

Is aberrant genome organization a cause or consequence of specific diseases?

Edited by

Eric C. Schirmer and Joanna M. Bridger

Published in

Frontiers in Cell and Developmental Biology



FRONTIERS EBOOK COPYRIGHT STATEMENT

The copyright in the text of individual articles in this ebook is the property of their respective authors or their respective institutions or funders. The copyright in graphics and images within each article may be subject to copyright of other parties. In both cases this is subject to a license granted to Frontiers.

The compilation of articles constituting this ebook is the property of Frontiers.

Each article within this ebook, and the ebook itself, are published under the most recent version of the Creative Commons CC-BY licence. The version current at the date of publication of this ebook is CC-BY 4.0. If the CC-BY licence is updated, the licence granted by Frontiers is automatically updated to the new version.

When exercising any right under the CC-BY licence, Frontiers must be attributed as the original publisher of the article or ebook, as applicable.

Authors have the responsibility of ensuring that any graphics or other materials which are the property of others may be included in the CC-BY licence, but this should be checked before relying on the CC-BY licence to reproduce those materials. Any copyright notices relating to those materials must be complied with.

Copyright and source acknowledgement notices may not be removed and must be displayed in any copy, derivative work or partial copy which includes the elements in question.

All copyright, and all rights therein, are protected by national and international copyright laws. The above represents a summary only. For further information please read Frontiers' Conditions for Website Use and Copyright Statement, and the applicable CC-BY licence.

ISSN 1664-8714
ISBN 978-2-8325-3464-9
DOI 10.3389/978-2-8325-3464-9

About Frontiers

Frontiers is more than just an open access publisher of scholarly articles: it is a pioneering approach to the world of academia, radically improving the way scholarly research is managed. The grand vision of Frontiers is a world where all people have an equal opportunity to seek, share and generate knowledge. Frontiers provides immediate and permanent online open access to all its publications, but this alone is not enough to realize our grand goals.

Frontiers journal series

The Frontiers journal series is a multi-tier and interdisciplinary set of open-access, online journals, promising a paradigm shift from the current review, selection and dissemination processes in academic publishing. All Frontiers journals are driven by researchers for researchers; therefore, they constitute a service to the scholarly community. At the same time, the *Frontiers journal series* operates on a revolutionary invention, the tiered publishing system, initially addressing specific communities of scholars, and gradually climbing up to broader public understanding, thus serving the interests of the lay society, too.

Dedication to quality

Each Frontiers article is a landmark of the highest quality, thanks to genuinely collaborative interactions between authors and review editors, who include some of the world's best academicians. Research must be certified by peers before entering a stream of knowledge that may eventually reach the public - and shape society; therefore, Frontiers only applies the most rigorous and unbiased reviews. Frontiers revolutionizes research publishing by freely delivering the most outstanding research, evaluated with no bias from both the academic and social point of view. By applying the most advanced information technologies, Frontiers is catapulting scholarly publishing into a new generation.

What are Frontiers Research Topics?

Frontiers Research Topics are very popular trademarks of the *Frontiers journals series*: they are collections of at least ten articles, all centered on a particular subject. With their unique mix of varied contributions from Original Research to Review Articles, Frontiers Research Topics unify the most influential researchers, the latest key findings and historical advances in a hot research area.

Find out more on how to host your own Frontiers Research Topic or contribute to one as an author by contacting the Frontiers editorial office: frontiersin.org/about/contact

Is aberrant genome organization a cause or consequence of specific diseases?

Topic editors

Eric C. Schirmer — University of Edinburgh, United Kingdom

Joanna M. Bridger — Brunel University London, United Kingdom

Citation

Schirmer, E. C., Bridger, J. M., eds. (2023). *Is aberrant genome organization a cause or consequence of specific diseases?* Lausanne: Frontiers Media SA.
doi: 10.3389/978-2-8325-3464-9

Table of contents

- 04 **Editorial: Is aberrant genome organization a cause or consequence of specific diseases?**
Eric C. Schirmer and Joanna M. Bridger
- 06 **Biology and Model Predictions of the Dynamics and Heterogeneity of Chromatin-Nuclear Lamina Interactions**
Julia Madsen-Østerbye, Aurélie Bellanger, Natalia M. Galigniana and Philippe Collas
- 19 **Breaking the aging epigenetic barrier**
Sweta Sikder, Ganesan Arunkumar, Daniël P. Melters and Yamini Dalal
- 36 **Erratum: Breaking the aging epigenetic barrier**
Frontiers Production Office
- 37 **MeCP2 heterochromatin organization is modulated by arginine methylation and serine phosphorylation**
Annika Schmidt, Jana Frei, Ansgar Poetsch, Alexandra Chittka, Hui Zhang, Chris Aßmann, Anne Lehmkuhl, Uta-Maria Bauer, Ulrike A. Nuber and M. Cristina Cardoso
- 59 **Emerin interacts with histone methyltransferases to regulate repressive chromatin at the nuclear periphery**
Nicholas Marano and James M. Holaska
- 72 **Genome organization in cardiomyocytes expressing mutated A-type lamins**
Marie Kervella, Maureen Jahier, Albano C. Meli and Antoine Muchir
- 81 **The role of prelamin A post-translational maturation in stress response and 53BP1 recruitment**
Cristina Capanni, Elisa Schena, Maria Letizia Di Giampietro, Alessandra Montecucco, Elisabetta Mattioli and Giovanna Lattanzi
- 96 **Nuclear envelope, chromatin organizers, histones, and DNA: The many achilles heels exploited across cancers**
A. K. Balaji, Santam Saha, Shruti Deshpande, Darshini Poola and Kundan Sengupta
- 117 **Nuclear envelope transmembrane proteins involved in genome organization are misregulated in myotonic dystrophy type 1 muscle**
Vanessa Todorow, Stefan Hintze, Benedikt Schoser and Peter Meinke



OPEN ACCESS

EDITED AND REVIEWED BY

Davide Marenduzzo,
SUPA, School of Physics and Astronomy,
University of Edinburgh, United Kingdom

*CORRESPONDENCE

Joanna M. Bridger,
✉ joanna.bridger@brunel.ac.uk

RECEIVED 02 August 2023

ACCEPTED 17 August 2023

PUBLISHED 29 August 2023

CITATION

Schirmer EC and Bridger JM (2023),
Editorial: Is aberrant genome
organization a cause or consequence of
specific diseases?
Front. Cell Dev. Biol. 11:1271790.
doi: 10.3389/fcell.2023.1271790

COPYRIGHT

© 2023 Schirmer and Bridger. This is an
open-access article distributed under the
terms of the [Creative Commons
Attribution License \(CC BY\)](#). The use,
distribution or reproduction in other
forums is permitted, provided the original
author(s) and the copyright owner(s) are
credited and that the original publication
in this journal is cited, in accordance with
accepted academic practice. No use,
distribution or reproduction is permitted
which does not comply with these terms.

Editorial: Is aberrant genome organization a cause or consequence of specific diseases?

Eric C. Schirmer¹ and Joanna M. Bridger^{2*}

¹Institute of Cell Biology, University of Edinburgh, Edinburgh, United Kingdom, ²Centre of Genome Engineering and Maintenance, Biosciences, Department of Life Sciences, College of Health, Medicine and Life Sciences, Brunel University London, Uxbridge, United Kingdom

KEYWORDS

genome organization, ageing, lamina associated domains, cancer, laminopathies, epigenetics, DNA repair, lamin A

Editorial on the Research Topic

[Is aberrant genome organization a cause or consequence of specific diseases?](#)

The past four decades have seen technological advances in the field of genome behaviour that have enabled a pretty clear overview of genome behaviour in healthy cells and how it changes upon external stimuli and during differentiation/senescence. However, ongoing discussions abound regarding mechanisms and functional consequences of gene/chromatin positioning, folding, and dynamics, and how its disruption links with disease. Furthermore, we remain far from completely understanding the involvement of the various nuclear structures, and how even some of these structures are built, let alone their functional, spatial, and temporal association with the genome. There is, however, plenty of evidence and consensus in the field that the nuclear envelope is an immensely important structure with respect to anchoring the genome and the regulation of genome function, not only directly at the nuclear edge but throughout the nucleoplasm. Furthermore, epigenetic control of the genome is partly controlled by nuclear envelope proteins. It is very obvious that genome organization is altered in a wide range of diseases from cancer to tissue degenerative diseases including neural, muscular, skin, metabolic, bone, and fertility, as well as diseases associated with premature ageing. As it has been suggested that most remaining disease alleles to be identified will lie outside of coding regions, to map all genome changes and their impact on gene expression in all diseases will be a major undertaking; therefore, it makes sense to first reflect on the problem to identify underlying common mechanisms for genome organization alterations and establish a defined set of criteria and quality assurances to adhere to, that could also lead to biomarker discovery. This led us to ask the question for this Research Topic: *Is aberrant genome organization a cause or consequence of specific diseases?*

The response yielded the publication of a range of excellent research articles and thoughtful, impactful reviews on epigenetic control and remodelling, the importance of the nuclear envelope and its role in genome organization, and roles of chromatin remodellers for gene regulation; all highlighting best practices needed in the field. Studying genome organization in diseased cells and tissues is not straightforward, as most data are simply correlative, and proper testing requires complex genome-engineered controls.

Some articles were focused more on chromatin remodelling and epigenetics, such as the identification of several new MeCP2 post-translational modifications specifically in the brain

that alter its binding kinetics and targeting, which could explain the effects of some Rett syndrome mutations. Here, [Schmidt et al.](#) found that R106 that is mutated in Rett syndrome normally becomes dimethylated in the brain and this increases its DNA-binding affinity. A role for the nuclear envelope in chromatin remodelling and epigenetics was made very clear by [Marano and Holaska](#), who demonstrated that emerin at the nuclear envelope interacts with the histone modifiers HDAC3, EZH2, and G9a and altered HDAC3 binding in emerin mutants, resulting in more repressed chromatin at the edge of the nucleus affecting the cell cycle and myogenic differentiation. A comprehensive review on chromatin structural changes in ageing details how ageing genomes suffer histone loss, instability, altered epigenetics, and compositional differences in senescence-associated heterochromatin foci. [Sikder et al.](#) also discuss how these alterations to the epigenome and spatial organization as cells age are inherently coupled with cancer progression and differ across the evolutionary landscape.

Evidence for a more direct role of the nuclear envelope in cancer progression was collated by [Balaji et al.](#) that involved both nuclear pore complex functions and nuclear membrane structural functions related to 3D-spatial genome organization, oncohistones, and nuclear envelope functions in senescence. Other articles also focused on the nuclear envelope regulation of genome organization. [Kervella et al.](#) reviewed how mutations in lamin A causing cardiomyopathy lead to reorganization of nuclear envelope-genome tethers called lamina-associated-domains (LADs) that in turn alter gene expression specifically in cardiomyocytes. They compared data from four different methods to measure genome organization and emphasized the need to apply genome editing tools in patient cells to clarify how genome mis-organization causes disease. [Madsen-Østerbye et al.](#) argue the benefits of using combinatorial approaches for 3D-computer modelling of chromosomes and their interactions with the nuclear envelope at LADs to distinguish the most functionally relevant interactions. Importantly, the authors highlight to the field the heterogeneity of these interactions in various cell types, differentiation, senescence, and disease situations where they observed fascinating new patterns.

Finally, other important genome functions linked to the nuclear envelope were considered in two last research articles. [Capanni et al.](#) used proximity ligation assays to show that changing pre-lamin A levels are temporally linked to the regulation of early stress responses and DNA repair by 53BP1 that gets recruited to lamin A/C. [Todorow et al.](#) focused on a disorder previously not linked to the nuclear envelope, Myotonic dystrophy (DM1). Since DM1 is associated with massive alternative splicing, the authors questioned whether nuclear envelope proteins linked to other

muscle disorders are mis-spliced in DM1, finding that structural proteins such as SYNE 1 and 3, SUN1 and 2, and Samp1 were misspliced as well as nuclear membrane proteins involved in musclespecific 3D-genome organization.

Overall, this Research Topic has highlighted the importance of using combinatorial approaches together with some best practices such as genome engineering of patient cells needed to address this important question. It has also shown that there remain previously un-investigated functions that could explain the effects of altered genome organization on specific diseases. Our core Research Topic question of whether aberrant genome organization is a cause or consequence of disease is still unanswered; however, the data argue that where a pathology-causing effect of genome mis-organization has not yet been found, it likely exists and will require scientific creativity like that demonstrated in these Research Topic articles, together with best practices enumerated here to find it.

Author contributions

ES: Conceptualization, Writing–original draft, Writing–review and editing. JB: Conceptualization, Writing–original draft, Writing–review and editing.

Conflict of interest

The authors declare that the research was conducted in the absence of any commercial or financial relationships that could be construed as a potential conflict of interest.

The handling editor DM declared a shared affiliation with the author ES at the time of review.

The author(s) declared that they were an editorial board member of Frontiers, at the time of submission. This had no impact on the peer review process and the final decision.

Publisher's note

All claims expressed in this article are solely those of the authors and do not necessarily represent those of their affiliated organizations, or those of the publisher, the editors and the reviewers. Any product that may be evaluated in this article, or claim that may be made by its manufacturer, is not guaranteed or endorsed by the publisher.



Biology and Model Predictions of the Dynamics and Heterogeneity of Chromatin-Nuclear Lamina Interactions

Julia Madsen-Østerbye¹, Aurélie Bellanger¹, Natalia M. Galigniana^{1,2} and Philippe Collas^{1,2*}

¹Department of Molecular Medicine, Institute of Basic Medical Sciences, Faculty of Medicine, University of Oslo, Oslo, Norway,

²Department of Immunology and Transfusion Medicine, Oslo University Hospital, Oslo, Norway

OPEN ACCESS

Edited by:

Eric C. Schirmer,
University of Edinburgh,
United Kingdom

Reviewed by:

Davide Marenduzzo,
University of Edinburgh,
United Kingdom
Chiara Lanzuolo,
Institute of Cell Biology and
Neurobiology (CNR), Italy

*Correspondence:

Philippe Collas
philc@medisin.uio.no

Specialty section:

This article was submitted to
Nuclear Organization and Dynamics,
a section of the journal
Frontiers in Cell and Developmental
Biology

Received: 06 April 2022

Accepted: 12 May 2022

Published: 26 May 2022

Citation:

Madsen-Østerbye J, Bellanger A,
Galigniana NM and Collas P (2022)
Biology and Model Predictions of the
Dynamics and Heterogeneity of
Chromatin-Nuclear
Lamina Interactions.
Front. Cell Dev. Biol. 10:913458.
doi: 10.3389/fcell.2022.913458

Associations of chromatin with the nuclear lamina, at the nuclear periphery, help shape the genome in 3 dimensions. The genomic landscape of lamina-associated domains (LADs) is well characterized, but much remains unknown on the physical and mechanistic properties of chromatin conformation at the nuclear lamina. Computational models of chromatin folding at, and interactions with, a surface representing the nuclear lamina are emerging in attempts to characterize these properties and predict chromatin behavior at the lamina in health and disease. Here, we highlight the heterogeneous nature of the nuclear lamina and LADs, outline the main 3-dimensional chromatin structural modeling methods, review applications of modeling chromatin-lamina interactions and discuss biological insights inferred from these models in normal and disease states. Lastly, we address perspectives on future developments in modeling chromatin interactions with the nuclear lamina.

Keywords: chromatin, interaction, LAD, lamina-associated domain, nuclear envelope, polymer modeling, restraint

INTRODUCTION

The 3-dimensional (3D) conformation of the genome is critical for the orchestration of gene expression regulating development, cell differentiation and tissue homeostasis. Genome organization relies on chromosomal interactions (Rowley and Corces, 2018) and at the nuclear periphery, associations of chromatin with the nuclear lamina (NL) via lamina-associated domains (LADs) (Briand and Collas, 2020). Some LADs change during differentiation or are altered in disease, and laminopathies, pathologies caused by mutations in nuclear lamins (Shin and Worman, 2022), underscore the importance of maintaining a proper radial genome organization. Whereas the genomic landscape of LADs is getting well characterized, surprisingly little is known on how LADs are physically and mechanistically repositioned in the genome.

Computational modeling of chromatin structure (Parmar et al., 2019; Jerkovic and Cavalli, 2021) creates opportunities to better understand the patterns, dynamics and mechanisms of chromatin-NL interactions in normal and disease states. Polymer physics modeling provides quantitative information on the physical properties of chromatin folding. In addition, restraint-based methods model 3D chromatin structures represented by points and restraints between them dictated by wet-lab data. Both approaches can accommodate positional constraints for chromatin, for example imposing interactions between similar chromatin domains or interactions with a nuclear body or with a surface representing a NL.

Here, we highlight the heterogeneous nature of the NL and LADs, outline the main 3D chromatin structural modeling methods currently used, review computational models of chromatin-NL

interactions, and discuss biological insights deduced from these models in normal and pathological conditions. Lastly, we address perspectives on applications of modeling interactions of chromatin with the NL with the aim of better appreciating the multiple facets of functional genome organization.

HETEROGENEITY OF THE NUCLEAR LAMINA AND LAMINA-ASSOCIATED DOMAINS

Current views of 3D nuclear architecture depict a hierarchical and dynamic environment where chromatin can alter its composition and conformation in response to stimuli (Rowley and Corces, 2018). Within chromosome territories, chromatin is divided into active and inactive compartments, within which smaller topological domains reflect a high frequency of chromosomal contacts thought to regulate gene expression. These topological domains can also form dynamic long-range interactions within chromosomes, while some also interact with the NL *via* LADs, and thereby radially organize the genome (Marti-Renom et al., 2018; Buchwalter et al., 2019).

The Heterogeneous Nuclear Lamina

At the nuclear periphery, the NL interfaces the inner nuclear membrane and chromatin as a meshwork of intermediate filaments built from polymers of A-type lamins (lamins A and C, splice variants of the *LMNA* gene) and B-type lamins (lamins B1 and B2, products of the *LMNB1* and *LMNB2* genes) (Burke and Stewart, 2013). The NL plays a critical role in maintaining nuclear shape. It provides mechanical support to chromatin and anchors chromatin modifying enzymes, transcription factors and signaling molecules, imposing a spatio-temporal regulation of genome compaction, DNA replication and transcription (Buchwalter et al., 2019). Studies combining cryo-electron tomography and microscopy reveal that the NL forms a heterogeneous structure with distinct but interacting networks of A- and B-type lamin homopolymers and void space occupied by other proteins and chromatin (Shimi et al., 2008; Shimi et al., 2015; Turgay et al., 2017). Additional imaging data show that lamin B1 and lamin A/C form concentric but overlapping networks with lamin B1 localized more outwards, adjacent to the inner nuclear membrane (Nmezi et al., 2019). Interestingly, models of NL structure inferred from these findings have been shown to predict NL behavior, the roles of lamin B1 and A/C networks and impacts of their perturbation on nuclear function (Nmezi et al., 2019). Whether this structural organization of the NL provides a basis for differential interactions of A- and B-type lamins with chromatin (Forsberg et al., 2019) remains unknown but is a possibility. As addressed later in this review, these observations bring about options to enhance the prediction potential of 3D models of chromatin folding and interactions with the NL. Computational models of the relationship between components of the nuclear envelope have been discussed elsewhere (Nmezi et al., 2019; Sapra et al., 2020; Tenga and Medalia, 2020; Kittisopikul et al., 2021) and provide complementary insights to those highlighted here on the

structural organization of the periphery of the mammalian nucleus.

Lamina-Associated Domains Are Diverse and Dynamic Genome Organizers

In mammalian cells, hundreds of LADs have been mapped throughout the genome (**Figure 1A**) using various wet-lab and bioinformatics methods (Briand and Collas, 2020; Manzo et al., 2022). Irrespective of these methods, LADs have been identified as domains of about 10 kilobases (kb) to 10 megabases (mb) unevenly distributed between chromosomes and within chromosomes. LADs are AT-rich and of low gene density, and enriched in long interspersed nuclear elements (LINEs) and features of heterochromatin such as histone H3 lysine 9 dimethylation (H3K9me2) and H3K9me3 (Guelen et al., 2008). LADs tend to display relatively sharp borders (sharp transitions between LAD and non-LAD regions) and are typically flanked by active genes, and within 50–200 kb of these borders, by domains of H3K27me3 (Harr et al., 2015; Paulsen et al., 2019). As a result, most genes in LADs are silent or expressed at low levels and overall, LADs form repressive domains at the nuclear periphery. Likely as a result of their compact state, LADs are excluded sites of viral (e.g., HIV-1) integration despite preferred virus insertions at the nuclear periphery (Marini et al., 2015), and constitute domains of low DNA lesion repair capacity presumably due to limited access to the DNA repair machinery (Garcia-Nieto et al., 2017).

LADs are a general feature of genome organization, but not all LADs have similar properties (**Figure 1B**). Some are well conserved between cell types (Keough et al., 2020; Meuleman et al., 2013), during differentiation (Madsen-Østerbye et al., 2022; Peric-Hupkes et al., 2010; Rønningen et al., 2015) and across circadian time (Brunet et al., 2019). These constitutive LADs (cLADs) are characterized by high lamin B1-chromatin contact frequency and are viewed as the genomic backbone of chromosome anchoring to the nuclear envelope. Other LADs are less conserved between cell types (**Figure 1B**). Variable (v) LADs are smaller than cLADs, display lower lamin B1 enrichment, harbor a higher gene density and are less heterochromatic. vLADs are a feature of differentiation where entire LADs or LAD edges associate with or detach from the NL (Madsen-Østerbye et al., 2022). Some loci in vLADs are repositioned away from the NL when they lose lamin association (Reddy et al., 2008), but this is not systematic (Robson et al., 2016; Forsberg et al., 2019; Czapiewski et al., 2022). LAD repositioning also occasionally concurs with activation of cell type-specific genes (Peric-Hupkes et al., 2010; Robson et al., 2016; Keough et al., 2020; Czapiewski et al., 2022; Madsen-Østerbye et al., 2022) or disease-specific genes (Kohler et al., 2020). vLADs may also function as regulators of transcription by releasing enhancers that in turn regulate expression of neighboring genes (Robson et al., 2016; Czapiewski et al., 2022) (**Figure 1C**).

In spite of their overall conservation, increasing evidence indicates that cLADs are not homogeneous in their chromatin composition. Approximately 10% of genes in cLADs have initially

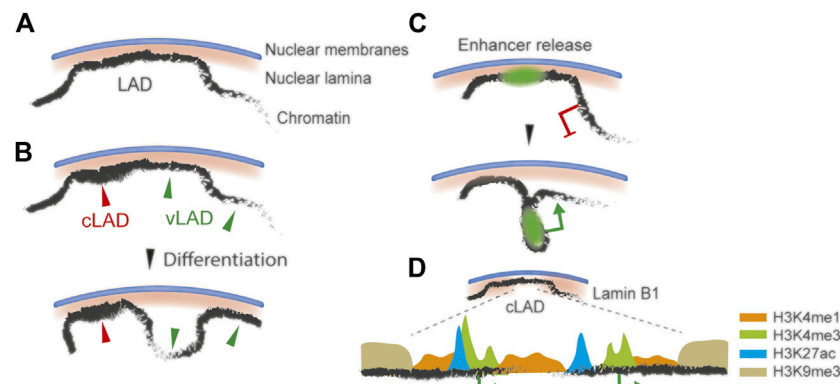


FIGURE 1 | Dynamics and heterogeneity of LADs **(A)** Interaction of chromatin with the NL via a LAD **(B)** Variable LADs (vLADs) are repositioned in the genome during differentiation **(C)** Enhancer (green area) release from the NL by LAD detachment, and activation of a nearby gene (green arrow) **(D)** Active cLAD sub-domain of lower lamin B1 level than the rest of the LAD, depleted of H3K9me3 but enriched in euchromatic histone modifications (H3K4me1, H3K4me3 and H3K27ac). Genes in these sub-domains escape the heterochromatic repressive environment of LADs.

been found to be expressed and to escape the repressive NL environment (Guelen et al., 2008), a figure which has been confirmed in many studies regardless of cell type and species. Lower local lamin B1 enrichment, promoter sequence properties and active histone modifications may account for this apparent discrepancy (Brueckner et al., 2020; Leemans et al., 2019; Madsen-Østerbye et al., 2022; Wu and Yao, 2017) (Figure 1D). These regions also appear to be more prone to alterations in epigenetic states and chromatin accessibility than the more constitutive heterochromatic domains of LADs. For example, in diseases caused by lamin mutations such as Hutchinson-Gilford Progeria Syndrome (HGPS), a premature aging laminopathy caused by mutations in the *LMNA* gene (Kohler et al., 2020; Shin and Worman, 2022).

Additionally, a subset of LADs bound by A-type lamins harbors features of euchromatin (Lund et al., 2015; Gesson et al., 2016), and lamin C, when phosphorylated, can bind H3K27-acetylated enhancers (Ikegami et al., 2020). A fraction of B-type lamins also intriguingly binds active genes during the epithelial-to-mesenchymal transition (Pascual-Reguant et al., 2018), through currently unidentified mechanisms. This variation of chromatin states in LADs creates opportunities to better appreciate the physics of chromatin-NL interactions and tentatively predict their functional implications.

3D MODELS OF CHROMOSOMES PROVIDE MECHANISTIC AND STATISTICAL INSIGHTS INTO CHROMATIN DYNAMICS

One strategy to investigate spatial genome dynamics is to generate 3D models of chromatin and analyze properties of the models. Modeling enables statistical and mechanistic insights into principles of chromatin folding or interaction with a surface representing, for example, the NL. Models of

chromatin have been generated using two main approaches: 1) polymer physics models chromatin as a semi-flexible polymer chain that can adopt many configurations within physical constraints applied to the chain; 2) restraint-based modeling represents chromatin by beads in a Euclidian space with restrained interactions between them commonly determined from chromosome interaction data. We next provide an account of these modeling approaches in light of their relevance for modeling chromatin configuration at the NL. For details on 3D genome modeling methods, we refer to an excellent exhaustive review (Jerkovic and Cavalli, 2021).

Polymer Models of Chromosomes

Polymer modeling provides quantitative information on the physical properties of chromatin folding and on chromosome dynamics in the nucleus (Fiorillo et al., 2019; Tortora et al., 2020). Polymer models can predict statistical quantities such as end-to-end (Euclidian) distances or interaction frequencies between monomers in the polymer. A chromosome or chromosome segment is typically modeled as a semi-flexible polymer chain (Parmar et al., 2019). Semi-flexible polymers can in principle adopt an infinite number of configurations, but these are in reality limited by the persistence length L_p of the polymer—that is, the length under which the polymer behaves as a rigid rod and above which it behaves as a flexible chain. The repeating units of chromatin, modeled as monomers in the polymer chain, further limit the number of conformations the polymer can adopt during simulations; this limitation is typically achieved by introducing a self-avoidance effect to prevent clashes between monomers (Chiariello et al., 2016).

Block copolymer modeling is a broadly used generic and minimal chromatin modeling technique. It operates on the assumption that chromatin is a self-avoiding polymer whose folding is dictated by preferential interactions between domains (blocks) of similar epigenomic signatures, or “colors” (Jost et al., 2014) (Figure 2A). Self-avoiding consecutive monomers (beads) are connected *via* a harmonic potential and

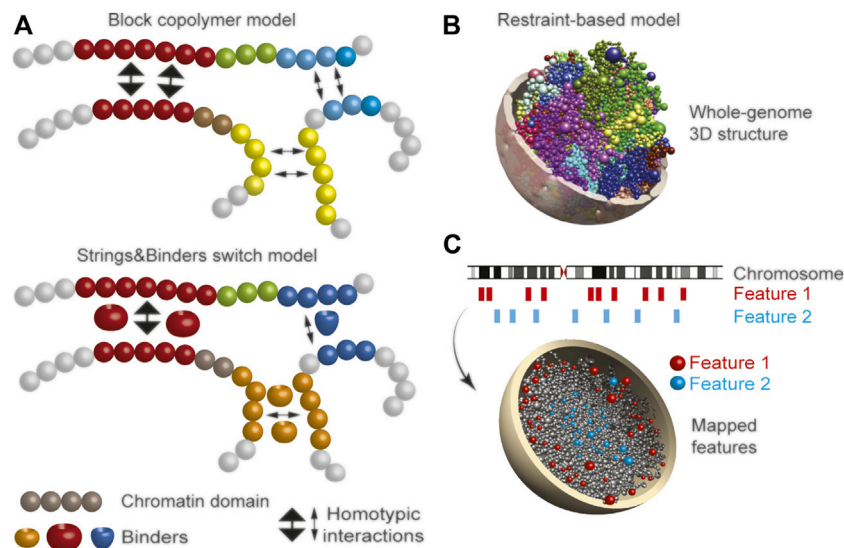


FIGURE 2 | Main polymer physics modeling approaches for chromatin **(A)** Top, block copolymer modeling of chromatin folding relying on homotypic interactions between domains (blocks) of similar epigenomic signatures (colors). Variations the strength of these interactions are introduced to model heterochromatic (thick arrows) or euchromatic (thin arrows) homotypic interactions. Bottom, a variant of block copolymer modeling: here, “binders” (e.g., transcription factors) mediate homotypic chromatin interactions **(B,C)** Restraint-based modeling **(B)** 3D model example of a whole human genome structure; each color defines a chromosome as a chain of beads, with one bead representing a topological domain identified from Hi-C data (here, in adipose stem cells). The model integrates Hi-C and lamin B1 ChIP-seq (LAD) restraints for chromatin and is generated with our Chrom3D platform (Paulsen et al., 2017) **(C)** 3D chromatin modeling enables spatial visualization of genomic features not detectable in 1D data; here, feature 1 is more peripherally located than feature 2.

an interaction strength between beads can be added *via* a tuneable attraction potential: for example, a strong potential can model homotypic heterochromatic interactions reflecting a compact structure, while a weaker potential models homotypic euchromatic interactions reflecting the more open state of active chromatin (Jost et al., 2014). Despite their simplicity and the exclusion of biological aspects of chromatin folding, block co-polymer models can recapitulate large scale Hi-C contact maps including A/B compartments and topological domains when built from epigenomes (Jost et al., 2014).

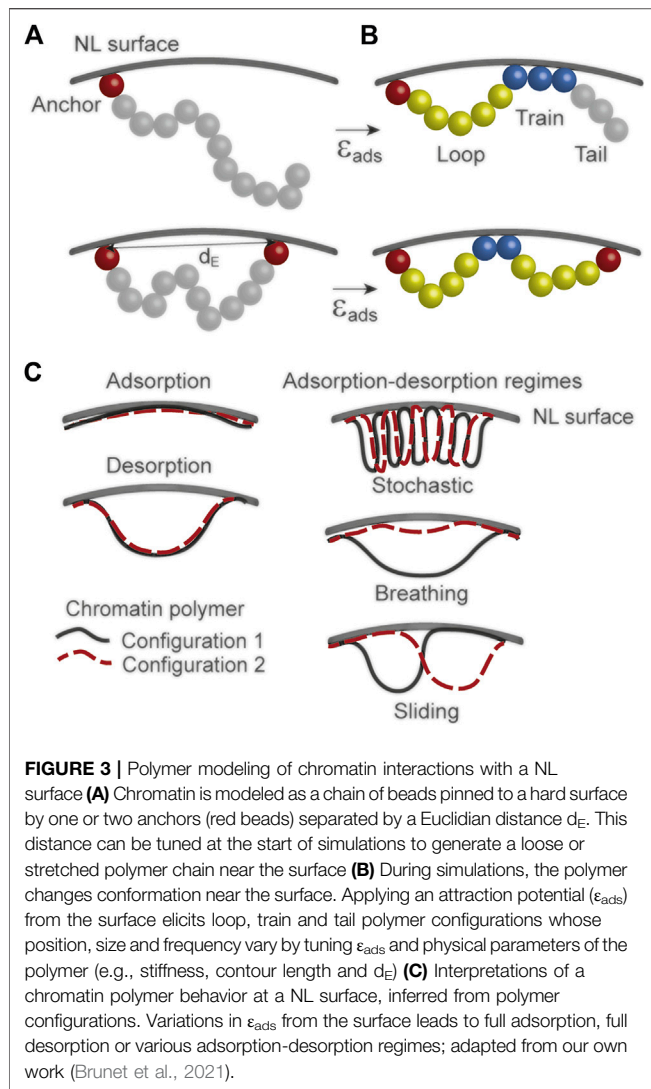
A variation of block copolymer modeling referred to as Strings & Binders switch modeling, allows interaction of chromatin with factors (binders) that mediate these interactions (Annunziatella et al., 2018; Barbieri et al., 2012) (**Figure 2A**). Again, beads are given a chromatin state (color) based on the type of binder they are attracted to, such as architectural proteins (e.g., HP1 α /CBX5, CTCF), histone-modifying enzymes (e.g., histone deacetylase HDAC3) or transcription factors (e.g., SREBP1). Beads tend to interact with binders and other beads of the same type as binder concentration increases, forming homotypic interactions. These models can be initiated from contact matrices by applying polymer physics laws, or by applying *a priori* knowledge of the modeled chromatin region, such as chromatin states or transcription factor binding profiles. Block copolymer simulations can also model the behavior of a chromatin chain that can assume various thicknesses and compositions, providing a more realistic view of chromatin (Buckle et al., 2018). Polymer models have mainly been limited to intra-chromosomal interactions, but with modifications,

can also model interactions between multiple chromosomes (Oliveira Junior et al., 2021).

Restraint-Based Modeling of Chromatin

Other chromatin 3D modeling approaches use restraint-based methods to infer spatial information directly from experimental data and reconstruct structures without assumptions on folding mechanisms. Contact matrices derived from Hi-C or other 3C-sequencing data are used to identify pairs of interacting domains as primary constraints. One restraint-based approach is to reconstruct a single consensus structure representing the average of 3D conformations in the cell population under study (Duan et al., 2010; Hu et al., 2013; Zhang et al., 2013; Lesne et al., 2014; Szalaj et al., 2016; Zou et al., 2016; Wlasnowolski et al., 2020). Consensus structures provide insights into genome architecture, but by definition do not capture variations in chromatin conformation seen between cells in a population (Nagano et al., 2013; Cheng et al., 2020).

To enable this, other methods simulate many structures. Resampling methods carry out a large number of independent optimizations from the same input data. Optimizations start from, most commonly, a random chromosome configuration and use the same scoring function aiming to reach a state where no constraint violations remain, producing a quasi-stable structure (Bau and Marti-Renom, 2011; Di Stefano et al., 2016; Kalhor et al., 2012; Le Dily et al., 2014; Meluzzi and Arya, 2013; Paulsen et al., 2017; Tjong et al., 2012) (**Figure 2B**). Of note, optimization can also be initialized from a determined (phenomenological) chromosome disposition based on existing data, for example, describing the radial positioning of



chromosomes in the nucleus (Di Stefano et al., 2016). Other methods deconvolute Hi-C data into a population of 3D structures using various techniques (Tjong et al., 2016; Li et al., 2017; Zhu et al., 2017). To enhance accuracy of the models, chromatin constraints can be added to for instance prevent clash between beads (motivated by chromatin thickness), position beads towards a nucleolus, or direct them towards a NL (Duan et al., 2010; Di Stefano et al., 2016; Li et al., 2017; Paulsen et al., 2017; Pouokam et al., 2019). Hi-C-constrained models of the diploid human genome have been shown to recapitulate features of spatial genome organization, including associations with a nuclear envelope (by including LAD constraints), with functional relevance (Di Stefano et al., 2016).

We have also reported ensembles of chromatin structures (Paulsen et al., 2017) relying on Hi-C and lamin B1 ChIP-seq (LAD) data, which faithfully recover characteristics of radial genome organization and stability observed in single cells (Kind et al., 2015). The structures allow inference on the regionalization of chromatin states (Di Stefano et al., 2016;

Paulsen et al., 2018; Paulsen et al., 2019), and on radial positioning of loci (Briand et al., 2018), disease-associated LADs (Paulsen et al., 2017) and cancer mutations (Garcia-Nieto et al., 2017) (**Figure 2C**). It will be interesting to compare outputs of restraint-based model ensembles and of models generated from single-cell data (Cardozo Gizzi, 2021; Kos et al., 2021) to determine the most powerful strategy for predicting chromatin structure dynamics. This would be relevant in the study of 3D cancer genomes, as cell-to-cell heterogeneity within tumors hampers many investigations.

MODELING INTERACTIONS OF CHROMATIN WITH THE NUCLEAR LAMINA

Chromatin folding at, and interactions with, the NL have been modeled in attempts to identify physical processes driving these events, infer mechanisms of chromatin association with, and dissociation from, the NL, and provide more accurate spatial genome structures at the nucleus level.

Basic Physical Considerations in Modeling Interactions of a Chromatin Polymer With a NL Surface

We have recently assessed the extent to which basic physical properties of a polymer, such as stiffness and stretching, would influence its configurations near an impermeable (hard) surface representing a NL, fitted with an attraction potential towards the polymer (Brunet et al., 2021). Chromatin is modeled as a polymer of hard beads of contour length L_C 360 nm representing a ~50 kb region to enable modeling interactions of small vLADs or euchromatic sub-LAD regions (Madsen-Østerbye et al., 2022). The polymer is configured with one or two ends anchored to the surface with increasing Euclidean distance d_E between them, yielding a relaxed or stretched chain (**Figure 3A**). Further, by varying the persistence length L_p , or stiffness, of the polymer, the behavior of euchromatin (low persistence length) or heterochromatin (higher persistence length) at the NL can be approximated (Brunet et al., 2021).

Data from simulations indicate that in the absence of attraction potential from the NL surface, the polymer must be pinned by at least one bead to enable any interactions with the surface. Second, a flexible chain explores a greater area than a semi-flexible or rigid chain, so one may infer that a euchromatic region can explore a greater space near the NL than a more rigid heterochromatic domain (Brunet et al., 2021). Third, interaction profiles of the polymer with the surface, described as trains, tails and loops (**Figure 3B**) during simulations suggest that more flexible (eu)chromatin as opposed to more rigid (hetero)chromatin can adopt more variable and dynamic configurations at the NL, reflecting biological observations (Madsen-Østerbye et al., 2022). It will be informative to investigate the functional impact of this property of euchromatic LADs (Pascual-Reguant et al., 2018; Ikegami et al., 2020; Liu and Ikegami,

2020) or sub-LAD domains (Madsen-Østerbye et al., 2022) on gene expression dynamics in these regions.

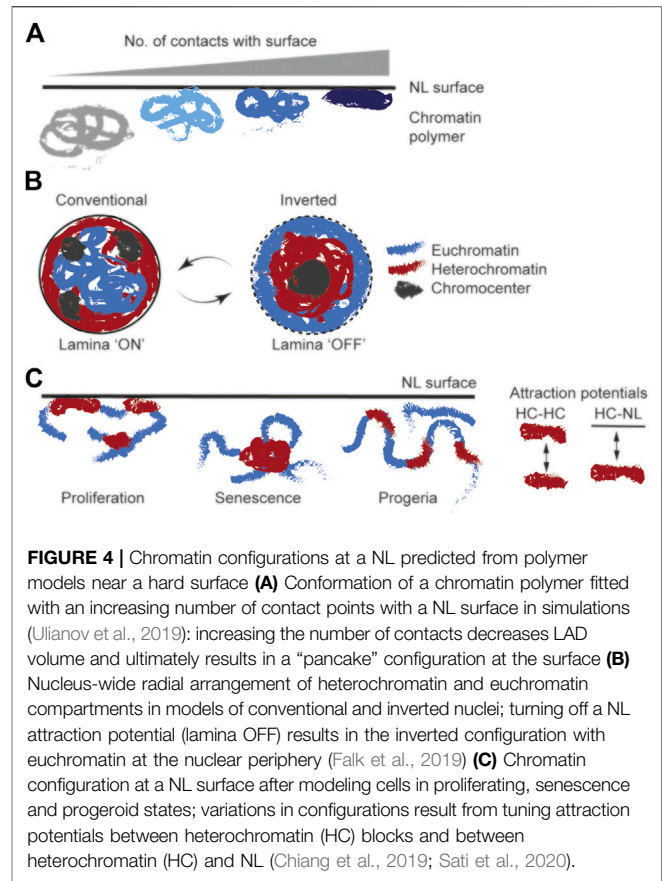
Without attraction potential, polymer interactions with the surface are only transient and barely detectable (except at the anchors). This is consistent with other models where turning off an attraction potential between the NL surface and a chromatin polymer promotes polymer detachment (Chiang et al., 2019; Falk et al., 2019; Sati et al., 2020; Amiad-Pavlov et al., 2021). In contrast, applying an attraction potential to the NL is essential for persistent interactions. Tuning this potential yields interaction profiles ranging from stable adsorption (strong potential) to stable desorption (weak potential), with in between, adsorption-desorption regimes yielding multiple configurations at the surface (Brunet et al., 2021) (Figure 3C). These experiments together identify fundamental physical parameters which in combination contribute to predict chromatin behavior at the NL.

The absence of attraction potential towards a NL may still enable expected polymer positioning relative to a physical constraint. Indeed, when a self-avoiding polymer is confined to a nucleus sphere, non-specific entropic forces alone can remarkably shape and position chromatin polymers in the sphere and approximate high-order localization of loose (thin) and compact (thick) segments in the sphere center or periphery, respectively (Cook and Marenduzzo, 2009).

Modeling Nucleus-Wide Chromatin Reconfiguration With a Minimal Set of Physical Parameters

These findings have been extended by modifying the polymer-surface interaction parameter as a fraction of the chromatin polymer bound to the NL, and introducing a chromatin volume fraction (modeling a hydration effect) and an intra-chromatin attraction potential (Bajpai et al., 2021). Tuning these parameters in simulations of chromatin behavior in a nucleus sphere yields transitions in chromatin reconfigurations, from peripheral heterochromatin enrichment to a fully central “collapsed” localization when the LAD parameter is turned off. The data reveal that a theoretical competition between chromatin-NL and chromatin-chromatin attraction strengths is sufficient to determine large-scale chromatin arrangement in the nucleus (Bajpai et al., 2021).

Identification of a minimalistic set of parameters able to predict chromatin conformation is useful (Bajpai et al., 2021); however the models would gain from the inclusion of attraction potentials regulating homotypic and heterotypic chromatin interactions. For instance, abrogating chromatin-NL interactions should not result in chromatin clumping in the nucleus center. Rather, turning off chromatin-NL interactions has been shown to reconstitute the central localization of heterochromatin observed in “inverted” nuclei, with a peripheral localization of euchromatin (Falk et al., 2019) (see also below). Similarly, turning off the LAD parameter in restraint-based genome models results in less stable peripheral localization of peripheral chromosomes across simulations, but chromatin does not collapse in the nucleus center despite persistent



interactions between topological domains (Paulsen et al., 2017). That said, the models of Bajpai et al. seem to recapitulate *in vivo* chromatin imaging observations and, with only a small number of parameters, account for changes in phase separation (chromatin vs. aqueous) that may drive mesoscale chromatin reconfiguration in developing *Drosophila* larvae (Amiad-Pavlov et al., 2021).

WHEN MODELING MEETS BIOLOGY

Polymer Models Predict That Attachment to the NL Compacts Chromatin

Polymer simulations of *Drosophila* S2 cell chromatin shows that interactions with a surface are sufficient to compact chromatin, with the degree of compaction being proportional to the number of contact points, ultimately reaching a “pancake” configuration (Ulianov et al., 2019) (Figure 4A). This is consistent with our theoretical findings from simulations of the dynamics of polymer adsorption to a surface (Brunet et al., 2021). Conversely, the models predict that release of LADs from the NL coincides with local decompaction of LAD chromatin, which was confirmed by microscopy (Ulianov et al., 2019). However, this does not imply that chromatin decompaction is a nucleus-wide phenomenon, because non-LAD domains undergo compaction upon LAD release from the NL (Sawh et al., 2020), presumably as a result

of tension release in chromatin (Ulianov et al., 2019; Sawh et al., 2020).

Polymer Models of Nuclear Inversion Uncouple Chromatin Compartmentalization From NL Interaction in the Radial Arrangement of the Genome

Block copolymer models have been used to disentangle the role of hetero-/euchromatin compartmentalization and of the NL in the radial disposition of chromatin in conventional vs. inverted nuclei in which heterochromatin is concentrated in the center while euchromatin lies towards the periphery (Falk et al., 2019). Simulations were done considering pericentric constitutive heterochromatic-, heterochromatic- and euchromatic-type monomers with or without interactions with a NL surface. These monomers were conferred with homotypic and heterotypic short-range interactions enabled by attraction potentials of various strengths. Remarkably, the models recapitulate genome compartmentalization seen in Hi-C data and produce the inverted radial chromatin conformation (Falk et al., 2019) reported in nuclei in the absence of lamin A or of the lamin B receptor (LBR) (Solovei et al., 2013) (**Figure 4B**). Only when short-range attraction potentials between heterochromatin monomers and the NL surface are introduced in simulations do the models adopt a conventional nucleus configuration with heterochromatin at the periphery (Falk et al., 2019); this is notably reversible (**Figure 4B**). Supporting original microscopy observations (Solovei et al., 2013), these models suggest that homotypic heterochromatic interactions are sufficient to drive the segregation of heterochromatin from euchromatin, whereas interaction with the NL is necessary to confer a conventional radial nuclear configuration (Falk et al., 2019).

Modeling Chromatin Rearrangement and NL Dissociation During Senescence

Hallmarks of senescence are the formation of senescence-associated heterochromatic foci (SAHF) and degradation of the NL, which releases heterochromatin from the nuclear envelope and elicits SAHFs (Sadaie et al., 2013; Shah et al., 2013). To disentangle heterochromatin compaction from LAD repositioning in SAHF formation, block copolymer models have been generated, with tuneable attraction potentials between monomers in a chain modeling a senescence-associated heterochromatin domain, and between monomers and a NL surface (Sati et al., 2020) (**Figure 4C**). Modeling proliferating cells produces structures where heterochromatin masses interact but also occur away from the NL (**Figure 4C**). Moreover, a “membrane release” scenario where chromatin-NL attraction is brought to zero during simulations, effectively recapitulates LAD detachment from the NL. This results in local chromatin polymer decompaction and large-scale interactions consistent with SAHF formation away from the NL (**Figure 4C**). Tuning the attraction potential between monomers in the chromatin chain approximates imaging data (Sati et al., 2020), indicating that polymer

models recapitulate both chromatin folding patterns and dynamic interactions with the NL.

Senescence-associated loss of heterochromatin at the NL also occurs after down-regulation of LBR, a protein of the inner nuclear membrane anchoring heterochromatin at the nuclear envelope (Herman et al., 2021). A role of LBR in mediating chromatin-NL interactions could be tested *in silico* by introducing LBR as a “binder” mediating these interactions in block copolymer models (see **Figure 2A**). Large-scale changes in nuclear morphology observed upon LBR down-regulation-elicited senescence (Kohler et al., 2020) would provide a valuable dataset to predict chromatin structural alterations at the nucleus level in restraint-based 3D genome models.

MODELING CHROMATIN-NL INTERACTIONS TO BETTER UNDERSTAND DISEASE?

Disruption of chromatin architectural genomic elements or proteins has emerged as a mechanism underlying diseases ranging from developmental defects to laminopathies and certain cancers (Lupianez et al., 2016; Evangelisti et al., 2022; Shin and Worman, 2022). The discovery of nuclear architectural defects linked to these diseases provides opportunities to test whether modeling would help understand consequences of the diseases on genome integrity, and in the most optimistic scenarios help identify causes of the pathologies.

Polymer modeling of dynamic chromatin-NL interactions under normal and senescence conditions not only yields predictions on large-scale chromatin refolding upon detachment from the NL, but also extends our understanding of chromatin behavior at the NL in HGPS. By tuning only two attraction potentials controlling heterochromatin-heterochromatin and heterochromatin-NL interactions, simulations reproduce the distinct chromatin conformation changes occurring in senescent cells and in progeroid syndromes (Chiang et al., 2019) (**Figure 4C**). These simulations reveal euchromatic beads close to the NL despite the absence of specified attraction force between them, recapitulating the loss of peripheral heterochromatin reported in cells from HGPS patients (Shumaker et al., 2006; Kohler et al., 2020; Sebestyen et al., 2020).

Cell culture models of HGPS also provide opportunities to develop more elaborate and arguably more realistic models of chromatin changes in disease. Recent work highlights that alterations in chromatin accessibility, based on sequential extraction of chromatin fractions, in cells from HGPS patients can be measured in early passage HGPS cells prior to changes in heterochromatin composition (H3K9me3), which are only detectable in later passage (Sebestyen et al., 2020). Nonetheless, epigenetic remodeling by Polycomb (H3K27me3) seems to coincide with the structural changes of chromatin. These observations provide opportunities to temporally uncouple and mechanistically disentangle, in models of chromatin, the physical processes driving changes in chromatin structure and epigenomic changes, which most current models of chromatin

assume are coincident. Because LADs are also monitored in the study (Sebestyen et al., 2020), temporal models of structural and biochemical alterations of chromatin in relation to the loss of association with the NL would also be plausible (Chiang et al., 2019).

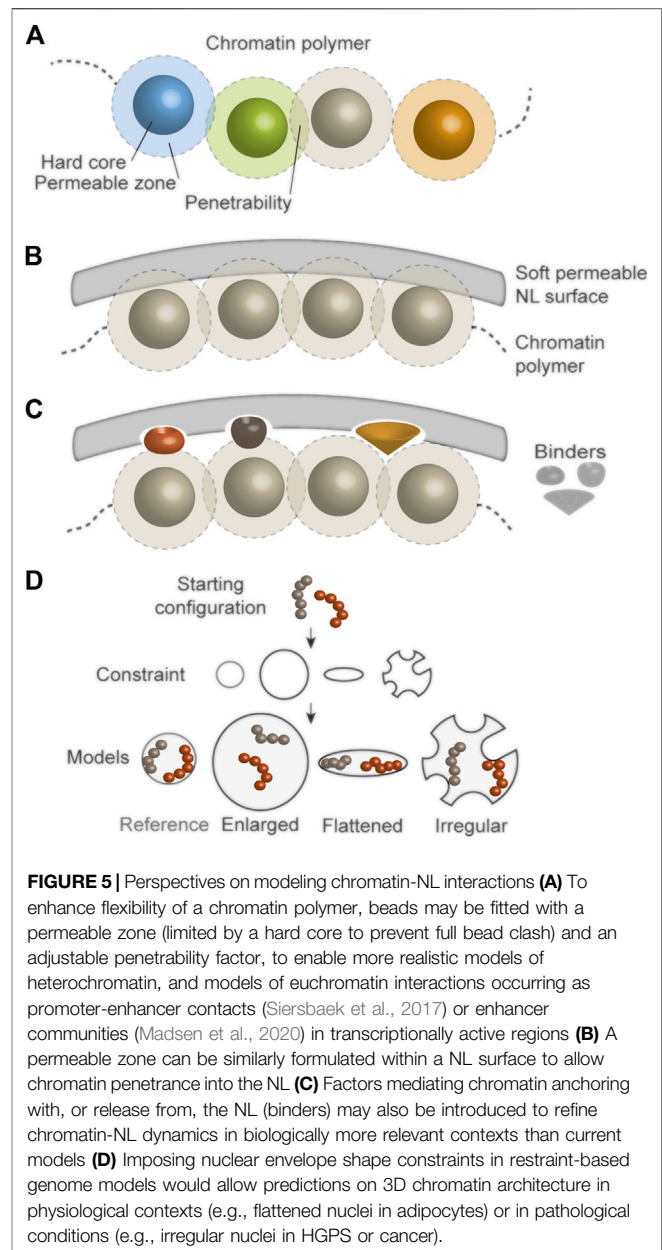
Explaining or Recapitulating Genome-Lamina Interactions With Modeling?

Data from simulations are not uncommonly interpreted as “explaining” a biological observation, as exemplified in some recent studies (Chiang et al., 2019; Sati et al., 2020). Whereas models may predict a biological outcome, they are a result of simulations carried out under minimalistic conditions and, we would argue, cannot per se explain biological phenomena. Results from simulation recapitulate a biological observation because parameters are appropriately tuned to mimic these observations. Notwithstanding, polymer models can generate useful working hypotheses on chromatin folding principles or mechanisms (defined by a minimal set of impactful parameters) underlying chromatin conformation and changes therein, e.g., in pathological contexts. Even based on simple rules or biophysical ingredients, models are believed to have the most useful if, on top of recapitulating biological observations, they can predict new ones. Models do not always need to be particularly sophisticated or detailed to achieve high predictive power, provided they capture sufficient details for the questions they aim to answer.

Restraint-Based Models Enable New Hypotheses on Mechanisms Underlying a Pathology

Integration of genomic datasets from wet-lab experiments into restraint-based models of 3D genome structure have provided new spatial insights into genomic consequences of pathological states, which may open to new therapeutic avenues. For instance, statistical analyses of Chrom3D models of human fibroblast genomes indicate that UV-induced DNA lesions are predominantly detected in LADs, suggesting greater UV-susceptibility of chromosomes at the nuclear periphery (Garcia-Nieto et al., 2017). Even more relevant for cancer, nearly 80% of genes mutated in melanomas are not only found in LADs but also statistically enriched at the nuclear periphery in 3D genome models, while genes not mutated in melanomas are more centrally located (Garcia-Nieto et al., 2017).

Corroborating these findings, 3D genome models generated from Hi-C and radial positional information of loci reveal a decrease in the frequency of single nucleotide polymorphisms from the nuclear periphery towards the nucleus center, especially of those associated with melanomas or lung cancer (Girelli et al., 2020). This is again consistent with the higher frequency of cancer-linked mutations in late-replicating LAD heterochromatin (Schuster-Bockler and Lehner, 2012; Liu et al., 2013; Morganello et al., 2016). In



contrast, loci implicated in gene fusions catalogued in The Cancer Genome Atlas are more centrally located than loci not involved in fusions; accordingly, the frequency of DNA double-strand breaks, which contribute the pathogenesis of gene fusions in cancers, also augments towards the nucleus center (Girelli et al., 2020). In another line of pathologies, altered lamin A/C-genome associations in nuclei from patients with a lipodystrophic laminopathy seem to occur preferentially in the nucleus center in 3D genome models of fibroblasts generated using public Hi-C data and control-vs. patient-specific lamin A/C ChIP-seq data (Paulsen et al., 2017).

These studies provide seminal examples of how restraint-based genome models may generate predictions on

consequences of pathological insults or mutations on genome integrity with a 3D perspective. Currently, these models cannot explain a pathology, but hypotheses generated from statistical analyses of modeled structures open the door to better designed studies aiming to target specific regions in a 3D nucleus space which would not be predicted from one-dimensional data.

Modeling to Enable New Wet-Lab Methods and Biological Insights on Chromatin Behavior

A powerful outcome of computational models of chromatin behavior is the opportunity to generate testable hypotheses on the physical properties of chromatin. A recent elegant example is the use of block copolymer models of chromatin to make predictions on the nature and dynamics of homotypic chromatin interactions occurring in microphase-separated compartment throughout the nucleus (Belaghal et al., 2021). Testing these properties interestingly required further developments of the Hi-C methodology (which maps chromosomal interactions genome-wide) to accommodate a liquid chromatin phase (Belaghal et al., 2021).

PERSPECTIVES

Considering Softness and Heterogeneity of the Nuclear Lamina

Despite their increasing complexity and power, chromatin models still ignore some information inherent to chromosome structure important for nuclear function, such as additional physical properties of chromatin. For example, chromatin domains can intermingle or partly invade the NL. So chromatin cannot simply be considered as a hard entity (non-penetrable beads in models). Instead, beads may be fitted with a soft permeable outer zone and an adjustable penetrability factor to enhance flexibility of the chromatin chain and better approximate chromosome compaction (Figure 5A). Similarly, a soft attraction potential may be introduced for interactions with a NL surface, a view justified by the void spaces penetrated by chromatin in the NL (Turgay et al., 2017). Thus, a NL surface should not necessarily be hard but be penetrable by polymer beads (Figure 5B).

Recent analyses of NL structure and organization (Nmezi et al., 2019; Turgay et al., 2017) suggest new options to improve models of chromatin-NL interactions. First, the distinct A- and B-type lamin networks of the NL, together with the identification of lamin A/C- and B-specific LADs (Forsberg et al., 2019) suggests that the strength of interaction potentials of chromatin with A- or B-type lamins could differentially be tuned. Second, the void volume of the NL could create space for binders mediating chromatin-NL interactions in block copolymer models, (Figure 5C). Binders, e.g., mimicking the lamin A-associated histone deacetylase HDAC3 (Demmerle et al., 2012), could also be introduced to simulate changes in chromatin states in LADs, such as those occurring in senescence (Chandra et al., 2012; Sadaie et al., 2013)

or cancer (Dawson and Kouzarides, 2012). Other binders might control the release of chromatin from the NL during differentiation, senescence, or in disease.

Modeling Interactions of the Nuclear Lamina With Euchromatin

Polymer models of chromatin folding at the NL in progeroid cells (Chiang et al., 2019) predict proximity of euchromatin to the NL only by tuning two parameters (see Figure 4C). This concept could be extended to model euchromatic and active LAD sub-domain, euchromatic regions dragged alongside heterochromatic LADs towards the NL, or associations of lamins with euchromatin in the nuclear interior. Locally fitting attraction potentials to these regions as a function of gene activity or epigenomic states should predict minimal conditions required to promote and maintain weaker NL-chromatin interactions. In this context, adding “binders” based on experimental evidence of factors involved in the modulation of chromatin-NL interactions, either as LADs or focal domains in LADs (e.g., CTCF) (van Schaik et al., 2021; Kaczmarczyk et al., 2022), should enable advances in our mechanistic understanding of these interactions. Modeling the behavior of a chromatin polymer with various thicknesses (Buckle et al., 2018) may also predict the dynamics of chromatin domains with varying compaction levels at the NL. By extension, it should also be possible to model lamin A interactions with euchromatin, which are modulated by histone acetylation (Ikegami et al., 2020).

Introducing Nuclear Envelope Perturbations in 3D Genome Models

Further developments of 3D genome modeling to yield mechanistic insights into changes in nuclear architecture linked to disease would also be beneficial. Evidence implicates lamin mutations in alterations in LADs and chromatin conformation, and nucleus size and shape are also affected in cancer cells (de Leeuw et al., 2018). Introducing perturbations in the shape of the nucleus shell in restraint-based models may enable inference of unsuspected features of higher-order chromatin architecture linked to disease or differentiation (Katiyar et al., 2019; Dickinson et al., 2022) (Figure 5D). Such more advanced models could also in principle be supplemented with binders mediating chromatin interactions with nuclear bodies.

Repetitive Elements in 3D Genome Models?

DNA repeats constitute more than half of the human genome and play a role in re-wiring epigenomes and gene expression programs in a variety of developmental and pathological conditions (Rebollo et al., 2012). Repeat elements are also frequently epigenetically altered in cancers (Dawson and Kouzarides, 2012). L1 elements (containing LINEs) are AT-rich, heterochromatic and enriched in LADs, whereas Alu repeats are more CG-rich and mainly found in euchromatic gene-rich A compartments. Accordingly, L1 and Alu repeats are relevant elements to consider in 3D genome models.

To our knowledge however, 3D models of chromatin have largely ignored DNA repeats because, 1) due to their repeat nature, repeat sequence reads are often discarded from analyses, 2) they are not relevant for the questions asked, or 3) they can simply be modeled as monomers (beads) alike any other chromatin domain. The latter is illustrated by the hidden inclusion of L1 repeats as LAD-associated topological domains (beads) in restraint-based whole-genome 3D models (Paulsen et al., 2017; Paulsen et al., 2018). Today however, repeats can in principle be explicitly included in 3D models as increasingly performant long-read sequencing technologies (De Bustos et al., 2016) and bioinformatics tools (Fernandes et al., 2020) provide more accurate estimates of their genomic localization. Their epigenetic states are also well characterized, and fluorescence *in situ* hybridization techniques allow their visualization in nuclei (Lu et al., 2021). Altogether, this information should be able to guide a phenomenological positioning of chromosome regions relative to a nuclear structure or boundary (e.g., peripheral positioning of L1-rich LADs) in simulation initiations, and validations of model predictions. It would also allow introduction of attraction potentials typical for heterochromatin (to cluster L1 elements) and of weaker potentials (to model Alu repeat aggregation). This view is supported by recent Hi-C and microscopy evidence of homotypic clustering of L1 and Alu repeats which compartmentalize the 3D genome (Falk et al., 2019; Lu et al., 2021).

Enhancers and 3D Genome-Wide Association Studies

Recent evidence indicates that the NL constrains enhancers at the nuclear periphery, within LADs (Robson et al., 2017; Czapiewski et al., 2022; Madsen-Østerbye et al., 2022) and between LADs (Smith et al., 2021). By releasing these elements from the NL, disruption of NL-chromatin associations in laminopathies (McCord et al., 2013; Perovanovic et al., 2016; Paulsen et al., 2017) or cancer (Lenain et al., 2017) may alter the 3D interaction

landscape of these elements in a manner reflected in genome-wide association studies (GWAS). GWAS typically link a genetic variant to a differentially expressed linearly proximal gene (an expression quantitative trait locus, or eQTL) using the nearest gene method. However, GWAS variants turn out to be located mainly outside genes, with only a minor fraction impacting nearby genes (Fadason et al., 2017; Mumbach et al., 2017; Fu et al., 2018). In a 3D space, variants likely affect more genes than projected and new eQTLs can be identified (Fadason et al., 2018; Buxton et al., 2019). Integration of 3D genomic perspectives, including LAD information, into GWAS studies may enhance identification of new genes and mechanisms underlying complex diseases, and in designing new treatments.

CONCLUSION

Combinations of more sophisticated computational approaches with rapidly evolving wet-lab technologies such as high-throughput genome editing (Akhtar et al., 2013), live chromatin imaging (Germier et al., 2017), high-throughput fluorescence *in situ* hybridization (Finn et al., 2019) and biophysical techniques (Keizer et al., 2021), will expectedly lead to a clearer understanding of altered genome organization being a cause or consequence of disease.

AUTHOR CONTRIBUTIONS

All authors listed have made a substantial, direct, and intellectual contribution to the work and approved it for publication.

FUNDING

Our work is supported by the University of Oslo, the Research Council of Norway, The Norwegian Cancer Society and South-East Health Norway.

REFERENCES

- Akhtar, W., de Jong, J., Pindyurin, A. V., Pagie, L., Meuleman, W., de Ridder, J., et al. (2013). Chromatin Position Effects Assayed by Thousands of Reporters Integrated in Parallel. *Cell* 154, 914–927. doi:10.1016/j.cell.2013.07.018
- Amiad-Pavlov, D., Lorber, D., Bajpai, G., Reuveny, A., Roncato, F., Alon, R., et al. (2021). Live Imaging of Chromatin Distribution Reveals Novel Principles of Nuclear Architecture and Chromatin Compartmentalization. *Sci. Adv.* 7, eabf6251. doi:10.1126/sciadv.abf6251
- Annunziatella, C., Chiariello, A. M., Esposito, A., Bianco, S., Fiorillo, L., and Nicodemi, M. (2018). Molecular Dynamics Simulations of the Strings and Binders Switch Model of Chromatin. *Methods* 142, 81–88. doi:10.1016/j.ymeth.2018.02.024
- Bajpai, G., Amiad Pavlov, D., Lorber, D., Volk, T., and Safran, S. (2021). Mesoscale Phase Separation of Chromatin in the Nucleus. *Elife* 10, e63976. doi:10.7554/eLife.63976
- Barbieri, M., Chotalia, M., Fraser, J., Lavitas, L.-M., Dostie, J., Pombo, A., et al. (2012). Complexity of Chromatin Folding Is Captured by the Strings and Binders Switch Model. *Proc. Natl. Acad. Sci. U.S.A.* 109, 16173–16178. doi:10.1073/pnas.1204799109
- Baù, D., and Marti-Renom, M. A. (2011). Structure Determination of Genomic Domains by Satisfaction of Spatial Restraints. *Chromosome Res.* 19, 25–35. doi:10.1007/s10577-010-9167-2
- Belaghzal, H., Borrmann, T., Stephens, A. D., Lafontaine, D. L., Venev, S. V., Weng, Z., et al. (2021). Liquid Chromatin Hi-C Characterizes Compartment-dependent Chromatin Interaction Dynamics. *Nat. Genet.* 53, 367–378. doi:10.1038/s41588-021-00784-4
- Briand, N., and Collas, P. (2020). Lamina-associated Domains: Peripheral Matters and Internal Affairs. *Genome Biol.* 21, 85. doi:10.1186/s13059-020-02003-5
- Briand, N., Guénant, A.-C., Jeziorowska, D., Shah, A., Mantecon, M., Capel, E., et al. (2018). The Lipodystrophic Hotspot Lamin A p.R482W Mutation Deregulates the Mesodermal Inducer T/Brachyury and Early Vascular Differentiation Gene Networks. *Hum. Mol. Genet.* 27, 1447–1459. doi:10.1093/hmg/ddy055
- Brueckner, L., Zhao, P. A., van Schaik, T., Leemans, C., Sima, J., Peric-Hupkes, D., et al. (2020). Local Rewiring of Genome-Nuclear Lamina Interactions by Transcription. *EMBO J.* 39, e103159. doi:10.15252/embj.2019103159

- Brunet, A., Destainville, N., and Collas, P. (2021). Physical Constraints in Polymer Modeling of Chromatin Associations with the Nuclear Periphery at Kilobase Scale. *Nucleus* 12, 6–20. doi:10.1080/19491034.2020.1868105
- Brunet, A., Forsberg, F., Fan, Q., Sæther, T., and Collas, P. (2019). Nuclear Lamin B1 Interactions with Chromatin during the Circadian Cycle Are Uncoupled from Periodic Gene Expression. *Front. Genet.* 10, 917. doi:10.3389/fgene.2019.00917
- Buchwalter, A., Kaneshiro, J. M., and Hetzer, M. W. (2019). Coaching from the Sidelines: the Nuclear Periphery in Genome Regulation. *Nat. Rev. Genet.* 20, 39–50. doi:10.1038/s41576-018-0063-5
- Buckle, A., Brackley, C. A., Boyle, S., Marenduzzo, D., and Gilbert, N. (2018). Polymer Simulations of Heteromorphic Chromatin Predict the 3D Folding of Complex Genomic Loci. *Mol. Cell* 72, 786–797. doi:10.1016/j.molcel.2018.09.016
- Burke, B., and Stewart, C. L. (2013). The Nuclear Lamins: Flexibility in Function. *Nat. Rev. Mol. Cell Biol.* 14, 13–24. doi:10.1038/nrm3488
- Buxton, D. S., Batten, D. J., Crofts, J. J., and Chuzhanova, N. (2019). Predicting Novel Genomic Regions Linked to Genetic Disorders Using GWAS and Chromosome Conformation Data - a Case Study of Schizophrenia. *Sci. Rep.* 9, 17940. doi:10.1038/s41598-019-54514-2
- Cardozo Gizzi, A. M. (2021). A Shift in Paradigms: Spatial Genomics Approaches to Reveal Single-Cell Principles of Genome Organization. *Front. Genet.* 12, 780822. doi:10.3389/fgene.2021.780822
- Chandra, T., Kirschner, K., Thuret, J.-Y., Pope, B. D., Ryba, T., Newman, S., et al. (2012). Independence of Repressive Histone Marks and Chromatin Compaction during Senescent Heterochromatic Layer Formation. *Mol. Cell* 47, 203–214. doi:10.1016/j.molcel.2012.06.010
- Cheng, R. R., Contessoto, V. G., Lieberman Aiden, E., Wolynes, P. G., Di Pierro, M., and Onuchic, J. N. (2020). Exploring Chromosomal Structural Heterogeneity across Multiple Cell Lines. *Elife* 9, e60312. doi:10.7554/eLife.60312
- Chiang, M., Michieletto, D., Brackley, C. A., Rattanaivirotkul, N., Mohammed, H., Marenduzzo, D., et al. (2019). Polymer Modeling Predicts Chromosome Reorganization in Senescence. *Cell Rep.* 28, 3212–3223. doi:10.1016/j.celrep.2019.08.045
- Chiariello, A. M., Annunziatella, C., Bianco, S., Esposito, A., and Nicodemi, M. (2016). Polymer Physics of Chromosome Large-Scale 3D Organisation. *Sci. Rep.* 6, 29775. doi:10.1038/srep29775
- Cook, P. R., and Marenduzzo, D. (2009). Entropic Organization of Interphase Chromosomes. *J. Cell Biol.* 186, 825–834. doi:10.1083/jcb.200903083
- Czapiewski, R., Batrakou, D. G., de las Heras, J. I., Carter, R. N., Sivakumar, A., Sliwinski, M., et al. (2022). Genomic Loci Mispositioning in Tmem120a Knockout Mice Yields Latent Lipodystrophy. *Nat. Commun.* 13, 321. doi:10.1038/s41467-021-27869-2
- Dawson, M. A., and Kouzarides, T. (2012). Cancer Epigenetics: from Mechanism to Therapy. *Cell* 150, 12–27. doi:10.1016/j.cell.2012.06.013
- De Bustos, A., Cuadrado, A., and Jouve, N. (2016). Sequencing of Long Stretches of Repetitive DNA. *Sci. Rep.* 6, 36665. doi:10.1038/srep36665
- de Leeuw, R., Gruenbaum, Y., and Medalia, O. (2018). Nuclear Lamins: Thin Filaments with Major Functions. *Trends Cell Biol.* 28, 34–45. doi:10.1016/j.tcb.2017.08.004
- Demmerle, J., Koch, A. J., and Holaska, J. M. (2012). The Nuclear Envelope Protein Emerin Binds Directly to Histone Deacetylase 3 (HDAC3) and Activates HDAC3 Activity. *J. Biol. Chem.* 287, 22080–22088. doi:10.1074/jbc.m111.325308
- Di Stefano, M., Paulsen, J., Lien, T. G., Hovig, E., and Micheletti, C. (2016). Hi-C-constrained Physical Models of Human Chromosomes Recover Functionally-Related Properties of Genome Organization. *Sci. Rep.* 6, 35985. doi:10.1038/srep35985
- Dickinson, R. B., Katiyar, A., Dubell, C. R., and Lele, T. P. (2022). Viscous Shaping of the Compliant Cell Nucleus. *Appl. Bioeng.* 6, 010901. doi:10.1063/5.0071652
- Duan, Z., Andronescu, M., Schutz, K., McIlwain, S., Kim, Y. J., Lee, C., et al. (2010). A Three-Dimensional Model of the Yeast Genome. *Nature* 465, 363–367. doi:10.1038/nature08973
- Evangelisti, C., Rusciano, I., Mongiorgi, S., Ramazzotti, G., Lattanzi, G., Manzoli, L., et al. (2022). The Wide and Growing Range of Lamin B-Related Diseases: from Laminopathies to Cancer. *Cell. Mol. Life Sci.* 79, 126. doi:10.1007/s00018-021-04084-2
- Fadason, T., Ekblad, C., Ingram, J. R., Schierding, W. S., and O'Sullivan, J. M. (2017). Physical Interactions and Expression Quantitative Traits Loci Identify Regulatory Connections for Obesity and Type 2 Diabetes Associated SNPs. *Front. Genet.* 8, 150. doi:10.3389/fgene.2017.00150
- Fadason, T., Schierding, W., Lumley, T., and O'Sullivan, J. M. (2018). Chromatin Interactions and Expression Quantitative Trait Loci Reveal Genetic Drivers of Multimorbidities. *Nat. Commun.* 9, 5198. doi:10.1038/s41467-018-07692-y
- Falk, M., Feodorova, Y., Naumova, N., Imakaev, M., Lajoie, B. R., Leonhardt, H., et al. (2019). Heterochromatin Drives Compartmentalization of Inverted and Conventional Nuclei. *Nature* 570, 395–399. doi:10.1038/s41586-019-1275-3
- Fernandes, J. D., Zamudio-Hurtado, A., Clawson, H., Kent, W. J., Haussler, D., Salama, S. R., et al. (2020). The UCSC Repeat Browser Allows Discovery and Visualization of Evolutionary Conflict across Repeat Families. *Mob. DNA* 11, 13. doi:10.1186/s13100-020-00208-w
- Finn, E. H., Pegoraro, G., Brandão, H. B., Valton, A.-L., Oomen, M. E., Dekker, J., et al. (2019). Extensive Heterogeneity and Intrinsic Variation in Spatial Genome Organization. *Cell* 176, 1502–1515. doi:10.1016/j.cell.2019.01.020
- Fiorillo, L., Bianco, S., Esposito, A., Conte, M., Sciarretta, R., Musella, F., et al. (2019). A Modern Challenge of Polymer Physics: Novel Ways to Study, Interpret, and Reconstruct Chromatin Structure. *WIREs Comput. Mol. Sci.*, e1454. doi:10.1002/wcms.1454
- Forsberg, F., Brunet, A., Ali, T. M. L., and Collas, P. (2019). Interplay of Lamin A and Lamin B LADs on the Radial Positioning of Chromatin. *Nucleus* 10, 7–20. doi:10.1080/19491034.2019.1570810
- Fu, Y., Tessner, K. L., Li, C., and Gaffney, P. M. (2018). From Association to Mechanism in Complex Disease Genetics: the Role of the 3D Genome. *Arthritis Res. Ther.* 20, 216. doi:10.1186/s13075-018-1721-x
- García-Nieto, P. E., Schwartz, E. K., King, D. A., Paulsen, J., Collas, P., Herrera, R. E., et al. (2017). Carcinogen Susceptibility Is Regulated by Genome Architecture and Predicts Cancer Mutagenesis. *EMBO J.* 36, 2829–2843. doi:10.15252/embj.201796717
- Germier, T., Kocanova, S., Walther, N., Bancaud, A., Shaban, H. A., Sellou, H., et al. (2017). Real-Time Imaging of a Single Gene Reveals Transcription-Initiated Local Confinement. *Biophysical J.* 113, 1383–1394. doi:10.1016/j.bpj.2017.08.014
- Gesson, K., Rescheneder, P., Skoruppa, M. P., von Haeseler, A., Dechat, T., and Foissner, R. (2016). A-type Lamins Bind Both Hetero- and Euchromatin, the Latter Being Regulated by Lamina-Associated Polypeptide 2 Alpha. *Genome Res.* 26, 462–473. doi:10.1101/gr.196220.115
- Girelli, G., Custodio, J., Kallas, T., Agostini, F., Wernersson, E., Spanjaard, B., et al. (2020). GPSeq Reveals the Radial Organization of Chromatin in the Cell Nucleus. *Nat. Biotechnol.* 38, 1184–1193. doi:10.1038/s41587-020-0519-y
- Guelen, L., Pagie, L., Brasset, E., Meuleman, W., Faza, M. B., Talhout, W., et al. (2008). Domain Organization of Human Chromosomes Revealed by Mapping of Nuclear Lamina Interactions. *Nature* 453, 948–951. doi:10.1038/nature06947
- Harr, J. C., Luperchio, T. R., Wong, K., Cohen, E., Wheelan, S. J., and Reddy, K. L. (2015). Directed Targeting of Chromatin to the Nuclear Lamina Is Mediated by Chromatin State and A-type Lamins. *J. Cell Biol.* 208, 33–52. doi:10.1083/jcb.201405110
- Herman, A. B., Anerillas, C., Harris, S. C., Munk, R., Martindale, J. L., Yang, X., et al. (2021). Reduction of Lamin B Receptor Levels by miR-340-5p Disrupts Chromatin, Promotes Cell Senescence and Enhances Senolysis. *Nucleic Acids Res.* 49, 7389–7405. doi:10.1093/nar/gkab538
- Hu, M., Deng, K., Qin, Z., Dixon, J., Selvaraj, S., Fang, J., et al. (2013). Bayesian Inference of Spatial Organizations of Chromosomes. *PLoS Comput. Biol.* 9, e1002893. doi:10.1371/journal.pcbi.1002893
- Ikegami, K., Secchia, S., Almakki, O., Lieb, J. D., and Moskowitz, I. P. (2020). Phosphorylated Lamin A/C in the Nuclear Interior Binds Active Enhancers Associated with Abnormal Transcription in Progeria. *Dev. Cell* 52, 699–713. doi:10.1016/j.devcel.2020.02.011
- Jerkovic, I., and Cavalli, G. (2021). Understanding 3D Genome Organization by Multidisciplinary Methods. *Nat. Rev. Mol. Cell Biol.* 22, 511–528. doi:10.1038/s41580-021-00362-w
- Jost, D., Carrivain, P., Cavalli, G., and Vaillant, C. (2014). Modeling Epigenome Folding: Formation and Dynamics of Topologically Associated Chromatin Domains. *Nucleic Acids Res.* 42, 9553–9561. doi:10.1093/nar/gku698

- Kaczmarczyk, L. S., Levi, N., Segal, T., Salmon-Divon, M., and Gerlitz, G. (2022). CTCF Supports Preferentially Short Lamina-Associated Domains. *Chromosome Res.* 30, 123–136. doi:10.1007/s10577-022-09686-5
- Kalhor, R., Tjong, H., Jayathilaka, N., Alber, F., and Chen, L. (2012). Genome Architectures Revealed by Tethered Chromosome Conformation Capture and Population-Based Modeling. *Nat. Biotechnol.* 30, 90–98. doi:10.1038/nbt.2057
- Katiyar, A., Tocco, V. J., Li, Y., Aggarwal, V., Tamashunas, A. C., Dickinson, R. B., et al. (2019). Nuclear Size Changes Caused by Local Motion of Cell Boundaries Unfold the Nuclear Lamina and Dilate Chromatin and Intracellular Bodies. *Soft Matter* 15, 9310–9317. doi:10.1039/c9sm01666j
- Keizer, V. I. P., Grosse-Holz, S., Wöringer, M., Zambon, L., Aizel, K., Bongaerts, M., et al. (2021). Live-cell Micromanipulation of a Genomic Locus Reveals Interphase Chromatin Mechanics. *bioRxiv*. doi:10.1101/2021.04.20.439763
- Keough, K. C., Shah, P. P., Gjoni, K., Santini, G. T., Wickramasinghe, N. M., Dundes, C. E., et al. (2020). An Atlas of Lamina-Associated Chromatin across Twelve Human Cell Types Reveals an Intermediate Chromatin Subtype. *bioRxiv*. doi:10.1101/2020.07.23.218768
- Kind, J., Pagie, L., de Vries, S. S., Nahidiazar, L., Dey, S. S., Bienko, M., et al. (2015). Genome-wide Maps of Nuclear Lamina Interactions in Single Human Cells. *Cell* 163, 134–147. doi:10.1016/j.cell.2015.08.040
- Kittisopikul, M., Shimi, T., Tatli, M., Tran, J. R., Zheng, Y., Medalia, O., et al. (2021). Computational Analyses Reveal Spatial Relationships between Nuclear Pore Complexes and Specific Lamins. *J. Cell Biol.* 220, e202007082. doi:10.1083/jcb.202007082
- Köhler, F., Bormann, F., Raddatz, G., Gutekunst, J., Corless, S., Musch, T., et al. (2020). Epigenetic Deregulation of Lamina-Associated Domains in Hutchinson-Gilford Progeria Syndrome. *Genome Med.* 12, 46. doi:10.1186/s13073-020-00749-y
- Kos, P. I., Galitsyna, A. A., Ulianov, S. V., Gelfand, M. S., Razin, S. V., and Chertovich, A. V. (2021). Perspectives for the Reconstruction of 3D Chromatin Conformation Using Single Cell Hi-C Data. *PLoS Comput. Biol.* 17, e1009546. doi:10.1371/journal.pcbi.1009546
- Le Dily, F., Batü, D., Pohl, A., Vicent, G. P., Serra, F., Soronellas, D., et al. (2014). Distinct Structural Transitions of Chromatin Topological Domains Correlate with Coordinated Hormone-Induced Gene Regulation. *Genes Dev.* 28, 2151–2162. doi:10.1101/gad.241422.114
- Leemans, C., van der Zwalm, M. C. H., Brueckner, L., Comoglio, F., van Schaik, T., Pagie, L., et al. (2019). Promoter-Intrinsic and Local Chromatin Features Determine Gene Repression in LADs. *Cell* 177, 852–864. doi:10.1016/j.cell.2019.03.009
- Lenain, C., de Graaf, C. A., Pagie, L., Visser, N. L., de Haas, M., de Vries, S. S., et al. (2017). Massive Reshaping of Genome-Nuclear Lamina Interactions during Oncogene-Induced Senescence. *Genome Res.* 27, 1634–1644. doi:10.1101/gr.225763.117
- Lesne, A., Riposo, J., Roger, P., Cournac, A., and Mozziconacci, J. (2014). 3D Genome Reconstruction from Chromosomal Contacts. *Nat. Methods* 11, 1141–1143. doi:10.1038/nmeth.3104
- Li, Q., Tjong, H., Li, X., Gong, K., Zhou, X. J., Chiolo, I., et al. (2017). The Three-Dimensional Genome Organization of *Drosophila melanogaster* through Data Integration. *Genome Biol.* 18, 145. doi:10.1186/s13059-017-1264-5
- Liu, L., De, S., and Michor, F. (2013). DNA Replication Timing and Higher-Order Nuclear Organization Determine Single-Nucleotide Substitution Patterns in Cancer Genomes. *Nat. Commun.* 4, 1502. doi:10.1038/ncomms2502
- Liu, S. Y., and Ikegami, K. (2020). Nuclear Lamin Phosphorylation: an Emerging Role in Gene Regulation and Pathogenesis of Laminopathies. *Nucleus* 11, 299–314. doi:10.1080/19491034.2020.1832734
- Lu, J. Y., Chang, L., Li, T., Wang, T., Yin, Y., Zhan, G., et al. (2021). Homotypic Clustering of L1 and B1/Alu Repeats Compartmentalizes the 3D Genome. *Cell Res.* 31, 613–630. doi:10.1038/s41422-020-00466-6
- Lund, E. G., Duband-Goulet, I., Oldenburg, A., Buendia, B., and Collas, P. (2015). Distinct Features of Lamin A-Interacting Chromatin Domains Mapped by ChIP-Sequencing from Sonicated or Micrococcal Nuclease-Digested Chromatin. *Nucleus* 6, 30–39. doi:10.4161/19491034.2014.990855
- Lupianez, D. G., Spielmann, M., and Mundlos, S. (2016). Breaking TADs: How Alterations of Chromatin Domains Result in Disease. *Trends Genet.* 32, 225–237. doi:10.1016/j.tig.2016.01.003
- Madsen, J. G. S., Madsen, M. S., Rauch, A., Traynor, S., Van Hauwaert, E. L., Haakonsson, A. K., et al. (2020). Highly Interconnected Enhancer Communities Control Lineage-Determining Genes in Human Mesenchymal Stem Cells. *Nat. Genet.* 52, 1227–1238. doi:10.1038/s41588-020-0709-z
- Madsen-Østerbye, J., Abdelhalim, M., Baudement, M. O., and Collas, P. (2022). Local Euchromatin Enrichment in Lamina-Associated Domains Anticipates Their Repositioning in the Adipogenic Lineage. *Genome Biol.* 23, 91. doi:10.1186/s13059-022-02662-6
- Manzo, S. G., Dauban, L., and van Steensel, B. (2022). Lamina-associated Domains: Tethers and Looseners. *Curr. Opin. Cell Biol.* 74, 80–87. doi:10.1016/j.ccb.2022.01.004
- Marini, B., Kertesz-Farkas, A., Ali, H., Lucic, B., Lisek, K., Manganaro, L., et al. (2015). Nuclear Architecture Dictates HIV-1 Integration Site Selection. *Nature* 521, 227–231. doi:10.1038/nature14226
- Marti-Renom, M. A., Almouzni, G., Bickmore, W. A., Bystricky, K., Cavalli, G., Fraser, P., et al. (2018). Challenges and Guidelines toward 4D Nucleome Data and Model Standards. *Nat. Genet.* 50, 1352–1358. doi:10.1038/s41588-018-0236-3
- McCord, R. P., Nazario-Toole, A., Zhang, H., Chines, P. S., Zhan, Y., Erdos, M. R., et al. (2013). Correlated Alterations in Genome Organization, Histone Methylation, and DNA-Lamin A/C Interactions in Hutchinson-Gilford Progeria Syndrome. *Genome Res.* 23, 260–269. doi:10.1101/gr.138032.112
- Meluzzi, D., and Arya, G. (2013). Recovering Ensembles of Chromatin Conformations from Contact Probabilities. *Nucleic Acids Res.* 41, 63–75. doi:10.1093/nar/gks1029
- Meuleman, W., Peric-Hupkes, D., Kind, J., Beaudry, J.-B., Pagie, L., Kellis, M., et al. (2013). Constitutive Nuclear Lamina-Genome Interactions Are Highly Conserved and Associated with A/T-rich Sequence. *Genome Res.* 23, 270–280. doi:10.1101/gr.141028.112
- Morganella, S., Alexandrov, L. B., Glodzik, D., Zou, X., Davies, H., Staaf, J., et al. (2016). The Topography of Mutational Processes in Breast Cancer Genomes. *Nat. Commun.* 7, 11383. doi:10.1038/ncomms11383
- Mumbach, M. R., Satpathy, A. T., Boyle, E. A., Dai, C., Gowen, B. G., Cho, S. W., et al. (2017). Enhancer Connectome in Primary Human Cells Identifies Target Genes of Disease-Associated DNA Elements. *Nat. Genet.* 49, 1602–1612. doi:10.1038/ng.3963
- Nagano, T., Lubling, Y., Stevens, T. J., Schoenfelder, S., Yaffe, E., Dean, W., et al. (2013). Single-cell Hi-C Reveals Cell-To-Cell Variability in Chromosome Structure. *Nature* 502, 59–64. doi:10.1038/nature12593
- Nmezi, B., Xu, J., Fu, R., Armiger, T. J., Rodriguez-Bey, G., Powell, J. S., et al. (2019). Concentric Organization of A- and B-type Lamins Predicts Their Distinct Roles in the Spatial Organization and Stability of the Nuclear Lamina. *Proc. Natl. Acad. Sci. U.S.A.* 116, 4307–4315. doi:10.1073/pnas.1810070116
- Oliveira Junior, A. B., Contessoto, V. G., Mello, M. F., and Onuchic, J. N. (2021). A Scalable Computational Approach for Simulating Complexes of Multiple Chromosomes. *J. Mol. Biol.* 433, 166700. doi:10.1016/j.jmb.2020.10.034
- Parmar, J. J., Wöringer, M., and Zimmer, C. (2019). How the Genome Folds: The Biophysics of Four-Dimensional Chromatin Organization. *Annu. Rev. Biophys.* 48, 231–253. doi:10.1146/annurev-biophys-052118-115638
- Pascual-Reguant, L., Blanco, E., Galan, S., Le Dily, F., Cuartero, Y., Serra-Bardenys, G., et al. (2018). Lamin B1 Mapping Reveals the Existence of Dynamic and Functional Euchromatin Lamin B1 Domains. *Nat. Commun.* 9, 3420. doi:10.1038/s41467-018-05912-z
- Paulsen, J., Liyakat Ali, T. M., and Collas, P. (2018). Computational 3D Genome Modeling Using Chrom3D. *Nat. Protoc.* 13, 1137–1152. doi:10.1038/nprot.2018.009
- Paulsen, J., Liyakat Ali, T. M., Nekrasov, M., Delbarre, E., Baudement, M.-O., Kurscheid, S., et al. (2019). Long-range Interactions between Topologically Associating Domains Shape the Four-Dimensional Genome during Differentiation. *Nat. Genet.* 51, 835–843. doi:10.1038/s41588-019-0392-0
- Paulsen, J., Sekelja, M., Oldenburg, A. R., Barateau, A., Briand, N., Delbarre, E., et al. (2017). Chrom3D: Three-Dimensional Genome Modeling from Hi-C and Nuclear Lamin-Genome Contacts. *Genome Biol.* 18, 21. doi:10.1186/s13059-016-1146-2
- Peric-Hupkes, D., Meuleman, W., Pagie, L., Bruggeman, S. W. M., Solovei, I., Brugman, W., et al. (2010). Molecular Maps of the Reorganization of Genome-Nuclear Lamina Interactions during Differentiation. *Mol. Cell* 38, 603–613. doi:10.1016/j.molcel.2010.03.016

- Perovanovic, J., Dell'Orso, S., Gnoci, V. F., Jaiswal, J. K., Sartorelli, V., Vigouroux, C., et al. (2016). Laminopathies Disrupt Epigenomic Developmental Programs and Cell Fate. *Sci. Transl. Med.* 8, 335ra58. doi:10.1126/scitranslmed.aad4991
- Pouokam, M., Cruz, B., Burgess, S., Segal, M. R., Vazquez, M., and Arsuaga, J. (2019). The Rab1 Configuration Limits Topological Entanglement of Chromosomes in Budding Yeast. *Sci. Rep.* 9, 6795. doi:10.1038/s41598-019-42967-4
- Rebollo, R., Romanish, M. T., and Mager, D. L. (2012). Transposable Elements: an Abundant and Natural Source of Regulatory Sequences for Host Genes. *Annu. Rev. Genet.* 46, 21–42. doi:10.1146/annurev-genet-110711-155621
- Reddy, K. L., Zullo, J. M., Bertolino, E., and Singh, H. (2008). Transcriptional Repression Mediated by Repositioning of Genes to the Nuclear Lamina. *Nature* 452, 243–247. doi:10.1038/nature06727
- Robson, M. I., de Las Heras, J. I., Czapiewski, R., Sivakumar, A., Kerr, A. R. W., and Schirmer, E. C. (2017). Constrained Release of Lamina-Associated Enhancers and Genes from the Nuclear Envelope during T-Cell Activation Facilitates Their Association in Chromosome Compartments. *Genome Res.* 27, 1126–1138. doi:10.1101/gr.212308.116
- Robson, M. I., de las Heras, J. I., Czapiewski, R., Lê Thành, P., Booth, D. G., Kelly, D. A., et al. (2016). Tissue-Specific Gene Repositioning by Muscle Nuclear Membrane Proteins Enhances Repression of Critical Developmental Genes during Myogenesis. *Mol. Cell* 62, 834–847. doi:10.1016/j.molcel.2016.04.035
- Rønningen, T., Shah, A., Oldenburg, A. R., Vekterud, K., Delbarre, E., Moskaug, J. Ø., et al. (2015). Prepatterning of Differentiation-Driven Nuclear Lamin A/C-associated Chromatin Domains by GlcNAcylated Histone H2B. *Genome Res.* 25, 1825–1835. doi:10.1101/gr.193748.115
- Rowley, M. J., and Corces, V. G. (2018). Organizational Principles of 3D Genome Architecture. *Nat. Rev. Genet.* 19, 789–800. doi:10.1038/s41576-018-0060-8
- Sadaie, M., Salama, R., Carroll, T., Tomimatsu, K., Chandra, T., Young, A. R. J., et al. (2013). Redistribution of the Lamin B1 Genomic Binding Profile Affects Rearrangement of Heterochromatic Domains and SAHF Formation during Senescence. *Genes Dev.* 27, 1800–1808. doi:10.1101/gad.217281.113
- Sapra, K. T., Qin, Z., Dubrovsky-Gaupp, A., Aebi, U., Müller, D. J., Buehler, M. J., et al. (2020). Nonlinear Mechanics of Lamin Filaments and the Meshwork Topology Build an Emergent Nuclear Lamina. *Nat. Commun.* 11, 6205. doi:10.1038/s41467-020-20049-8
- Sati, S., Bonev, B., Szabo, Q., Jost, D., Bensadoun, P., Serra, F., et al. (2020). 4D Genome Rewiring during Oncogene-Induced and Replicative Senescence. *Mol. Cell* 78, 522–538. doi:10.1016/j.molcel.2020.03.007
- Sawh, A. N., Shafer, M. E. R., Su, J.-H., Zhuang, X., Wang, S., and Mango, S. E. (2020). Lamina-Dependent Stretching and Unconventional Chromosome Compartments in Early *C. elegans* Embryos. *Mol. Cell* 78, 96–111. e116. doi:10.1016/j.molcel.2020.02.006
- Schuster-Böckler, B., and Lehner, B. (2012). Chromatin Organization Is a Major Influence on Regional Mutation Rates in Human Cancer Cells. *Nature* 488, 504–507. doi:10.1038/nature11273
- Sebestyén, E., Marullo, F., Lucini, F., Petrini, C., Bianchi, A., Valsoni, S., et al. (2020). SAMMY-seq Reveals Early Alteration of Heterochromatin and Deregulation of Bivalent Genes in Hutchinson-Gilford Progeria Syndrome. *Nat. Commun.* 11, 6274. doi:10.1038/s41467-020-20048-9
- Shah, P. P., Donahue, G., Otte, G. L., Capell, B. C., Nelson, D. M., Cao, K., et al. (2013). Lamin B1 Depletion in Senescent Cells Triggers Large-Scale Changes in Gene Expression and the Chromatin Landscape. *Genes Dev.* 27, 1787–1799. doi:10.1101/gad.223834.113
- Shimi, T., Kittisopikul, M., Tran, J., Goldman, A. E., Adam, S. A., Zheng, Y., et al. (2015). Structural Organization of Nuclear Lamins A, C, B1, and B2 Revealed by Superresolution Microscopy. *MBoC* 26, 4075–4086. doi:10.1091/mbc.e15-07-0461
- Shimi, T., Pflieger, K., Kojima, S.-i., Pack, C.-G., Solovei, I., Goldman, A. E., et al. (2008). The A- and B-type Nuclear Lamin Networks: Microdomains Involved in Chromatin Organization and Transcription. *Genes Dev.* 22, 3409–3421. doi:10.1101/gad.1735208
- Shin, J.-Y., and Worman, H. J. (2022). Molecular Pathology of Laminopathies. *Annu. Rev. Pathol. Mech. Dis.* 17, 159–180. doi:10.1146/annurev-pathol-042220-034240
- Shumaker, D. K., Dechat, T., Kohlmaier, A., Adam, S. A., Bozovsky, M. R., Erdos, M. R., et al. (2006). Mutant Nuclear Lamin A Leads to Progressive Alterations of Epigenetic Control in Premature Aging. *Proc. Natl. Acad. Sci. U.S.A.* 103, 8703–8708. doi:10.1073/pnas.0602569103
- Siersbæk, R., Madsen, J. G. S., Javierre, B. M., Nielsen, R., Bagge, E. K., Cairns, J., et al. (2017). Dynamic Rewiring of Promoter-Anchored Chromatin Loops during Adipocyte Differentiation. *Mol. Cell* 66, 420–e5. doi:10.1016/j.molcel.2017.04.010
- Smith, C. L., Poleshko, A., and Epstein, J. A. (2021). The Nuclear Periphery Is a Scaffold for Tissue-specific Enhancers. *Nucleic Acids Res.* 49, 6181–6195. doi:10.1093/nar/gkab392
- Solovei, I., Wang, A. S., Thanisch, K., Schmidt, C. S., Krebs, S., Zwerger, M., et al. (2013). LBR and Lamin A/C Sequentially Tether Peripheral Heterochromatin and Inversely Regulate Differentiation. *Cell* 152, 584–598. doi:10.1016/j.cell.2013.01.009
- Szalaj, P., Tang, Z., Michalski, P., Pietal, M. J., Luo, M. J., Sadowski, O. J., et al. (2016). An Integrated 3-Dimensional Genome Modeling Engine for Data-Driven Simulation of Spatial Genome Organization. *Genome Res.* 26, 1697–1709. doi:10.1101/gr.205062.116
- Tenga, R., and Medalia, O. (2020). Structure and Unique Mechanical Aspects of Nuclear Lamin Filaments. *Curr. Opin. Struct. Biol.* 64, 152–159. doi:10.1016/j.sbi.2020.06.017
- Tjong, H., Li, W., Kalhor, R., Dai, C., Hao, S., Gong, K., et al. (2016). Population-based 3D Genome Structure Analysis Reveals Driving Forces in Spatial Genome Organization. *Proc. Natl. Acad. Sci. U. S. A.* 113, E1663–E1672. doi:10.1073/pnas.1512577113
- Tjong, H., Gong, K., Chen, L., and Alber, F. (2012). Physical Tethering and Volume Exclusion Determine Higher-Order Genome Organization in Budding Yeast. *Genome Res.* 22, 1295–1305. doi:10.1101/gr.129437.111
- Tortora, M. M., Salari, H., and Jost, D. (2020). Chromosome Dynamics during Interphase: a Biophysical Perspective. *Curr. Opin. Genet. Dev.* 61, 37–43. doi:10.1016/j.gde.2020.03.001
- Turgay, Y., Eibauer, M., Goldman, A. E., Shimi, T., Khayat, M., Ben-Harush, K., et al. (2017). The Molecular Architecture of Lamins in Somatic Cells. *Nature* 543, 261–264. doi:10.1038/nature21382
- Ulianov, S. V., Doronin, S. A., Khrameeva, E. E., Kos, P. I., Luzhin, A. V., Starikov, S. S., et al. (2019). Nuclear Lamina Integrity Is Required for Proper Spatial Organization of Chromatin in *Drosophila*. *Nat. Commun.* 10, 1176. doi:10.1038/s41467-019-09185-y
- van Schaik, T., Liu, N. Q., Manzo, S. G., Peric-Hupkes, D., de Wit, E., and van Steensel, B. (2021). CTCF and Cohesin Promote Focal Detachment of DNA from the Nuclear Lamina. *bioRxiv* 13, 460079. doi:10.1101/2021.1109.1113.460079
- Wlasnowolski, M., Sadowski, M., Czarnota, T., Jodkowska, K., Szalaj, P., Tang, Z., et al. (2020). 3D-GNOME 2.0: a Three-Dimensional Genome Modeling Engine for Predicting Structural Variation-Driven Alterations of Chromatin Spatial Structure in the Human Genome. *Nucleic Acids Res.* 48, W170–W176. doi:10.1093/nar/gkaa388
- Wu, F., and Yao, J. (2017). Identifying Novel Transcriptional and Epigenetic Features of Nuclear Lamina-Associated Genes. *Sci. Rep.* 7, 100. doi:10.1038/s41598-017-00176-x
- Zhang, Z., Li, G., Toh, K.-C., and Sung, W.-K. (2013). 3D Chromosome Modeling with Semi-definite Programming and Hi-C Data. *J. Comput. Biol.* 20, 831–846. doi:10.1089/cmb.2013.0076
- Zhu, Y., Gong, K., Denholtz, M., Chandra, V., Kamps, M. P., Alber, F., et al. (2017). Comprehensive Characterization of Neutrophil Genome Topology. *Genes Dev.* 31, 141–153. doi:10.1101/gad.293910.116
- Zou, C., Zhang, Y., and Ouyang, Z. (2016). HSA: Integrating Multi-Track Hi-C Data for Genome-Scale Reconstruction of 3D Chromatin Structure. *Genome Biol.* 17, 40. doi:10.1186/s13059-016-0896-1

Conflict of Interest: The authors declare that the research was conducted in the absence of any commercial or financial relationships that could be construed as a potential conflict of interest.

Publisher's Note: All claims expressed in this article are solely those of the authors and do not necessarily represent those of their affiliated organizations, or those of the publisher, the editors and the reviewers. Any product that may be evaluated in this article, or claim that may be made by its manufacturer, is not guaranteed or endorsed by the publisher.

Copyright © 2022 Madsen-Østerbye, Bellanger, Galigniana and Collas. This is an open-access article distributed under the terms of the Creative Commons Attribution License (CC BY). The use, distribution or reproduction in other forums is permitted, provided the original author(s) and the copyright owner(s) are credited and that the original publication in this journal is cited, in accordance with accepted academic practice. No use, distribution or reproduction is permitted which does not comply with these terms.



OPEN ACCESS

EDITED BY

Eric C. Schirmer,
University of Edinburgh,
United Kingdom

REVIEWED BY

Giovanna Lattanzi,
Consiglio Nazionale delle Ricerche
(Bologna), Italy
Craig Peterson,
University of Massachusetts Medical
School, United States

*CORRESPONDENCE

Yamini Dalal,
dalaly@mail.nih.gov

SPECIALTY SECTION

This article was submitted to Nuclear
Organization and Dynamics,
a section of the journal
Frontiers in Cell and Developmental
Biology

RECEIVED 13 May 2022

ACCEPTED 04 July 2022

PUBLISHED 01 August 2022

CITATION

Sikder S, Arunkumar G, Melters DP and
Dalal Y (2022), Breaking the aging
epigenetic barrier.
Front. Cell Dev. Biol. 10:943519.
doi: 10.3389/fcell.2022.943519

COPYRIGHT

© 2022 Sikder, Arunkumar, Melters and
Dalal. This is an open-access article
distributed under the terms of the
[Creative Commons Attribution License](#)
(CC BY). The use, distribution or
reproduction in other forums is
permitted, provided the original
author(s) and the copyright owner(s) are
credited and that the original
publication in this journal is cited, in
accordance with accepted academic
practice. No use, distribution or
reproduction is permitted which does
not comply with these terms.

Breaking the aging epigenetic barrier

Sweta Sikder, Ganesan Arunkumar, Daniël P. Melters and
Yamini Dalal*

Chromatin Structure and Epigenetic Mechanisms, Laboratory of Receptor Biology and Gene
Expression, Center for Cancer Research, NCI, NIH, Bethesda, MD, United States

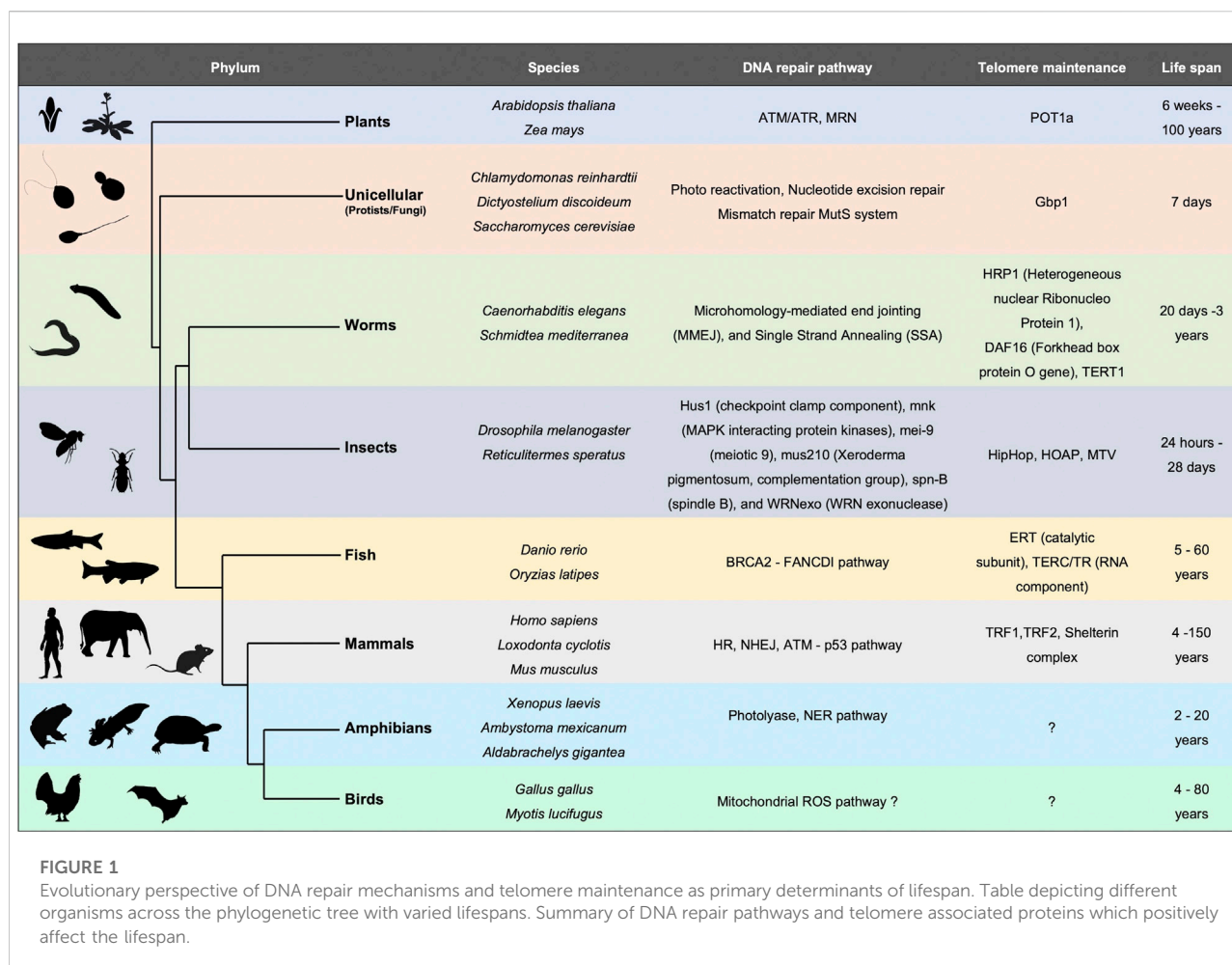
Aging is an inexorable event occurring universally for all organisms characterized by the progressive loss of cell function. However, less is known about the key events occurring inside the nucleus in the process of aging. The advent of chromosome capture techniques and extensive modern sequencing technologies have illuminated a rather dynamic structure of chromatin inside the nucleus. As cells advance along their life cycle, chromatin condensation states alter which leads to a different epigenetic landscape, correlated with modified gene expression. The exact factors mediating these changes in the chromatin structure and function remain elusive in the context of aging cells. The accumulation of DNA damage, reactive oxygen species and loss of genomic integrity as cells cease to divide can contribute to a tumor stimulating environment. In this review, we focus on genomic and epigenomic changes occurring in an aged cell which can contribute to age-related tumor formation.

KEYWORDS

senescence, histone variants, chromatin dynamics, cancer, nucleosomes

Introduction

The mystery of who we are, why we are here, why we age, and die has intrigued the human intellect, spanning art, literature, music, religion, and even the earliest experimental science. For instance, in ancient Egypt, incantations from funerary scrolls of the Book of the Dead dating around 2,323 B.C.E–2,291 B.C.E. were typically painted on the ceiling of tombs with the hope that it would protect and resurrect the deceased in a vividly imagined afterlife. In ancient Mayan culture, the Popul Vuh, one of the last codices to survive the erstwhile Spanish invasion of Mexico, details a cycle of life, death, and eventual resurrection. In the modern scientific era, however, a long-sought-after goal has been to retard or even reverse human aging, by trying to decipher its molecular basis and use chemicals to block or reverse phenotypes associated with aging. This is no trivial feat, as aging is now understood to be a multifactorial process manifested by the gradual decline of physiological functions from the organ all the way down to the cellular, possibly even the molecular level. The phenomenon of functional loss is seen in almost all living organisms ranging from unicellular to multicellular organisms (Figure 1). To gain a deeper understanding of the molecular mechanisms underlying the aging process, several studies have unveiled cellular senescence at a systemic level (Hornsby,



2002; McHugh and Gil, 2018). Cellular senescence was first described almost four decades ago by Hayflick and colleagues, who showed that human cells grown in culture have a finite lifespan (Hayflick, 1965). This finding led to the elucidation of the contrasting effects of cellular senescence. While cell cycle arrest leads to decline of tissue regeneration and repair activity (Hornsby, 2002), it might also serve as a possible tumor-suppressive role by inhibiting cancer cells to proliferate indefinitely (Aunan et al., 2017). Molecular determinants of cellular senescence have established it as a complex phenomenon, as it can be triggered by extrinsic and intrinsic factors, such as radiation or oxidative stress, nutrient deprivation, inflammation, mitogenic signals, progressive telomere shortening, epigenetic changes, chromatin disorganization, perturbed proteostasis, amongst many others (Mikula-Pietrasik et al., 2020). The molecular signatures of each type of senescence are quite diverse, thus altering its functional outcome. To gain further insights, it is important to understand how organisms age across all life forms. For example, what are the common hallmarks, at the organismal, cellular, and molecular levels? Do these events occur in a spatiotemporally uniform fashion or are they random? In this

review, we highlight current advances illuminating the causes of cellular senescence specifically in the context of genome organization and genome integrity. We speculate that such nuclear changes may be intricately intertwined with carcinogenesis.

Evolutionary theories for aging

Lifespan varies tremendously among species ranging from a few hours (bacteria) to thousands of years (sea sponges) (Finch, 1990) (Figure 1). This observation implies a diverse rate of senescence. Fisher (Fisher, 1958), Haldane (Finch, 2010), and later Medawar (Medawar, 1946) proposed that aging occurs when natural selection for fitness traits decreases, or even ceases at a post-reproductive age. This hypothesis further (Medawar, 1946; Medawar, 1952) states that as most organisms die before they reach old age, individuals have a very small probability of being alive and reproductive at an advanced age (Moorad and Promislow, 2010). Consequently, selection primarily occurs in younger generations. A second hypothesis is based on mutation accumulation (Medawar,

1946; Medawar, 1952) states that deleterious mutations within an individual accumulate with age. If these mutations occur after the organism is reproductively active, they will not impact the fitness of the population (Charlesworth, 2001; Hughes and Reynolds, 2005). This is observed in diseases like Huntington's or Alzheimer's where the mutation sets on at an older age in humans. A third hypothesis (Williams, 1957) argues for pleiotropic effects of mutation at different ages. For example, a genetic variation could be beneficial early in life when selection is strong, but deleterious late in life when selection is weak. Taking these various modes of evolution into consideration, it would seem unlikely that a single model would suffice to capture diversity in aging mechanisms (or lack thereof) across the species.

Studies across bacteria to mammals have concluded that genome stability is a key factor regulating lifespan (Lidzbarsky et al., 2018) (Figure 1). From bacteria and archaea to eukaryotes, DNA repair mechanisms correlate positively with lifespan (White and Allers, 2018). This sets the stage for DNA-interacting proteins such as replicative/repair polymerases and repair and recombination enzymes, to be implicated in the process of senescence. Unicellular organisms like *E. coli*, the budding yeast *Saccharomyces cerevisiae* or the *Caulobacter crescentus* which undergo asymmetric cell division demonstrate a progressive decline in reproductive potential (Ackermann et al., 2003; Erjavec et al., 2008). Upon deprivation of nutrients, and onset of stress, the bacterial genome undergoes changes. The DNA interacting protein composition also alters dramatically, for example in stationary phase the amount of Dps (DNA binding protein from starved cells) increases, whereas, the highly abundant protein of active genome, FIS, decreases (Ussery et al., 2001). In plants too, DNA repair pathway components as well as organization of the chromatin play an important role in leaf senescence (Guo et al., 2021). Ataxia Telangiectasia Mutated (ATM), suppresses double-strand break-induced expression of senescence-associated transcription factors such as ANAC016, WRKY6, WRKY53, and WRKY75 through histone lysine methylation, thus delaying leaf senescence in *Arabidopsis* (Ay et al., 2009). Although the diversity of proteins involved in maintaining the integrity of DNA among various species is large, understanding how the genome is organized and repaired might hold a clue to the basis of, and potential retardation of the aging process.

Chromatin structure: An important regulator of aging in eukaryotes

The nucleoprotein complex, chromatin, exists within the limited three-dimensional space of the nucleus (Li and Reinberg, 2011). Chromatin forms a beads-on-a-string

structure where each bead is a nucleosome (McGinty and Tan, 2015). Access to nucleosomes on the chromatin fiber is regulated through various epigenetic modifiers such as chromatin remodelers, transcription factors and long noncoding RNAs (Khosraviani et al., 2019). Apart from canonical histones, there are additional histone variants which are incorporated to nucleosomes in a replication-independent manner (Malik and Henikoff, 2003). Incorporation of these histone variants by their chaperones into nucleosome changes not only the physical nature of the nucleosomes, but also lead to the formation of differential chromatin structure either by signaling or by enhanced affinity for additional factors (Kamakaka and Biggins, 2005; Melters et al., 2019). This chromatin variation is found at the centromeres where the canonical histone H3 is replaced by Centromeric protein-A (CENP-A) which helps in assembling the kinetochore and mediating faithful cell segregation (Kamakaka and Biggins, 2005). The importance of histone variants, such as CENP-A, H2A.Z1, and H3.3, are highlighted by their knockout phenotypes which are either embryonic lethal or lead to adverse effects. (Howman et al., 2000; Faast et al., 2001; Tang et al., 2015). Interestingly, all these histone variants have been shown to maintain genomic stability and chromatin integrity (Kamakaka and Biggins, 2005). In the absence of replication-dependent replenishment, does the natural turnover of histones result in gaps in the chromatin fiber that are more susceptible to downstream DNA damage (Lowe et al., 2020)? Conversely, does restoring the epigenetic landscape by overexpressing histone restore genome integrity? It is therefore important to investigate the nucleosomal structure and composition of the aging chromatin.

Loss of canonical histones over the lifespan of an organism

Due to the finite lifespan of the budding yeast and ease of genetic manipulation and screening, *S. cerevisiae* has long served as a model to study eukaryotic aging. In a stunning series of experiments, simply overexpressing core histones in aging yeast cells lengthened their lifespan (Feser et al., 2010). Silent Information Regulator 4 (SIR4) along with SIR2 and SIR3 silence the yeast mating genes and genes in the subtelomere region through heterochromatinization (Kennedy et al., 1995). This SIR-mediated gene silencing is lost as the yeast ages (Khosraviani et al., 2019) suggesting a role of heterochromatin in aging. Furthermore, a gain of function SIR4 mutant was shown to extend its lifespan (Kennedy et al., 1995). Twenty-five years ago, Villeponteau hypothesized that global heterochromatin loss results in aging of mammalian cells including normal human cell lines (Villeponteau, 1997;

Tsurumi and Li, 2012; Lee et al., 2020). This hypothesis posits that as cells proceed through successive cell cycles and enter a stage of permanent growth arrest (i.e., replicative senescence), there is a progressive loss of the canonical histones. This histone loss leads to the disruption of heterochromatin at a global scale. This in turn, would lead to perturbation of the transcriptional landscape and expression of previously silenced regions of the genome. In addition to the budding yeast, this concept of chromatin architectural erosion has been documented in organisms like *C. elegans*, *Drosophila*, mice, and humans (Feser and Tyler, 2011). These studies show a characteristic reduction of repressive histone marks of H3K9me3 and H4K20me3 as well as delocalization of Heterochromatin protein 1 (HP1). In the same vein, overexpression of the heterochromatin binding protein HP1 in fruit flies resulted in a longer lifespan and maintenance of muscle integrity (Larson et al., 2012). In parallel with these model organism findings, the loss of repressive chromatin has also been observed in models of premature aging diseases in humans, such as Hutchinson-Gilford progeria syndrome (HGPS) and Werner syndrome. HGPS patients harbor germline mutations in *lamin A* gene (at chromosome 1q21) resulting in a c-terminal truncated version of the prelamin A called the progerin (Eriksson et al., 2003). The precursor prelamin A contains a carboxyl-terminal cysteine-aliphatic-aliphatic-any amino acid (CAAX) motif which undergoes farnesylation and subsequent cleavage by the zinc metalloprotease ZMPSTE24 (Barrowman et al., 2012). This cleavage results in the formation of mature unfarnesylated lamin A. Mechanistically, the mutation in *lamin A* gene found in HGPS (G608G) activates a cryptic RNA splice donor site, causing an internal deletion of 50 amino acids from prelamin A. This truncated, farnesylated prelamin A variant (progerin) fails to undergo cleavage resulting in accumulation in HGPS patients (Worman and Michaelis, 2018). Studies from cultured cells of HGPS patients replicate features of chronologically aged cells like enlarged nuclei, disorganized nuclear structure, reduction of H3K9me3 and loss of HP1 expression (Scaffidi and Misteli, 2006a; Shumaker et al., 2006). Werner syndrome is another accelerated aging model caused by the mutation in DNA repair gene *wrn*. Mesenchymal cells from mice and human which have been depleted of WRN showed drastic reduction of histone methyltransferase SUV39H1, which plays a vital role in the formation of heterochromatin and its maintenance (Zhang et al., 2015). Thus, global heterochromatin loss holds true for both replicative senescence as well as in premature aging models.

A burning question is: why do histone levels decrease during aging? A study in the replicative senescent IMR90 fibroblasts (obtained from human lung) indicate reduction in Stem Loop Binding Protein (SLBP), which is an important factor regulating histone mRNA stability (O'Sullivan et al., 2010). Genes encoding canonical histones are mostly expressed during S phase of the cell cycle. Transcription of these genes are regulated by the cyclin E-

cdk2 mediated phosphorylation of the Nuclear Protein Mapped to the AT locus (NPAT) trans-activator protein (DeRan et al., 2008). As cells divide continuously there is gradual shortening of telomeres resulting in an activated DNA damage response. This in turn, inhibits the phosphorylation of NPAT, thereby decreasing the transcription of histone genes (DeRan et al., 2008). These data point to a surprising connection between sensing of telomere length and homeostasis of core histone genes. A more recent study on chromatin degradation through lysosome mediated pathways also extends this concept of histone loss during senescence (Ivanov et al., 2013).

Despite several studies supporting the general hypothesis of canonical histone degradation over age, there are some contradicting reports that merit closer examination. A recent study in mice tissues obtained from different time points of the mouse lifespan reanalyzed histone H3 occupancy genome wide (Chen et al., 2020). Their results indicate alteration in the H3 occupancy (both increased and decreased) at specific genomic sites, but no profound changes in total H3 expression levels were found. A potential limitation of the study was the use of H3 specific antibody which recognizes all H3 isoforms (variants) rather than specifically recognizing a particular histone H3 variant. This study indicates that histone loss and resultant reduction of heterochromatin in an aging cell is predominantly cell-type and context-specific. A later study demonstrates that histone variant H3.3 may be recruited at novel genomic sites in aged cells resulting in a significant change in combinatorial histone H3 post translational modifications (Tvardovskiy et al., 2017). This study also highlights the crucial role of histone modifications and the epigenetic enzymes in mediating cell fate regulation. Histone modifying enzymes like that of, Histone deacetylase 4 (HDAC4), was shown to be downregulated in both replication-dependent and oncogene-induced senescent cells (Di Giorgio et al., 2020). A follow up study demonstrated the mechanism of the onset of senescence by specific HDAC4/H3K27ac interactions at senescence super-enhancer regions (Di Giorgio et al., 2021). Depletion of histone acetyl transferases p300, have also been shown to delay replicative senescence in fibroblasts by suppressing senescence-related gene expression (Sen et al., 2019). These studies demonstrate the direct modulation of the chromatin state at specific loci through epigenetic enzymes.

Collectively, these studies signify the chromatin regulation through histone variants or their post translational modifications. Are these genomic sites specific, or do they vary in a cell type or tissue specific manner? How does this replacement affect the chromatin structure at the localized sites? Does replacement of canonical histones with their corresponding variants have implications in mediating long range interactions across the genome? It is interesting to consider how an eroding chromatin landscape is rewired in an aged cell, and whether this impacts gene expression.

Reorganization of chromatin into senescence associated heterochromatin foci

Striking nuclear structures associated with aging are senescence associated heterochromatin foci (SAHF) (Narita et al., 2003; Zhang et al., 2007). Several studies have focused on deciphering the detailed structure of SAHF. The inner core of the SAHF is enriched for H3K9me3, an accepted proxy for constitutive heterochromatin. This is surrounded by the facultative heterochromatin layer denoted by H3K27me3 (Chandra et al., 2012). Furthermore, several architectural proteins like High Mobility Group A (HMGA) are an integral part of SAHF (Narita et al., 2006). Knockdown of HMGA leads to drastic reduction of SAHF in cells, proving its essential role in SAHF formation and maintenance (Chandra et al., 2012). In addition, SAHF is enriched for the histone variant macroH2A but not H3.3.

One could speculate that SAHF might be enriched with histone variants. It is indeed found that macroH2A is associated with the facultative heterochromatin region (H3K9me2) of SAHF (Zhang et al., 2007) indicating that the nucleosomal composition of SAHF might be enriched with histone variants. It has long been anticipated that the histone variant H3.3 might replace the canonical histone H3 in SAHF particularly because its chaperone histone regulator A (HIRA) is essential for the heterochromatin foci formation (Zhang et al., 2005; Ye et al., 2007; Zhang et al., 2007). Surprisingly, a more recent study shows that H3.3 is not enriched in SAHF but is contained at the promyelocytic leukemia nuclear bodies (PML-NBs) with another H3.3 chaperone ATRX/DAXX in both proliferating and oncogene-induced senescent cells (Corpet et al., 2014). These data signify novel functions of not just histone variants, but also their associated chaperones in oncogenic transformation of aged cells. These data also uncover additional functions of other histone variants in senescence apart from formation of heterochromatin foci.

Further studies on histone composition of aged nuclei could be informative to better designate functional roles in regulating the behavior of senescent cells. In this regard, it is interesting to note that mass spectrometric analysis of aged mouse neurons and human postmortem brains reveal an increased H3.3 pool (Maze et al., 2015). The decrease of canonical H2A histones is replaced by H2A.Z and H2A.J both in mouse and human aged tissues (Contrepois et al., 2017; Stefanelli et al., 2018). Apart from the core histones, linker histone H1 variants, which are primarily involved in local and global chromatin condensation and accessibility (Brockers and Schneider, 2019), is understudied during ageing. One preliminary study suggested exclusion of H1 from SAHF relevant to the observation of chromatin decompaction in SAHF (Funayama et al., 2006). Another study on H1 demonstrates increase in H1.0 both at protein and mRNA level in human dermal fibroblasts when aged in

culture (Seker-Pataryas and Sourlingas, 2007). The essential centromeric histone variant CENP-A, which mediates faithful and accurate cell division, was found to be reduced in human fibroblasts aged *in vitro* (Maehara et al., 2010). CENP-A is downregulated in both ras induced and replicatively senescent human cells. However, the functional consequence of such downregulation remains to be deciphered. Table 1 lists the histones, histone modifiers and associated proteins implicated in aging. It is to be noted here that several studies predict that the main function of the SAHF is to repress proliferative gene expression in an epigenetic fashion. However, the significance of the histone variants and other gene regulatory factors present outside the SAHF remain open avenues for exploration. Does histone variant replacement alter the accessibility of the chromatin structure? Do the modified nucleosomes harbor different histone posttranslational modifications? Does this impact gene expression, three-dimensional folding, replication timing, repair kinetics, or indeed any other aspect of nuclear biology? Investigating these avenues might provide insights into senescent chromatin structure and function.

Organization of senescent associated heterochromatin foci chromatin in a three-dimensional fashion

Multiple chromatin immunoprecipitation studies revealed that the formation of SAHF is induced by the dissociation of constitutive heterochromatin from the nuclear lamina (Chandra et al., 2015; Scaffidi et al., 2006b). Lamin associated domains (LADs) usually consist of heterochromatic regions which interact with the nuclear lamina (Briand and Collas, 2020). During aging there is a gradual degradation of nuclear lamin protein (Lamin B1) which causes the LADs to detach from the nuclear envelope resulting in a redistribution of the heterochromatin from the periphery to the interior. This process might induce the formation of SAHF (Sadaie et al., 2013). Loss of constitutive heterochromatin also leads to decondensation and activation of satellite repeats. This mechanism is referred to as senescence associated distension of satellites (SADS) (Swanson et al., 2013). SADS formation is an early event found in both mouse and human cells and does not require SAHF formation (Short, 2013). It is also fascinating that although centromeric alpha satellite regions decondense, there is no large-scale change in the classic heterochromatin marks H3K9me3/H3K27me3. These data suggest a distinct higher order chromatin organization at the centromeric regions (Swanson et al., 2015). The implication of loss of constitutive heterochromatin from the nuclear periphery cannot only be attributed to SAHF formation as (HGPS) progeroid cells are devoid of SAHF (Chandra et al., 2015).

One logical speculation is that the reorganization of chromatin in a senescent cell is a two-step process, the decompaction of heterochromatin, followed by the spatial

TABLE 1 Histones and Chromatin modifiers which are altered during ageing.

Name	Type	Expression pattern	Model organism	References
Histones				
H3, H4, H2A, H2B	Canonical histones	Loss	Yeast	Feser and Tyler, (2011)
H3	Canonical histone	Loss	<i>C.elegans</i>	Faget et al. (2019)
H3, H2A.1, H4	Canonical histone	Loss	Human fibroblasts	Kennedy et al. (1995)
mH2A, H2A.Z, H2A.J	Histone variant	Accumulation	Human, mouse	(Narita et al., 2003; Chandra et al., 2012; Di Giorgio et al., 2020)
H3.3	Histone variant	Accumulation	Human, mouse	(Zhang et al., 2007; Sen et al., 2019)
H1.0	Histone variant	Accumulation	Human fibroblasts	Eriksson et al. (2003)
Chromatin remodelers				
SWI/SNF	ATP chromatin remodeler	Loss results in shorter lifespan	<i>C.elegans</i>	Malaquin et al. (2013)
ISW1/ITCH	Chromatin remodeler	Loss results in extended lifespan	Yeast	Kaur et al. (2019)
Histone modifying enzymes				
SET-1	Histone lysine methyltransferase (ASH-2 complex subunit)	Loss	<i>C.elegans</i>	Oberdoerffer and Sinclair, (2007)
EZH2	Histone methyltransferase	Loss	Mouse, human fibroblasts	Zhang et al. (2020)
SUV39H1	Histone methyltransferase	Loss	Human and mouse hematopoietic stem cells	Ocampo et al. (2016)
HP1 beta	Heterochromatin associated protein	Accumulation	Mice and primate tissues	Li et al. (2010)

bundling of the decompacted chromatin (Figure 2). The global chromatin organizing factor CTCF, along with cohesin, acts to assemble the higher order chromatin structure. Strikingly, a recent report showed that CTCF is downregulated in aged cells (Hou et al., 2021). Furthermore, in aged cells CTCF DNA binding capacity is impaired upon aberrant transcription of pericentromeric DNA resulting in the expression of senescence associated inflammatory genes examples (Miyata et al., 2021). Taken together, these studies signify the interconnected roles of nuclear architecture, chromatin binding proteins, and region-specific chromatin condensation events in shaping a reformed nuclear landscape during aging.

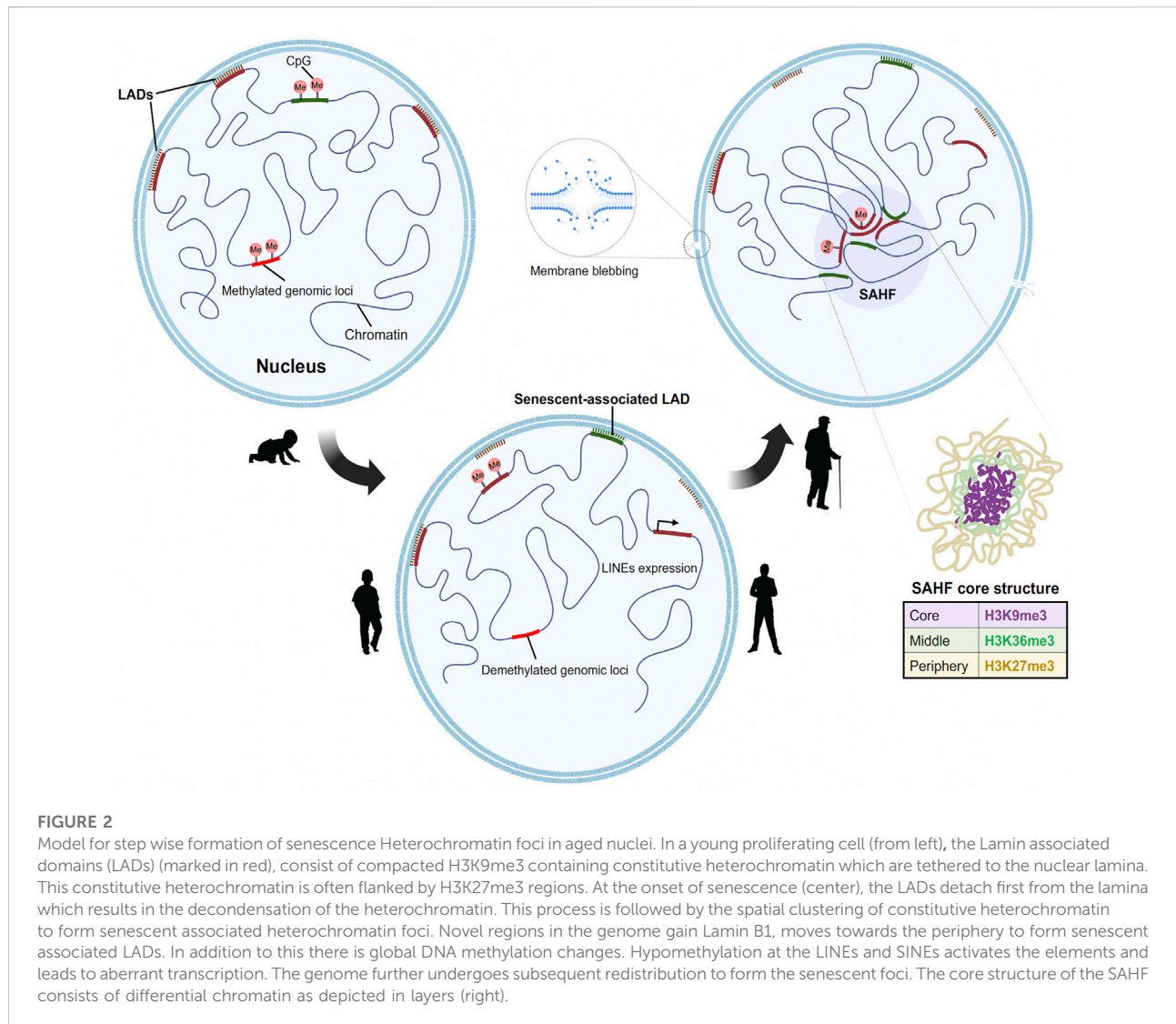
Genome integrity and senescence

The process of senescence is prompted by several factors, like accumulation of DNA damage, telomere attrition, epigenetic changes culminating in permanent cell cycle arrest and eventually organismal death. Accumulation of genomic abnormalities during aging can arise due to amassing of unrepaired DNA lesions across the genome owing to the declining quality of repair pathways (Lombard et al., 2005). The term “DNA damage” is quite broad, therefore we categorized them into two main classes based on their origin: endogenous and exogenous DNA damage. Endogenous DNA

damage is predominantly caused by replication errors, DNA base mismatches, and formation of topoisomerase-DNA complexes (Chatterjee and Walker, 2017) which are based on cellular enzymatic factors. Reactive oxygen species induce hydrolytic cleavage of the glycosidic bond and deamination of bases (De Bont and van Larebeke, 2004; Alexandrov et al., 2013). Cells have several safeguard mechanisms to repair these lesions. The four major DNA damage repair mechanisms are mentioned as follows. In case of double stranded breaks, cells exploit homologous recombination (HR) or non-homologous end joining (NHEJ) repair depending on the cell cycle stage. Single strand DNA breaks SBs are fixed through the base- or nucleotide excision repair pathways (BER and NER, respectively) whereas mismatched bases are rectified by the mismatch repair (MMR) mechanism (Lindahl, 1976; Pan et al., 2016). Here we discuss the type of DNA damage and disruption of repair pathways which occur in aging and their possible biological significance.

DNA modifications and reactivation of transposable elements

DNA methylation has been implicated in senescence and acts as a biological clock to determine the progression of age (Horvath, 2013; Weidner et al., 2014). Aberrant DNA methylation is both a signature of extensive hypermethylation



and silencing of tumor suppressor genes like that of p21, p16INK4a, and DNA repair genes like BRCA1 which occur in cancer cells (Daniel and Tollefsbol, 2015). Age-dependent hypomethylation of specific long interspersed nuclear element-1 (LINE-1) activates proto-oncogenes such as MET, RAB3IP, and CHRM3 in metastatic colorectal and lung cancer (Hur et al., 2014; Søs et al., 2014). Notably, activation of transposable elements because of DNA hypomethylation and loss of repressive chromatin structure is a common event during aging (Figure 2) (Villeponteau, 1997; Wood and Helfand, 2013). This reactivation could further lead to chromosomal breaks and relocations often characteristic of an oncogenic cell. Collectively these studies suggest a provocative, testable link between non-coding RNA, DNA methylation, altered gene expression and cancer progression. For example, we recently showed that when lncRNA PCAT2 gene is introduced to a naïve chromosome locus it acts in cis to mislocalize centromeric specific histone variant, thus altering

the epigenetic memory and chromatin structure at the locus from where it was transcribed (Arunkumar et al., 2022). LncRNAs can also interact with DNA to form RNA–DNA hybrids such as R-loops, to modulate chromatin architecture and accessibility of the transcription machinery to the underlying DNA. Antisense lncRNA TARID forms an R-loop, recognized by growth arrest and DNA damage-inducible- α (GADD45A), at the promoter of tumor suppressor gene TCF21 to trigger local DNA demethylation through TET1 and promote TCF21 gene expression (Arab et al., 2019). Nuclear-abundant lncRNAs NEAT1 and MALAT1 are shown to localize to hundreds of genomic sites in human cells, preferentially to active genes (West et al., 2014). NEAT1 regulates aberrant self-renewal of bone marrow mesenchymal stem cell lineage during skeletal aging by mediating mitochondrial function (Zhang et al., 2022). Whereas, in vascular endothelial cells SIRT6-mediated suppression of MALAT1 resulted in aging-induced endothelial to mesenchymal transition through Snail upregulation (Qin

et al., 2019). Therefore, consistent with the role of lncRNAs in the organization of higher-ordered chromatin structure, chromatin-interacting lncRNAs play a major role in the regulation of the chromatin architecture and spatial organization during aging and cancer development. Genome instability through specific DNA or lncRNA mutations then remain a key avenue ripe for exploration.

A genetic mutational basis for aging

Single nucleotide polymorphisms (SNPs) are the largest source of sequence variation in a DNA sequence among individuals. SNPs act as chromosomal tags and can be used for variations that may be involved in a human disease or disorder. SNP profiling of an individual's genome helps to study the mechanisms of the aging process as well. Nevertheless, studies showed that mitochondrial DNA (mtDNA) SNPs of individuals reaching a long life, such as the centenarians, are different from that at a younger age (Bessenyei et al., 2004). A longevity-associated mitochondrial genotype, called Mt5178A, that decelerates the frequency of mtDNA mutation in the oocytes, is shown to be present at a higher frequency in individuals reaching a longer life (Kokaze, 2005). Nuclear DNA genotypes as is indicated in the previous section are also associated with aging and related diseases. Studying the frequency of HLA-DR alleles, revealed that allelic distributions were significantly different between control and longevous groups. A high DR13 frequency is commonly seen among both genders in centenarians, whereas males had a higher DR7, and female had a higher DR11 frequency in specific (Ivanova et al., 1998). Expression quantitative trait locus (eQTL) is a genomic locus that associate transcriptomic data sets from an individual to identify gene expression phenotype. A longitudinal twin cohort study using whole-blood gene expression data showed that the expression pattern of subset of genes (2,213) are differential over time (Bryois et al., 2017). This study suggests widespread effects of quantitative trait locus on the transcriptome with an aging signature. In another comprehensive study of 11,672 complex disease-associated SNPs study, Yao et al. (2013) identified 14 sex- and 10 age-interacting eQTLs with significant association. They identified 3 age associated SNPs that have a strong association for SLC44A4 expression due to alternative splicing.

Thus, it is evident that accumulation of mutational events that increase in age could be strongly correlated with gender, ethnicity and ancestral background. As senescence sets in, the system's capacity to remove cells carrying altered genotypes is hampered resulting in pathophysiological conditions. Genetic mosaicism arises when balanced or imbalanced chromosomal aberrations such as deletion or duplication occur as cells divide (Lin dstrom et al., 2011; Ma chiesta and Chanock, 2017). These altered chromosomes might be formed during early embryonic

development or later in life. Thus, these studies indicate a genetic component to aging. However, whether specific DNA sequence alterations result in cell growth inhibition and whether these mutations are enough to potentiate the process of aging remains to be established.

DNA repair pathway is compromised in ageing tissues

Why do aged cells accumulate mutations? One approach to address this seemingly straightforward question is to compare closely related short- and long-lived animals. A study comparing long-lived and short-lived bats revealed that two genes involved in mismatch repair (MSH2 and MLH1) were significantly reduced in short-lived bats compared to the long-lived ones (Conde-Pérezprina et al., 2012). This indicates that changes in efficiency of DNA repair pathways might contribute to the speed of aging. Furthermore, the study showed that the short-lived bats exhibited increased microsatellite instability with age while the long-lived bats were protected through the expression of enhanced levels of antioxidant enzyme activities (Conde-Pérezprina et al., 2012). Studies from naked mole rats (longest lived rodents with low cancer incidence) also demonstrate similar results in terms of DNA repair activity. A comparative study in mice, naked mole rats, and humans, revealed increased expression of DNA repair genes in humans and naked mole rats that are important for DNA repair pathways such as MMR, NHEJ, and the BER (MacRae et al., 2015). Insights obtained from different DNA repair defective related syndromes demonstrate that defective DNA damage repair pathways lead to premature-aging syndromes (de Boer et al., 2002; Lombard et al., 2005; de Renty and Ellis, 2017). Mice encoding a mutation in DNA helicase gene XPD (trichothiodystrophy (TTD) show premature aging with symptoms such as osteoporosis and cachexia (de Boer et al., 2002). Table 2 lists some of the genetic diseases of DNA repair pathways which exhibit a disrupted aging pattern. Thus, aging of the genome may also be correlated with loss of fidelity or competence in DNA damage repair activity. With a frail repair system, the damaged DNA lesions are uncorrected thus leading to DNA mutations and exit from the cell cycle. Will improving DNA repair activity alone rejuvenate aged cells?

Telomere attrition as a source of DNA damage

Apart from the DNA lesions and variations, cellular senescence can be triggered through other mechanisms. An important factor is telomere attrition which is evolutionarily conserved (Figure 1). Telomeres are short tandem repeats of DNA that functions as a protective cap at the ends of the

TABLE 2 Age-associated disorders which directly affect DNA repair and genome maintenance.

Disease	Genes mutated	Pathway affected	Aging-related symptoms	References
Werner syndrome	WRN	Telomere maintenance, DNA replication and recombination repair	Arthritis, cardiovascular diseases, sarcopenia, atherosclerosis, and increased risk of cancer	Sinclair, (2005)
Bloom syndrome	BLM	DNA replication, recombination	High incidence of cancer, pulmonary disease, diabetes	Ivanova et al. (1998)
XFE progeroid syndrome	ERCC4	ICL, NER	Anemia, cardiovascular and kidney disease, neurodegeneration, sensory loss	Bartkova et al. (2006)
Trichothiodystrophy	TTDA, TTDN1, XPB, XPD, XPG	TC-NER	Bone marrow exhaustion, higher risk of cancer	Bryois et al. (2017)
Ataxia telangiectasia	ATM	DSB repair	Bone marrow exhaustion, diabetes, neurodegeneration	Kosar et al. (2011)
Hutchinson-Guilford progeria syndrome	LMNA	Nuclear lamina function, chromatin architecture	Alopecia, arthritis, cardiovascular diseases, skin aging and atrophy	Eriksson et al. (2003)
Cockayne syndrome	CSA, CSB, XPB, XPD, XPG	TC-NER	Ataxia, cataracts, muscular and neurodegeneration	Hauer and Gasser, (2017)
Fanconi anemia	FANCA-FANCW	ICL	Premature bone marrow exhaustion	Armeev et al. (2021)

ICL, Interstrand DNA crosslinks; TC-NER, Transcription coupled nucleotide excision repair; NER, Nucleotide excision repair.

chromosomes to prevent it from double strand breaks at consecutive cell divisions. The Hayflick limit is based on the shortening of telomeres, limiting cellular longevity to a finite number of cell divisions (40–60 for human diploid fibroblast cell lines) ([Aunan et al., 2017](#)). This happens due to the low fidelity of DNA polymerases which prevent it from copying the entire sequence at the DNA ends at each cell division subsequently leading to shorter telomere length ([Vaiserman and Krasnienkov, 2021](#)). In the mammalian systems, G-quadruplex rich telomeric DNA is more predisposed to oxidative damage compared to other genomic sites ([Petersen et al., 1998](#)), and telomere-bound proteins (TRF1 and TRF2) also inhibit DNA repair machinery to access the telomeres ([Palm and de Lange, 2008](#)). This prevents the resolution of DNA breaks/lesions, leading to persistent DNA damage signaling stimulated by telomeric DNA ([Cesare et al., 2013](#)). In addition to this, recent evidence on the transcriptional events occurring at the telomeres, suggest induction of telomeric diRNAs (tdiRNAs) and telomeric DDRNAs (tDDRNs) during senescence ([Aguado et al., 2020](#)). These non-coding transcripts are essential for the maintenance of DNA damage response activation at dysfunctional telomeres. Sequence specific inhibition of these lncRNAs through antisense oligonucleotides ameliorated the aging effects in HGPS mouse model ([Aguado et al., 2019](#)). Furthermore, the DNA damage signaling at the telomeres, can also be prevented by the enzyme telomerase, which is present in limiting amounts in most human somatic cells and in most mammals ([Hornsby, 2007](#)). Telomeric chromatin is shown to undergo significant remodeling during aging. Telomerase deficient mice as well as aged human fibroblasts exhibit reduced heterochromatin markers H3K9me3, H4K20me3, and CBX3 at the telomeres, while the euchromatin marker like H3K9ac increases ([Benetti et al., 2007](#)).

These findings connect the concepts of heterochromatin loss and telomere shortening, signifying that aging is driven by simultaneous endogenous events. The gradual shortening of telomeres can be prevented by the expression of hTERT (telomerase) which is used to immortalize cultured cells ([Bodnar et al., 1998](#)) and can be efficiently used for tissue engineering ([Shay and Wright, 2000](#)). Despite being an efficient anti-aging therapy, hTERT overexpression has its own shortcomings. A heightened telomerase activity is a signature of cancerous cells ([Horn et al., 2013](#); [Jafri et al., 2016](#)). Therefore, further exploration of mechanisms to prevent aging defects is required to prevent its neoplastic transformation.

Tumor formation in the aging background

The progressive decline of physiological functions during aging results in various pathological conditions including cancer ([Yancik, 1997](#); [Berger et al., 2006](#)). Although aging and cancer share some common mechanisms such as disruption of telomere length, genomic instability, diverse epigenetic changes, altered proteostasis, disrupted nutrient sensing and metabolic pathways ([Gemble et al., 2015](#); [Gemble et al., 2016](#); [Berben et al., 2021](#)), they lead to divergent cell fates. The process of cellular senescence also plays a crucial role in the process of transformation of an aged cell to malignancy. On the surface, cancer cells and aged cells display conflicting features. Cancer cells are highly proliferative cells, harboring mutations enabling prompt cell division, resulting in high consumption of energy; whereas aged cells accumulate mutations which pose a disadvantage for cell growth and

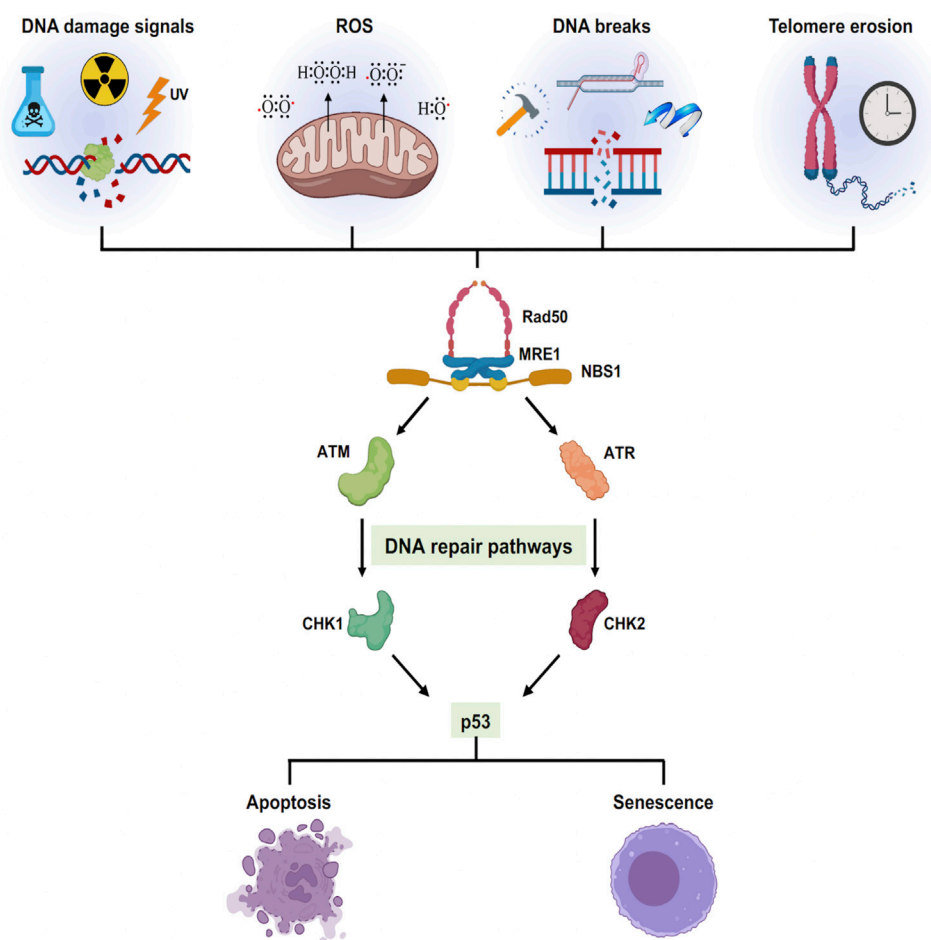


FIGURE 3

Cellular senescence triggered by different stress signals: Different exogenous and endogenous events trigger a stress response pathway. The stress elicits a DNA damage responsive pathway via ATM/ATR converging onto p53 which decides the cellular fate either to cell death or cell growth arrest.

proliferation. However, several studies have associated cellular senescence with cancer development (Berger et al., 2006).

Genome instability: A common cause of aging and cancer

The progressive buildup of DNA damage and mutations are prime drivers of both cancer and aging (Sinclair and Oberdoerffer, 2009). Extensive exposure to endogenous and exogenous DNA damage factors such as ionizing radiation, ultraviolet radiation, tobacco smoking, toxins, reactive electrophiles, alkylating agents, and environmental stress play a significant role in driving genome instability. In mammalian cells, the production of double-strand breaks (DSBs) initiates DNA damage Response (DDR), a global cellular response by triggering checkpoint signaling and DNA repair mechanisms.

The MRN (MRE11/RAD50/NBS1) complex binds to double-strand breaks facilitating the activation of ATM signaling to initiate DDR (Uziel et al., 2003). PARP1 and PARP2 are among the first molecules recruited to DNA breaks induced by irradiation as the MRN complex (Haince et al., 2008) followed by γ H2AX, an H2A histone variant, accumulation at the damage site and its phosphorylation is amplified by recruitment of MDC1 (Stucki et al., 2005). MDC1 contributes to the recruitment of multiple DNA Damage Response (DDR) pathway members such as RAP80, 53BP1, KAP-1, and BRCA1 (Thompson, 2012). The overall signaling pathway phosphorylates CHK2, p53, and CDC25 to trigger checkpoint activation and cell cycle arrest (Deng, 2006; Huen et al., 2007; Sakasai and Tibbetts, 2008). Remarkably, PARP1 has a dual role, acting as a longevity factor at a younger age, while playing an aging-promoting factor at an older age or in pathophysiological conditions (Haince et al., 2008). Similarly, γ H2AX, p53, and

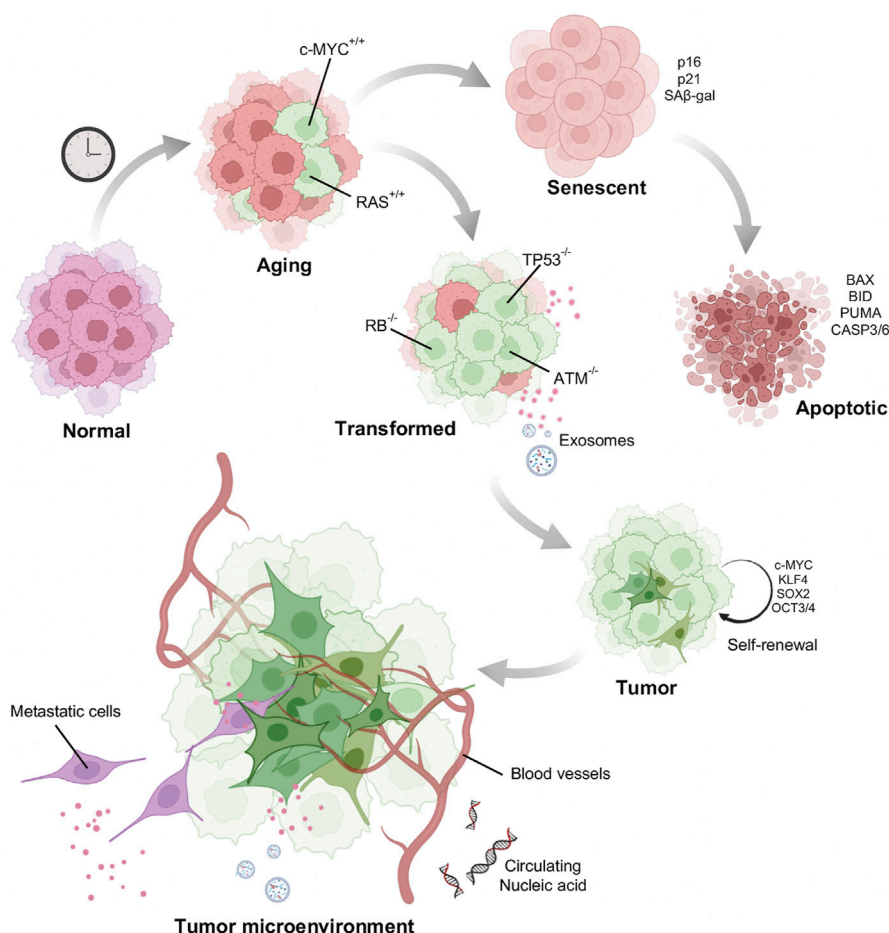


FIGURE 4

Model of how aged cells potentiate tumor formation: Normal young cells accumulate DNA damage and senesce. A few of the damaged old cells acquire mutations such as activation of oncogenes to induce oncogene induced senescence. Senescent cells after acquiring enormous DNA damage might be directed towards apoptotic pathway. Some cells however, escape death by acquiring other mutations and gain self-renewal property behaving as potential stem cells. Tumor cells once formed is also facilitated by the aging stroma for its growth and metastasis.

BRCA1 are all shown to be involved in aging and related diseases (Mah et al., 2010; Ben-Aharon et al., 2018; Wu and Prives, 2018). Therefore, accumulation of DNA damage caused by both endogenous and exogenous factors over time will promote growth arrest, apoptosis, or cellular senescence (Figure 3). In this context, examining PARP inhibitors and their effect on aging, bears further experimental examination.

Progressive inactivation of tumor suppressors with age

Adult stem cells after acquiring enough mutations, epigenetic alterations, depart from the proliferative pool (Santos Franco et al., 2015) (Figure 4). This phenomenon of cell cycle arrest is particularly dependent on p53. The p53 protein encoded by the

TP53 gene activates cyclin dependent kinase (CDK) inhibitor p21, which further restricts the activity of CDK4/6 activity. The P16INK4a gene encodes two proteins p14ARF, regulates p53 stability and the p16INK4A protein, an inhibitor of CDK4/6. Thus, both the pathways converge at inactivating the CDK4/6. Inhibition of CDK4/6 activity prevents the phosphorylation of the retinoblastoma protein (pRB). This results in cell cycle arrest at the G1 phase (Ye et al., 2007; McHugh and Gil, 2018). A study by Tyner et al. (2002) compared the propensity of tumor development in wild type, p53 knockout, and mutant p53 (gain of function) background. These data demonstrated high tumor occurrence in p53 knockout mice (Tyner et al., 2002). Mice with a gain of function p53 exhibited very low occurrence of tumor, but fascinatingly, showed signs of premature aging, such as sparse ruffled fur, loss of weight and lethargy. Telomere shortening,

another activator of senescence, is also p53 dependent (Chin et al., 1999). Mice carrying extra copies of p53 DNA do not accumulate telomere damage thereby reducing telomere driven aging (García-Ca o et al., 2006). This advantage has also been observed in elephants, which carry extra copies of p53 which is associated with enhanced apoptotic clearance of cells with DNA damage (Seluanov et al., 2018). This response is thought to be a reason why elephants have a low incidence of cancer. All these observations point to the anti-tumorigenic effect of p53 dependent senescence. However, some cells may escape these cellular degradation pathways by acquiring additional strategic mutations allowing them to proliferate even in the presence of an eroded and damaged chromatin landscape. Escaped somatic cells might form a niche in a later stage to develop malignant tumors. The presence of senescent cells in tumor tissues have been reported to arise either spontaneously or through activation of oncogenes (Mikula-Pietrasik et al., 2020).

Chemically induced senescence can be promoted by anti-cancer drugs such as aphidicolin, bleomycin, cisplatin, doxorubicin, etoposide, mitoxantrone, retinols, hydroxyurea, carboplatin combined with docetaxel, and many others (Mikula-Pietrasik et al., 2020). This can be triggered by induction of DNA damage, accumulation of reactive oxygen species or by inhibition of DNA polymerases (Ewald et al., 2010). Although chemically induced senescence might have severe side-effects as it can promote cancer cell proliferation (Alspach et al., 2013). Induction of senescence, particularly by the inactivation of certain tumor suppressors like that of SHP2 (Serrano, 2015) and PTEN (Toso et al., 2014) also facilitate tumor growth. These studies propose a two-hit hypothesis for cancer development from aged cells. Like one bad apple in a basket which spoils the whole lot, a logical question to ask is whether an aged cell acquiring an oncogenic mutation could potentiate tumor cell population? In other words, does the aging cell provide a favorable microenvironment for tumor growth?

Aged microenvironment favors tumor growth

In the last two decades there have been studies trying to decipher the molecular mechanism of pro-oncogenic activity of senescence. An important factor might be the formation of an immunosuppressive tissue microenvironment. Senescent cells elicit a secretory phenotype called SASP (senescent associated secretory phenotype), characterized by an overproduction of a variety of chemokines, growth factors (EGF, bGF, VEGF, and TGF- β 1), cytokines along with several extracellular matrix constituents and remodeling proteins (fibronectin, collagens, laminin, MMP-1, -3). Apart from causing major chronic inflammation, SASP also act *via* autocrine and paracrine pathways (Acosta et al., 2008; Acosta et al., 2013). This enables SASP to inhibit cell growth and promote senescence

spreading to distant healthy bystander cells. The proteins such as IL-6, IL-8 (Kojima et al., 2013; Ortiz-Montero et al., 2017), MMP-1 have been shown to induce the paracrine responses and play an active role in tumor progression and metastasis (Faget et al., 2019). Replicative senescent skin fibroblasts secreting MMP-1 and MMP-2 displayed activation of PAR-1 in tumorigenic keratinocytes and enhanced their invasive activity (Malaquin et al., 2013). Aged human skin fibroblast expresses reduced levels of hyaluronan and proteoglycan link protein 1 (HAPLN1) leading to a more organized ECM, which promotes the metastasis of melanoma cells (Kaur et al., 2019) (Figure 4).

Conclusion and perspectives

Comprehending the role of molecular processes such as DNA damage repair, telomere shortening, nuclear (Oberdoerffer and Sinclair, 2007) and chromatin changes along with epigenetic alterations which drive aging as well as aging related diseases may hold a key to the “elixir of life.” Of late the resurrection of aged cells back to cellular proliferation has garnered attention from various molecular biologists. The use of Yamanaka factors (OCT4, NANOG, SOX2, KLF4, and MYC) reprograms cells to a partially undifferentiated stage which is shown to ameliorate some of the functions of aged fibroblasts as well as fibroblasts obtained from progeroid models (Zhang et al., 2020). The transient expression of these factors rescued the levels of H3K9me3 and DNA damage marks such as γ -H2AX (Ocampo et al., 2016). Caloric restriction is another mode of rejuvenation of aged cells extensively studied in mice and human cells (Sinclair, 2005; Li et al., 2010). Interestingly, this mode of rejuvenation also acts through the epigenome. Glucose restriction induced increase in H3K4me2 at hTERT and H3K9me3 at the p16INK4a promoter, respectively which accelerated cellular lifespan by activation of hTERT and repression of p16INK4a (Li et al., 2010). All these studies fortify the beneficial role of heterochromatin in protecting the genome from DNA damage and neoplastic transformation.

However, there remain several uncharted domains: Is heterochromatin alone sufficient to extend lifespan? Is the reorganization of the heterochromatin guided by the changed DNA methylome in aged cells? A varied number of histone variants are expressed inside as well as outside of the SAHF. What directs them to their specific genomic location upon senescence? The complexity and confusion arise as cells induced by different stress mediated pathways show different epigenetic signatures or varied chromatin organization. Senescent cells found in the pre-cancerous lesions exhibit increased levels of heterochromatic histone modifications (H3K9me2/3 and HP1 γ) (Bartkova et al., 2006) but lack in SAHF (Kosar et al., 2011). This discrepancy might be due to the variation in the extent of heterochromatinization of the genome.

We posit that analyzing the biophysical and mechanical nature of aged chromatin polymer in different cell types might provide clues to its natural decay and dysfunction. Despite current technological challenges, even elucidating the half-life or turnover of chromatin factors, including post-translational modifications of nucleosomes, repair factors, chromatin remodelers could be an important start. Knowing these parameters, we can better understand and potentially model how the nuclear landscape changes as cells age. How do these different half-lives impact protein-complex composition and functional stability of transcriptionally active and inactive regions of the genome? Genomic regions which exhibit distinct functions such as promoter, enhancers, and constitutive heterochromatin are marked by the presence of histone PTMs (post translational modifications). Ideally, established histone PTMs are maintained to continue the faithful expression of tissue-specific genes. Rare and unconventional PTMs, such as glypiation, neddylation, siderophorylation, AMPylation, and cholesteroylation, are expected to accumulate in senescent cells, purely by change, or chance, acting as driver epimutations. These PTMs influence protein structure and function (Basak et al., 2016). DNA damage also increase histone degradation (Hauer and Gasser, 2017) and histone tail cleavage has been associated with various cellular processes (Yi and Kim 2018). All-atom computational modeling shows that histone tail dynamics modulate the DNA accessibility (Armeev et al., 2021; Peng et al., 2021) and DNA methylation leads to more curved under-twisted DNA (Li et al., 2022). Taking these factors into account, one might predict dramatic differences between the biophysical properties of aged chromatin versus young chromatin. Exploring how material properties of nucleosomes impact the functional outcome of a chromatin fiber and how these properties age, we argue, is the next frontier of chromatin biology. Indeed, development of experimental approaches to circumvent the limitations of time and optimizations of methods are required to study aging chromatin in a microfluidic tube.

Finally, the study of aging needs to be expanded from murine/human cells to that of long-lived whales, termites or even plants which live for hundreds of years. These species may provide unanticipated and novel mechanisms of aging and rejuvenation (Holtze et al., 2021) that have eluded our own species. Will the secret “ambrosia of Greek Gods” be found in the genomes of more age-resilient species, such as that of the humble tardigrade (Hashimoto et al., 2016)? It is remarkable that the 21st century thus far has been marked by devastation caused by nanopathogens and non-pathogenic climate extremes. To quote

from a recent novella by the brilliant sci-fi writer Ted Chiang “Four things do not come back: the spoken word, the sped arrow, the past life, and the neglected opportunity.” Billionaire Trekkie space pioneers compete with each other, to boldly go where no human has gone before, in the hopes of terraforming distant planets. Examining how human lifespan and aging impacts our potential for exploration is now no longer in the arena of futuristic sci-fi, but an opportunity for nano-exploration rooted firmly to our species’ survival on this planet.

Author contributions

SS and YD conceived of the draft SS and GA made the figures SS, GA, and DM (in this order) co-wrote a draft, YD edited the draft as senior author.

Funding

All authors were supported by the Intramural Research Program of the National Institutes of Health.

Acknowledgments

The authors thank Drs Minh Bui and Ankita Saha for critical reading of the manuscript. The authors also thank Dr Payel Sen, NIA for valuable contributions in an ongoing collaborative project on epigenetics of aging.

Conflict of interest

The authors declare that the research was conducted in the absence of any commercial or financial relationships that could be construed as a potential conflict of interest.

Publisher’s note

All claims expressed in this article are solely those of the authors and do not necessarily represent those of their affiliated organizations, or those of the publisher, the editors and the reviewers. Any product that may be evaluated in this article, or claim that may be made by its manufacturer, is not guaranteed or endorsed by the publisher.

References

- Ackermann, M., Stearns, S. C., and Jenal, U. (2003). Senescence in a bacterium with asymmetric division. *Science* 300, 1920. doi:10.1126/science.1083532
- Acosta, J. C., Banito, A., Wuestefeld, T., Georgilis, A., Janich, P., Morton, J. P., et al. (2013). A complex secretory program orchestrated by the inflammasome controls paracrine senescence. *Nat. Cell Biol.* 15, 978–990. doi:10.1038/ncb2784
- Acosta, J. C., O'Loughlin, A., Banito, A., Guijarro, M. V., Augert, A., Raguz, S., et al. (2008). Chemokine signaling via the CXCR2 receptor reinforces senescence. *Cell* 133, 1006–1018. doi:10.1016/j.cell.2008.03.038
- Aguado, J., d'Adda di Fagnana, F., and Wolvetang, E. (2020). Telomere transcription in ageing. *Ageing Res. Rev.* 62, 101115. doi:10.1016/j.arr.2020.101115
- Aguado, J., Sola-Carvajal, A., Cancila, V., Revêchon, G., Ong, P. F., Jones-Weinert, C. W., et al. (2019). Inhibition of DNA damage response at telomeres improves the detrimental phenotypes of Hutchinson–Gilford Progeria Syndrome. *Nat. Commun.* 10, 4990. doi:10.1038/s41467-019-13018-3
- Alexandrov, L. B., Nik-Zainal, S., Wedge, D. C., Aparicio, S. A. J. R., Behjati, S., Biankin, A. V., et al. (2013). Signatures of mutational processes in human cancer. *Nature* 500, 415–421. doi:10.1038/nature12477
- Alspach, E., Fu, Y., and Stewart, S. A. (2013). Senescence and the pro-tumorigenic stroma. *Crit. Rev. Oncog.* 18, 549–558. doi:10.1615/critrevoncog.2014010630
- Arab, K., Karaulanov, E., Musheev, M., Trnka, P., Schäfer, A., Grummt, I., et al. (2019). GADD45A binds R-loops and recruits TET1 to CpG island promoters. *Nat. Genet.* 51, 217–223. doi:10.1038/s41588-018-0306-6
- Armeev, G. A., Kniazeva, A. S., Komarova, G. A., Kirpichnikov, M. P., and Shaytan, A. K. (2021). Histone dynamics mediate DNA unwrapping and sliding in nucleosomes. *Nat. Commun.* 12, 2387. doi:10.1038/s41467-021-22636-9
- Arunkumar, G., Baek, S., Sturgill, D., Bui, M., and Dalal, Y. (2022). Oncogenic lncRNAs alter epigenetic memory at a fragile chromosomal site in human cancer cells. *Sci. Adv.* 8, eabl5621. doi:10.1126/sciadv.abl5621
- Aunan, J. R., Cho, W. C., and Søreide, K. (2017). The biology of aging and cancer: A brief overview of shared and divergent molecular hallmarks. *Ageing Dis.* 8, 628–642. doi:10.14336/AD.2017.0103
- Ay, N., Irmeler, K., Fischer, A., Uhlemann, R., Reuter, G., and Humbeck, K. (2009). Epigenetic programming via histone methylation at WRKY53 controls leaf senescence in *Arabidopsis thaliana*. *Plant J.* 58 (2), 333–346. doi:10.1111/j.1365-3113.2008.03782.x
- Barrowman, J., Wiley, P. A., Hudon-Miller, S. E., Hrycyna, C. A., and Michaelis, S. (2012). Human ZMPSTE24 disease mutations: Residual proteolytic activity correlates with disease severity. *Hum. Mol. Genet.* 21, 4084–4093. doi:10.1093/hmg/dd233
- Bartkova, J., Rezaei, N., Lontos, M., Karakaidos, P., Kletsas, D., Issaeva, N., et al. (2006). Oncogene-induced senescence is part of the tumorigenesis barrier imposed by DNA damage checkpoints. *Nature* 444, 633–637. doi:10.1038/nature05268
- Basak, S., Lu, C., and Basak, A. (2016). Post-translational protein modifications of rare and unconventional types: Implications in functions and diseases. *Curr. Med. Chem.* 23, 714–745.
- Ben-Aharon, I., Levi, M., Margel, D., Yerushalmi, R., Rizel, S., Perry, S., et al. (2018). Premature ovarian aging in BRCA carriers: A prototype of systemic precocious aging? *Oncotarget* 9, 15931–15941. doi:10.18632/oncotarget.24638
- Benetti, R., García-Cao, M., and Blasco, M. A. (2007). Telomere length regulates the epigenetic status of mammalian telomeres and subtelomeres. *Nat. Genet.* 39, 243–250. doi:10.1038/ng1952
- Benben, L., Floris, G., Wildiers, H., and Hatse, S. (2021). Cancer and aging: Two tightly interconnected biological processes. *Cancers (Basel)* 13, 1400. doi:10.3390/cancers13061400
- Berger, N. A., Savvides, P., Koroukian, S. M., Kahana, E. F., Deimling, G. T., Rose, J. H., et al. (2006). Cancer in the elderly. *Trans. Am. Clin. Climatol. Assoc.* 117, 147–155.
- Bessenyei, B., Márka, M., Urbán, L., Zehner, M., and Semsei, I. (2004). Single nucleotide polymorphisms: Aging and diseases. *Biogerontology* 5, 291–303. doi:10.1007/s10522-004-2567-y
- Bodnar, A. G., Ouellette, M., Frolkis, M., Holt, S. E., Chiu, C. P., Morin, G. B., et al. (1998). Extension of life-span by introduction of telomerase into normal human cells. *Science* 279, 349–352. doi:10.1126/science.279.5349.349
- Briand, N., and Collas, P. (2020). Lamina-associated domains: Peripheral matters and internal affairs. *Genome Biol.* 21, 85. doi:10.1186/s13059-020-02003-5
- Brockers, K., and Schneider, R. (2019). Histone H1, the forgotten histone. *Epigenomics* 11, 363–366. doi:10.2217/epi-2019-0018
- Bryois, J., Buil, A., Ferreira, P. G., Panousis, N. I., Brown, A. A., Vinuela, A., et al. (2017). Time-dependent genetic effects on gene expression implicate aging processes. *Genome Res.* 27, 545–552. doi:10.1101/gr.207688.116
- Cesare, A. J., Hayashi, M. T., Crabbe, L., and Karlseder, J. (2013). The telomere deprotection response is functionally distinct from the genomic DNA damage response. *Mol. Cell* 51, 141–155. doi:10.1016/j.molcel.2013.06.006
- Chandra, T., Ewels, P. A., Schoenfelder, S., Furlan-Magaril, M., Wingett, S. W., Kirschner, K., et al. (2015). Global reorganization of the nuclear landscape in senescent cells. *Cell Rep.* 10, 471–483. doi:10.1016/j.celrep.2014.12.055
- Chandra, T., Kirschner, K., Thuret, J. Y., Pope, B. D., Ryba, T., Newman, S., et al. (2012). Independence of repressive histone marks and chromatin compaction during senescent heterochromatic layer formation. *Mol. Cell* 47, 203–214. doi:10.1016/j.molcel.2012.06.010
- Charlesworth, B. (2001). Patterns of age-specific means and genetic variances of mortality rates predicted by the mutation-accumulation theory of ageing. *J. Theor. Biol.* 210, 47–65. doi:10.1006/jtbi.2001.2296
- Chatterjee, N., and Walker, G. C. (2017). Mechanisms of DNA damage, repair, and mutagenesis. *Environ. Mol. Mutagen.* 58, 235–263. doi:10.1002/em.22087
- Chen, Y., Bravo, J. I., Son, J. M., Lee, C., and Benayoun, B. A. (2020). Remodeling of the H3 nucleosomal landscape during mouse aging. *Transl. Med. Aging* 4, 22–31. doi:10.1016/j.tma.2019.12.003
- Chin, L., Artandi, S. E., Shen, Q., Tam, A., Lee, S. L., Gottlieb, G. J., et al. (1999). p53 deficiency rescues the adverse effects of telomere loss and cooperates with telomere dysfunction to accelerate carcinogenesis. *Cell* 97, 527–538. doi:10.1016/s0092-8674(00)80762-x
- Conde-Pérezprina, J. C., Luna-López, A., González-Puertos, V. Y., Zenteno-Savín, T., León-Galván, M. A., Königsberg, M., et al. (2012). DNA MMR systems, microsatellite instability and antioxidant activity variations in two species of wild bats: *Myotis velifer* and *Desmodus rotundus*, as possible factors associated with longevity. *Age (Dordr)* 34, 1473–1492. doi:10.1007/s11357-012-9399-5
- Contrepois, K., Coudereau, C., Benayoun, B. A., Schuler, N., Roux, P.-F., Bischof, O., et al. (2017). Histone variant H2A.J accumulates in senescent cells and promotes inflammatory gene expression. *Nat. Commun.* 8, 14995. doi:10.1038/ncomms14995
- Corpet, A., Olbrich, T., Gwerder, M., Fink, D., and Stucki, M. (2014). Dynamics of histone H3.3 deposition in proliferating and senescent cells reveals a DAXX-dependent targeting to PML-NBs important for pericentromeric heterochromatin organization. *Cell Cycle* 13, 249–267. doi:10.4161/cc.26988
- Daniel, M., and Tollefsbol, T. O. (2015). Epigenetic linkage of aging, cancer and nutrition. *J. Exp. Biol.* 218, 59–70. doi:10.1242/jeb.107110
- de Boer, J., Andressoo, J. O., de Wit, J., Huijman, J., Beems, R. B., van Steeg, H., et al. (2002). Premature aging in mice deficient in DNA repair and transcription. *Science* 296, 1276–1279. doi:10.1126/science.1070174
- De Bont, R., and van Larebeke, N. (2004). Endogenous DNA damage in humans: A review of quantitative data. *Mutagenesis* 19, 169–185. doi:10.1093/mutage/geh025
- de Renty, C., and Ellis, N. A. (2017). Bloom's syndrome: Why not premature aging?: A comparison of the blm and wrn helicases. *Ageing Res. Rev.* 33, 36–51. doi:10.1016/j.arr.2016.05.010
- Deng, C. X. (2006). BRCA1: Cell cycle checkpoint, genetic instability, DNA damage response and cancer evolution. *Nucleic Acids Res.* 34, 1416–1426. doi:10.1093/nar/gkl010
- DeRan, M., Pulvino, M., Greene, E., Su, C., and Zhao, J. (2008). Transcriptional activation of histone genes requires NPAT-dependent recruitment of TRRAP-Tip60 complex to histone promoters during the G1/S phase transition. *Mol. Cell Biol.* 28, 435–447. doi:10.1128/MCB.00607-07
- Di Giorgio, E., Dalla, E., Franforte, E., Paluvai, H., Minisini, M., Trevisanut, M., et al. (2020). Different class IIa HDACs repressive complexes regulate specific epigenetic responses related to cell survival in leiomyosarcoma cells. *Nucleic Acids Res.* 48, 646–664. doi:10.1093/nar/gkz1120
- Di Giorgio, E., Paluvai, H., Dalla, E., Ranzino, L., Renzini, A., Moresi, V., et al. (2021). HDAC4 degradation during senescence unleashes an epigenetic program driven by AP-1/p300 at selected enhancers and super-enhancers. *Genome Biol.* 22, 129. doi:10.1186/s13059-021-02340-z
- Eriksson, M., Brown, W. T., Gordon, L. B., Glynn, M. W., Singer, J., Scott, L., et al. (2003). Recurrent de novo point mutations in lamin A cause Hutchinson–Gilford progeria syndrome. *Nature* 423, 293–298. doi:10.1038/nature01629

- Erjavec, N., Cvijovic, M., Klipp, E., and Nyström, T. (2008). Selective benefits of damage partitioning in unicellular systems and its effects on aging. *Proc. Natl. Acad. Sci. U. S. A.* 105, 18764–18769. doi:10.1073/pnas.0804550105
- Ewald, J. A., Desotelle, J. A., Wilding, G., and Jarrard, D. F. (2010). Therapy-induced senescence in cancer. *J. Natl. Cancer Inst.* 102, 1536–1546. doi:10.1093/jnci/djq364
- Faast, R., Thonglairoam, V., Schulz, T. C., Beall, J., Wells, J. R. E., Taylor, H., et al. (2001). Histone variant H2A.Z is required for early mammalian development. *Curr. Biol.* 11, 1183–1187. doi:10.1016/s0960-9822(01)00329-3
- Faget, D. V., Ren, Q., and Stewart, S. A. (2019). Unmasking senescence: Context-dependent effects of SASP in cancer. *Nat. Rev. Cancer* 19, 439–453. doi:10.1038/s41568-019-0156-2
- Feser, J., Truong, D., Das, C., Carson, J. J., Kieft, J., Harkness, T., et al. (2010). Elevated histone expression promotes life span extension. *Mol. Cell* 39, 724–735. doi:10.1016/j.molcel.2010.08.015
- Feser, J., and Tyler, J. (2011). Chromatin structure as a mediator of aging. *FEBS Lett.* 585, 2041–2048. doi:10.1016/j.febslet.2010.11.016
- Finch, C. E. (2010). Evolution in health and medicine sackler colloquium: Evolution of the human lifespan and diseases of aging: Roles of infection, inflammation, and nutrition. *Proc. Natl. Acad. Sci. U. S. A.* 107 (Suppl. 1), 1718–1724. doi:10.1073/pnas.0909606106
- Finch, C. (1990). *Longevity, senescence, and the genome/Caleb E. Finch*. Chicago: University of Chicago Press.
- Fisher, R. A. (1958). *The genetical theory of natural selection*. Harpenden, England: ПиШол Классик.
- Funayama, R., Saito, M., Tanobe, H., and Ishikawa, F. (2006). Loss of linker histone H1 in cellular senescence. *J. Cell Biol.* 175, 869–880. doi:10.1083/jcb.200604005
- García-Cao, I., García-Cao, M., Tomás-Loba, A., Martín-Caballero, J., Flores, J. M., Klatt, P., et al. (2006). Increased p53 activity does not accelerate telomere-driven ageing. *EMBO Rep.* 7, 546–552. doi:10.1038/sj.embor.7400667
- Gemble, S., Ahuja, A., Buhagiar-Labarchède, G., Onclercq-Delic, R., Dairou, J., Biard, D. S., et al. (2015). Pyrimidine pool disequilibrium induced by a cytidine deaminase deficiency inhibits PARP-1 activity, leading to the under replication of DNA. *PLoS Genet.* 11, e1005384. doi:10.1371/journal.pgen.1005384
- Gemble, S., Buhagiar-Labarchède, G., Onclercq-Delic, R., Biard, D., Lambert, S., Amor-Guérét, M., et al. (2016). A balanced pyrimidine pool is required for optimal Chk1 activation to prevent ultrafine anaphase bridge formation. *J. Cell Sci.* 129, 3167–3177. doi:10.1242/jcs.187781
- Guo, Y., Ren, G., Zhang, K., Li, Z., Miao, Y., Guo, H., et al. (2021). Leaf senescence: Progression, regulation, and application. *Mol. Hortic.* 1, 5. doi:10.1186/s43897-021-00006-9
- Haince, J. F., McDonald, D., Rodrigue, A., Dery, U., Masson, J. Y., Hendzel, M. J., et al. (2008). PARP1-dependent kinetics of recruitment of MRE11 and NBS1 proteins to multiple DNA damage sites. *J. Biol. Chem.* 283, 1197–1208. doi:10.1074/jbc.M706734200
- Hashimoto, T., Horikawa, D. D., Saito, Y., Kuwahara, H., Kozuka-Hata, H., Shin-I, T., et al. (2016). Extremotolerant tardigrade genome and improved radiotolerance of human cultured cells by tardigrade-unique protein. *Nat. Commun.* 7, 12808. doi:10.1038/ncomms12808
- Hauer, M. H., and Gasser, S. M. (2017). Chromatin and nucleosome dynamics in DNA damage and repair. *Genes Dev.* 31, 2204–2221. doi:10.1101/gad.307702.117
- Hayflick, L. (1965). The limited *in vitro* lifetime of human diploid cell strains. *Exp. Cell Res.* 37, 614–636. doi:10.1016/0014-4827(65)90211-9
- Holtze, S., Gorshkova, E., Braude, S., Cellerino, A., Dammann, P., Hildebrandt, T. B., et al. (2021). Alternative animal models of aging research. *Front. Mol. Biosci.* 8, 660959. doi:10.3389/fmolb.2021.660959
- Horn, S., Figl, A., Rachakonda, P. S., Fischer, C., Sucker, A., Gast, A., et al. (2013). TERT promoter mutations in familial and sporadic melanoma. *Science* 339, 959–961. doi:10.1126/science.1230062
- Hornsby, P. J. (2002). Cellular senescence and tissue aging *in vivo*. *Journals Gerontology Ser. A Biol. Sci. Med. Sci.* 57, B251–B256. doi:10.1093/gerona/57.7.b251
- Hornsby, P. J. (2007). Telomerase and the aging process. *Exp. Gerontol.* 42, 575–581. doi:10.1016/j.exger.2007.03.007
- Horvath, S. (2013). DNA methylation age of human tissues and cell types. *Genome Biol.* 14, R115. doi:10.1186/gb-2013-14-10-r115
- Hou, Y., Song, Q., Gao, S., Zhang, X., Wang, Y., Liu, J., et al. (2021). CTCF mediates replicative senescence through POLD1. *Front. Cell Dev. Biol.* 9, 618586. doi:10.3389/fcell.2021.618586
- Howman, E. V., Fowler, K. J., Newson, A. J., Redward, S., MacDonald, A. C., Kalitsis, P., et al. (2000). Early disruption of centromeric chromatin organization in centromere protein A (Cenpa) null mice. *Proc. Natl. Acad. Sci. U. S. A.* 97, 1148–1153. doi:10.1073/pnas.97.3.1148
- Huen, M. S., Grant, R., Manke, I., Minn, K., Yu, X., Yaffe, M. B., et al. (2007). RNF8 transduces the DNA-damage signal via histone ubiquitylation and checkpoint protein assembly. *Cell* 131, 901–914. doi:10.1016/j.cell.2007.09.041
- Hughes, K. A., and Reynolds, R. M. (2005). Evolutionary and mechanistic theories of aging. *Annu. Rev. Entomol.* 50, 421–445. doi:10.1146/annurev.ento.50.071803.130409
- Hur, K., Cejas, P., Feliu, J., Moreno-Rubio, J., Burgos, E., Boland, C. R., et al. (2014). Hypomethylation of long interspersed nuclear element-1 (LINE-1) leads to activation of proto-oncogenes in human colorectal cancer metastasis. *Gut* 63, 635–646. doi:10.1136/gutjnl-2012-304219
- Ivanov, A., Pawlikowski, J., Manoharan, I., van Tuyn, J., Nelson, D. M., Rai, T. S., et al. (2013). Lysosome-mediated processing of chromatin in senescence. *J. Cell Biol.* 202, 129–143. doi:10.1083/jcb.201212110
- Ivanova, R., Hénon, N., Lepage, V., Charron, D., Vicaute, E., Schächter, F., et al. (1998). HLA-DR alleles display sex-dependent effects on survival and discriminate between individual and familial longevity. *Hum. Mol. Genet.* 7, 187–194. doi:10.1093/hmg/7.2.187
- Jafri, M. A., Ansari, S. A., Alqahtani, M. H., and Shay, J. W. (2016). Roles of telomeres and telomerase in cancer, and advances in telomerase-targeted therapies. *Genome Med.* 8, 69. doi:10.1186/s13073-016-0324-x
- Kamakaka, R. T., and Biggins, S. (2005). Histone variants: Deviants? *Genes Dev.* 19, 295–310. doi:10.1101/gad.1272805
- Kaur, A., Ecker, B. L., Douglass, S. M., Kugel, C. H., 3rd, Webster, M. R., Almeida, F. V., et al. (2019). Remodeling of the collagen matrix in aging skin promotes melanoma metastasis and affects immune cell motility. *Cancer Discov.* 9, 64–81. doi:10.1158/2159-8290.CD-18-0193
- Kennedy, B. K., Austriaco, N. R., Jr., Zhang, J., and Guarente, L. (1995). Mutation in the silencing gene SIR4 can delay aging in *S. cerevisiae*. *Cell* 80, 485–496. doi:10.1016/0092-8674(95)90499-9
- Khosravi, N., Ostrowski, L. A., and Mekhail, K. (2019). Roles for non-coding RNAs in spatial genome organization. *Front. Cell Dev. Biol.* 7, 336. doi:10.3389/fcell.2019.00336
- Kojima, H., Inoue, T., Kunimoto, H., and Nakajima, K. (2013). IL-6-STAT3 signaling and premature senescence. *JAKSTAT* 2, e25763. doi:10.4161/jkst.25763
- Kokaze, A. (2005). Genetic epidemiological studies of longevity-associated mitochondrial DNA 5178 C/A polymorphism. *Environ. Health Prev. Med.* 10, 319–323. doi:10.1007/BF02898191
- Kosar, M., Bartkova, J., Hubackova, S., Hodny, Z., Lukas, J., Bartek, J., et al. (2011). Senescence-associated heterochromatin foci are dispensable for cellular senescence, occur in a cell type- and insult-dependent manner and follow expression of p16(ink4a). *Cell Cycle* 10, 457–468. doi:10.4161/cc.10.3.14707
- Larson, K., Yan, S. J., Tsurumi, A., Liu, J., Zhou, J., Gaur, K., et al. (2012). Heterochromatin formation promotes longevity and represses ribosomal RNA synthesis. *PLoS Genet.* 8, e1002473. doi:10.1371/journal.pgen.1002473
- Lee, J. H., Kim, E. W., Croteau, D. L., and Bohr, V. A. (2020). Heterochromatin: An epigenetic point of view in aging. *Exp. Mol. Med.* 52, 1466–1474. doi:10.1038/s12276-020-00497-4
- Li, G., and Reinberg, D. (2011). Chromatin higher-order structures and gene regulation. *Curr. Opin. Genet. Dev.* 21, 175–186. doi:10.1016/j.gde.2011.01.022
- Li, S., Peng, Y., Landsman, D., and Panchenko, A. R. (2022). DNA methylation cues in nucleosome geometry, stability and unwrapping. *Nucleic Acids Res.* 50, 1864–1874. doi:10.1093/nar/gkac097
- Li, Y., Liu, L., and Tollefsbol, T. O. (2010). Glucose restriction can extend normal cell lifespan and impair precancerous cell growth through epigenetic control of hTERT and p16 expression. *Faseb J.* 24, 1442–1453. doi:10.1096/fj.09-149328
- Lidzbarsky, G., Gutman, D., Shekhdem, H. A., Sharvit, L., and Atzmon, G. (2018). Genomic instabilities, cellular senescence, and aging: *In vitro*, *in vivo* and aging-like human syndromes. *Front. Med.* 5, 104. doi:10.3389/fmed.2018.00104
- Lindstrom, D. L., Leverich, C. K., Henderson, K. A., and Gottschling, D. E. (2011). Replicative age induces mitotic recombination in the ribosomal RNA gene cluster of *Saccharomyces cerevisiae*. *PLoS Genet.* 7, e1002015. doi:10.1371/journal.pgen.1002015
- Lindahl, T. (1976). New class of enzymes acting on damaged DNA. *Nature* 259, 64–66. doi:10.1038/259064a0

- Lombard, D. B., Chua, K. F., Mostoslavsky, R., Franco, S., Gostissa, M., Alt, F. W., et al. (2005). DNA repair, genome stability, and aging. *Cell* 120, 497–512. doi:10.1016/j.cell.2005.01.028
- Lowe, D. J., Herzog, M., Mosler, T., Cohen, H., Felton, S., Beli, P., et al. (2020). Chronic irradiation of human cells reduces histone levels and deregulates gene expression. *Sci. Rep.* 10, 2200. doi:10.1038/s41598-020-59163-4
- Machiela, M. J., and Chanock, S. J. (2017). The ageing genome, clonal mosaicism and chronic disease. *Curr. Opin. Genet. Dev.* 42, 8–13. doi:10.1016/j.gde.2016.12.002
- MacRae, S. L., Croken, M. M., Calder, R. B., Aliper, A., Milholland, B., White, R. R., et al. (2015). DNA repair in species with extreme lifespan differences. *Aging (Albany NY)* 7, 1171–1184. doi:10.18632/aging.100866
- Maehara, K., Takahashi, K., and Saitoh, S. (2010). CENP-A reduction induces a p53-dependent cellular senescence response to protect cells from executing defective mitoses. *Mol. Cell. Biol.* 30, 2090–2104. doi:10.1128/MCB.01318-09
- Mah, L. J., El-Osta, A., and Karagiannis, T. C. (2010). GammaH2AX as a molecular marker of aging and disease. *Epigenetics* 5, 129–136. doi:10.4161/epi.5.2.11080
- Malaquin, N., Vercamer, C., Bouali, F., Martien, S., Deruy, E., Wernert, N., et al. (2013). Senescent fibroblasts enhance early skin carcinogenic events via a paracrine MMP-PAR-1 axis. *PLoS One* 8, e63607. doi:10.1371/journal.pone.0063607
- Malik, H. S., and Henikoff, S. (2003). Phylogenomics of the nucleosome. *Nat. Struct. Biol.* 10, 882–891. doi:10.1021/cr500373h
- Maze, I., Wenderski, W., Noh, K. M., Bagot, R. C., Tzavaras, N., Purushothaman, I., et al. (2015). Critical role of histone turnover in neuronal transcription and plasticity. *Neuron* 87, 77–94. doi:10.1016/j.neuron.2015.06.014
- McGinty, R. K., and Tan, S. (2015). Nucleosome structure and function. *Chem. Rev.* 115, 2255–2273. doi:10.1021/cr500373h
- McHugh, D., and Gil, J. (2018). Senescence and aging: Causes, consequences, and therapeutic avenues. *J. Cell Biol.* 217, 65–77. doi:10.1083/jcb.201708092
- Medawar, P. B. (1952). *An unsolved problem of biology*. London: Published for the College by H.K. Lewis.
- Medawar, P. B. (1946). Old age and natural death. *Mod. Quart.* 2, 30–49.
- Melters, D. P., Pitman, M., Rakshit, T., Dimitriadis, E. K., Bui, M., Papoian, G. A., et al. (2019). Intrinsic elasticity of nucleosomes is encoded by histone variants and calibrated by their binding partners. *Proc. Natl. Acad. Sci. U. S. A.* 116, 24066–24074. doi:10.1073/pnas.1911880116
- Mikula-Pietrasik, J., Niklas, A., Uruski, P., Tykarski, A., and Ksiazek, K. (2020). Mechanisms and significance of therapy-induced and spontaneous senescence of cancer cells. *Cell. Mol. Life Sci.* 77, 213–229. doi:10.1007/s00018-019-03261-8
- Miyata, K., Imai, Y., Hori, S., Nishio, M., Loo, T. M., Okada, R., et al. (2021). Pericentromeric noncoding RNA changes DNA binding of CTCF and inflammatory gene expression in senescence and cancer. *Proc. Natl. Acad. Sci. U. S. A.* 118, e2025647118. doi:10.1073/pnas.2025647118
- Moorad, J. A., and Promislow, D. E. (2010). Evolution: Aging up a tree? *Curr. Biol.* 20, R406–R408. doi:10.1016/j.cub.2010.03.016
- Narita, M., Narita, M., Krizhanovsky, V., Nunez, S., Chicas, A., Hearn, S. A., et al. (2006). A novel role for high-mobility group proteins in cellular senescence and heterochromatin formation. *Cell* 126, 503–514. doi:10.1016/j.cell.2006.05.052
- Narita, M., Nuñez, S., Heard, E., Narita, M., Lin, A. W., Hearn, S. A., et al. (2003). Rb-mediated heterochromatin formation and silencing of E2F target genes during cellular senescence. *Cell* 113, 703–716. doi:10.1016/s0092-8674(03)00401-x
- O'Sullivan, R. J., Kubicek, S., Schreiber, S. L., and Karlseder, J. (2010). Reduced histone biosynthesis and chromatin changes arising from a damage signal at telomeres. *Nat. Struct. Mol. Biol.* 17, 1218–1225. doi:10.1038/nsmb.1897
- Oberdoerffer, P., and Sinclair, D. A. (2007). The role of nuclear architecture in genomic instability and ageing. *Nat. Rev. Mol. Cell Biol.* 8, 692–702. doi:10.1038/nrm2238
- Ocampo, A., Reddy, P., Martinez-Redondo, P., Platero-Luengo, A., Hatanaka, F., Hishida, T., et al. (2016). *In vivo* amelioration of age-associated hallmarks by partial reprogramming. *Cell* 167, 1719–1733. e12. doi:10.1016/j.cell.2016.11.052
- Ortiz-Montero, P., Londoño-Vallejo, A., and Vernot, J.-P. (2017). Senescence-associated IL-6 and IL-8 cytokines induce a self- and cross-reinforced senescence/inflammatory milieu strengthening tumorigenic capabilities in the MCF-7 breast cancer cell line. *Cell Commun. Signal.* 15, 17. doi:10.1186/s12964-017-0172-3
- Palm, W., and de Lange, T. (2008). How shelterin protects mammalian telomeres. *Annu. Rev. Genet.* 42, 301–334. doi:10.1146/annurev.genet.41.110306.130350
- Pan, M. R., Li, K., Lin, S. Y., and Hung, W. C. (2016). Connecting the dots: From DNA damage and repair to aging. *Int. J. Mol. Sci.* 17, E685. doi:10.3390/ijms17050685
- Peng, S., Guo, P., Lin, X., An, Y., Sze, K. H., Lau, M. H. Y., et al. (2021). CAG RNAs induce DNA damage and apoptosis by silencing NUDT16 expression in polyglutamine degeneration. *Proc. Natl. Acad. Sci. U. S. A.* 118, e2022940118. doi:10.1073/pnas.2022940118
- Petersen, S., Saretzki, G., and Zglinicki, T. V. (1998). Preferential accumulation of single-stranded regions in telomeres of human fibroblasts. *Exp. Cell Res.* 239, 152–160. doi:10.1006/excr.1997.3893
- Qin, W., Zhang, L., Li, Z., Xiao, D., Zhang, Y., Yang, H., et al. (2019). SIRT6-mediated transcriptional suppression of MALAT1 is a key mechanism for endothelial to mesenchymal transition. *Int. J. Cardiol.* 295, 7–13. doi:10.1016/j.ijcard.2019.07.082
- Santos Franco, S., Raveh-Amit, H., Kobilák, J., Alqahtani, M. H., Mobasher, A., Dinnyes, A., et al. (2015). The crossroads between cancer stem cells and aging. *BMC Cancer* 15 (Suppl. 1), S1. doi:10.1186/1471-2407-15-S1-S1
- Sadaie, M., Salama, R., Carroll, T., Tomimatsu, K., Chandra, T., Young, A. R., et al. (2013). Redistribution of the Lamin B1 genomic binding profile affects rearrangement of heterochromatic domains and SAHF formation during senescence. *Genes Dev.* 27, 1800–1808. doi:10.1101/gad.217281.113
- Sakasai, R., and Tibbetts, R. (2008). RNF8-dependent and RNF8-independent regulation of 53BP1 in response to DNA damage. *J. Biol. Chem.* 283, 13549–13555. doi:10.1074/jbc.M710197200
- Scaffidi, P., and Misteli, T. (2006a). Lamin A-dependent nuclear defects in human aging. *Science* 312, 1059–1063. doi:10.1126/science.1127168
- Scaffidi, P., and Misteli, T. (2006b). Good news in the nuclear envelope: Loss of lamin A might be a gain. *J. Clin. Invest.* 116, 632–634.
- Sekeri-Pataryas, K. E., and Sourlingas, T. G. (2007). The differentiation-associated linker histone, H1.0, during the *in vitro* aging and senescence of human diploid fibroblasts. *Ann. N. Y. Acad. Sci.* 1100, 361–367. doi:10.1196/annals.1395.039
- Seluanov, A., Gladyshev, V. N., Vijg, J., and Gorbunova, V. (2018). Mechanisms of cancer resistance in long-lived mammals. *Nat. Rev. Cancer* 18, 433–441. doi:10.1038/s41568-018-0004-9
- Sen, P., Lan, Y., Li, C. Y., Sidoli, S., Donahue, G., Dou, Z., et al. (2019). Histone acetyltransferase p300 induces de novo super-enhancers to drive cellular senescence. *Mol. Cell* 73, 684–698. e8. doi:10.1016/j.molcel.2019.01.021
- Serrano, M. (2015). SHP2: A new target for pro-senescence cancer therapies. *EMBO J.* 34, 1439–1441. doi:10.15252/embj.201591616
- Shay, J. W., and Wright, W. E. (2000). The use of telomerized cells for tissue engineering. *Nat. Biotechnol.* 18, 22–23. doi:10.1038/71872
- Short, B. (2013). Senescent cells have a case of the SADS. *J. Cell Biol.* 203, 866. doi:10.1083/jcb.203611
- Shumaker, D. K., Dechat, T., Kohlmaier, A., Adam, S. A., Bozovsky, M. R., Erdos, M. R., et al. (2006). Mutant nuclear lamin A leads to progressive alterations of epigenetic control in premature aging. *Proc. Natl. Acad. Sci. U. S. A.* 103, 8703–8708. doi:10.1073/pnas.0602569103
- Sinclair, D. A., and Oberdoerffer, P. (2009). The ageing epigenome: Damaged beyond repair? *Ageing Res. Rev.* 8, 189–198. doi:10.1016/j.arr.2009.04.004
- Sinclair, D. A. (2005). Toward a unified theory of caloric restriction and longevity regulation. *Mech. Ageing Dev.* 126, 987–1002. doi:10.1016/j.mad.2005.03.019
- Soes, S., Dugaard, I. L., Sørensen, B. S., Carus, A., Mattheisen, M., Alsner, J., et al. (2014). Hypomethylation and increased expression of the putative oncogene ELMO3 are associated with lung cancer development and metastases formation. *Oncoscience* 1, 367–374. doi:10.18632/oncoscience.42
- Stefanelli, G., Azam, A. B., Walters, B. J., Brimble, M. A., Gettens, C. P., Bouchard-Cannon, P., et al. (2018). Learning and age-related changes in genome-wide H2A.Z binding in the mouse Hippocampus. *Cell Rep.* 22, 1124–1131. doi:10.1016/j.celrep.2018.01.020
- Stucki, M., Clapperton, J. A., Mohammad, D., Yaffe, M. B., Smerdon, S. J., Jackson, S. P., et al. (2005). MDC1 directly binds phosphorylated histone H2AX to regulate cellular responses to DNA double-strand breaks. *Cell* 123, 1213–1226. doi:10.1016/j.cell.2005.09.038
- Swanson, E. C., Manning, B., Zhang, H., and Lawrence, J. B. (2013). Higher-order unfolding of satellite heterochromatin is a consistent and early event in cell senescence. *J. Cell Biol.* 203, 929–942. doi:10.1083/jcb.201306073
- Swanson, E. C., Rapkin, L. M., Bazett-Jones, D. P., and Lawrence, J. B. (2015). Unfolding the story of chromatin organization in senescent cells. *Nucleus* 6, 254–260. doi:10.1080/19491034.2015.1057670

- Tang, M. C., Jacobs, S. A., Mattiske, D. M., Soh, Y. M., Graham, A. N., Tran, A., et al. (2015). Contribution of the two genes encoding histone variant h3.3 to viability and fertility in mice. *PLoS Genet.* 11, e1004964. doi:10.1371/journal.pgen.1004964
- Thompson, L. H. (2012). Recognition, signaling, and repair of DNA double-strand breaks produced by ionizing radiation in mammalian cells: The molecular choreography. *Mutat. Res.* 751, 158–246. doi:10.1016/j.mrrev.2012.06.002
- Toso, A., Revandkar, A., Di Mitri, D., Guccini, I., Proietti, M., Sarti, M., et al. (2014). Enhancing chemotherapy efficacy in Pten-deficient prostate tumors by activating the senescence-associated antitumor immunity. *Cell Rep.* 9, 75–89. doi:10.1016/j.celrep.2014.08.044
- Tsurumi, A., and Li, W. X. (2012). Global heterochromatin loss: A unifying theory of aging? *Epigenetics* 7, 680–688. doi:10.4161/epi.20540
- Tvardovskiy, A., Schwämmle, V., Kempf, S. J., Rogowska-Wrzesinska, A., and Jensen, O. N. (2017). Accumulation of histone variant H3.3 with age is associated with profound changes in the histone methylation landscape. *Nucleic Acids Res.* 45, 9272–9289. doi:10.1093/nar/gkx696
- Tyner, S. D., Venkatachalam, S., Choi, J., Jones, S., Ghebranious, N., Igelmann, H., et al. (2002). p53 mutant mice that display early ageing-associated phenotypes. *Nature* 415, 45–53. doi:10.1038/415045a
- Ussery, D., Schou Larsen, T., Trevor Wilkes, K., Friis, C., Worning, P., Krogh, A., et al. (2001). Genome organisation and chromatin structure in *Escherichia coli*. *Biochimie* 83, 201–212. doi:10.1016/s0300-9084(00)01225-6
- Uziel, T., Lerenthal, Y., Moyal, L., Andegeko, Y., Mittelman, L., Shiloh, Y., et al. (2003). Requirement of the MRN complex for ATM activation by DNA damage. *EMBO J.* 22, 5612–5621. doi:10.1093/emboj/cdg541
- Vaiserman, A., and Krasnienkov, D. (2021). Telomere length as a marker of biological age: State-of-the-Art, open issues, and future perspectives. *Front. Genet.* 11, 630186. doi:10.3389/fgene.2020.630186
- Villeponteau, B. (1997). The heterochromatin loss model of aging. *Exp. Gerontol.* 32, 383–394. doi:10.1016/s0531-5565(96)00155-6
- Weidner, C. I., Lin, Q., Koch, C. M., Eisele, L., Beier, F., Ziegler, P., et al. (2014). Aging of blood can be tracked by DNA methylation changes at just three CpG sites. *Genome Biol.* 15, R24. doi:10.1186/gb-2014-15-2-r24
- West, J. A., Davis, C. P., Sunwoo, H., Simon, M. D., Sadreyev, R. I., Wang, P. I., et al. (2014). The long noncoding RNAs NEAT1 and MALAT1 bind active chromatin sites. *Mol. Cell* 55, 791–802. doi:10.1016/j.molcel.2014.07.012
- White, M. F., and Allers, T. (2018). DNA repair in the archaea—An emerging picture. *FEMS Microbiol. Rev.* 42, 514–526. doi:10.1093/femsre/fuy020
- Williams, G. C. (1957). Pleiotropy, natural selection, and the evolution of senescence. *Evolution* 11, 398. doi:10.2307/2406060
- Wood, J. G., and Helfand, S. L. (2013). Chromatin structure and transposable elements in organismal aging. *Front. Genet.* 4, 274. doi:10.3389/fgene.2013.00274
- Worman, H. J., and Michaelis, S. (2018). Permanently farnesylated prelamin A, progeria, and atherosclerosis. *Circulation* 138, 283–286. doi:10.1161/CIRCULATIONAHA.118.034480
- Wu, D., and Prives, C. (2018). Relevance of the p53–MDM2 axis to aging. *Cell Death Differ.* 25, 169–179. doi:10.1038/cdd.2017.187
- Yancik, R. (1997). Cancer burden in the aged: An epidemiologic and demographic overview. *Cancer* 80, 1273–1283. doi:10.1002/(sici)1097-0142(19971001)80:7<1273::aid-cnrcr13>3.0.co;2-4
- Yao, C., Joehanes, R., Johnson, A. D., Huan, T., Esko, T., Ying, S., et al. (2013). Sex- and age-interacting eQTLs in human complex diseases. *Hum. Mol. Genet.* 23, 1947–1956. doi:10.1093/hmg/ddt582
- Ye, X., Zerlanko, B., Zhang, R., Somaiah, N., Lipinski, M., Salomoni, P., et al. (2007). Definition of pRB- and p53-dependent and -independent steps in HIRA/ASF1a-Mediated formation of senescence-associated heterochromatin foci. *Mol. Cell. Biol.* 27, 2452–2465. doi:10.1128/MCB.01592-06
- Yi, S. J., and Kim, K. (2018). Histone tail cleavage as a novel epigenetic regulatory mechanism for gene expression. *BMB Rep.* 51, 211–218.
- Zhang, H., Xu, R., Li, B., Xin, Z., Ling, Z., Zhu, W., et al. (2022). LncRNA NEAT1 controls the lineage fates of BMSCs during skeletal aging by impairing mitochondrial function and pluripotency maintenance. *Cell Death Differ.* 29, 351–365. doi:10.1038/s41418-021-00858-0
- Zhang, R., Chen, W., and Adams, P. D. (2007). Molecular dissection of formation of senescence-associated heterochromatin foci. *Mol. Cell. Biol.* 27, 2343–2358. doi:10.1128/MCB.02019-06
- Zhang, R., Poustovoitov, M. V., Ye, X., Santos, H. A., Chen, W., Daganzo, S. M., et al. (2005). Formation of MacroH2A-containing senescence-associated heterochromatin foci and senescence driven by ASF1a and HIRA. *Dev. Cell* 8, 19–30. doi:10.1016/j.devcel.2004.10.019
- Zhang, W., Li, J., Suzuki, K., Qu, J., Wang, P., Zhou, J., et al. (2015). Aging stem cells. A Werner syndrome stem cell model unveils heterochromatin alterations as a driver of human aging. *Science* 348, 1160–1163. doi:10.1126/science.aaa1356
- Zhang, W., Qu, J., Liu, G. H., and Belmonte, J. C. I. (2020). The ageing epigenome and its rejuvenation. *Nat. Rev. Mol. Cell Biol.* 21, 137–150. doi:10.1038/s41580-019-0204-5



OPEN ACCESS

APPROVED BY

Frontiers Editorial Office,
Frontiers Media SA, Switzerland

*CORRESPONDENCE

Frontiers Production Office,
production.office@frontiersin.org

SPECIALTY SECTION

This article was submitted to Nuclear Organization and Dynamics, a section of the journal Frontiers in Cell and Developmental Biology

RECEIVED 24 August 2022

ACCEPTED 24 August 2022

PUBLISHED 13 September 2022

CITATION

Frontiers Production Office (2022),
Erratum: Breaking the aging
epigenetic barrier.
Front. Cell Dev. Biol. 10:1027162.
doi: 10.3389/fcell.2022.1027162

COPYRIGHT

© 2022 Frontiers Production Office.
This is an open-access article
distributed under the terms of the
[Creative Commons Attribution License](https://creativecommons.org/licenses/by/4.0/)
(CC BY). The use, distribution or
reproduction in other forums is
permitted, provided the original
author(s) and the copyright owner(s) are
credited and that the original
publication in this journal is cited, in
accordance with accepted academic
practice. No use, distribution or
reproduction is permitted which does
not comply with these terms.

Erratum: Breaking the aging epigenetic barrier

Frontiers Production Office*

Frontiers Media SA, Lausanne, Switzerland

KEYWORDS

senescence, histone variants, chromatin dynamics, cancer, nucleosomes

An erratum on

[Breaking the aging epigenetic barrier](https://doi.org/10.3389/fcell.2022.943519)

by Sikder S, Arunkumar G, Melters DP and Dalal Y (2022) *Front. Cell Dev. Biol.* 10:943519. doi: [10.3389/fcell.2022.943519](https://doi.org/10.3389/fcell.2022.943519)

Due to a production error, the umlaut in author Daniël P. Melters' name was omitted.
The publisher apologizes for this mistake.

The original version of this article has been updated.



OPEN ACCESS

EDITED BY

Joanna M. Bridger,
Brunel University London,
United Kingdom

REVIEWED BY

Hengbin Wang,
Virginia Commonwealth University,
United States
Ines Castro,
Heidelberg University Hospital,
Germany

*CORRESPONDENCE

Ulrike A. Nuber,
nuber@bio.tu-darmstadt.de
M. Cristina Cardoso,
cardoso@bio.tu-darmstadt.de

[†]These authors have contributed equally
to this work

SPECIALTY SECTION

This article was submitted to Nuclear
Organization and Dynamics,
a section of the journal
Frontiers in Cell and Developmental
Biology

RECEIVED 11 May 2022

ACCEPTED 19 August 2022

PUBLISHED 12 September 2022

CITATION

Schmidt A, Frei J, Poetsch A, Chittka A,
Zhang H, Aßmann C, Lehmkuhl A,
Bauer U-M, Nuber UA and Cardoso MC
(2022), MeCP2 heterochromatin
organization is modulated by arginine
methylation and
serine phosphorylation.
Front. Cell Dev. Biol. 10:941493.
doi: 10.3389/fcell.2022.941493

COPYRIGHT

© 2022 Schmidt, Frei, Poetsch, Chittka,
Zhang, Aßmann, Lehmkuhl, Bauer,
Nuber and Cardoso. This is an open-
access article distributed under the
terms of the [Creative Commons
Attribution License \(CC BY\)](#). The use,
distribution or reproduction in other
forums is permitted, provided the
original author(s) and the copyright
owner(s) are credited and that the
original publication in this journal is
cited, in accordance with accepted
academic practice. No use, distribution
or reproduction is permitted which does
not comply with these terms.

MeCP2 heterochromatin organization is modulated by arginine methylation and serine phosphorylation

Annika Schmidt¹, Jana Frei^{2†}, Ansgar Poetsch^{3,4,5†},
Alexandra Chittka^{6,7}, Hui Zhang¹, Chris Aßmann⁸,
Anne Lehmkuhl¹, Uta-Maria Bauer⁸, Ulrike A. Nuber^{2*} and
M. Cristina Cardoso^{1*}

¹Cell Biology and Epigenetics, Department of Biology, Technical University of Darmstadt, Darmstadt, Germany, ²Stem Cell and Developmental Biology, Department of Biology, Technical University of Darmstadt, Darmstadt, Germany, ³Queen Mary School, Medical College, Nanchang University, Nanchang, China, ⁴Plant Biochemistry, Ruhr University Bochum, Bochum, Germany, ⁵College of Marine Life Sciences, Ocean University of China, Qingdao, China, ⁶Division of Medicine, The Wolfson Institute for Biomedical Research, University College London, London, United Kingdom, ⁷Department of Neuromuscular Diseases, Queen Square Institute of Neurology, University College London, London, United Kingdom, ⁸Institute of Molecular Biology and Tumor Research, Philipps University Marburg, Marburg, Germany

Rett syndrome is a human intellectual disability disorder that is associated with mutations in the X-linked *MECP2* gene. The epigenetic reader MeCP2 binds to methylated cytosines on the DNA and regulates chromatin organization. We have shown previously that *MECP2* Rett syndrome missense mutations are impaired in chromatin binding and heterochromatin reorganization. Here, we performed a proteomics analysis of post-translational modifications of MeCP2 isolated from adult mouse brain. We show that MeCP2 carries various post-translational modifications, among them phosphorylation on S80 and S421, which lead to minor changes in either heterochromatin binding kinetics or clustering. We found that MeCP2 is (di)methylated on several arginines and that this modification alters heterochromatin organization. Interestingly, we identified the Rett syndrome mutation site R106 as a dimethylation site. In addition, co-expression of protein arginine methyltransferases (PRMT1 and PRMT6) lead to a decrease of heterochromatin clustering. Altogether, we identified and validated novel modifications of MeCP2 in the brain and show that these can modulate its ability to bind as well as reorganize heterochromatin, which may play a role in the pathology of Rett syndrome.

KEYWORDS

arginine (di)methylation, heterochromatin organization, MeCP2, protein arginine methyltransferases, Rett syndrome

Highlights

- 1) MeCP2 from mouse brain is methylated on arginines and phosphorylated on serines
- 2) Phosphorylation on serine 80 increases MeCP2 chromatin binding kinetics
- 3) Phosphorylation on serine 421 increases chromatin clustering
- 4) MeCP2 is arginine methylated on R91, R162, R167, and this modulates heterochromatin organization
- 5) R106 is dimethylated and its mutation results in reduced DNA binding and heterochromatin clustering abilities

1 Introduction

The methyl-CpG-binding protein 2 (MeCP2) is the founding member of the methyl-CpG binding domain (MBD) protein family and specifically binds to methylated CpGs *via* its MBD. As DNA methylation is mainly found on the less transcriptionally active heterochromatin, MeCP2 is prominently localized *in vivo* at pericentric chromatin regions, which contain highly methylated major satellite DNA repeats (Lewis et al., 1992). In addition to the MBD, MeCP2 contains a transcriptional repression domain (TRD) (Nan et al., 1997), the interdomain region (ID) and, more recently, the N-CoR/SMRT interacting domain (NID) has also been mapped (Lyst et al., 2013). MeCP2 binds to multiple interaction partners *via* these regions (reviewed in (Schmidt et al., 2020)). Several of the interacting partners are components of transcriptional repression complexes, for example Sin3A, HDAC and N-CoR (Jones et al., 1998; Nan et al., 1998; Kokura et al., 2001; Lunyak et al., 2002; Lyst et al., 2013). MeCP2 might also be involved in transcriptional activation as it associates with CREB1 (Chahrour et al., 2008). Aside from the MBD, which shows structurally conserved motifs, MeCP2 was reported to be an intrinsically disordered protein (Adams et al., 2007).

In mouse cells, pericentric heterochromatin from different chromosomes forms densely packed chromatin clusters in interphase called chromocenters ((Baccarini, 1908), see review (Jost et al., 2012)). Increased MeCP2 levels, either occurring during cell differentiation or upon exogenous expression of fusion protein constructs, cause large-scale reorganization of heterochromatin, which can be visualized as fusion events of heterochromatin clusters in mouse cells (Brero et al., 2005; Agarwal et al., 2007; Bertulat et al., 2012). As constitutive heterochromatin has been shown to organize chromosomes within the cell nucleus (Falk et al., 2019), its reorganization has potential impact on the general chromosome distribution. Recently, we and others proposed that heterochromatin cluster fusion events might be mediated by liquid-liquid phase separation (Larson et al., 2017; Strom et al., 2017), as MeCP2 was shown to undergo phase separation under physiological conditions (Fan et al., 2020; Wang et al., 2020;

Zhang et al., 2022). MeCP2 shows characteristic properties of phase separating proteins including intrinsically disordered regions and multivalency, and it was reported to interact with itself and several other interaction partners *via* regions outside of the MBD (Becker et al., 2013).

Mutations in the *MECP2* gene were linked to Rett syndrome, a human neurological disorder affecting mainly females, that is associated with intellectual disability among other symptoms (Amir et al., 1999). *MECP2* mutations in males can lead to a wide spectrum of phenotypes ranging from mild intellectual impairment to severe neonatal encephalopathy and premature death (Inuzuka et al., 2021). Missense mutations in the MBD domain of *MECP2* affect heterochromatin accumulation due to reduced DNA binding ability, but also heterochromatin clustering (Agarwal et al., 2011). The clustering function of some mutations could be rescued by retargeting MeCP2 to heterochromatin (Casas-Delucchi et al., 2012).

Importantly, MeCP2 is post-translationally modified and although many modifications have been identified, only a few were validated and functionally characterized (reviewed in (Bellini et al., 2014; Schmidt et al., 2020)). The phosphorylation of serine 421 in the C-terminal domain of MeCP2 was identified upon neuronal activity and stress exclusively in the brain, indicating a specific function under this condition (Zhou et al., 2006; Tao et al., 2009). Serine 80 phosphorylation in the N-terminal domain of MeCP2 was found in mouse and rat brain (Tao et al., 2009). Serine to alanine mutated knock-in mice of both modification sites were reported to display opposing phenotypes, as S421A mice show increased, whereas S80A mice show decreased locomotor activity. In line with these results, membrane depolarization in cortical neurons results in dephosphorylation of serine 80 and phosphorylation of serine 421. Interestingly, the S80A mutation results in a decrease of MeCP2 chromatin binding affinity to *Pomc* and *Gtl2* promoters evaluated by ChIP-qPCR but did not lead to significant changes in gene transcription (Tao et al., 2009). Besides, MeCP2 was found to be poly(ADP-ribosyl)ated in mouse brain tissue at ID and TRD, and this led to decreased DNA binding and heterochromatin clustering (Becker et al., 2016).

In this study, we aimed to identify post-translational modifications of MeCP2 from mouse brain (*in vivo*) and determine whether these modifications are involved in MeCP2 chromatin binding and clustering. 23% of the MeCP2 protein is composed of positively charged amino acids and we found only a few modified arginines compared to many modified lysines. In addition, we identified several phosphorylated serine and threonine residues, including the previously reported S80 and S421. We show that arginine methylation and to a much lesser extent also serine phosphorylation affect heterochromatin accumulation and binding kinetics and MeCP2 heterochromatin clustering function. In addition, coexpression of MeCP2 variants and the

protein arginine methyltransferase 6 (PRMT6) reveals differences in heterochromatin clustering.

2 Materials and methods

2.1 Nuclei isolation from mouse brains

3-month-old C57BL/6 mice (Charles River Laboratories, Inc., Wilmington, MA) were sacrificed according to the animal care and use regulations (Government of Hessen, Germany), and the organs were collected from the sacrificed animals, washed with PBS and frozen in liquid nitrogen. For nuclei isolation the frozen mouse brains were crushed to powder and homogenized in 0.25 M sucrose solution (20 mM triethanolamine-HCl (pH 7.6), 30 mM KCl, 10 mM MgCl₂, 1 mM DTT, 1 mM PMSF). After centrifugation for 10 min at 1,000 × g, the supernatant was discarded and the pellet resuspended in sucrose buffer to a final sucrose concentration of 2.1 M. The raw nuclei fraction was obtained by ultracentrifugation for 30 min at 50,000 × g. The pellet was resuspended in 0.25 M sucrose solution and centrifuged at 1,000 × g. During the procedure, samples were taken after resuspension of the tissue, after homogenization and after nuclei isolation, fixed with 3.7% formaldehyde in solution for 15 min, dropped on slides, dried and counterstained with 4',6-diamidino-2-phenylindole (DAPI) for microscopic examination of the individual steps.

2.2 Protein enrichment

For the MeCP2 enrichment from mouse brain tissue we made use of its natural hepta-histidine tag for protein pull-down with Ni-IDA beads (His60 Ni Superflow resin, Clontech Laboratories, Inc., Mountain View, CA). First, 10⁷ mouse brain nuclei in PBS were pelleted by centrifugation at 1,000 × g for 10 min. The nuclei were resuspended in buffer B (0.2% Triton X-100, 50 mM triethanolamine-HCl (pH 7.6), 5 mM MgCl₂), incubated on ice for 10 min and centrifuged at 1,000 × g for 10 min. The supernatant was discarded and the pellet washed three times by resuspension in 100 µl buffer C (2 mM triethanolamine-HCl (pH 7.6), 0.5 mM MgCl₂) and centrifugation for 10 min at 1,000 × g. The pellet was resuspended in 500 µl 1 M NaCl equilibration buffer (50 mM sodium phosphate, 20 mM imidazole, pH 7.4), followed by sonication 3 × 20 s (250–450 Sonicator, BRANSON ultrasonic corporation, Danbury, CT) with microscopic control after each step. Subsequently, the lysate was diluted using 500 µl equilibration buffer without NaCl and added to the Nickel-Iminodiacetic acid (Ni-IDA) beads for incubation overnight at 4°C with rotation. The beads were washed with 300 mM NaCl equilibration buffer, then

with wash buffer (50 mM sodium phosphate, 300 mM NaCl, 40 mM imidazole, pH 7.4). The Ni-IDA beads were then resuspended in Laemmli buffer (2% SDS, 50 mM Tris (pH 6.8), 10% glycerol, 0.01% bromophenol blue, 100 mM DTT), incubated at 95°C for 10 min and separated using sodium dodecylsulfate polyacrylamide gel electrophoresis (SDS-PAGE). The protein enrichment from *E. coli* BL21 (DE3) was performed using the pTYB1-MeCP2wt plasmid coding for MeCP2 with a C-terminal intein-CBD tag allowing protein binding to chitin beads and subsequent elution by cleavage as described before (Zhang et al., 2022).

2.3 Mass spectrometry

The samples to be analyzed by mass spectrometry were analyzed by SDS-PAGE and the gel was stained with Coomassie staining solution (5% aluminium sulfate-(14)-(18)-hydrate, 10% ethanol p.a., 0.02% CBB-G250 (Coomassie brilliant blue), 2% orthophosphoric acid (Dybala and Metzger, 2009)) over night. The in-gel tryptic digestion was performed as described before (Cerletti et al., 2015). Briefly, the gel was destained using Coomassie destaining solution (10% ethanol p.a., 2% orthophosphoric acid, LC-MS grade) two times for 10 min, equilibrated in ddH₂O (MS grade), the bands of interest were excised, cut to small cubes and dried using a vacuum concentrator. For destaining the gel pieces were covered with destaining solution (40 mM ammonium bicarbonate, 50% acetonitrile, LC-MS grade), incubated at 37°C for 30 min with shaking and the solution was removed. Destaining was repeated at least two times and the gel pieces were dried using a vacuum concentrator. For trypsin digestion the gel pieces were covered with 12.5 ng/µl trypsin (sequencing grade modified trypsin, V5111, Promega Corporation, Madison, WI) in 40 mM ammonium bicarbonate and incubated at 37°C with shaking overnight. The peptides were eluted by adding elution solution (50% acetonitrile, 0.5% trifluoroacetic acid, LC-MS grade), incubation for 20 min in an ultrasonic bath, transfer of the peptide solution to a new tube and drying using a vacuum concentrator. Samples were resuspended in 20 µl buffer (0.1% formic acid in 2% acetonitrile, LC-MS grade), incubated in an ultrasonic bath for 5 min and transferred to HPLC vials. Subsequent drying of the samples in a vacuum concentrator allowed storage at room temperature in the dark until the measurement.

The HPLC-MS/MS measurement was performed with the setup described before (Cerletti et al., 2015). Briefly, an UPLC HSS T3 column and an UPLC Symmetry C18 trapping column for LC were used in combination with the nanoACQUITY gradient UPLC pump system (Waters, Milford, MA) coupled to a LTQ Orbitrap Elite mass spectrometer (Thermo Fisher Scientific, Waltham, MA). The LTQ Orbitrap Elite was operated in a data-dependent mode using Xcalibur software

either in collision-induced dissociation (CID) TOP20 or in TOP10 with high-energy collisional dissociation (HCD) and CID fragmentation for every precursor ion. For elution of the peptides a linear gradient from 5%–30% for 60 min (CID TOP20) or 150 min (TOP10 HCD, CID) of buffer B (0.1 formic acid in acetonitrile, UPLC/MS grade) was applied, followed by a step gradient from 30%–85% acetonitrile for 5 min at a flow rate of 400 nl/min.

Data analysis was performed using Proteome discoverer 1.3 (Thermo Fisher Scientific) with SEQUEST (Eng et al., 1994) and MaxQuant (version 2.0.3.0) with Andromeda (Tyanova et al., 2016) algorithms searching against the complete UniProt database (UniProt Consortium, 2021) for *Mus musculus*. A maximum of two missed tryptic cleavages was accepted and methionine oxidation, N-terminal acetylation, N-terminal pyroglutamate, lysine acetylation, lysine ubiquitination, lysine and arginine mono-methylation or di-methylation and serine/threonine/tyrosine phosphorylation were set as variable modifications. To identify all methylation and dimethylation sites, the search was repeated including either only lysine/arginine methylation or dimethylation. The MaxQuant search was run with default parameters having matching between runs enabled.

2.4 Plasmids

All plasmids used in this study are listed in [Supplementary Table S1](#). The tetracycline inducible (Tet-On® 3G) pmMeCP2 wt expression plasmid was assembled from several plasmids: pEGFP-N1_MeCP2(WT) was a gift from Adrian Bird (Addgene plasmid #110186; <http://n2t.net/addgene:110186>; RRID:Addgene_110186) (Tillotson et al., 2017), AAVS1-TRE3G-EGFP was a gift from Su-Chun Zhang (Addgene plasmid #52343; <http://n2t.net/addgene:52343>; RRID:Addgene_52343) (Qian et al., 2014), HSC1-HS4-GiP was a gift from James Ellis (Addgene plasmid #58540; <http://n2t.net/addgene:58540>; RRID:Addgene_58540) (Rival-Gervier et al., 2013), pSpCas9(BB)-2A-Puro (PX459) V2.0 was a gift from Feng Zhang (Addgene plasmid #62988; <http://n2t.net/addgene:62988>; RRID:Addgene_62988) (Ran et al., 2013). The linker peptide as well as additionally required restriction sites were added during PCR amplification using accordingly designed primers ([Supplementary Table S2](#)). Three HS4 insulators were inserted flanking the cDNA sequence of *Mecp2-EGFP* under the control of the TRE3G promoter and flanking the Tet-On® 3G expression cassette under control of the CAG promoter to reduce leaky expression of *Mecp2-EGFP*. All cDNA sequences for MeCP2 modification site mutants were generated using overlap extension PCR (Heckman and Pease, 2007) with the primers listed in [Supplementary Table S2](#). Mutant *Mecp2* cDNA sequences (PCR products) were inserted into pmMeCP2G wt to replace WT *Mecp2* cDNA through a cloning step using unique

restriction sites of SalI and BamHI. The pTYP1-MeCP2wt plasmid used for bacterial expression was a gift from Christopher L. Woodcock (Georgel et al., 2003).

For the cloning of *hPRMT1*, the cDNA of PRMT1 transcript variant 2 (Goulet et al., 2007) was generated as a gBlock with an artificial nucleotide sequence due to gBlock optimization. The gBlock and pcDNA3.1 vector were digested with HindIII and XhoI and subsequently ligated to obtain the phPRMT1-pcDNA3.1 plasmid. The *mPRMT4* cDNA fragment was amplified by PCR from pSG5-HA_PRMT4 (Chen et al., 1999) and subsequently cloned *via* EcoRI and XhoI into pcDNA3.1. The *hPRMT5* transcript variant 1 (NM_006109) sequence was obtained by PCR using hPRMT5-fwd and hPRMT5-rev primers generating BamHI and EcoRI sites, which enabled cloning of *PRMT5* into pcDNA3.1.

2.5 Cell culture and transfection

C2C12 mouse myoblast cells (female), MTF mouse tail fibroblast (male) MeCP2 ^{-/-} cells (see [Supplementary Table S3](#)) and human embryonic kidney (HEK) 293T cells (female) were grown in Dulbecco's modified Eagle Medium (DMEM) with high glucose (#D6429, Sigma-Aldrich, St. Louis, MO) supplemented with 20% (C2C12) or 10% (MTF ^{-/-}, HEK293T) fetal bovine serum (#F7524, Sigma-Aldrich), 1x glutamine (#G7513, Sigma-Aldrich) and 1 μM gentamicin (#G1397, Sigma-Aldrich) at 37°C and 5% CO₂ in a humidified incubator. *Mycoplasma* tests were performed regularly and all cell lines are listed in [Supplementary Table S3](#). C2C12 cells were tested for the ability to differentiate to myotubes, MTF ^{-/-} cells were proven to be MeCP2 negative by immunofluorescence staining and HEK293T cells were authenticated by STR profiling.

Transient transfections of C2C12 and MTF ^{-/-} cells were performed using the Neon transfection System (Thermo Fisher Scientific, Waltham, MA) according to the manufacturer's instructions. For cotransfections of MeCP2 mutants and PRMTs a plasmid amount ratio of 1:5 (2 μg, 10 μg) was used. After transfection, cells were seeded on gelatin-coated coverslips and grown at 37°C and 5% CO₂ in a humidified incubator. 7 h after transfection, cells were washed with PBS and transcription was induced by adding medium supplemented with 2 μM tetracycline. 20 h after induction, cells were washed with PBS and fixed either with ice cold methanol for 6 min (MTF ^{-/-}) or with 3.7% formaldehyde (C2C12) for 15 min. HEK293T cells were transfected using polyethylenimine (PEI, Sigma-Aldrich) as described previously (Agarwal et al., 2007).

2.6 Protein salt extraction

C2C12 cells were transfected with plasmids expressing MeCP2-WT, S80D, or 3L and treated 7 h with 1 μg/ml

tetracycline followed by incubation for 20 h. The cells were harvested by trypsinization, washed using PBS, counted, and aliquoted into four tubes with the same cell number. Cells were resuspended in 100 μ l lysis buffer (20 mM Tris-HCl, pH 8.0, 0.5 mM EDTA, 0.5% NP-40, protease inhibitors, and 150, 450, 600, or 1,000 mM NaCl separately). Cells were lysed by syringe treatment (21G needle, 20 strokes), followed by 25 min incubation on ice. The lysate was collected by centrifugation at $4,600 \times g$ for 15 min at 4°C. The pellet was dissolved in 2% SDS in water. Both lysate and pellet were mixed with Laemmli buffer, and boiled at 95°C for 5 min before Western blot analysis.

2.7 Western blot analysis

Mouse brain nuclei were lysed in Laemmli buffer (see above), mechanically disrupted and incubated for 5 min at 95°C. The samples were analyzed by SDS-PAGE and transferred to a nitrocellulose membrane using a semi-dry blotting system at 25 V for 35 min. For detection of post-translational modifications, membranes were blocked with 5% BSA in TBS-T (0.1% Tween 20 in TBS) for 1 h and incubated with anti-PTM antibody diluted in TBS-T (antibodies and dilutions are listed in [Supplementary Table S4](#)) at 4°C with shaking overnight. Membranes were washed three times with TBS, blocked for 30 min with 5% low-fat milk in PBS and incubated overnight with anti-MeCP2 monoclonal rat antibody mix (4H7, 4G10, 4E1 undiluted, ([Jost et al., 2011](#))). After three washing steps with 0.1% PBST (0.1% Tween 20 in PBS), membranes were incubated with Cy3-conjugated anti-rat IgG secondary antibody diluted 1:1,000 in 3% milk in PBS for 1 h, washed three times with PBST and the fluorescent signal for MeCP2 was detected using Amersham AI600 imager (see [Supplementary Table S5](#)). Subsequently, membranes were incubated with HRP-coupled secondary antibodies (either rabbit or mouse IgG) diluted in 3% milk for 1 h, washed three times with PBST, stained with ECL solution (Clarity Western ECL substrate, #1705061, Bio-Rad, Hercules, CA) and the chemiluminescence signal for the PTMs detected using an Amersham AI600 imager.

All other Western blots were performed similarly to MeCP2 detection. Briefly, membranes were blocked for 30 min with 5% low-fat milk in PBS, incubated with primary antibody diluted in 5% low-fat milk overnight at 4°C shaking, washed three times with PBST, incubated 1 h at room temperature with secondary antibody diluted in 3% low-fat milk, washed three times with PBST and signals were detected using an Amersham imager.

2.8 Immunofluorescence staining

After fixation either with ice cold methanol for 6 min (MTF -/y) or with 3.7% formaldehyde (C2C12) for 15 min and washing

with PBS, cells were permeabilized with 0.7% Triton X-100 in PBS for 20 min and washed three times with 0.01% PBST. Cells were either directly stained with DAPI or blocked with 2% BSA in PBST for 20 min and incubated with primary antibody diluted in 2% BSA in PBST for 2 h (primary and secondary antibodies with their respective dilutions are listed in [Supplementary Table S4](#)). After washing three times with 0.1% PBST, secondary antibody in 2% BSA was applied for 1 h in the dark, followed by three times washing with 0.1% PBST, 12 min DAPI staining in the dark, washing with PBST and water and mounting in Mowiol 4-88 (#81381, Sigma-Aldrich; 4.3 M Mowiol 4-88 in 0.2 M Tris-HCl pH 8.5 with 30% glycerol) supplemented with 2.5% DABCO antifade (1,4-diazabicyclo (2.2.2)octan, #D27802, Sigma-Aldrich).

2.9 Fluorescence microscopy and image analysis

All characteristics of the microscopy systems used including lasers/lamps, filters, objectives, detection and incubation systems are listed in [Supplementary Table S5](#).

2.9.1 Microscopic analysis of subcellular localization

Fluorescence and DIC images of transfected C2C12 cells were taken using a Nikon Eclipse TiE2 system with a 40x air Plan Apo λ DIC objective. Fluorescence images of transfected MTF -/y cells were acquired using a confocal microscope Leica TCS SPEII and intensities were measured using ImageJ (<https://imagej.nih.gov/ij/>).

2.9.2 Microscopic analysis of heterochromatin accumulation

Fluorescence images of transfected C2C12 cells for calculation of heterochromatin accumulation were acquired on a Zeiss Axiovert 200 microscope. Image segmentation was performed using an ImageJ macro described previously ([Zhang et al., 2022](#)). First, the cell nuclei were segmented semi-manually based on the DAPI intensity and a difference of gaussian blur filter was applied. For heterochromatin segmentation individual pixel intensities were calculated, local maxima were determined in squares of 30×30 pixels and pixel intensities were binned into 42 bins with the local maximum defining the intensity of the highest bin per square. Heterochromatin masks were obtained by thresholding the pixel intensities based on their respective bins, taking all pixels with bins ≥ 21 for total, ≥ 37 for core heterochromatin cluster regions. The nucleoplasm area was calculated by subtracting the total heterochromatin cluster areas from the nucleus area. The heterochromatin accumulation of MeCP2 mutants for each individual heterochromatin cluster was calculated by dividing the mean intensity of the

heterochromatin cluster core by the mean intensity of the nucleoplasm (see [Supplementary Figure S1](#)). To analyze the protein level-dependency of accumulation differences, the cells were divided into low and high protein levels based on their GFP intensity as described before ([Zhang et al., 2022](#)). Briefly, the log10 GFP sum intensity of the cells was plotted and divided into 40 bins. In comparison to the GFP intensity of untransfected cells, bins 1 to 11 were defined as negative, while cells in bins 13 to 21 were considered as low and cells in bins 24 to 32 as high expressing.

2.9.3 Microscopic analysis of heterochromatin clustering

High-content screening microscopy of transfected C2C12 cells was performed using a PerkinElmer Operetta imaging system and analyzed using the supplier's software Harmony (Version 3.5.1, PerkinElmer Life Sciences, United Kingdom). Briefly, cell nuclei were segmented based on the DAPI channel image considering nuclei with a size of 110–250 μm^2 and roundness coefficient >0.8 that are not touching the edges of the image. Heterochromatin segmentation was also performed using the DAPI channel image, identifying high intensity spots within the nuclei. Spots with a spot-to-region intensity ratio of at least 0.35, an area of at least five px^2 and a relative spot intensity of 0.0253 were considered. The nucleus and heterochromatin masks generated based on the DAPI channel image were used to segment the images of the other channels and intensity and morphology properties of nuclei and heterochromatin clusters were measured (see [Supplementary Figure S2](#)). MeCP2 intensity bins based on GFP intensity were defined as described for the Axiovert images. Not all images obtained were considered for analysis, as the cell numbers per replicate and condition were different caused by differing transfection efficiencies. Thus, either the number of images (three biological replicates) was reduced to achieve comparable cell numbers or the number of cells (two biological replicates) was adjusted to achieve exactly the same number of cells per condition and replicate.

For the cell cycle analysis, the frequencies of the DAPI sum intensities per nucleus were plotted as histogram. The DAPI intensities of the different samples were normalized as described before ([Heinz et al., 2018](#)). The intervals for G1, S and G2/M phase were set manually and the percentages of the cells within each interval were plotted as bar diagrams.

2.9.4 Fluorescence recovery after photobleaching analysis of heterochromatin binding kinetics

Live cell imaging for fluorescence recovery after photobleaching (FRAP) experiments was carried out on a confocal microscope Leica SP5 II with a HCX PL APO $\times 63$ oil lambda blue objective equipped with an ACU live cell chamber at 37°C, 5% CO_2 and 60% humidity. MTF

-y cells were transfected with MeCP2 mutation constructs, seeded on gelatin-coated glass bottom p35 plates followed by induction with 1 μM tetracycline 7 h later and DNA staining with 100 nM SiR-DNA (SiR-Hoechst) (#SC007, Spirochrome) in presence of 5 μM verapamil (included in #SC007). 16 h later heterochromatin clusters were bleached with a 488 nm argon laser at 100% intensity for 2 s and confocal images were taken with a frame size of 256 \times 256 with 200 Hz and a pinhole of one AU in time intervals of 1.5 s. For analysis the image series were registration corrected using ImageJ plugin StackReg (correction based on GFP channel) or HyperStackReg (correction based on DNA staining). The mean fluorescence intensities of the (pre- and post-bleach) bleached and unbleached region were background subtracted for each time point. For single normalization, intensities were normalized to the mean of the prebleach intensities. Fluorescence recovery curves were fitted in ImageJ and t-half values and mobile fraction were obtained from the fitted curves. At least 10 cells were analyzed for each construct and the means of the fitted curves, t-half values and mobile fractions were plotted.

2.9.5 Protein *in situ* extractions

The protein extractability was measured in live cells. In brief, the C2C12 cells were transfected with plasmids expressing MeCP2-WT, S80D, or 3 L, plated onto μ -Slide eight Well plate (#80826, Ibidi), and treated 7 h with 1 $\mu\text{g}/\text{ml}$ tetracycline followed by incubation for 20 h. Live-cell imaging was performed on an UltraVIEW VoX spinning disc system (PerkinElmer Life Sciences) mounted on a Nikon Ti microscope equipped with an oil immersion 60 Plan-Apochromat NA 1.45 objective lens at 37°C, 5% CO_2 . Confocal z-stacks were acquired at 30 s intervals for 20 min. Z-stack images were taken first in PBS/EDTA and then in PBS with 0.5% Triton X-100 for 20 min with 30 s intervals. Quantifications were performed using Volocity (PerkinElmer Life Sciences). The mean fluorescence intensity signal at the heterochromatin clusters/cell at each time was calculated and normalized to the mean fluorescence intensity of heterochromatin clusters before Triton X-100 treatment.

3 Results

3.1 MeCP 2 is post-translationally modified in mouse brain

To identify post-translational modifications (PTMs) of MeCP2, we first isolated nuclei from mouse brain tissue using a sucrose buffer in combination with ultracentrifugation. Then, we enriched MeCP2 from mouse brain nuclei using its natural hepta-histidine sequence localized in its C-terminal domain (see [Figures 1A,B](#)) for protein pull down with Ni-IDA beads ([Supplementary Figure S3](#)). Subsequently, the enriched proteins were separated by SDS-PAGE, in-gel digested using

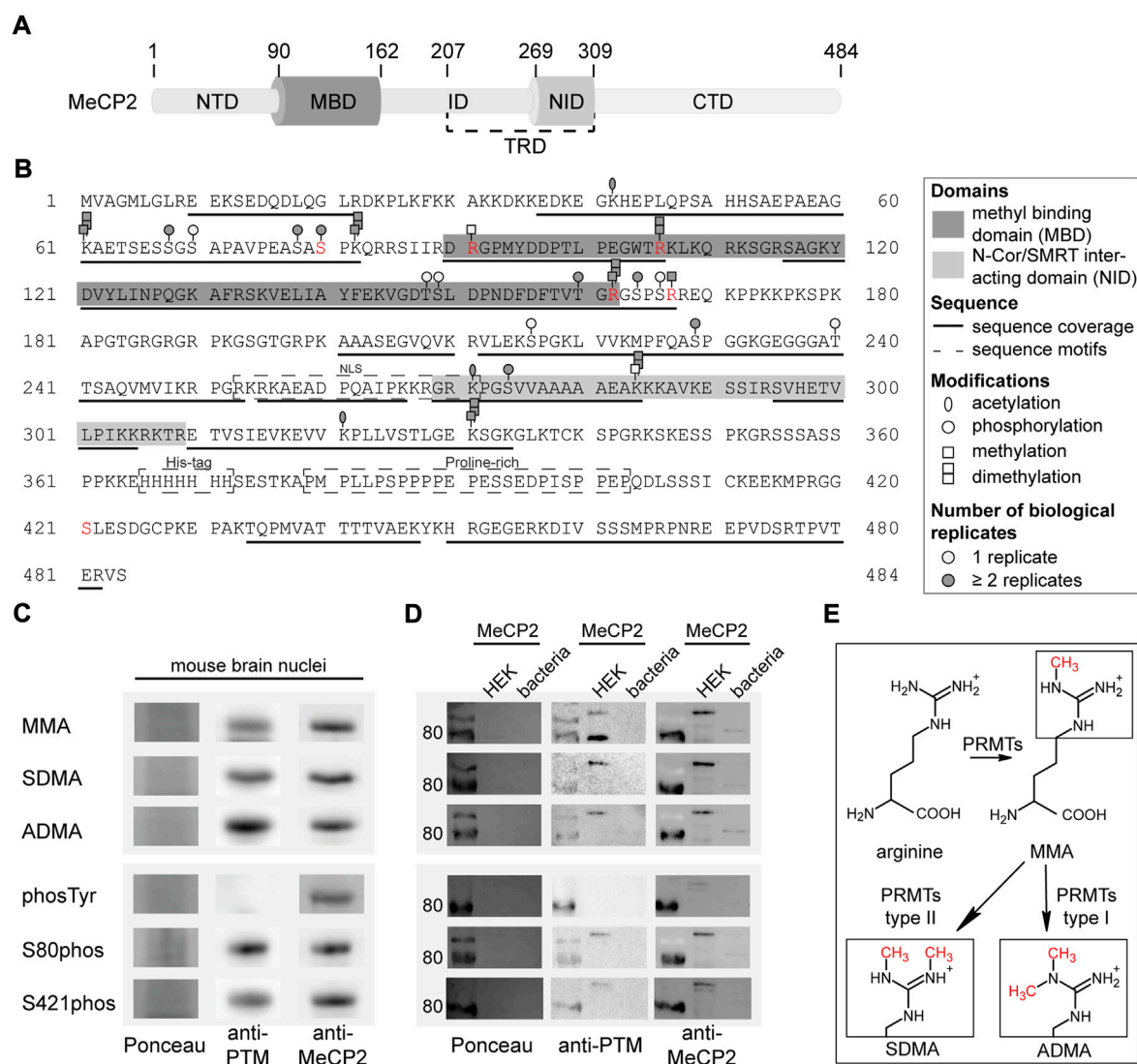


FIGURE 1

Post-translational modifications of MeCP2 from mouse brain identified by mass spectrometry analysis. (A) MeCP2 domain structure comprising N-terminal domain (NTD), methyl-CpG binding domain (MBD), intervening domain (ID), N-CoR/SMRT interacting domain (NID), transcriptional repression domain (TRD) and C-terminal domain (CTD). (B) MeCP2 protein sequence with modifications identified by mass spectrometry. MBD and NID, sequence coverage, sequence motifs, PTMs (acetylation, phosphorylation, methylation, dimethylation) and the number of biological replicates from independent experiments are marked as indicated. Modifications selected for further validation are marked in red. The software-based annotation of spectra and modification sites shown were obtained from Proteome Discoverer and MaxQuant. The arginine methylation sites selected for further validation were additionally manually inspected (see [Supplementary Figures S4–6](#)). The location of modifications identified on the same peptide might be uncertain. (C) Western blot analysis of mouse brain nuclei extracts tested for monomethyl arginine (MMA), symmetric dimethyl arginine (SDMA), asymmetric dimethyl arginine (ADMA), tyrosine phosphorylation (phosTyr), S80 and S421 phosphorylation (phos) and reprobated with MeCP2 specific antibodies. The full membranes of the Western blots are shown in [Supplementary Figure S7](#). (D) Western blot analysis of MeCP2-GFP purified from human HEK cells and MeCP2 purified from *E. coli* probed with the same modification specific antibodies and reprobated with MeCP2 specific antibodies. The Ponceau stain visualizes the total proteins on the membrane and the full membranes are shown in [Supplementary Figure S7](#). (E) Scheme of the arginine methylation reaction: protein arginine methyltransferases (PRMTs) can catalyze the monomethylation of arginine and subsequently the dimethylation, which can occur either on the same nitrogen (ADMA, catalyzed by type I PRMTs) or on the unmodified nitrogen (SDMA, catalyzed by type II PRMTs).

trypsin and subjected to mass spectrometry analysis using a TOP10 shotgun method with a combination of HCD and CID fragmentation for improved sequence coverage and modification identification. The mass spectrometry analysis of MeCP2 from

mouse brain yielded a sequence coverage of 60.1% and a series of PTMs, including lysine methylation and acetylation, arginine methylation and phosphorylation on serines and threonines. [Figure 1B](#) depicts the MeCP2 protein sequence with the

modifications identified. The peptides on which the modifications were identified and the number of identifications obtained from automated data analysis using either Proteome Discoverer or MaxQuant software are listed in [Supplementary Table S7](#). We decided to functionally characterize especially arginine methylation sites, as 7% of the MeCP2 amino acids are arginines, but we found only 11.4% of the arginines modified. In addition, a large number of *MECP2* mutations identified in Rett syndrome patients affect arginine residues. The arginine methylation sites identified on MeCP2-E2 isoform (starting in exon 2) namely R91, R106, R162, and R167 were selected for further analysis and were validated by manual inspection of the spectra (see [Supplementary Figures S4–6](#)). The arginines R162 and R167 are located on the same peptide and were both identified as monomethylated and R162 also as dimethylated in the automated analysis. It was not possible to unambiguously determine the localization of the methylation sites on this peptide from the spectra (see [Supplementary Figures S4–6](#)).

As the MeCP2 sequence comprises 13.2% of lysines and 7% of arginines, it is likely that some regions could not be covered in our measurements due to the generation of very short peptides by trypsin which cuts after lysine and arginine. In addition, there is a long sequence without any lysines and arginines in the C-terminus of MeCP2, containing the hepta-histidine sequence and a proline-rich region (see [Figure 1B](#)) that was, thus, not accessible. Of note, it was reported that post-translational modifications like methylation lower the efficiency of trypsin mediated cleavage. Therefore, we tried to increase sequence coverage using other enzymes for digestion but were unable to cover the missing regions (data not shown).

The results were validated by immunoblot detection of mono and dimethyl arginine, serine/threonine/tyrosine phosphorylation as well as serine 80 and serine 421 phosphorylation on mouse brain nuclei extracts ([Figure 1C](#); [Supplementary Figure S7](#)). The same membranes were incubated with anti-MeCP2 antibody to validate that the PTM signal was specific to MeCP2. We could show that MeCP2 is monomethylated as well as symmetrically and asymmetrically dimethylated on arginines. In addition, it is phosphorylated on serines, but not on tyrosines. The published MeCP2 phosphorylation sites S80 and S421 ([Zhou et al., 2006](#); [Tao et al., 2009](#)) were also detected on MeCP2 isolated from mouse brains ([Figure 1C](#)). In addition, recombinant MeCP2-GFP was enriched from human HEK cells and MeCP2 from *E. coli* to confirm the antibody specificity by Western blot ([Figure 1D](#)). [Figure 1E](#) shows a scheme of the arginine methylation reaction catalyzed by protein arginine methyl transferases (PRMTs). First, arginine residues can be monomethylated by PRMT enzymes of class I and II, subsequent asymmetric dimethylation is catalyzed by PRMT enzymes type I, symmetric dimethylation by PRMT enzymes of type II. Of note, the arginine keeps its charge in the methylated state, but shows a different charge distribution due to the bulky methylation groups.

3.2 Arginine methylation and serine phosphorylation site mutations do not influence MeCP2 subcellular localization with exception of MeCP2 R106 mutations

To investigate the functional consequences of MeCP2 PTMs, we generated recombinant MeCP2 proteins tagged with GFP and altered at PTM sites. While most published work utilizes the amino acid substitutes aspartate (D) to mimic phosphorylation or alanine (A) to prevent phosphorylation, there are no commonly used substitutions for methylated arginines. Thus, we decided to mutate the arginines identified to be methylated to lysine (K) to retain the positive charge, to glutamine (Q) to sterically mimic a methylated arginine and to leucine (L) to obtain methyl groups similar to a methylated arginine (compare [Supplementary Figure S8C](#) and [Figure 1E](#)). In addition, arginine substitutions to glutamine and leucine were identified in Rett syndrome patients. Of note, none of these mutations is an ideal mimic for methylated or unmethylated arginine. In methylated arginine the positive charge of the arginine is kept with the addition of the sterically hindering additional methyl group(s). These amino acid substitutions can, thus, only partially mimic these changes, either the positive charge (K), the methyl group (L) or a polar and sterically larger side chain (Q). MeCP2 arginine R106 was detected as methylated in our proteomic screen ([Figure 1B](#)) and is found mutated to tryptophan (R106W) or glutamine (R106Q), with very low frequency also to glycine (R106G) and leucine (R106L) in Rett syndrome patients (online RettBASE, ([Krishnaraj et al., 2017](#))). We therefore generated recombinant MeCP2 with the R106 mutated to produce lysine, glutamine, leucine, tryptophan and glycine, thus including the previously explained substitutions for arginine methylated sites (K, Q, and L) and all reported R106 Rett syndrome mutations (W, Q, G, and L).

The MeCP2-GFP plasmids point mutated for modified sites ([Figure 2A](#)) were transfected into male mouse tail fibroblasts MTF-/y ([Supplementary Figures S8A,B](#)), which are MeCP2 null cells, and C2C12 female myoblast cells ([Figures 2B–D](#)), which have a very low to undetectable level of MeCP2 ([Zhang et al., 2022](#)) and, thus, can be used as a functional MeCP2-null system. In the following, the constructs are abbreviated as: 3K (triple R91K R162K R167K), 3Q (triple R91Q R162Q R167Q), and 3L (triple R91L R162L R167L).

First, we analyzed the subcellular localization of the altered MeCP2 proteins and compared them with the wild type MeCP2 protein. Like wild type MeCP2, the MeCP2 proteins with 3K, 3Q, and 3L substitutions ([Figure 2B](#), [Supplementary Figure S8A](#)) as well as all the phosphorylation site altered proteins ([Figure 2C](#), [Supplementary Figure S8B](#)) were enriched at heterochromatin, visualized as dense DAPI stained DNA regions in the images. All R106 altered MeCP2 proteins, as reported earlier for MeCP2 R106W and R106Q ([Ballestar et al., 2000](#); [Yang et al., 2016](#)), tend to lose their heterochromatin enrichment and mislocalize to the negatively charged RNA-enriched nucleolar compartment ([Figure 2D](#)). The nucleolar compartment is visualized in the

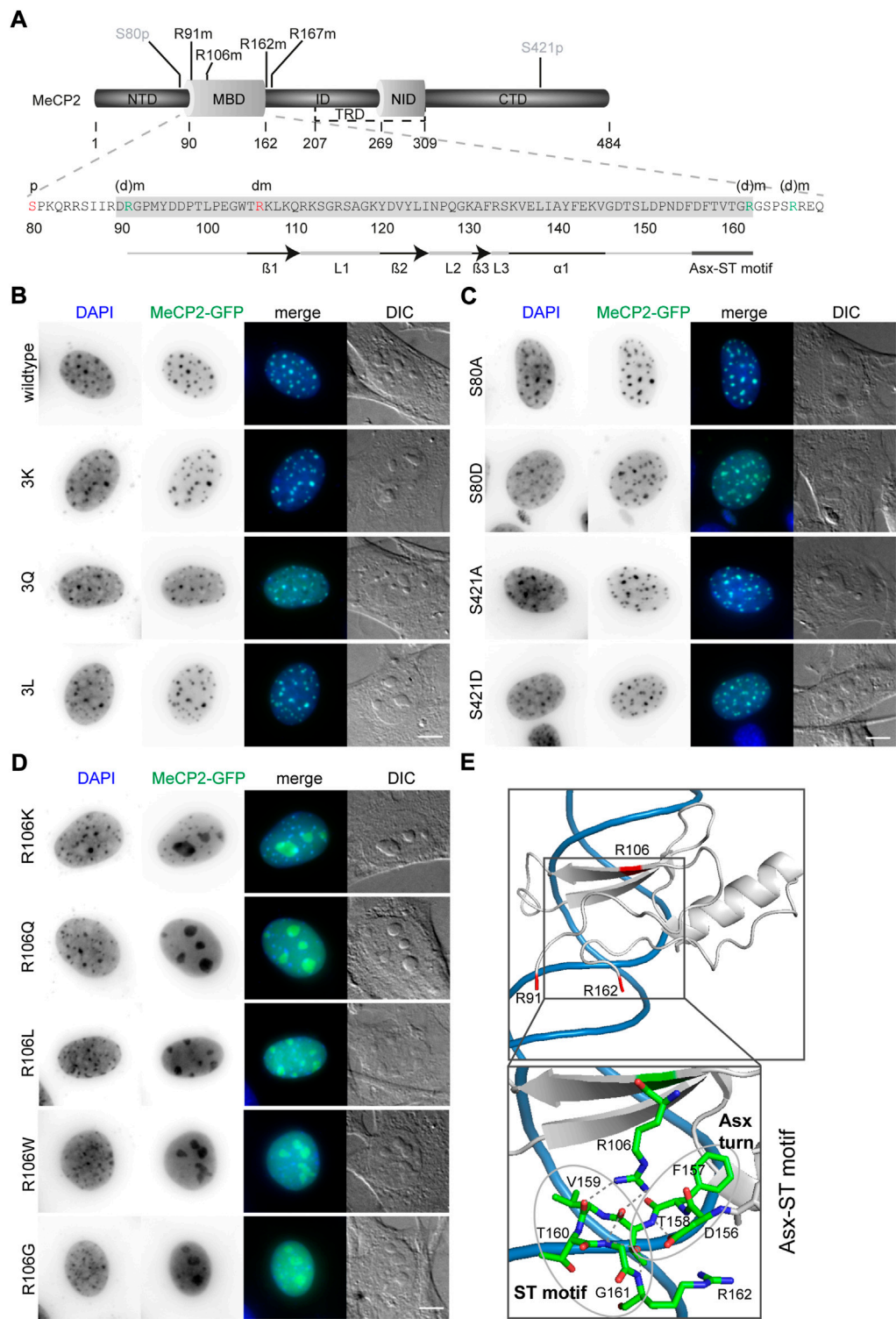
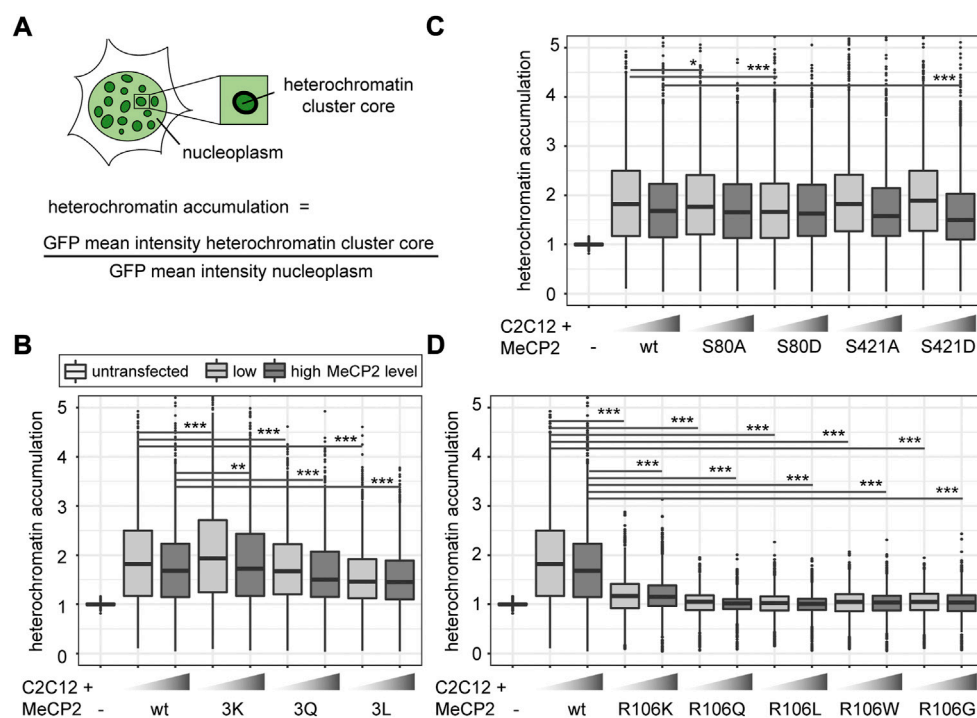


FIGURE 2
 Subcellular localization of MeCP2-GFP mutant constructs transfected in C2C12 mouse myoblast cells. **(A)** MeCP2 domain structure and MBD amino acid sequence with the modification sites selected for functional validation indicated in red (S80phos, R106dimet) or green (R91, R162, and R167, referred to as 3x). **(B–D)** MeCP2 wild type and 3K, 3Q, and 3L mutations **(B)** as well as S80 and S421 mutations **(C)** colocalized with DAPI dense heterochromatic regions, whereas R106 mutations lose their DAPI colocalization and mislocalized to the nucleoli **(D)**. Scale bar 5 μ m. **(E)** X-ray structure of the MeCP2 methyl-binding domain (MBD, shown in gray) in complex with methylated DNA (shown in blue) with the methylated arginine sites R91, R106, and R162 highlighted in red (structure information from (Ho et al., 2008); PDB accession code 3C2I). The enlarged image shows the (Continued)

FIGURE 2 (Continued)

Asx-ST motif stabilizing the MBD binding to methylated DNA. The Asx turn composed of D156, F157, and T158 is stabilized by a hydrogen bond between the carboxylate side chain of D156 and T158 main chain nitrogen. The ST motif of the amino acids 158 to 161 comprises two hydrogen bonds, one between the side chain hydroxyl group of T158 and the main chain nitrogens of G161 and R162, the second one between the main chain carbonyl group of T158 and G161 main chain nitrogen (Ho et al., 2008). The structural data was generated and color-coded using PyMOL software.

**FIGURE 3**

Comparative analysis of heterochromatin accumulation of MeCP2 mutant constructs transfected in C2C12 mouse myoblast cells. **(A)** Heterochromatin accumulation was calculated as the ratio of GFP mean intensity at heterochromatin versus nucleoplasm. The boxplots depict the heterochromatin accumulation of mutant MeCP2 including R91, R162, and R167 **(B)**, S80 and S421 **(C)**, and R106 **(D)** constructs for low and high MeCP2 levels in the cells. Three biological replicates, statistical significance calculated using Wilcoxon-Rank test. * $p < 0.05$, ** $p < 0.005$, *** $p < 0.001$. p -values and n -values are summarized in [Supplementary Table S6](#).

DIC images where it appears as prominent large structures within the cell nucleus. Interestingly, it was described that peptides with high occurrence of arginines tend to localize at the negatively charged nucleoli (Martin et al., 2015). While MeCP2 R106 K still shows some heterochromatin localization, the other R106 mutant proteins localized nearly exclusively within the nucleoli and showed higher intensities in the nucleoplasm compared to the wild type (Figure 2D). These results might be explained by the role of R106 in MBD binding to the DNA. It was reported that MeCP2 binding to methyl-CpG on the DNA is mediated by direct contact of the three amino acids D121, R111, and R133 and might involve five water molecules (Ho et al., 2008). Arginine 106 stabilizes the Asx-ST motif, a motif stabilizing MeCP2 DNA interaction ((Ho et al., 2008), see Figure 2E). Interestingly, also the frequent Rett

syndrome missense mutation T158M is localized in this motif. Both missense mutations occur very frequently and reduce DNA binding, emphasizing the importance of this motif for proper methyl-CpG binding and MeCP2 function.

3.3 MeCP2 arginine methylation and serine phosphorylation site mutants accumulate differently in heterochromatin

To quantitatively analyze heterochromatin accumulation of the MeCP2 mutant constructs, we performed a cellular DNA/chromatin binding assay. C2C12 cells were transfected with the mutant constructs, fixed and counterstained with the DNA dye

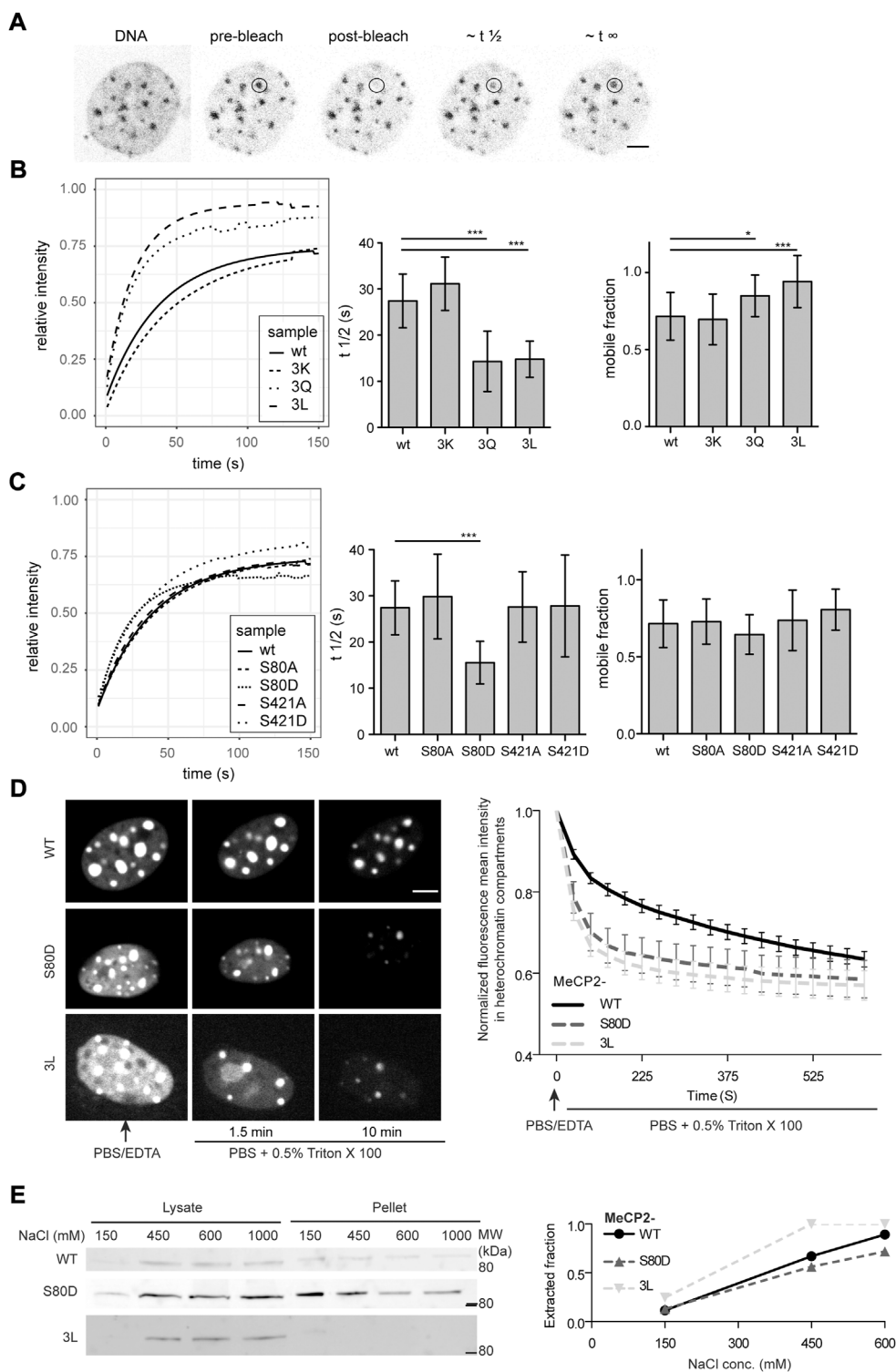


FIGURE 4
Analysis of the dynamics of MeCP2 mutants in cells. **(A)** Exemplary MTF *Mecp2*^{-/-} cell transfected with wild type MeCP2 expression construct stained with the cell-permeable DNA dye SIR Hoechst and GFP signal is shown pre-bleaching, post-bleaching and during fluorescence recovery. **(B)** Fitted time curves for fluorescence recovery after photobleaching and bar diagrams showing the recovery half times ($t_{1/2}$) and mobile fractions for MeCP2 wild type (wt) and 3K, 3Q, and 3L mutations including R91, R162, and R167 **(B)** as well as for S80 and S421 mutations **(C)**. *p*-values calculated by Wilcoxon-Rank test. $**p < 0.05$, $***p < 0.001$. *p*-values and *n*-values are summarized in [Supplementary Table S6](#), single recovery curves with standard deviation are plotted in [Supplementary Figure S9](#). **(D)** *In situ* extraction of MeCP2 mutants expressed in C2C12 mouse cells. Shown are (Continued)

FIGURE 4 (Continued)

representative images at selected time points (left side) and the quantification curve (right side) depicting the mean and SEM. (E) C2C12 cells expressing the constructs as indicated were subjected to fractionation with different salt concentrations to ascertain chromatin binding and soluble fraction (lysate) as well as insoluble fraction (pellet) were loaded and probed with anti-MeCP2 antibodies. The plot depicts the ratio of the lysate intensity to the total intensity (sum of lysate plus pellet). Full blots are shown in [Supplementary Figure S10](#). Scale bars 5 μ m.

DAPI. After imaging the cells, the nuclei were segmented semi-manually and heterochromatin compartments were segmented using a self-made macro in ImageJ/Fiji [(Zhang et al., 2022), [Supplementary Figure S1](#)]. By calculating the ratio of the mean GFP intensity in the heterochromatin to the mean GFP intensity in the nucleoplasm, we obtained heterochromatin accumulation values ([Figure 3A](#)). As MeCP2 levels might have an influence on its degree of heterochromatin accumulation, the cells were classified into low and high MeCP2 levels according to their mean nuclear fluorescence intensity as described before (Zhang et al., 2022).

The quantitative analysis of heterochromatin accumulation revealed a slightly higher accumulation of MeCP2 3K than MeCP2 wild type. MeCP2 3Q showed a lower accumulation than wild type MeCP2 and MeCP2 3L an even lower accumulation compared to the MeCP2 3Q ([Figure 3B](#)). The heterochromatin accumulation values of the phosphorylation site mutants were all very similar, with only the phospho mimic mutants S80D showing a slightly lower accumulation at low levels and S421D a lower accumulation at high levels ([Figure 3C](#)). In line with the subcellular localization, the heterochromatin accumulation was drastically reduced in all R106 mutants ([Figure 3D](#)). Only R106K still showed some heterochromatin accumulation with a ratio clearly above one. Overall, all constructs show a lower accumulation in case of high protein levels, which might hint to a saturation effect of MeCP2 binding to chromatin at high protein levels.

3.4 MeCP2 arginine methylation and serine phosphorylation site mutations affect its heterochromatin binding kinetics

Next, we wanted to know whether the MeCP2 modification site mutants show differences in heterochromatin binding kinetics. Therefore, MTF-/y cells were transfected with the different constructs and heterochromatin compartments were photobleached using a focused laser microbeam on a confocal microscope. The fluorescence recovery was measured by taking images before and every 1.5 s after photobleaching ([Figure 4A](#)). Curve fitting of the intensity values over time allowed for calculation of fluorescence recovery half times and mobile fractions ([Figure 4](#), [Supplementary Figure S9](#)).

The comparison of the recovery half times of wild type MeCP2 with those of the triple mutants revealed that the MeCP2 3Q and 3L mutants recover much faster than the

wild type ([Figure 4B](#)). The MeCP2 3K mutant, retaining the positive charge, showed similar kinetics as wild type MeCP2, emphasizing the importance of the positive charge for chromatin binding. These results are in line with the heterochromatin accumulation results, which depicted a slightly higher accumulation for 3K, but a lower one for 3Q and 3L constructs compared to the wild type ([Figure 3B](#)). For the phosphorylation mutants only S80D showed faster recovery kinetics compared to wild type MeCP2, but no significant changes in the mobile fraction ([Figure 4C](#)). This result also agrees with the heterochromatin accumulation data ([Figure 3C](#)). The recovery data for 3L and S80D were validated with *in situ* extraction analysis and by lysing the cells with increasing salt concentrations followed by Western blot analysis of the soluble and insoluble fractions ([Figures 4D,E](#), [Supplementary Figure S10](#)). As the R106 mutants were shown to hardly localize or accumulate at heterochromatin, their recovery times were too fast to be measured under similar conditions as wild type MeCP2 and were, thus, not analyzed.

3.5 Arginine methylation and serine phosphorylation site mutations of MeCP2 influence its heterochromatin clustering

To investigate the influence of MeCP2 modifications on chromatin organization, we performed a cellular chromatin clustering assay. As reported before, many small heterochromatin clusters tend to fuse to build fewer bigger clusters with increasing MeCP2 protein levels and cellular differentiation (Brero et al., 2005). Thus, we aimed to analyze the cellular heterochromatin clustering in two ways, by observing the heterochromatin cluster number and the corresponding area ([Figure 5A](#)), which should develop in an inverse manner. The transfected C2C12 cells were imaged on a high-content screening microscope and nuclei and heterochromatin clusters were segmented ([Supplementary Figure S2](#)). We confirmed transfected cell viability by cell cycle profiling ([Supplementary Figure S10](#)). Depending on the GFP mean nuclear intensity, cells were classified into low and high MeCP2 levels and heterochromatin cluster numbers and areas were plotted ([Figure 5](#)).

In comparison to wild type MeCP2, MeCP2 3K showed a higher heterochromatin clustering function represented by lower cluster numbers and larger cluster areas. MeCP2 3L showed a

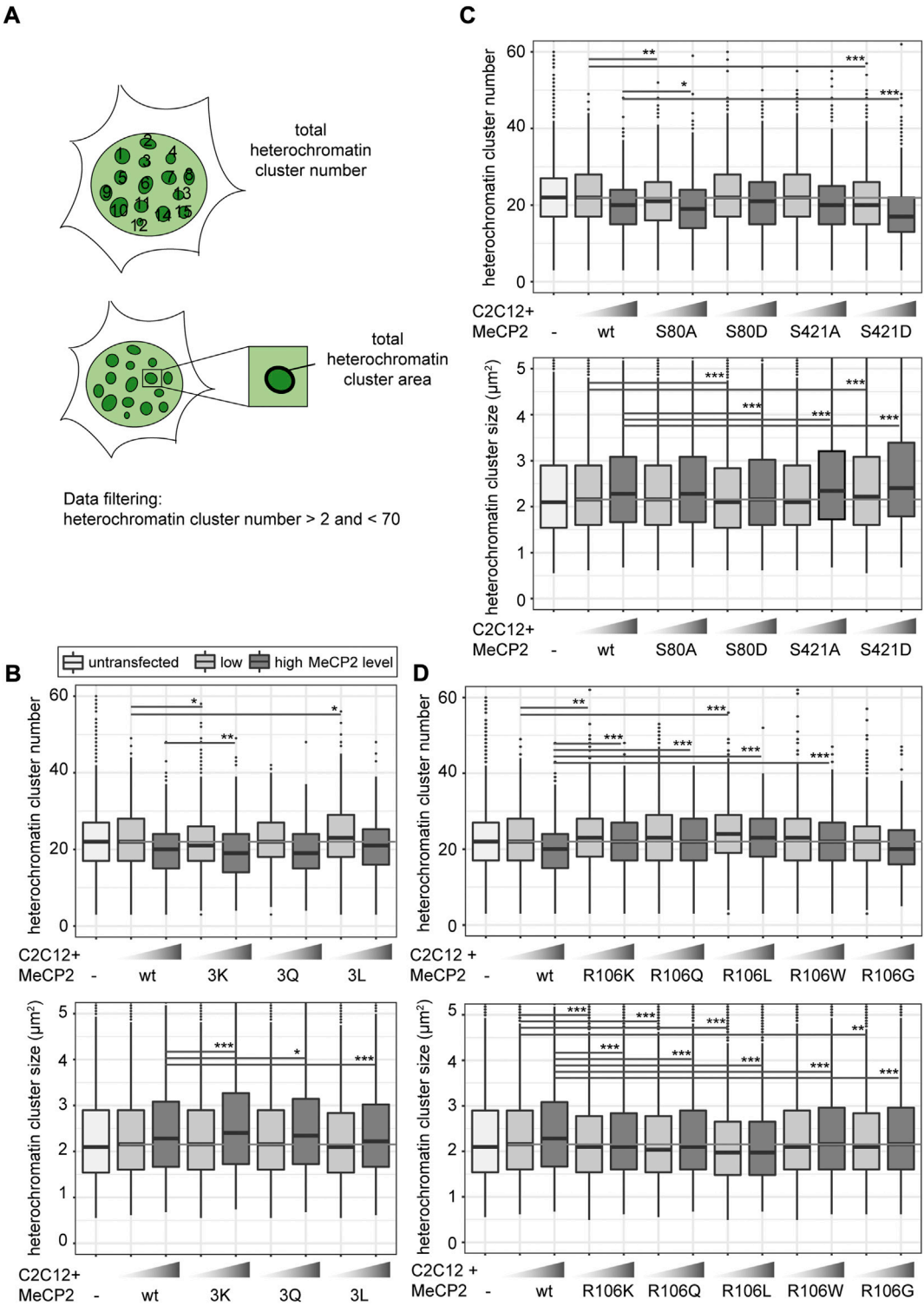


FIGURE 5
Heterochromatin clustering and cluster size of cells transfected with MeCP2 mutant constructs. Shown are the heterochromatin cluster numbers and areas scheme in (A) obtained for the arginine mutants including R91, R162, and R167 (B), arginine R106 (D) and S80, S421 phosphorylation (C) mutant constructs in C2C12 cells from high-content screening microscopy after segmentation of nuclei and heterochromatin clusters. Cells were divided into low and high MeCP2 levels based on their nuclear GFP signal. Three biological replicates, statistical significance calculated using Wilcoxon-Rank test. * $p < 0.05$, ** $p < 0.005$, *** $p < 0.001$, n. s Not significant. p -values and n -values are summarized in [Supplementary Table S6](#).

tendency to reduced heterochromatin clustering, while the results with MeCP2 3Q were not significantly different (Figure 5B). These findings correlate well with those obtained for heterochromatin accumulation and heterochromatin binding kinetics. 3K showed higher heterochromatin accumulation, while 3Q and 3L showed lower accumulation and faster heterochromatin binding kinetics (Figures 3B, 4B).

Regarding the phosphorylation site mutants, S421D showed the most striking clustering function difference to wild type MeCP2 represented by lower cluster numbers and larger cluster areas (Figure 5C). In the other functional assays, though, MeCP2 S421D showed lower accumulation than wild type at high protein levels but did not show any significant differences in the binding kinetics (Figures 3C, 4C). Hence, it is unclear how this amino acid substitution affects heterochromatin binding in relation to heterochromatin organization.

For MeCP2 arginine 106, all mutant constructs tested were associated with higher heterochromatin cluster numbers and smaller cluster areas than wild type MeCP2 (Figure 5D), possibly because of their lack of heterochromatin accumulation.

3.6 Protein arginine methyltransferases affect MeCP2 induced heterochromatin remodeling

As we observed changes in MeCP2 heterochromatin accumulation, clustering and binding kinetics for the constructs mutated for arginine methylation sites, we tested whether these changes are due to the mutations inserted or a consequence of arginine methylation. Therefore, we performed coexpression experiments of protein arginine methyltransferases (PRMTs) with *Mecp2* to test whether the PRMTs affect the MeCP2 heterochromatin clustering function. We confirmed transfected cell viability by cell cycle profiling (Supplementary Figure S10). We made use of recombinant PRMTs with a Myc-tag that could be used for detection. The PRMTs tested comprised three enzymes that catalyze mono- and asymmetric dimethylation on arginines namely PRMT1, 4, 6, as well as PRMT5 that catalyzes mono- and symmetric arginine dimethylation. We chose PRMT1, as it is the most common arginine methyltransferase responsible for about 85% of all arginine methylations (Nicholson et al., 2009). In addition, PRMT1 and PRMT6 preferentially methylate arginines in glycine and arginine rich (GAR) motifs (Bedford, 2007; Nicholson et al., 2009) and two of the sites identified, R91 and R162, are localized adjacent to lysines. PRMT4 and PRMT1 can cooperate in gene regulation (Kleinschmidt et al., 2008), but cannot substitute each other in all contexts (Herrmann et al., 2009). PRMT5 is the predominant type II PRMT catalyzing symmetric arginine methylation and was associated to transcriptional repression (Stopa et al., 2015). It was reported before that the subcellular localization of the PRMT enzymes is

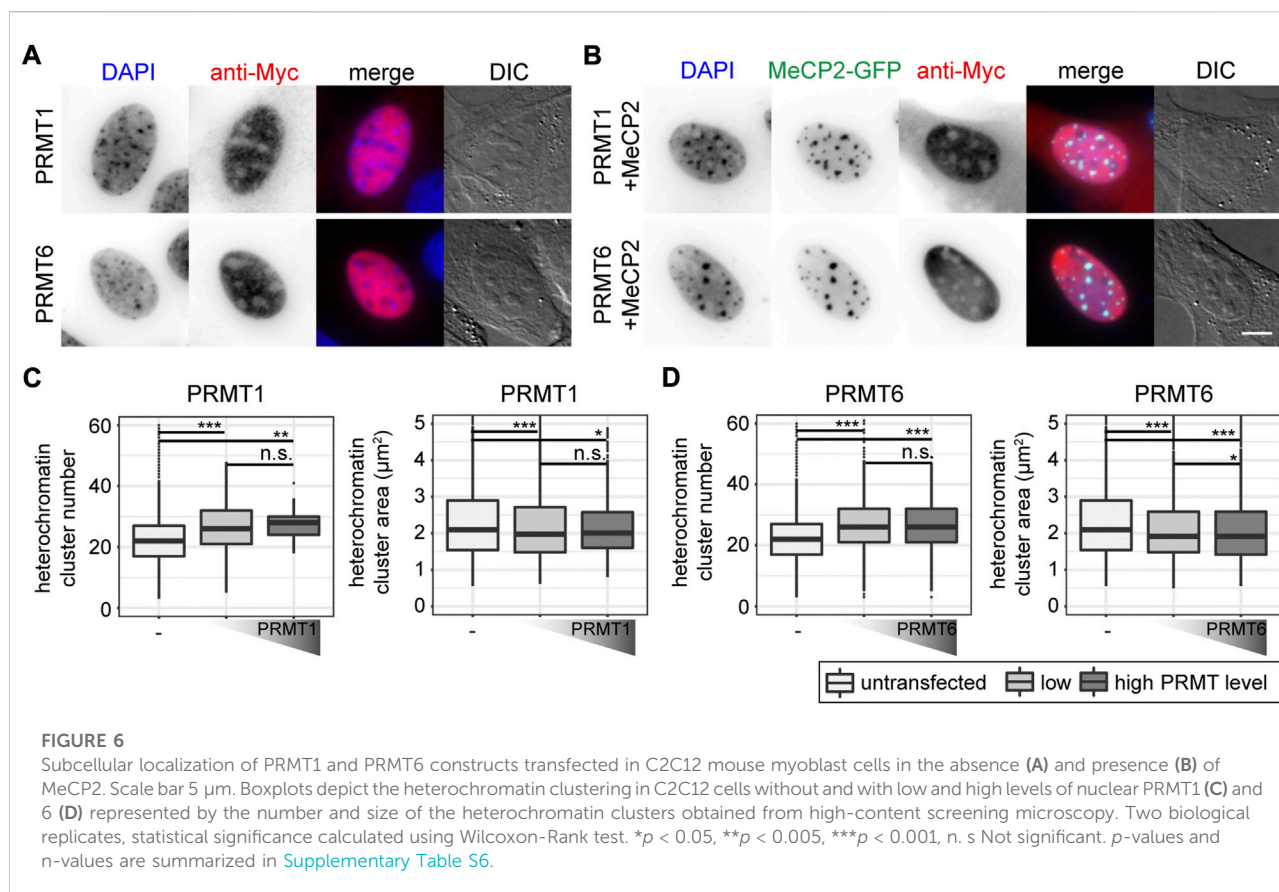
highly dependent on the cell type and the target proteins (Herrmann et al., 2009). Thus, to test for their subcellular localization, C2C12 cells were transfected with the PRMTs, fixed and stained using an antibody against the Myc tag. Of the four PRMTs tested, PRMT1 localized in the nucleus and to a lesser extent in the cytoplasm, while PRMT6 localized exclusively in the nucleus (Figures 6A,B), which is in line with previous studies (Frankel et al., 2002; Herrmann et al., 2009). PRMT4 and PRMT5 were localized in the cytoplasm and, thus, not considered in further experiments (Supplementary Figure S12). None of the PRMTs had an influence on MeCP2 localization (Figures 6A,B, Supplementary Figure S12).

First, we tested whether the PRMTs alone have an influence on heterochromatin clustering in C2C12 cells by plotting heterochromatin cluster numbers and areas (Figures 6C,D). The values for heterochromatin cluster numbers and areas were obtained from high-content microscopy data after segmentation of nuclei and heterochromatin clusters (Supplementary Figure S2) and binning of the cells into low and high protein levels based on their nucleus mean fluorescence intensities. The presence of PRMT1 and PRMT6 resulted in higher heterochromatin cluster numbers and smaller heterochromatin cluster areas compared to untransfected cells, meaning they counteract the clustering of heterochromatin compartments. This effect was observed independent of the PRMT level, as there was no difference in heterochromatin cluster numbers and areas between low and high PRMT levels (Figures 6C,D).

Next, C2C12 cells were cotransfected with *PRMT1* and *PRMT6* together with *Mecp2* wild type or mutant constructs, cells were fixed and stained for the Myc tag and subsequently imaged on a high-content microscope (Supplementary Figure S2). The heterochromatin cluster numbers (Figure 7) and areas (Supplementary Figure S13) were plotted as heatmaps for each PRMT in combination with the MeCP2 triple mutants.

Introduction of PRMT1 and PRMT6 together with MeCP2 wild type into cells resulted in a significantly decreased MeCP2 heterochromatin clustering shown by higher heterochromatin cluster numbers and smaller cluster areas (Figure 7; Supplementary Figure S13). While MeCP2 at high levels could still cluster heterochromatin in the presence of PRMT1, there was nearly no clustering in the presence of PRMT6.

The cotransfection experiments of MeCP2 and PRMTs revealed differences in heterochromatin clustering between MeCP2 modification site mutants and MeCP2 wild type. Comparing the triple mutations to MeCP2 wild type in presence of PRMT1, MeCP2 3Q showed a similar heterochromatin cluster number distribution as the wild type, while the heatmaps of 3K and 3L differed (Figure 7A). MeCP2 3K and 3L in presence of PRMT1 showed lower heterochromatin numbers in high levels compared to wildtype, but the changes observed were not statistically significant. The presence of



PRMT6 blocked the ability of MeCP2 wild type to induce heterochromatin clustering, and the same was observed for MeCP2 3Q (Figure 7B, Supplementary Figure S13B). MeCP2 3K, though, showed lower heterochromatin cluster numbers than wild type MeCP2 when cotransfected with PRMT6 and, thus, shows higher heterochromatin clustering. Thus, MeCP2 3K was able to reverse the negative effect of PRMT6 on heterochromatin clustering and the R to K substitution prevents its methylation by PRMTs. MeCP2 3L at high levels increased heterochromatin clustering (shown by lower heterochromatin cluster numbers and larger areas) in presence of PRMT6, but its clustering function was still impaired compared to its expression without PRMT6 (Figure 7B, Supplementary Figure S13B). Thus, we conclude that the presence of PRMTs influences the heterochromatin clustering function of MeCP2 and its triple mutants. The differences in clustering are specifically pronounced comparing the positively charged lysine mutation with the uncharged but still polar glutamine and the non-polar leucine, emphasizing the importance of the positive charge for the MeCP2 heterochromatin clustering function.

The cotransfection experiments of MeCP2 R106 mutants and PRMT1 and PRMT6 revealed that the mutation of R106 decreases MeCP2 heterochromatin clustering function

showing higher cluster numbers and smaller areas (Figures 7C,D, Supplementary Figures S12C,D). The R106 mutants could not counteract the reduced clustering function in the presence of PRMT1 and there was no clear difference in heterochromatin clustering between R106K, Q and L mutants. In the presence of PRMT6 MeCP2 R106Q showed no significant heterochromatin clustering, while the presence of R106K and R106L increased heterochromatin clustering when cotransfected with PRMT6. Thus, the influence of PRMT6 on the R106 mutant heterochromatin clustering shows similar tendencies as for the 3x mutants, but less pronounced.

4 Discussion

MeCP2 is post-translationally modified and some of these modifications might influence its transcriptional regulation and protein-protein interactions (Bellini et al., 2014), as well as its chromatin clustering abilities (Becker et al., 2016). Although many modifications have been reported, only few of them were functionally characterized or identified *in vivo*. In this study, we show that MeCP2 isolated from adult mouse brain is post-translationally phosphorylated on serines and threonines, methylated and acetylated on lysines and methylated on

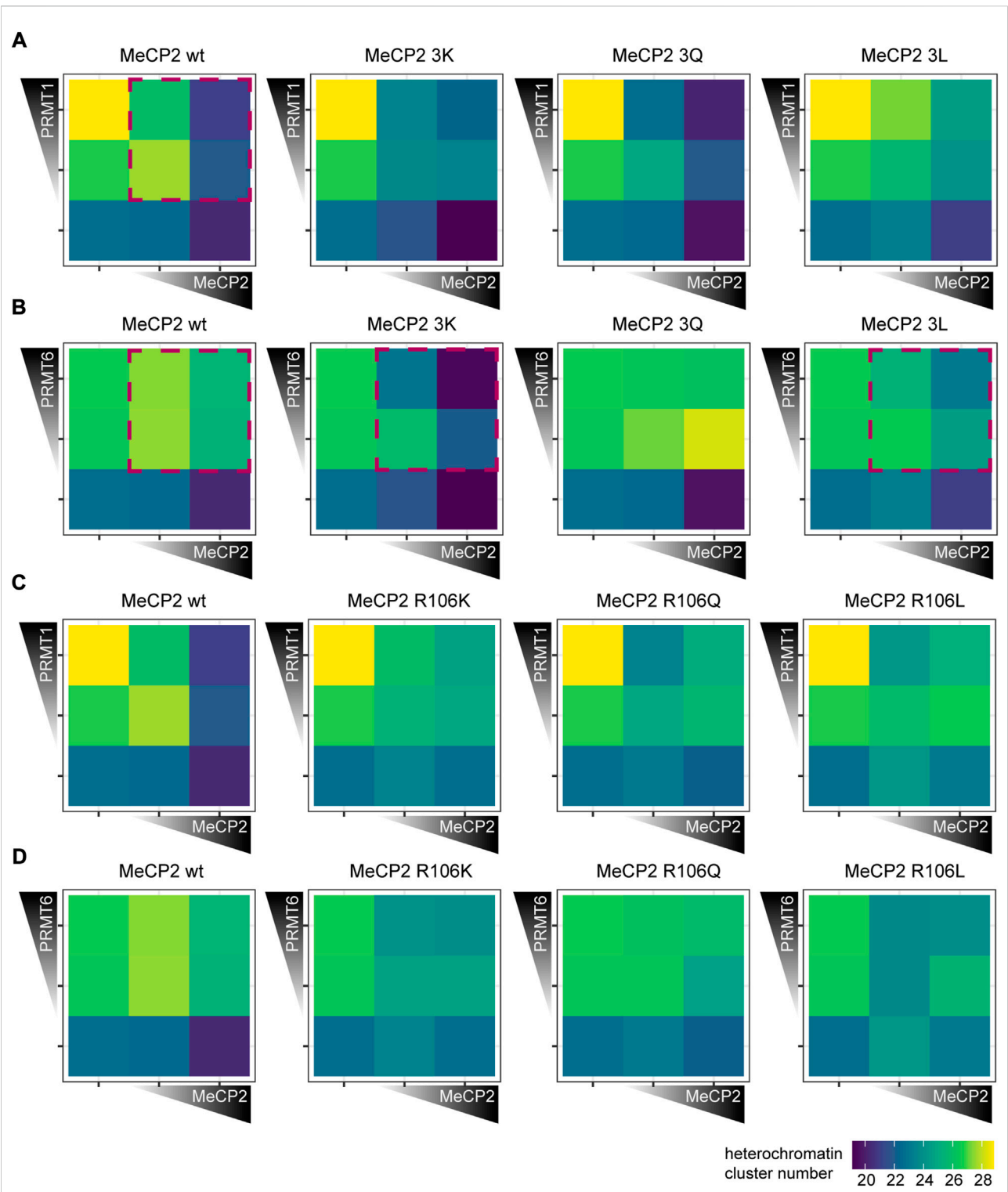
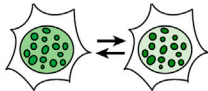
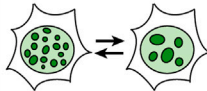
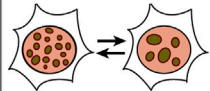
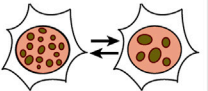

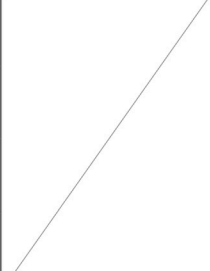
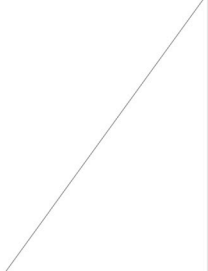











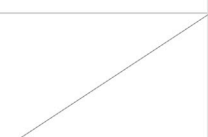






FIGURE 7
Heterochromatin clustering of cells transfected with MeCP2 mutant constructs in the presence of protein arginine methyltransferases (PRMTs) 1 and 6. Heatmaps show the heterochromatin cluster numbers obtained by high-content screening microscopy of C2C12 cells cotransfected with MeCP2 wild type or triple mutants and PRMT1 (A), wild type or triple mutants and PRMT6 (B), wild type or R106 mutants and PRMT1 (C) and wild type or R106 mutants and PRMT6 (D). Cells were binned for low and high fluorescence intensity according to their MeCP2 and PRMT levels. Heterochromatin cluster numbers are shown as means of at least 26 cells from at least two biological replicates. The *p*-values representing the statistical significance calculated using Wilcoxon-Rank test are listed in [Supplementary Table S6](#). Red boxes mark the most important observations.

		Cellular localization	Heterochromatin accumulation	Heterochromatin clustering	Heterochromatin clustering in presence of PRMTs		
							
serine phospho mutations	S80A		↓	—			
	S80D		↓	—			
	S421A		—	—			
	S421D		↓	↗			
arginine mutations	3x mutations (R91 R162 R167)	3K		↗	↗	—	↗
		3Q		↘	—	↘	—
		3L		↘	↘	↘	↗
	R106 mutations	R106K		↘	↘	↘	↗
		R106Q		↘	↘	—	—
		R106L		↘	↘	—	↘
		R106W		↘	↘		
		R106G		↘	↘		

Cellular localization		 heterochromatin & nucleoli
 heterochromatin	 nucleoli	

Differences compared to MeCP2 wildtype		
— no difference	↗ higher	↘ lower
	↗ higher n.s.	↘ lower n.s.

FIGURE 8
Summary of the functional characterization of MeCP2-induced heterochromatin organization. Functional differences of the MeCP2 PTM mutants in comparison to the wild type protein are represented as arrows showing increase (pointing up) and decrease (pointing down), if not statistically significant (n.s.) in gray, and no difference is marked by a line. Triple mutations stands for R91/R162/R167 mutations. Heterochromatin accumulation and clustering are MeCP2 dose-dependent. For the heterochromatin clustering in presence of PRMT1 and 6, only high PRMT levels were considered.

arginines. Although MeCP2 is rich in arginines (comprising 7.2% of the amino acids), we identified only a few of them as modified by methylation. One possible explanation is the removal of the modification during the experimental procedure. Although arginine methylation is considered a rather stable and permanent modification, recent reports argue for the existence of arginine demethylation enzymes (Bedford and Clarke, 2009; Wesche et al., 2017). On the one hand, studies involving drug treatments revealed rapid changes in arginine methylation (Le Romancer et al., 2008; Sylvestersen et al., 2014; Tsai et al., 2016).

On the other hand, candidate proteins catalyzing active arginine demethylation are discussed, among them several lysine demethylases (Chang et al., 2007; Walport et al., 2016; Wesche et al., 2017). Thus, although we might not have identified all possible arginine methylation sites, we conclude that arginine methylation on MeCP2 occurs mostly on a few specific sites and should be tightly regulated.

As MeCP2 serine 80 and 421 phosphorylation sites are well validated but not functionally characterized in the context of heterochromatin organization, we also analyzed their heterochromatin accumulation, clustering properties and binding kinetics (see Figure 8). The phospho-mimicking mutant S80D showed faster heterochromatin binding kinetics than wild type MeCP2, indicating reduced heterochromatin binding. By contrast, Tao et al. (2009) observed a decrease in MeCP2 chromatin binding affinity of the phospho-null MeCP2 S80A mutant to *Pomc* and *Gtl2* promoters by ChIP-qPCR. As with this method, the authors measured MeCP2 binding to selected genomic regions and not the overall MeCP2 heterochromatin binding kinetics, we used different methods to elucidate overall (hetero)chromatin association. Thus, our results contribute to understanding the function of MeCP2 S80 phosphorylation in global heterochromatin binding. MeCP2 S80 plays a role in heterochromatin association, but not in its clustering. In contrast, the serine 421 phosphorylation mimicking mutant S421D showed increased heterochromatin clustering (with lower heterochromatin cluster numbers and larger cluster areas) compared to wild type MeCP2. As S421 phosphorylation was found exclusively in the brain upon neuronal stimulation (Zhou et al., 2006; Tao et al., 2009), we propose that clustering of heterochromatin compartments plays a role in this process. Albeit heterochromatin binding often correlates to the ability of proteins to cluster heterochromatin together over time in the cell nucleus, it is not the only factor. In fact, whereas the binding of the Rett P101H mutant MeCP2 protein is similar to the wild type MeCP2, its clustering ability is totally impaired (Agarwal et al., 2011) and cannot be rescued by artificially targeting it to heterochromatin (Casas-Delucchi et al., 2012).

To observe the consequences of *PRMT1* and *PRMT6*, we introduced plasmids coding for PRMT one and six alone as well as together with MeCP2 in mouse myoblast cells. Solely the expression of *PRMT1* and *PRMT6* reduced the overall heterochromatin cluster size concomitantly increasing their numbers. PRMT1 mostly acts as a coactivator of transcription (An et al., 2004; Nicholson et al., 2009), whereas PRMT6 mostly acts as transcriptional repressor (Guccione et al., 2007; Hyllus et al., 2007; Stein et al., 2012; Stein et al., 2016), but it was also reported to contribute to gene activation (Bouchard et al., 2018). Interestingly, cells from cancer patients showed higher *PRMT1* and *PRMT6* expression than cells from healthy tissue, which seemed to be beneficial for tumor growth (Yoshimatsu et al.,

2011). Furthermore, *PRMT6* upregulation was found to correlate with DNA hypomethylation in mESCs and MCF7 cells (Veland et al., 2017), providing a possible explanation for the reduced heterochromatin clustering we observed upon *PRMT6* overexpression. Coexpression of *Mecp2* wild type and *PRMT1* and *PRMT6* lead to significantly decreased MeCP2-mediated heterochromatin clustering (indicated by higher cluster numbers and smaller areas), suggesting that a high degree of arginine methylation in the cells drastically impairs MeCP2 clustering function. This effect was more pronounced for PRMT6 than for PRMT1, although PRMT1 is considered responsible for the majority of cellular arginine methylation (Tang et al., 2000). Thus, PRMT6 might have a higher affinity for MeCP2 than PRMT1. Moreover, *PRMT1* and *PRMT6* expression was reported to depend on the MeCP2 level in a neuroblastoma cell line, thus suggesting a positive gene regulatory interaction between MeCP2 and these two genes (Vecsler et al., 2010).

The overall changes in heterochromatin clustering upon *PRMT* overexpression could be explained either by overall higher arginine methylation levels or by increased arginine methylation levels of MeCP2. To distinguish between these possibilities we made use of the MeCP2 arginine point mutations, which are not modifiable by the PRMTs. For this purpose, we generated MeCP2 constructs mutated for the modification sites identified (R91, R162, and R167) substituting the arginine with lysine (3K), glutamine (3Q) or leucine (3L). Although none of these substitutions can truly mimic the different arginine (modification) states, lysine retains the positive charge as (methylated) arginine, the polar glutamine should sterically mimic a methylated arginine and the unpolar leucine should mimic the methyl groups of methylated arginine (Supplementary Figure S8C, Figure 1E). Furthermore, arginine substitutions by glutamine and leucine were also found in Rett syndrome patients. Arginine substitution with the positively charged lysine increased heterochromatin accumulation and clustering in comparison to wild type MeCP2. In contrast, substitutions with glutamine and leucine reduced heterochromatin accumulation and lead to faster heterochromatin binding kinetics effectively reducing the $t_{1/2}$ to half of the one obtained with wild type MeCP2. These results indicate the importance of the positive charge on R91, R162, and R167 for MeCP2 heterochromatin accumulation and clustering but especially for heterochromatin binding kinetics. Of note, MeCP2 3Q seems to be the best MeCP2 mimic for heterochromatin clustering emphasizing that its polarity and steric properties are more similar to those of wild type MeCP2. The absence of charge and polarity clearly impacts all functional properties of MeCP2 tested here as seen with the MeCP2 3L mutant. Thus, we hypothesize that MeCP2 is methylated in brain at any given time at least at one of the arginine methylation sites identified and that this modification partially changes the positive charge distribution. Thus, methylated arginines might show similar properties as polar

amino acids. In fact, it was described that arginine methylation alters the charge distribution to more diffuse (especially in case of dimethylation) but still positive electrostatic properties (Evich et al., 2016; Lorton and Shechter, 2019). In addition, methylation changes arginine shape and reduces the number of possible hydrogen bonds (McBride and Silver, 2001; Bedford and Clarke, 2009). Cotransfection experiments of MeCP2 triple mutants and various PRMTs revealed differences in heterochromatin clustering between the mutants and the wild type protein, further strengthening the evidence for arginine methylation on one or more of the identified modification sites. In the presence of PRMT6, MeCP2 3K and 3L showed significantly higher heterochromatin clustering function represented by lower heterochromatin cluster numbers and larger areas than wild type MeCP2. MeCP2 3Q hardly induced any clustering, similar to MeCP2 wild type. MeCP2 3K showed higher clustering abilities (lower heterochromatin numbers and larger areas) than wild type MeCP2 and was able to reverse the effect of PRMT6 alone, which induced reduced clustering of heterochromatin. This effect might not be a direct result of the positive charge on heterochromatin clustering, but rather an indirect one as MeCP2 3K cannot be methylated by PRMTs on the mutated arginines. In comparison to the wild type protein, the MeCP2 3L mutant showed higher clustering when PRMT6 was introduced, although it showed decreased clustering without PRMT6. These results suggest a very high arginine methylation level of wild type MeCP2 in the coexpression experiment, which decreases its clustering ability to such an extent that even the MeCP2 3L mutant clusters more than the methylated wild type protein. From the increased heterochromatin clustering functions of the 3K and 3L mutant, which cannot be methylated on the substituted arginines, we conclude that MeCP2 gets methylated by PRMT6 on these sites. Of note, arginine methylation catalyzed by PRMT1 and PRMT6 often takes place on arginines flanked by one or more glycines in so called glycine and arginine rich (GAR) motifs (Lorton and Shechter, 2019) and MeCP2 R91 and R162 are localized adjacent to glycines. Although our results emphasize that MeCP2 gets methylated on arginines and in consequence shows reduced heterochromatin clustering abilities, we cannot exclude that consequences of high arginine methylation levels also indirectly impact MeCP2 heterochromatin clustering. Examples could be the modification of MeCP2 interacting proteins or other proteins involved in heterochromatin clustering, e.g., histones. Interestingly, MBD2, another member of the methyl-CpG binding protein family, was shown to undergo arginine methylation, which resulted in reduced DNA binding and reduced functionality in transcriptional repression (Tan and Nakielnny, 2006).

MeCP2 R106 was identified as dimethylated in our mass spectrometry analysis and is commonly mutated in Rett syndrome patients to tryptophan (W) and glutamine (Q), in very few cases also to glycine (G) and leucine (L).

MeCP2 R106W is a frequent Rett syndrome mutation causing severe phenotypes (Cuddapah et al., 2014) and the less common R106Q mutation was described to cause “classic” Rett syndrome (Bienvenu et al., 2000; Fukuda et al., 2005; Zahorakova et al., 2016), but there is insufficient clinical information reported for individuals with R106Q, R106G and R106L for a comparison of phenotypes (see RettBASE, (Krishnaraj et al., 2017)). R106 W was reported to abolish DNA binding, while R106Q reduced it (Ballestar et al., 2000; Yang et al., 2016). Accordingly, our experiments showed that all R106 mutants mainly lost heterochromatin accumulation and mislocalized to the negatively charged nucleoli due to the high amount of positively charged amino acids in MeCP2 (Martin et al., 2015). The reduced DNA binding and accumulation can be explained by the location of R106 close to the Asx-ST motif, which stabilizes MeCP2 DNA binding ((Ho et al., 2008), Figure 2E). H/DX experiments revealed similar dynamic protein behavior of MeCP2 R106W and wild type protein (Hansen et al., 2011) and circular dichroism spectra of R106W/Q showed no major changes in secondary structure compared to wild type MeCP2 (Ballestar et al., 2000; Yang et al., 2016). Instead, molecular modeling of the MeCP2 R106W/Q structures pointed towards local changes of hydrogen bonds and salt bridges (Kucukkal et al., 2015; Pedretti et al., 2016; Yang et al., 2016), which might cause changes in DNA binding as R106 is part of a β -strand in the MBD structure, stabilizes the Asx-ST motif and is buried and not exposed to the surrounding (Kucukkal et al., 2015; Pedretti et al., 2016). Thus, MeCP2 R106W/Q mutations have not been found to induce changes in overall MeCP2 structure but rather result in smaller local changes in amino acid interactions. The heterochromatin clustering was highly impaired in the MeCP2 R106 mutants as well. The reason might be the lack of binding to pericentric heterochromatin regions as the clustering abilities of some Rett mutants could be rescued by repositioning of the proteins to the heterochromatin regions (Casas-Delucchi et al., 2012). In addition, we recently showed that heterochromatin clustering *in vivo* can be modeled by *in vitro* phase separation (Zhang et al., 2022). The minimal basis for MeCP2 liquid-liquid phase separation was electrostatic self-interaction, but also DNA promoted *de novo* phase separation of MeCP2 in physiological salt conditions (Zhang et al., 2022). Thus, DNA binding as well as oligomerization *via* its ID and TRD domain (Becker et al., 2013) is involved in MeCP2 heterochromatin clustering. From the cotransfection experiments of PRMTs and MeCP2 R106 mutants it could be hypothesized that R106 is more likely to be methylated by PRMT6 than by PRMT1, as PRMT6 presence affected the clustering by MeCP2 R106 mutants. Altogether, our results demonstrate that post-translational modifications of MeCP2, in particular arginine methylation and to a lesser extent serine

phosphorylation, play an essential role in modulating MeCP2 function in heterochromatin organization.

Data availability statement

The datasets presented in this study can be found in online repositories. The names of the repositories and accession numbers can be found below: The data was uploaded to TUDDataLib accessible with the link <https://doi.org/10.48328/tudatalib-868>. The mass spectrometry proteomics data have been deposited to the ProteomeXchange Consortium via the PRIDE (Perez Riverol et al., 2019) partner repository with the dataset identifier PXD033696.

Author contributions

AS conceived the study. AS prepared the samples for mass spectrometry, performed parts of the mass spectrometry measurements, analyzed and visualized the mass spectrometry data. AS performed the Western blot analysis. AS performed all cell experiments, including immunofluorescence stainings, microscopy and data analysis. AS generated all figures and wrote the draft of the manuscript. AS implemented all comments from the coauthors, the bibliography, formatted the manuscript and organized and uploaded the data onto the repositories. JF contributed some of the dissected mouse brains used for Western blots. JF conceived, generated, characterized and validated the plasmids for inducible expression of MeCP2 wild type and PTM mutants. JF wrote the corresponding part of the methods section on plasmid generation. AP contributed the initial mass spectrometry data acquisition and helped in subsequent mass spectrometry data acquisition and analysis. AP supported AS on mass spectrometry data analysis, verification, database submission and presentation. AP commented and edited the manuscript. AC contributed preliminary data on arginine methylation and commented on the manuscript. HZ contributed to control immunofluorescence experiments and their analysis. HZ performed antibody testing and MeCP2 extraction analysis. CA conceived, generated, characterized and validated the plasmids for expression of PRMTs. AL provided assistance in cell culture during the cell experiments. U-MB conceived and supervised CA in the generation and characterization of the PRMT expression plasmids. U-MB commented and edited the manuscript. UN contributed to the conception of the project and to conceiving the MeCP2 PTM sites to be mutated and the design of how to generate the inducible expression plasmids for MeCP2 wild type and PTM mutants. UN proposed the PRMT overexpression experiments. UN commented and edited the manuscript, supervised JF and contributed to the supervision of

AS. UN interpreted data and acquired funding. MC conceived the study. MC supervised the project, discussed experiments, results and analysis. MC revised the manuscript and acquired the funding. All authors read and agreed to the manuscript.

Funding

The research was funded by the Deutsche Forschungsgemeinschaft (DFG, German Research Foundation) grants CA 198/10-1 project number 326470517 and CA198/16-1 project number 425470807 to MCC, grant UN 119/3-1 project number 326470517 to UAN, and grant BA 2292/1-4 to UMB. We acknowledge support by the Deutsche Forschungsgemeinschaft (DFG, German Research Foundation) and the Open Access Publishing Fund of Technical University of Darmstadt.

Acknowledgments

We thank Bianca Bertulat, Daniel Eck, Thomas Pfirzer, and Anica Ackermann for their contributions in the early stages of the project. We thank Alexander Rapp for experimental advice and Hector Romero for support with image analysis. We thank Diana Imblan for technical assistance and Mohamed El Hajjami for technical advice during mass spectrometry experiments. We thank Adrian Bird, Su-Chun Zhang, James Ellis, Feng Zhang, and Christopher L. Woodcock for providing plasmids.

Conflict of interest

The authors declare that the research was conducted in the absence of any commercial or financial relationships that could be construed as a potential conflict of interest.

Publisher's note

All claims expressed in this article are solely those of the authors and do not necessarily represent those of their affiliated organizations, or those of the publisher, the editors and the reviewers. Any product that may be evaluated in this article, or claim that may be made by its manufacturer, is not guaranteed or endorsed by the publisher.

Supplementary material

The Supplementary Material for this article can be found online at: <https://www.frontiersin.org/articles/10.3389/fcell.2022.941493/full#supplementary-material>

References

- Adams, V. H., McBryant, S. J., Wade, P. A., Woodcock, C. L., and Hansen, J. C. (2007). Intrinsic disorder and autonomous domain function in the multifunctional nuclear protein, MeCP2. *J. Biol. Chem.* 282, 15057–15064. doi:10.1074/jbc.M700855200
- Agarwal, N., Becker, A., Jost, K. L., Haase, S., Thakur, B. K., Brero, A., et al. (2011). MeCP2 Rett mutations affect large scale chromatin organization. *Hum. Mol. Genet.* 20, 4187–4195. doi:10.1093/hmg/ddr346
- Agarwal, N., Hardt, T., Brero, A., Nowak, D., Rothbauer, U., Becker, A., et al. (2007). MeCP2 interacts with HP1 and modulates its heterochromatin association during myogenic differentiation. *Nucleic Acids Res.* 35, 5402–5408. doi:10.1093/nar/gkm599
- Amir, R. E., Van den Veyver, I. B., Wan, M., Tran, C. Q., Francke, U., and Zoghbi, H. Y. (1999). Rett syndrome is caused by mutations in X-linked MECP2, encoding methyl-CpG-binding protein 2. *Nat. Genet.* 23, 185–188. doi:10.1038/13810
- An, W., Kim, J., and Roeder, R. G. (2004). Ordered cooperative functions of PRMT1, p300, and CARM1 in transcriptional activation by p53. *Cell* 117, 735–748. doi:10.1016/j.cell.2004.05.009
- Baccarini, P. (1908). Sulle cinesi vegetative del *Cynomorium coccineum* L. *N. Giorn. Bot. Ital. N. Ser.* 15, 189–203.
- Ballestar, E., Yusufzai, T. M., and Wolffe, A. P. (2000). Effects of Rett syndrome mutations of the methyl-CpG binding domain of the transcriptional repressor MeCP2 on selectivity for association with methylated DNA. *Biochemistry* 39, 7100–7106. doi:10.1021/bi0001271
- Becker, A., Allmann, L., Hofstätter, M., Casà, V., Weber, P., Lehmkuhl, A., et al. (2013). Direct homo- and hetero-interactions of MeCP2 and MBD2. *PLoS ONE* 8, e53730. doi:10.1371/journal.pone.0053730
- Becker, A., Zhang, P., Allmann, L., Meilinger, D., Bertulat, B., Eck, D., et al. (2016). Poly(ADP-ribosyl)ation of methyl CpG binding domain protein 2 regulates chromatin structure. *J. Biol. Chem.* 291, 4873–4881. doi:10.1074/jbc.M115.698357
- Bedford, M. T. (2007). Arginine methylation at a glance. *J. Cell Sci.* 120, 4243–4246. doi:10.1242/jcs.019885
- Bedford, M. T., and Clarke, S. G. (2009). Protein arginine methylation in mammals: Who, what, and why. *Mol. Cell* 33, 1–13. doi:10.1016/j.molcel.2008.12.013
- Bellini, E., Pavesi, G., Barbiero, I., Bergo, A., Chandola, C., Nawaz, M. S., et al. (2014). MeCP2 post-translational modifications: A mechanism to control its involvement in synaptic plasticity and homeostasis? *Front. Cell. Neurosci.* 8, 236. doi:10.3389/fncel.2014.00236
- Bertulat, B., De Bonis, M. L., Della Ragione, F., Lehmkuhl, A., Mildén, M., Storm, C., et al. (2012). MeCP2 dependent heterochromatin reorganization during neural differentiation of a novel Mecp2-deficient embryonic stem cell reporter line. *PLoS ONE* 7, e47848. doi:10.1371/journal.pone.0047848
- Bienvenu, T., Carrié, A., de Roux, N., Vinet, M. C., Jonveaux, P., Couvert, P., et al. (2000). MeCP2 mutations account for most cases of typical forms of Rett syndrome. *Hum. Mol. Genet.* 9, 1377–1384. doi:10.1093/hmg/9.9.1377
- Bouchard, C., Sahu, P., Meixner, M., Nötzold, R. R., Rust, M. B., Kremmer, E., et al. (2018). Genomic location of PRMT6-dependent H3R2 methylation is linked to the transcriptional outcome of associated genes. *Cell Rep.* 24, 3339–3352. doi:10.1016/j.celrep.2018.08.052
- Brero, A., Easwaran, H. P., Nowak, D., Grunewald, I., Cremer, T., Leonhardt, H., et al. (2005). Methyl CpG-binding proteins induce large-scale chromatin reorganization during terminal differentiation. *J. Cell Biol.* 169, 733–743. doi:10.1083/jcb.200502062
- Casas-Delucchi, C. S., Becker, A., Bolius, J. J., and Cardoso, M. C. (2012). Targeted manipulation of heterochromatin rescues MeCP2 Rett mutants and re-establishes higher order chromatin organization. *Nucleic Acids Res.* 40, e176. doi:10.1093/nar/gks784
- Cerletti, M., Paggi, R. A., Guevara, C. R., Poetsch, A., and De Castro, R. E. (2015). Global role of the membrane protease LonB in Archaea: Potential protease targets revealed by quantitative proteome analysis of a lonB mutant in *Haloferax volcanii*. *J. Proteomics* 121, 1–14. doi:10.1016/j.jprot.2015.03.016
- Chahrour, M., Jung, S. Y., Shaw, C., Zhou, X., Wong, S. T. C., Qin, J., et al. (2008). MeCP2, a key contributor to neurological disease, activates and represses transcription. *Science* 320, 1224–1229. doi:10.1126/science.1153252
- Chang, B., Chen, Y., Zhao, Y., and Bruick, R. K. (2007). JMJD6 is a histone arginine demethylase. *Science* 318, 444–447. doi:10.1126/science.1145801
- Chen, D., Ma, H., Hong, H., Koh, S. S., Huang, S. M., Schurter, B. T., et al. (1999). Regulation of transcription by a protein methyltransferase. *Science* 284, 2174–2177. doi:10.1126/science.284.5423.2174
- Cuddapah, V. A., Pillai, R. B., Shekar, K. V., Lane, J. B., Motil, K. J., Skinner, S. A., et al. (2014). Methyl-CpG-binding protein 2 (MECP2) mutation type is associated with disease severity in Rett syndrome. *J. Med. Genet.* 51, 152–158. doi:10.1136/jmedgenet-2013-102113
- Dyballa, N., and Metzger, S. (2009). Fast and sensitive colloidal coomassie G-250 staining for proteins in polyacrylamide gels. *JoVE* 1, 1431. doi:10.3791/1431
- Eng, J. K., McCormack, A. L., and Yates, J. R. (1994). An approach to correlate tandem mass spectral data of peptides with amino acid sequences in a protein database. *J. Am. Soc. Mass Spectrom.* 5, 976–989. doi:10.1016/1044-0305(94)80016-2
- Evich, M., Stroeve, E., Zheng, Y. G., and Germann, M. W. (2016). Effect of methylation on the side-chain pK_a value of arginine. *Protein Sci.* 25, 479–486. doi:10.1002/pro.2838
- Falk, M., Feodorova, Y., Naumova, N., Imakaev, M., Lajoie, B. R., Leonhardt, H., et al. (2019). Heterochromatin drives compartmentalization of inverted and conventional nuclei. *Nature* 570, 395–399. doi:10.1038/s41586-019-1275-3
- Fan, C., Zhang, H., Fu, L., Li, Y., Du, Y., Qiu, Z., et al. (2020). Rett mutations attenuate phase separation of MeCP2. *Cell Discov.* 6, 38. doi:10.1038/s41421-020-0172-0
- Frankel, A., Yadav, N., Lee, J., Branscombe, T. L., Clarke, S., and Bedford, M. T. (2002). The novel human protein arginine N-methyltransferase PRMT6 is a nuclear enzyme displaying unique substrate specificity. *J. Biol. Chem.* 277, 3537–3543. doi:10.1074/jbc.M108786200
- Fukuda, T., Yamashita, Y., Nagamitsu, S., Miyamoto, K., Jin, J.-J., Ohmori, I., et al. (2005). Methyl-CpG binding protein 2 gene (MECP2) variations in Japanese patients with rett syndrome: Pathological mutations and polymorphisms. *Brain Dev.* 27, 211–217. doi:10.1016/j.braindev.2004.06.003
- Georgel, P. T., Horowitz-Scherer, R. A., Adkins, N., Woodcock, C. L., Wade, P. A., and Hansen, J. C. (2003). Chromatin compaction by human MeCP2. *J. Biol. Chem.* 278, 32181–32188. doi:10.1074/jbc.M305308200
- Goulet, I., Gauvin, G., Boisvenue, S., and Côté, J. (2007). Alternative splicing yields protein arginine methyltransferase 1 isoforms with distinct activity, substrate specificity, and subcellular localization. *J. Biol. Chem.* 282, 33009–33021. doi:10.1074/jbc.M704349200
- Guccione, E., Bassi, C., Casadio, F., Martinato, F., Cesaroni, M., Schuchlantz, H., et al. (2007). Methylation of histone H3R2 by PRMT6 and H3K4 by an MLL complex are mutually exclusive. *Nature* 449, 933–937. doi:10.1038/nature06166
- Hansen, J. C., Wexler, B. B., Rogers, D. J., Hite, K. C., Panchenko, T., Ajith, S., et al. (2011). DNA binding restricts the intrinsic conformational flexibility of methyl CpG binding protein 2 (MeCP2). *J. Biol. Chem.* 286, 18938–18948. doi:10.1074/jbc.M111.234609
- Heckman, K. L., and Pease, L. R. (2007). Gene splicing and mutagenesis by PCR-driven overlap extension. *Nat. Protoc.* 2, 924–932. doi:10.1038/nprot.2007.132
- Heinz, K. S., Casas-Delucchi, C. S., Török, T., Cmarko, D., Rapp, A., Raska, I., et al. (2018). Peripheral re-localization of constitutive heterochromatin advances its replication timing and impairs maintenance of silencing marks. *Nucleic Acids Res.* 46, 6112–6128. doi:10.1093/nar/gky368
- Herrmann, F., Pably, P., Eckerich, C., Bedford, M. T., and Fackelmayer, F. O. (2009). Human protein arginine methyltransferases *in vivo* - distinct properties of eight canonical members of the PRMT family. *J. Cell Sci.* 122, 667–677. doi:10.1242/jcs.039933
- Ho, K. L., McNae, I. W., Schmiedeberg, L., Klose, R. J., Bird, A. P., and Walkinshaw, M. D. (2008). MeCP2 binding to DNA depends upon hydration at methyl-CpG. *Mol. Cell* 29, 525–531. doi:10.1016/j.molcel.2007.12.028
- Hyllus, D., Stein, C., Schnabel, K., Schiltz, E., Imhof, A., Dou, Y., et al. (2007). PRMT6-mediated methylation of R2 in histone H3 antagonizes H3 K4 trimethylation. *Genes Dev.* 21, 3369–3380. doi:10.1101/gad.447007
- Inuzuka, L. M., Guerra-Peixe, M., Macedo-Souza, L. I., Pedreira, C. C., Gurgel-Giannetti, J., Monteiro, F. P., et al. (2021). MECP2-related conditions in males: A systematic literature review and 8 additional cases. *Eur. J. Paediatr. Neurology* 34, 7–13. doi:10.1016/j.ejpn.2021.05.013
- Jones, P. L., Veenstra, G. J., Wade, P. A., Vermaak, D., Kass, S. U., Landsberger, N., et al. (1998). Methylated DNA and MeCP2 recruit histone deacetylase to repress transcription. *Nat. Genet.* 19, 187–191. doi:10.1038/561
- Jost, K. L., Bertulat, B., and Cardoso, M. C. (2012). Heterochromatin and gene positioning: Inside, outside, any side? *Chromosoma* 121, 555–563. doi:10.1007/s00412-012-0389-2
- Jost, K. L., Rottach, A., Mildén, M., Bertulat, B., Becker, A., Wolf, P., et al. (2011). Generation and characterization of rat and mouse monoclonal antibodies specific

- for MeCP2 and their use in X-inactivation studies. *PLoS ONE* 6, e26499. doi:10.1371/journal.pone.0026499
- Kleinschmidt, M. A., Streubel, G., Samans, B., Krause, M., and Bauer, U.-M. (2008). The protein arginine methyltransferases CARM1 and PRMT1 cooperate in gene regulation. *Nucleic Acids Res.* 36, 3202–3213. doi:10.1093/nar/gkn166
- Kokura, K., Kaul, S. C., Wadhwa, R., Nomura, T., Khan, M. M., Shinagawa, T., et al. (2001). The Ski protein family is required for MeCP2-mediated transcriptional repression. *J. Biol. Chem.* 276, 34115–34121. doi:10.1074/jbc.M105747200
- Krishnaraj, R., Ho, G., and Christodoulou, J. (2017). RettBASE: Rett syndrome database update. *Hum. Mutat.* 38, 922–931. doi:10.1002/humu.23263
- Kucukkal, T. G., Yang, Y., Uvarov, O., Cao, W., and Alexov, E. (2015). Impact of rett syndrome mutations on mcp2 MBD stability. *Biochemistry* 54, 6357–6368. doi:10.1021/acs.biochem.5b00790
- Larson, A. G., Elnatan, D., Keenen, M. M., Trnka, M. J., Johnston, J. B., Burlingame, A. L., et al. (2017). Liquid droplet formation by HP1a suggests a role for phase separation in heterochromatin. *Nature* 547, 236–240. doi:10.1038/nature22822
- Le Romancer, M., Treilleux, I., Leconte, N., Robin-Lespinasse, Y., Sents, S., Boucheikoua-Bouzagh, K., et al. (2008). Regulation of estrogen rapid signaling through arginine methylation by PRMT1. *Mol. Cell* 31, 212–221. doi:10.1016/j.molcel.2008.05.025
- Lewis, J. D., Meehan, R. R., Henzel, W. J., Maurer-Fogy, I., Jeppesen, P., Klein, F., et al. (1992). Purification, sequence, and cellular localization of a novel chromosomal protein that binds to methylated DNA. *Cell* 69, 905–914. doi:10.1016/0092-8674(92)90610-o
- Lorton, B. M., and Shechter, D. (2019). Cellular consequences of arginine methylation. *Cell. Mol. Life Sci.* 76, 2933–2956. doi:10.1007/s00018-019-03140-2
- Lunyak, V. V., Burgess, R., Prefontaine, G. G., Nelson, C., Sze, S.-H., Chenoweth, J., et al. (2002). Corepressor-dependent silencing of chromosomal regions encoding neuronal genes. *Science* 298, 1747–1752. doi:10.1126/science.1076469
- Lyst, M. J., Ekiert, R., Ebert, D. H., Merusi, C., Nowak, J., Selfridge, J., et al. (2013). Rett syndrome mutations abolish the interaction of MeCP2 with the NCoR/SMRT co-repressor. *Nat. Neurosci.* 16, 898–902. doi:10.1038/nn.3434
- Martin, R. M., Ter-Avetisyan, G., Herce, H. D., Ludwig, A. K., Lättig-Tünnemann, G., and Cardoso, M. C. (2015). Principles of protein targeting to the nucleolus. *Nucleus* 6, 314–325. doi:10.1080/19491034.2015.1079680
- McBride, A. E., and Silver, P. A. (2001). State of the arg. *Cell* 106, 5–8. doi:10.1016/s0092-8674(01)00423-8
- Nan, X., Campoy, F. J., and Bird, A. (1997). MeCP2 is a transcriptional repressor with abundant binding sites in genomic chromatin. *Cell* 88, 471–481. doi:10.1016/s0092-8674(00)81887-5
- Nan, X., Ng, H. H., Johnson, C. A., Laherty, C. D., Turner, B. M., Eisenman, R. N., et al. (1998). Transcriptional repression by the methyl-CpG-binding protein MeCP2 involves a histone deacetylase complex. *Nature* 393, 386–389. doi:10.1038/30764
- Nicholson, T. B., Chen, T., and Richard, S. (2009). The physiological and pathophysiological role of PRMT1-mediated protein arginine methylation. *Pharmacol. Res.* 60, 466–474. doi:10.1016/j.phrs.2009.07.006
- Pedretti, A., Granito, C., Mazzolari, A., and Vistoli, G. (2016). Structural effects of some relevant missense mutations on the MECP2-DNA binding: A md study analyzed by Rescore+, a versatile rescoring tool of the vega zz program. *Mol. Inf.* 35, 424–433. doi:10.1002/minf.201501030
- Perez-Riverol, Y., Csordas, A., Bai, J., Bernal-Llinares, M., Hewapathirana, S., Kundu, D. J., et al. (2019). The PRIDE database and related tools and resources in 2019: Improving support for quantification data. *Nucleic Acids Res.* 47, D442–D450. doi:10.1093/nar/gky1106
- Qian, K., Huang, C. T.-L., Chen, H., Blackburn, L. W., Chen, Y., Cao, J., et al. (2014). A simple and efficient system for regulating gene expression in human pluripotent stem cells and derivatives. *Stem Cells* 32, 1230–1238. doi:10.1002/stem.1653
- Ran, F. A., Hsu, P. D., Wright, J., Agarwala, V., Scott, D. A., and Zhang, F. (2013). Genome engineering using the CRISPR-Cas9 system. *Nat. Protoc.* 8, 2281–2308. doi:10.1038/nprot.2013.143
- Rival-Gervier, S., Lo, M. Y., Khattak, S., Pasceri, P., Lorincz, M. C., and Ellis, J. (2013). Kinetics and epigenetics of retroviral silencing in mouse embryonic stem cells defined by deletion of the D4Z4 element. *Mol. Ther.* 21, 1536–1550. doi:10.1038/mt.2013.131
- Schmidt, A., Zhang, H., and Cardoso, M. C. (2020). MeCP2 and chromatin compartmentalization. *Cells* 9, 878. doi:10.3390/cells9040878
- Stein, C., Nötzold, R. R., Riedl, S., Bouchard, C., and Bauer, U.-M. (2016). The arginine methyltransferase PRMT6 cooperates with polycomb proteins in regulating HOXA gene expression. *PLoS ONE* 11, e0148892. doi:10.1371/journal.pone.0148892
- Stein, C., Riedl, S., Ruthnick, D., Nötzold, R. R., and Bauer, U.-M. (2012). The arginine methyltransferase PRMT6 regulates cell proliferation and senescence through transcriptional repression of tumor suppressor genes. *Nucleic Acids Res.* 40, 9522–9533. doi:10.1093/nar/gks767
- Stopa, N., Krebs, J. E., and Shechter, D. (2015). The PRMT5 arginine methyltransferase: Many roles in development, cancer and beyond. *Cell. Mol. Life Sci.* 72, 2041–2059. doi:10.1007/s00018-015-1847-9
- Strom, A. R., Emelyanov, A. V., Mir, M., Fyodorov, D. V., Darzacq, X., and Karpen, G. H. (2017). Phase separation drives heterochromatin domain formation. *Nature* 547, 241–245. doi:10.1038/nature22989
- Sylvestersen, K. B., Horn, H., Jungmichel, S., Jensen, L. J., and Nielsen, M. L. (2014). Proteomic analysis of arginine methylation sites in human cells reveals dynamic regulation during transcriptional arrest. *Mol. Cell. Proteomics* 13, 2072–2088. doi:10.1074/mcp.O113.032748
- Tan, C. P., and Nakiely, S. (2006). Control of the DNA methylation system component MBD2 by protein arginine methylation. *Mol. Cell. Biol.* 26, 7224–7235. doi:10.1128/MCB.00473-06
- Tang, J., Frankel, A., Cook, R. J., Kim, S., Paik, W. K., Williams, K. R., et al. (2000). PRMT1 is the predominant type I protein arginine methyltransferase in mammalian cells. *J. Biol. Chem.* 275, 7723–7730. doi:10.1074/jbc.275.11.7723
- Tao, J., Hu, K., Chang, Q., Wu, H., Sherman, N. E., Martinowich, K., et al. (2009). Phosphorylation of MeCP2 at Serine 80 regulates its chromatin association and neurological function. *Proc. Natl. Acad. Sci. U.S.A.* 106, 4882–4887. doi:10.1073/pnas.0811648106
- Tillotson, R., Selfridge, J., Koerner, M. V., Gadalla, K. K. E., Guy, J., De Sousa, D., et al. (2017). Radically truncated MeCP2 rescues Rett syndrome-like neurological defects. *Nature* 550, 398–401. doi:10.1038/nature24058
- Tsai, W.-C., Gayatri, S., Reineke, L. C., Sbardella, G., Bedford, M. T., and Lloyd, R. E. (2016). Arginine demethylation of G3BP1 promotes stress granule assembly. *J. Biol. Chem.* 291, 22671–22685. doi:10.1074/jbc.M116.739573
- Tyanova, S., Temu, T., and Cox, J. (2016). The MaxQuant computational platform for mass spectrometry-based shotgun proteomics. *Nat. Protoc.* 11, 2301–2319. doi:10.1038/nprot.2016.136
- UniProt Consortium (2021). UniProt: The universal protein knowledgebase in 2021. *Nucleic Acids Res.* 49, D480–D489. doi:10.1093/nar/gkaa1100
- Vecsler, M., Simon, A. J., Amariglio, N., Rechavi, G., and Gak, E. (2010). MeCP2 deficiency down-regulates specific nuclear proteins that could be partially recovered by valproic acid *in vitro*. *Epigenetics* 5, 61–67. doi:10.4161/epi.5.1.10630
- Veland, N., Hardikar, S., Zhong, Y., Gayatri, S., Dan, J., Strahl, B. D., et al. (2017). The arginine methyltransferase PRMT6 regulates DNA methylation and contributes to global DNA hypomethylation in cancer. *Cell Rep.* 21, 3390–3397. doi:10.1016/j.celrep.2017.11.082
- Walport, L. J., Hopkinson, R. J., Chowdhury, R., Schiller, R., Ge, W., Kawamura, A., et al. (2016). Arginine demethylation is catalysed by a subset of JmJc histone lysine demethylases. *Nat. Commun.* 7, 11974. doi:10.1038/ncomms11974
- Wang, L., Hu, M., Zuo, M.-Q., Zhao, J., Wu, D., Huang, L., et al. (2020). Rett syndrome-causing mutations compromise MeCP2-mediated liquid-liquid phase separation of chromatin. *Cell Res.* 30, 393–407. doi:10.1038/s41422-020-0288-7
- Wesche, J., Kühn, S., Kessler, B. M., Salton, M., and Wolf, A. (2017). Protein arginine methylation: A prominent modification and its demethylation. *Cell. Mol. Life Sci.* 74, 3305–3315. doi:10.1007/s00018-017-2515-z
- Yang, Y., Kucukkal, T. G., Li, J., Alexov, E., and Cao, W. (2016). Binding analysis of methyl-CpG binding domain of MeCP2 and rett syndrome mutations. *ACS Chem. Biol.* 11, 2706–2715. doi:10.1021/acschembio.6b00450
- Yoshimatsu, M., Toyokawa, G., Hayami, S., Unoki, M., Tsunoda, T., Field, H. I., et al. (2011). Dysregulation of PRMT1 and PRMT6, Type I arginine methyltransferases, is involved in various types of human cancers. *Int. J. Cancer* 128, 562–573. doi:10.1002/ijc.25366
- Zahorakova, D., Lelkova, P., Gregor, V., Magner, M., Zeman, J., and Martasek, P. (2016). MECP2 mutations in Czech patients with rett syndrome and rett-like phenotypes: Novel mutations, genotype-phenotype correlations and validation of high-resolution melting analysis for mutation scanning. *J. Hum. Genet.* 61, 617–625. doi:10.1038/jhg.2016.19
- Zhang, H., Romero, H., Schmidt, A., Gagova, K., Qin, W., Bertulat, B., et al. (2022). MeCP2-induced heterochromatin organization is driven by oligomerization-based liquid-liquid phase separation and restricted by DNA methylation. *Nucleus* 13, 1–34. doi:10.1080/19491034.2021.2024691
- Zhou, Z., Hong, E. J., Cohen, S., Zhao, W.-N., Ho, H.-Y. H., Schmidt, L., et al. (2006). Brain-specific phosphorylation of MeCP2 regulates activity-dependent Bdnf transcription, dendritic growth, and spine maturation. *Neuron* 52, 255–269. doi:10.1016/j.neuron.2006.09.037



OPEN ACCESS

EDITED BY

Eric C. Schirmer,
University of Edinburgh,
United Kingdom

REVIEWED BY

Harinder Singh,
University of Pittsburgh, United States
Amos J. Simon,
Sheba Medical Center, Israel

*CORRESPONDENCE

James M. Holaska,
holaska@rowan.edu

SPECIALTY SECTION

This article was submitted to Nuclear Organization and Dynamics, a section of the journal Frontiers in Cell and Developmental Biology

RECEIVED 29 July 2022

ACCEPTED 20 September 2022

PUBLISHED 06 October 2022

CITATION

Marano N and Holaska JM (2022),
Emerin interacts with histone
methyltransferases to regulate
repressive chromatin at the
nuclear periphery.
Front. Cell Dev. Biol. 10:1007120.
doi: 10.3389/fcell.2022.1007120

COPYRIGHT

© 2022 Marano and Holaska. This is an open-access article distributed under the terms of the [Creative Commons Attribution License \(CC BY\)](https://creativecommons.org/licenses/by/4.0/). The use, distribution or reproduction in other forums is permitted, provided the original author(s) and the copyright owner(s) are credited and that the original publication in this journal is cited, in accordance with accepted academic practice. No use, distribution or reproduction is permitted which does not comply with these terms.

Emerin interacts with histone methyltransferases to regulate repressive chromatin at the nuclear periphery

Nicholas Marano and James M. Holaska*

Department of Biomedical Sciences, Cooper Medical School of Rowan University, Camden, NJ, United States

X-Linked Emery-Dreifuss muscular dystrophy is caused by mutations in the gene encoding emerin. Emerin is an inner nuclear membrane protein important for repressive chromatin organization at the nuclear periphery. Myogenic differentiation is a tightly regulated process characterized by genomic reorganization leading to coordinated temporal expression of key transcription factors, including MyoD, Pax7, and Myf5. Emerin was shown to interact with repressive histone modification machinery, including HDAC3 and EZH2. Using emerin-null myogenic progenitor cells we established several EDMD-causing emerin mutant lines in the effort to understand how the functional interaction of emerin with HDAC3 regulates histone methyltransferase localization or function to organize repressive chromatin at the nuclear periphery. We found that, in addition to its interaction with HDAC3, emerin interacts with the histone methyltransferases EZH2 and G9a in myogenic progenitor cells. Further, we show enhanced binding of emerin HDAC3-binding mutants S54F and Q133H to EZH2 and G9a. Treatment with small molecule inhibitors of EZH2 and G9a reduced H3K9me2 or H3K27me3 throughout differentiation. EZH2 and G9a inhibitors impaired cell cycle withdrawal, differentiation commitment, and myotube formation in wildtype progenitors, while they had no effect on emerin-null progenitors. Interestingly, these inhibitors exacerbated the impaired differentiation of emerin S54F and Q133H mutant progenitors. Collectively, these results suggest the functional interaction between emerin and HDAC3, EZH2, and G9a are important for myogenic differentiation.

KEYWORDS

emerin, Emery-Dreifuss muscular dystrophy, myogenic differentiation, repressive chromatin, EZH2, G9a

Introduction

X-linked Emery-Dreifuss muscular dystrophy (X-EDMD; EDMD1) is caused by mutations in the gene encoding emerin (Bione et al., 1994). Emerin is an integral inner nuclear membrane (INM) protein with putative roles in repressive chromatin organization at the nuclear periphery (Demmerle et al., 2012, 2013; Ranade et al.,

2019). Patients with EDMD1 experience skeletal muscle wasting and dilated cardiomyopathy (Heller et al., 2020). Skeletal muscle wasting may be attributed to the inability of the resident muscle stem cell pool to differentiate and regenerate damaged muscle (Koch and Holaska, 2014). Upon muscle injury or mechanical stimulation, these muscle stem cells (or myogenic progenitor cells) initiate the myogenic differentiation program, which is a tightly regulated process driven by the coordinated temporal expression of key transcription factors. Genomic reorganization is required for this transcriptional reprogramming during commitment to differentiation and formation of myotubes (Bharathy et al., 2013).

Purification of emerin-containing complexes from HeLa cells revealed interactions with chromatin associated proteins, such as barrier-to-autointegration factor (BAF) and histone deacetylases (HDAC) 1 and 3 (Holaska and Wilson, 2007). Emerin binds histone deacetylase 3 (HDAC3) in C2C12 myoblasts and in HeLa cells (Demmerle et al., 2012). HDAC3 is a class I lysine deacetylase and the catalytic subunit of the Nuclear CoRepressor complex (NCoR) (Moser et al., 2014) responsible for deacetylation of H4K5 (Bhaskara et al., 2010). *In vitro* studies showed that emerin binds directly to HDAC3 and activates its catalytic activity (Demmerle et al., 2012). Emerin-null myogenic progenitors showed a significant increase in transcriptionally active H4K5ac modification, which is the target of HDAC3 (Collins et al., 2017). Similar results were seen in emerin-downregulated HeLa cells (Demmerle et al., 2012). Differentiating emerin-null myogenic progenitors also had increased H4K5ac in promoters of key differentiation genes. Emerin-null progenitors also failed to coordinate the spatiotemporal localization of differentiation gene loci to the nuclear envelope, resulting in maintenance of their expression (Demmerle et al., 2013). Treatment with an HDAC3 activator rescued *Myf5* localization and myogenic differentiation (Demmerle et al., 2013), demonstrating the functional interaction between emerin and HDAC3 is important for differentiation. Treatment with histone acetyltransferase inhibitors specifically targeting H4K5 acetylation also rescued emerin-null differentiation (Bossone et al., 2020). We hypothesize that emerin is important for maintaining H4K5ac homeostasis during myogenic differentiation to ensure proper transcriptional reprogramming. It is possible emerin also regulates the coordinated deposition of H3K9me2/3 and H3K27me3 during differentiation.

Interestingly, EDMD1-causing emerin mutants (S54F, Δ95-99, Q133H, P183H) all failed to bind HDAC3 (Demmerle et al., 2012). Myogenic progenitors expressing the EDMD1 mutants in an emerin-null background exhibited impaired differentiation (Iyer and Holaska, 2020) suggesting the interaction of emerin with HDAC3 is vital for myogenic differentiation. Similar molecular pathways were disrupted in each of the EDMD1 mutants and emerin-null cells (Iyer et al.,

2017; Iyer and Holaska, 2020), suggesting similar mechanisms underly impaired differentiation in EDMD1. These observations suggest the emerin-HDAC3 interaction may be important for the impaired muscle regeneration seen in EDMD1 patients.

Msh homeobox 1 (Msx1) has been shown to colocalize with polycomb repressive complex 2 (PRC2) and H3K27me3 at the nuclear periphery in C2C12 cells and primary myoblasts (Wang et al., 2011). Emerin is responsible for the recruitment of Msx1 and EZH2 to the nuclear envelope (Ma et al., 2019). EZH2, the catalytic component of PRC2, mediates the trimethylation of H3K27 (Tan et al., 2014)—a repressive histone modification reported to be enriched in lamina-associated domains (van Steensel and Belmont, 2017). ChIP-Seq experiments show H3K27me3 enrichment and repression of transcriptional regulators *Myf5* and *MyoD* is dependent upon Msx1 (Wang et al., 2011). Localization of Msx1 and EZH2 at the nuclear envelope is emerin-dependent, as emerin-knockdown in C2C12 myoblasts caused both Msx1 and EZH2 localization to be lost at the inner nuclear membrane (Wang and Abate-Shen, 2012b; Ma et al., 2019).

Msx1 can also recruit euchromatic histone lysine methyltransferase 2 (EHMT2 or G9a) in C2C12 cells (Wang and Abate-Shen, 2012a). H3K9me2 enrichment at regulatory regions of key myogenic transcription factors is dependent on Msx1 (Wang and Abate-Shen, 2012a). G9a functions primarily as a heterodimer with lysine methyltransferase G9a-like protein (GLP) (Tachibana et al., 2005). Although G9a and GLP are structurally similar, they do serve distinct roles in myogenesis. Exogenous expression of G9a was shown to impair muscle differentiation in C2C12 cells (Ling et al., 2012), whereas knockdown of G9a favors muscle differentiation (Battisti et al., 2016). G9a was also shown to interact with the PRC2 complex (e.g., EZH2) and G9a knockdown led to decreased EZH2 and H3K27me3 at PRC2 target genes (Mozzetta et al., 2014). G9a and PRC2 may cooperate to organize repressive chromatin at the nuclear envelope and regulate myogenic differentiation, as genomic studies have suggested colocalization of PRC2 and H3K9 methyltransferases (Wang et al., 2008).

Collectively, these data support a model whereby emerin modulates repressive chromatin reorganization at the nuclear envelope during transcriptional reprogramming. How this occurs remains unknown. Thus, we set out to better understand the functional interaction between emerin, HDAC3, and EZH2 and G9a, and its role in myogenic differentiation. Here we show emerin interacts with both G9a and EZH2 in myogenic progenitors. We further demonstrate that emerin HDAC3-binding mutants show enhanced binding to G9a and EZH2, resulting in more H3K27me3 and H3K9me2 at the nuclear envelope and impaired differentiation. Using EZH2 and G9a inhibitors, we show these functional interactions are important for myogenic differentiation.

Methods

Cell culture

Myogenic progenitors from H2K wildtype and EMD^{-/-} mice were obtained from Tatiana Cohen and Terence Partridge (Children's National Medical Center, Washington DC, United States). Proliferating myogenic progenitors were counted in a Countess[®] II FL Automated Cell Counter (ThermoFisher Scientific), plated at 650 cells/cm², and incubated in proliferative media consisting of high-glucose DMEM (ThermoFisher Scientific) supplemented with 2% chick embryo extract (Accurate Chemical; #MDL-004-E), 20% heat-inactivated FBS (ThermoFisher Scientific; #MDL-004-E), 1% penicillin-streptomycin (ThermoFisher Scientific), 2% L-glutamine (ThermoFisher Scientific) and 20 units/mL γ -interferon (MilliporeSigma) at 33°C and 10% CO₂, as previously described (Iyer and Holaska, 2020). Emerin-null progenitor lines and emerin-null cell lines expressing wildtype emerin (+EMD), emerin EDMD1 mutants Q133H or S54F emerin, or vector alone control cell lines were previously established and grown in the presence of 6 μ g/ml puromycin, 10 μ g/ml puromycin, and 15 μ g/ml puromycin, respectively (Iyer and Holaska, 2020). For differentiation experiments, cells were plated at 25,000 cells/cm² in proliferative media at 33°C and 10% CO₂. Cells were washed once with PBS and incubated with differentiation media consisting of high-glucose DMEM, 2% horse serum, and 1% penicillin/streptomycin at 37°C and 5% CO₂.

Co-immunoprecipitation and western blotting

Dynabeads[™] protein G magnetic beads (ThermoFisher Scientific; #1007D) were washed once with washing buffer. Beads were then resuspended in antibody binding buffer and incubated with antibodies against emerin (Proteintech, #10351-1-AP), G9a (Abcam; #185050), or EZH2 (Active Motif #39239) overnight at 4°C with rotation. Wildtype and emerin-null progenitors expressing S54F or Q133H EDMD1 mutants were grown in 15 cm dishes coated with 0.01% gelatin in proliferative conditions, as described above. Cells were incubated with 0.05% Trypsin-EDTA (Gibco; #25300054) for 5 min at 37°C and 10% CO₂ and collected by centrifugation (160 g, 5 min). Cell pellets were lysed on ice in modified NEHN buffer (20% glycerol, 500 mM NaCl, 20 mM HEPES, 1 mM PMSF, 1 mM EDTA, 2 mM DTT, 1% NP-40, aprotinin, leupeptin, and pepstatin A). Whole cell lysates were then sonicated on ice with 30 s on/off intervals for 10 min and placed on ice for 5 min. This was repeated three more times. Lysates were spun at 16,300 g at 4°C for 20 min. Insoluble components were pelleted and the soluble fraction was

collected. Antibody-bound Dynabeads[™] protein G magnetic beads were washed twice with washing buffer and incubated overnight with soluble fractions. Beads were separated from the soluble fraction with a magnet and resuspended in washing buffer for three 5-min washes with rotation. Bound complexes were eluted from beads per manufacturer instructions (ThermoFisher Scientific). Eluted fractions were incubated with 1:1 mixture of 2X NuPage[™] LDS sample buffer at 75°C and 500 rpm for 10 min on a hot plate mixer (ThermoFisher Scientific; #NP0007). Samples were loaded and separated by SDS-PAGE at 150 V for 50 min. Gels were transferred to nitrocellulose membranes at 250 mA for 75 min on ice with stirring. Membranes were blocked with 5% non-fat milk (Giant Food Stores) in phosphate buffered saline (pH 7.4) containing 0.1% Tween-20 (PBST) for 1 hour at room temperature followed by incubation with antibodies against emerin (1:3,000; Leica Biosystems; #NCL-EMERIN), G9a (1:5,000; Proteintech; #66689-1-Ig) or EZH2 (1:5,000; Proteintech; #66476-1-Ig) diluted in 0.5% non-fat milk overnight at 4°C with mild shaking. Blots were washed with PBST at least 3 times for 5 min at room temperature and incubated with HRP-conjugated secondary antibodies against mouse IgG (ThermoFisher Scientific; #31432). Membranes were then washed with PBST at least 3 times for 5 min. Blots were incubated with SuperSignal[™] West PicoPlus chemiluminescent substrate solution (Life Technologies; #34580) and visualized. Images were taken on a Bio-Rad ChemiDoc MP imaging system. Densitometry was performed using Bio-Rad Image Lab[®] software. Ratios of bound to input were measured and plotted. Input and unbound sample lanes represent 2.5% of total. Bound lanes represent 50% of input.

Immunofluorescence microscopy

Myogenic progenitors were plated on gelatin-coated coverslips or directly in gelatin-coated 96-well dishes for immunofluorescence microscopy. Proliferative cells were plated on gelatin-coated coverslips and grown for 2 days (30%–40% confluent) at 33°C, 10% CO₂. Differentiation samples were plated at 25,000 cells/cm² and incubated in proliferative media overnight at 33°C and 10% CO₂. Coverslips and 96-well dishes were washed three times with phosphate buffered saline (PBS, pH 7.4), fixed with 3.7% formaldehyde in PBS for 15 min, washed once with PBS for 5 minutes at room temperature, permeabilized with PBS containing 0.2% Triton X-100 for 20 min at room temperature, followed by washing once with PBS for 5 minutes at room temperature. All washing and incubation steps are performed with moderate shaking. Coverslips or 96-well plates were blocked in PBS containing 3% BSA and 0.1% Triton X-100 for 2 h at room temperature, followed by incubation with antibodies against emerin (1:300; Leica

Biosystems; #NCL-Emerin), H3K9me2 (1:250; Active Motif; #39239), G9a (1:500; Abcam; #185050), H3K27me3 (1:200; Millipore Sigma; #MP 07-449) or EZH2 (1:250; Active Motif; #39901) overnight at 4°C with shaking. Coverslips were washed three times in PBS at room temperature and incubated with Alexa Fluor™-conjugated secondary antibodies against rabbit or mouse IgG (Invitrogen) for 1 h at room temperature shielded from light. All primary and secondary antibodies were diluted in PBS containing 3% BSA and 0.1% Triton X-100. Coverslips were mounted on slides with ProLong™ Diamond Antifade Mountant with DAPI (Life Technologies; #P36971). Myogenic differentiation was done in 96-well plates because myotubes can more readily detach from coverslips. For immunofluorescence microscopy on differentiating cells, the cells were plated at 25,000/cm² (differentiation density) and incubated overnight in proliferation media at 33°C and 10% CO₂. Wells were washed with PBS and differentiation media was added to each well and the cells were incubated for 24–72 h at 37°C, 5% CO₂. Blocking, fixing, washing, and incubating with primary and secondary antibodies was done as described for the coverslips. 96-well dishes were incubated with 0.2 µg/ml DAPI in PBS for 5 min and washed twice with PBS.

Confocal microscopy

Slides of myogenic progenitors were prepared as described above and confocal images were taken using a Nikon Eclipse Ti2-E Inverted Research Microscope equipped for confocal, brightfield and DIC imaging in conjunction with a Nikon A1rSi Laser Point Scanning Confocal System. All images were taken with a 60X oil-immersion objective (N.A. = 1.4). Nikon Imaging Software (NIS) Elements was used to record images. Each field was subject to the same light conditions and exposure times. At least 30 nuclei were imaged for each trial. Files were analyzed in NIS Elements Viewer software and ImageJ. Localization was measured using 21.1 µm lines that were drawn across similar axes of nuclei using ImageJ software. Fluorescence was quantified along the superimposed line in each field and measurements were plotted on the same graph.

Histone methyltransferase inhibition and myogenic differentiation assay

2.5 µM G9a inhibitor UNC0638 (BioVision; #1933) or 4.0 µM EZH2 inhibitor GSK126 (BioVision; #2282) were added to differentiation media upon differentiation induction ($t = 0$). At 24, 48, or 72 h after induction of differentiation, the cells were lysed in SDS-PAGE sample

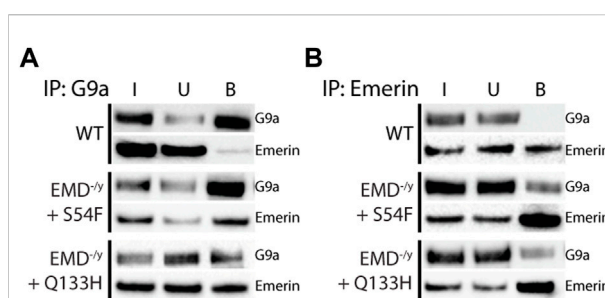
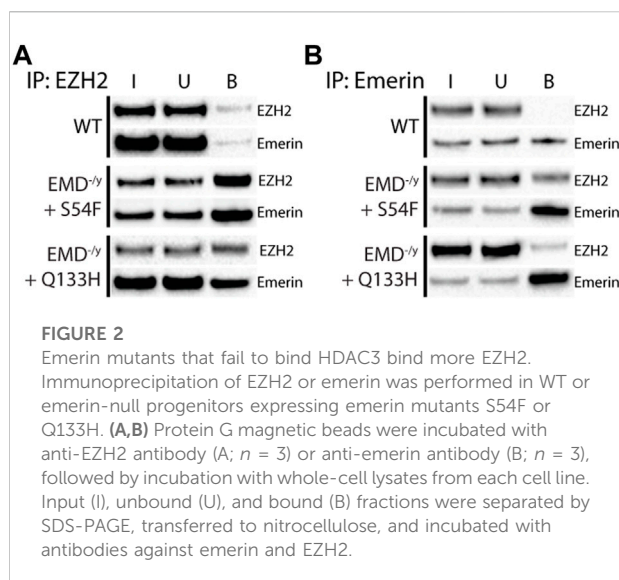


FIGURE 1
Emerin mutants that fail to bind HDAC3 bind more G9a. Immunoprecipitation of G9a or emerlin was performed in WT or emerlin-null progenitors expressing emerlin mutants S54F or Q133H. (A,B) Protein G magnetic beads were incubated with anti-G9a antibody (A; $n = 3$ for all cell lines) or anti-emerlin antibody (B; $n = 3$ for all cell lines), followed by incubation with whole-cell lysates from each cell line. Input (I), unbound (U), and bound (B) fractions were separated by SDS-PAGE, transferred to nitrocellulose, and incubated with antibodies against emerlin and G9a.

buffer, separated by SDS-PAGE, and western blotting was done using antibodies against H3K9me2 (1:2,000; Active Motif; #39239), H3K27me3 (1:1,500; Millipore Sigma; #MP 07-449), or γ -tubulin (1:10,000; ThermoFisher, Scientific). The levels of H3K9me2 and H3K27me3 were normalized to γ -tubulin expression and analyzed as described above. Validation of inhibitors was performed in all cell lines and two biological replicates were prepared for each treatment at each time point.

The ClickIt EdU reaction kit (ThermoFisher Scientific; #C10640) was used to assess cell cycle withdrawal. EdU was added to media 2 h prior to washing with PBS and fixing with 3.7% formaldehyde in PBS for 15 min. Cells were washed once with PBS, permeabilized with 0.2% Triton X-100 in PBS for 20 min at room temperature, and stained per manufacturer instructions. Nuclei were incubated with 0.2 µg/ml DAPI in PBS for 5 min at room temperature. Images of EdU (Alexa-647) and DAPI (405 nm) were taken using a 40X objective (N.A. = 0.65) on an Evos FL Auto 2 microscope. Differentiation was quantified by monitoring the expression of myosin heavy chain (MyHC) using MyHC antibodies (1:20; Santa Cruz Biotechnology; #SC-376157). A minimum of three biological replicates were prepared for each condition and at least three images were taken (random location) for each biological replicate in each field. At least 75 nuclei were imaged for each trial. Images were counted using the cell counter plugin on ImageJ and analyzed in Prism 9 software. Percentages of EdU-positive or MyHC-positive cells were compared to total nuclei (DAPI) for each replicate. Fusion index was determined by merging DAPI and MyHC channels and counting cells containing at least 3 nuclei sharing MyHC-stained cytoplasm.



Results

Emerin HDAC3-Binding mutants bind more G9a and EZH2

Our previous data suggests that emerlin binding to HDAC3 results in more chromatin deacetylation at the nuclear envelope which could recruit HMTs (e.g., EZH2 and G9a) to methylation targets and more stably repress nuclear envelope-associated chromatin. Emerlin was reported to interact with EZH2 *via* Mx1, so we tested whether emerlin and the EDMD1 mutants could bind to EZH2. H3K9me2 has also been implicated in organizing repressive chromatin at the nuclear envelope, so we also tested if emerlin could bind G9a.

Co-immunoprecipitation experiments with antibodies against emerlin, EZH2, or G9a were done on wildtype myogenic progenitors ($n = 3$) or emerlin-null progenitors expressing either emerlin S54F ($n = 3$) or Q133H ($n = 3$) at wildtype levels. A small fraction of endogenous emerlin bound G9a (Figure 1A; S1, 0.76% of input), whereas G9a bound a much larger fraction of S54F (80.9% of input) and Q133H (45.1% of input). Reciprocal experiments were done using antibodies against emerlin for the immunoprecipitation and similar results were seen with 0.2% of G9a binding to wildtype emerlin ($n = 3$) and 13.8% and 9.6% binding to S54F ($n = 3$) and Q133H ($n = 3$), respectively (Figure 1B; Supplementary Figure S1). We next analyzed emerlin binding to EZH2 by co-IP in myogenic progenitors and S54F and Q133H emerlin mutant myogenic progenitors. Immunoprecipitation with antibodies against EZH2 showed 0.7% emerlin bound EZH2 in wildtype progenitors (Figure 2A; Supplementary Figure S2; $n = 2$), whereas 71.8% of S54F ($n = 3$) and 77.8% of Q133H ($n = 2$) bound EZH2. Similar results were seen in the reciprocal immunoprecipitation,

with 2.4% EZH2 bound to wildtype emerlin ($n = 3$), and 57.9% and 89.4% of EZH2 binding to S54F ($n = 3$) and Q133H ($n = 2$), respectively (Figure 2B; Supplementary Figure S2).

More H3K9me2 and H3K27me3 localize to the nuclear envelope in S54F and Q133H myogenic progenitors

G9a mediates the mono- and di-methylation of H3K9 (Poulard et al., 2021) and EZH2 mediates the trimethylation of H3K27 (Tan et al., 2014). Thus, we tested if enhanced binding of S54F and Q133H to G9a and EZH2 affected their activity at the nuclear envelope. Confocal immunofluorescence microscopy was used to localize emerlin, EZH2, G9a, H3K9me2, and H3K27me3 in wildtype, emerlin-null, S54F, and Q133H myogenic progenitors (Figure 3; Supplementary Figure S1–S12; $n > 30$ for each). A line was drawn through each nucleus and relative fluorescence along this line was plotted to monitor spatial distribution of each protein and its associated modification. H3K9me2 (Figure 3A; Supplementary Figure S3) and H3K27me3 (Figure 3B; Supplementary Figure S8) images in wildtype progenitors show greater peripheral localization of each modification when compared to cells lacking emerlin. Emerlin-null progenitors had less H3K9me2 (Figure 3A; Supplementary Figure S4) and H3K27me3 (Figure 3B; Supplementary Figure S9), which was rescued by expression of wildtype emerlin (+EMD, Figures 3A,B; Supplementary Figure S5, S10). Both S54F and Q133H, which fail to bind HDAC3, show increased localization of H3K9me2 (Figure 3A; Supplementary Figure S6,S7) and H3K27me3 (Figure 3B; Supplementary Figure S11,12) at the nuclear periphery when compared to wildtype myogenic progenitors. G9a and EZH2 were not enriched at the nuclear envelope in wildtype progenitors nor in either of the EDMD1 mutant progenitors (data not shown), suggesting the interactions between emerlin and HMTs at the nuclear envelope may be transient. These results show that an increased interaction between these HDAC3-binding mutants results in an increased proportion of H3K9me2 and H3K27me3 chromatin localized at the nuclear envelope.

Inhibitors UNC0638 and GSK126 reduce H3K9me2 and H3K27me3 levels throughout differentiation

We reasoned higher relative levels of H3K9me2 and H3K27me3 at the nuclear envelope in HDAC3-binding emerlin mutants were due to increased binding of emerlin to G9a and EZH2. Thus, we tested if this increased H3K9 and H3K27 methylation may contribute to the impaired differentiation of S54F and Q133H progenitors. We used selective inhibitors of G9a (UNC0638) and EZH2 (GSK126)

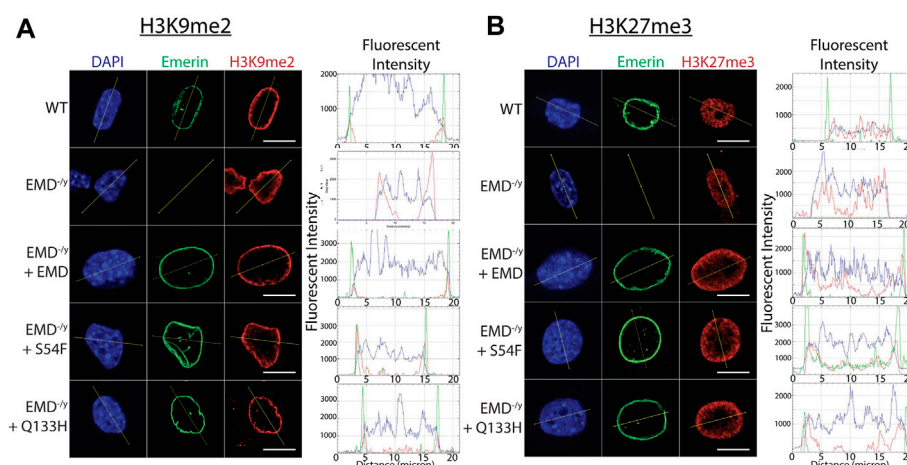


FIGURE 3

Confocal imaging shows enrichment of H3K9me2 and H3K27me3 at the nuclear periphery. **(A,B)** Wildtype myogenic progenitors or emerlin null myogenic progenitors expressing WT emerlin, S54F emerlin, or Q133H emerlin were fixed and incubated with antibodies against emerlin and H3K9me2 **(A)** or H3K27me3 **(B)**. Representative images of DAPI, emerlin, and H3K9me2 or H3K27me3 staining are shown. Images were analyzed using ImageJ software to measure enrichment at the nuclear envelope. A line was drawn across the nucleus in each field and fluorescence was quantified along the line. Representative line graphs are shown for each set of images ($N > 30$ for each cell line). Scale bars represent 10 μm .

to reduce H3K9me2 and H3K27me3 levels, respectively, to test this hypothesis. UNC0638 and GSK126 have reported IC_{50} values of 15 and 9.9 nM, respectively (BioVision). To validate our approach (Figure 4A), we first confirmed these inhibitors would be functional throughout differentiation (72 h) by measuring total levels of their respective histone modifications. Myogenic progenitors were plated at differentiation density, treated with UNC0638 and induced to differentiate. Cells were suspended in SDS-PAGE sample buffer at 0 h (upon introduction of differentiation media), 24 h, 48 h, and 72 h. Western-blotting was done on whole cell lysates using antibodies against H3K9me2 to confirm G9a inhibition throughout differentiation. H3K9me2 levels in wildtype, S54F and Q133H were reduced 61.3%, 31.7%, and 87.1%, after 72 h (Figures 4B,C; $n = 2$), respectively. H3K9me2 levels at 24 h showed a reduction of 35.2% in wildtype, 17.8% in S54F, and 26.7% in Q133H differentiating myogenic progenitors, demonstrating that UNC0638 remains functional throughout the differentiation assay. Treatment with UNC0638 lowered the levels of H3K9me2 at all time points, with the exception of emerlin-null cells (Figure 4C). Similar experiments were done using the EZH2 inhibitor, GSK126. Inhibition of EZH2 throughout differentiation was also seen, as H3K27me3 was reduced at all time points in the presence of GSK126 for all cell lines compared to control (Figures 4D,E; $n = 2$). H3K27me3 levels in wildtype, in S54F, in Q133H, and in emerlin-null cells were reduced 71.2%, 68.1%, 74.7%, and 71.5% after 72 h of differentiation (Figures 4D,E), respectively. Similar reductions of H3K27me3 were seen at 24 h (64.0% in wildtype, 68.8% in S54F, 67.0% in Q133H, and 82.1% in emerlin-null),

showing GSK126 remains functional throughout the differentiation assay.

Now that we confirmed functionality of UNC0638 and GSK126 throughout differentiation, we wanted to test the impact of G9a or EZH2 inhibition on wildtype and EDMD1 mutant myogenic differentiation. EdU incorporation was measured 24 h after differentiation induction to assess cell cycle withdrawal. G9a inhibition increased cell cycle withdrawal during differentiation of wildtype and S54F progenitors (Figures 5B,D, $n = 3$) but failed to rescue cell cycle withdrawal during differentiation of Q133H and emerlin-null progenitors (Figures 5B,D; $n = 3$). EZH2 inhibition failed to significantly alter cell cycle exit in any of the progenitor lines tested compared (Figures 5C,D; $n = 3$).

We next measured the differentiation index (number of nuclei in MyHC⁺ multinucleated myotubes + number of nuclei in MyHC⁺ mono- or di-nuclear cells/total nuclei) and the fusion index (number of nuclei in MyHC⁺ multi-nucleated myotubes (≥ 3 nuclei/total nuclei)) to assess myoblast commitment and fusion to form myotubes, respectively, in the presence of UNC0638 and GSK126. To monitor myoblast commitment and fusion, expression of MyHC was detected by immunofluorescence microscopy 48 h after differentiation induction, while the fusion index is determined at 72 h post-induction. G9a inhibition significantly decreased the differentiation index in wildtype emerlin and S54F mutant cells (Figures 6B,D; $n = 3$), while no significant difference was detected in emerlin-null and Q133H mutant cells (Figures 6B,D). Inhibition of EZH2 reduced the differentiation index of wildtype emerlin and Q133H mutant cells, while no significant change was

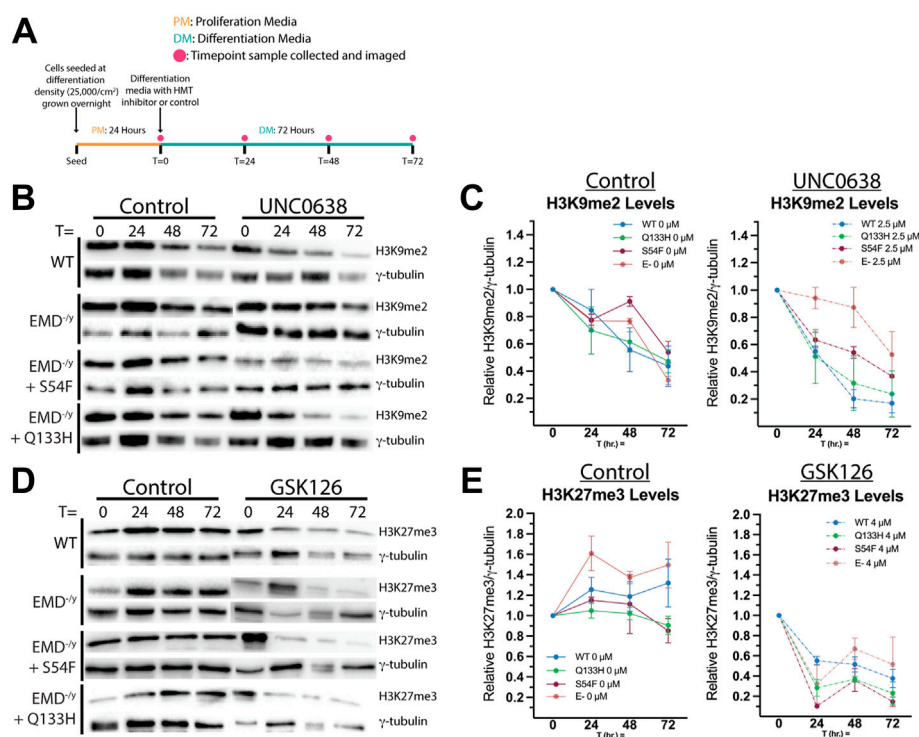


FIGURE 4

H3K9me2 and H3K27me3 are reduced by histone methyltransferase inhibitors throughout differentiation. (A) Schematic of the experimental approach for validating inhibitors UNC0638 and GSK126 is shown. Wildtype, emerin-null (E-), S54F, or Q133H myogenic progenitors were seeded at 25,000 cells/cm² and grown overnight in proliferation media at 10% CO₂ and 33°C. At t = 0 h, differentiation was induced by replacing the media with differentiation media and incubating at 5% CO₂ and 37°C. Differentiation media contained 2.5 μ M UNC0638, 4 μ M GSK126, or ethanol alone. Images and samples were collected at 0, 24, 48, and 72 h. UNC0638 (B) and GSK126 (D) samples were separated by SDS-PAGE and visualized by western blot. Quantitation was performed via densitometry analysis of H3K9me2 [(C); n = 2] and H3K27me3 [(E); n = 2] at each time point and plotted. Bands were normalized to γ -tubulin expression. Error bars represent SEM.

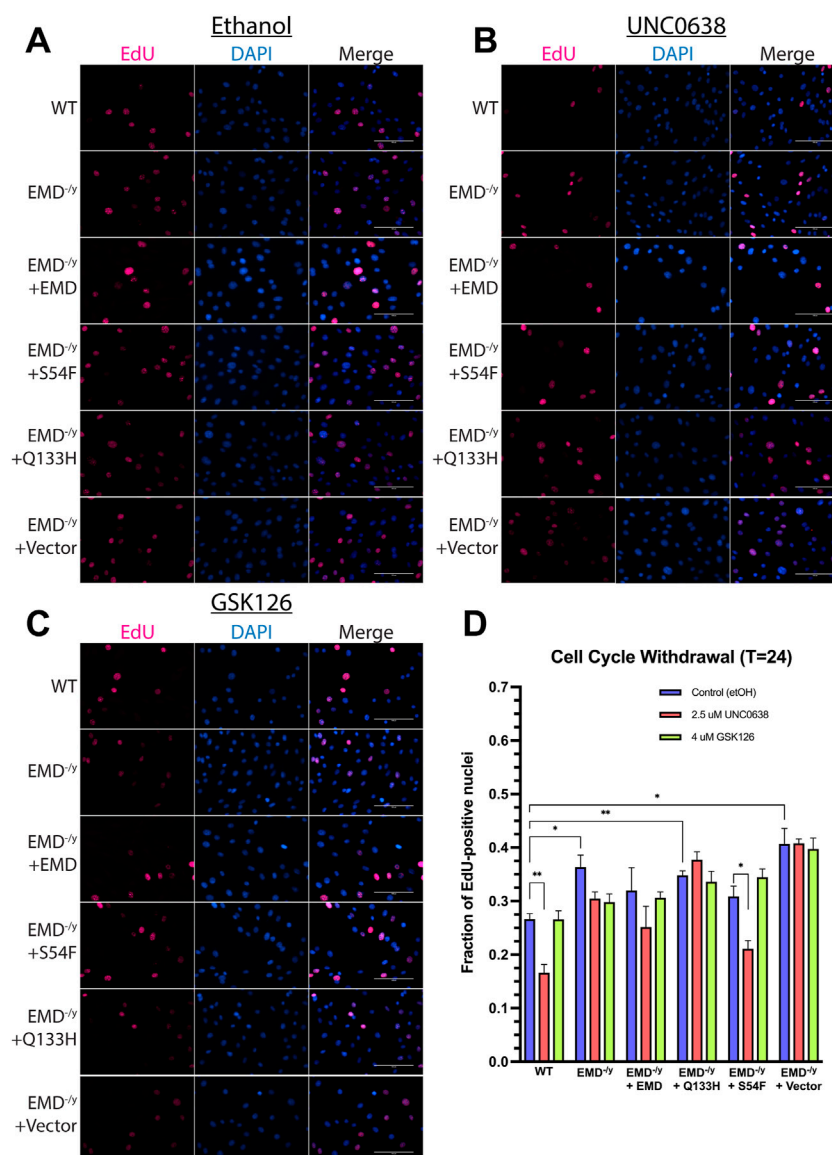
detected in emerin-null and S54F mutant cells (Figures 6C,D; n = 3). The fusion index was significantly decreased in emerin-null and Q133H mutant cells upon treatment with UNC0638 (Figures 6B,E; n = 3), while no effect was seen in emerin-null and S54F mutant cells. Treatment with GSK126 decreased myotube formation in wildtype emerin, emerin-null and Q133H mutant cells (Figures 6C,E; n = 3), while no significant difference was seen in S54F mutant cells.

Discussion

The myogenic differentiation program is a coordinated process dependent upon epigenetic mechanisms to regulate proper gene expression, including modulating histone modifications (Bharathy et al., 2013), RNA-mediated silencing (Bianchi et al., 2017), and DNA methylation (Yang et al., 2021) at specific gene loci. In differentiating adult stem cells, coordinated repression and activation of developmentally regulated loci occurs by association of chromatin with the nuclear lamina at

the nuclear envelope (Wong et al., 2014; van Steensel and Belmont, 2017). These Lamina Associated Domains (LADs) consist of both developmentally regulated genes (facultative LADs; fLADs) and constitutively inactive domains (constitutive LADs; cLADs) (Meuleman et al., 2013; Zheng et al., 2015). fLADs consist of developmental genes that alter their association with the nuclear lamina during differentiation and are enriched for the histone modifications H3K9me2 and H3K27me3 (Luperchio et al., 2014; Kind et al., 2015). fLAD reorganization is seen during tissue-specific differentiation resulting in the coordinated temporal expression of key differentiation genes in neuronal differentiation (Peric-Hupkes et al., 2010), myogenic differentiation (Demmerle et al., 2013), and cardiac progenitor differentiation (Poleshko et al., 2017).

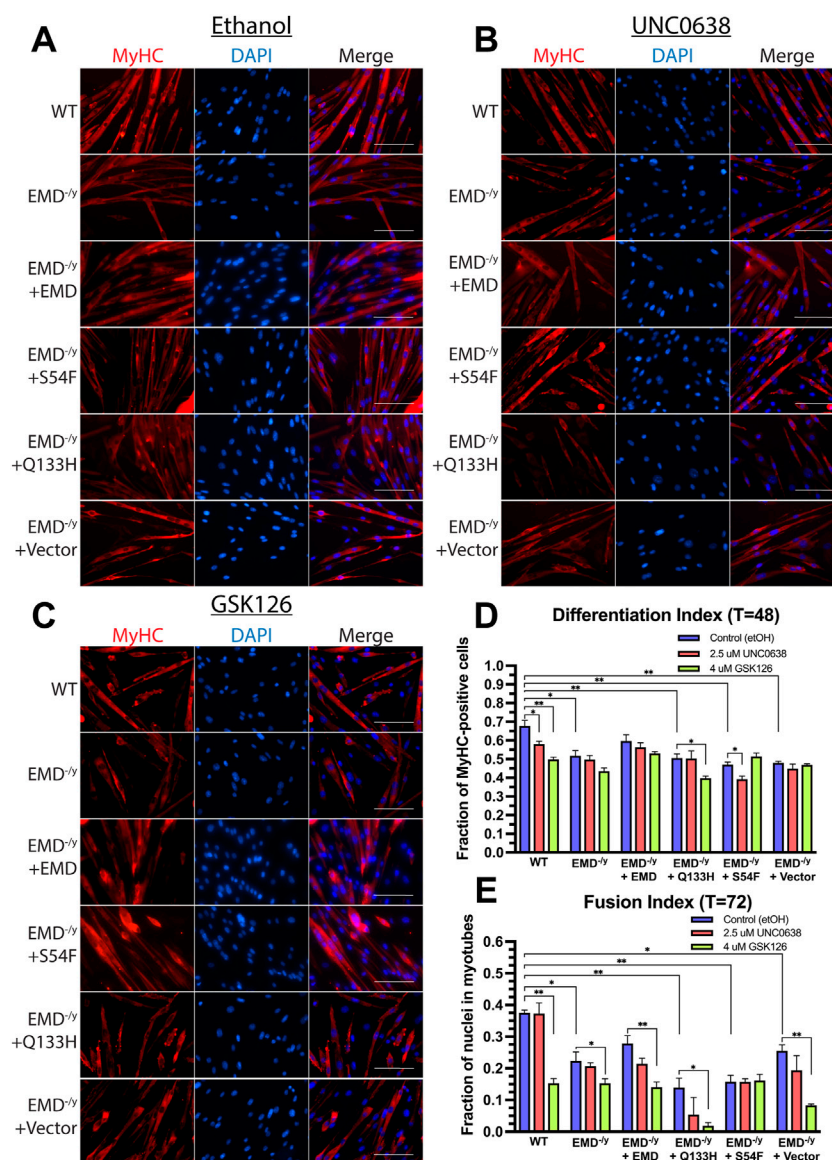
Increasing evidence demonstrates the importance of epigenetic modifications on cell fate, but the mechanism by which repressive chromatin is dynamically organized at the nuclear periphery remains unclear. Previous work in our lab and by others have shown emerin is an important regulator of chromatin organization through its interaction with, and

**FIGURE 5**

UNC0638 and GSK126 treatment fails to rescue impaired cell cycle withdrawal of emerin-null, S54F, and Q133H myogenic progenitors. The indicated myogenic progenitor cell lines were induced to differentiate in the presence of ethanol alone (A), UNC0638 (B) or GSK126 (C) for 24 h. Cells were incubated with EdU for 2 h prior to fixing and imaging to monitor cell cycle withdrawal. EdU-positive cells were counted and plotted [(D); $n > 225$ for each cell line]. Scale bars represent 100 μ m. Error bars represent SEM. (Student's t-test; * $p < 0.05$ ** $p < 0.01$)

activation of, HDAC3 (Demmerle et al., 2012, 2013; Collins et al., 2017). Emerin and HDAC3 are required for localizing LADs to the nuclear envelope to repress transcription (Demmerle et al., 2012, 2013). Targeting H4K5 acetylation or deacetylation by pharmacological activators or inhibitors to decrease total H4K5ac levels in emerin-null myogenic progenitors rescued their differentiation defects (Collins et al., 2017; Bossone et al., 2020). This suggests histone modifications are important in regulating myogenic fLAD organization. Nuclear envelope-localized HDAC3 is also required for cardiomyocyte

differentiation (Poleshko et al., 2017), suggesting this mechanism may be conserved in adult stem cell differentiation. Methylation of H3K9 was also shown to be important for LAD localization (Towbin et al., 2012). H3K9me2 and H3K27me3 are the products of G9a (Shinkai and Tachibana, 2011) and EZH2 (Tan et al., 2014), respectively, and inhibition of these HMTs disrupts LAD formation (Towbin et al., 2012; Harr et al., 2015). The mechanism of HMT recruitment to LADs remains unclear, but HDAC3 was shown to recruit EZH2 to repressive loci (Wang et al., 2011; Zhang et al.,

**FIGURE 6**

Inhibition of G9a and EZH2 fails to rescue emerin-null, S54F, and Q133H myogenic progenitor differentiation, but exacerbates their differentiation defects. The indicated myogenic progenitor cell lines were induced to differentiate in the presence of ethanol alone (A), UNC0638 (B), or GSK126 (C) for 48 or 72 h. Cells were fixed, incubated with antibodies against MyHC, and stained with DAPI. The differentiation index (D) is the number of nuclei in MyHC⁺ multinucleated myotubes plus the number of nuclei in MyHC mono- or di-nuclear cells/total nuclei after 48 h. The fusion index (E) is the number of nuclei in MyHC⁺ multi-nucleated myotubes (≥ 3 nuclei/total nuclei) after 72 h. Scale bars represent 100 μ m. Error bars represent SEM. (Student's t-test; * $p < 0.05$ ** $p < 0.01$).

2012; Emmett and Lazar, 2019) and emerlin was shown to recruit EZH2 and H3K27me3 to the nuclear periphery in C2C12 myoblasts and 293T cells (Ma et al., 2019).

In this study, we show emerlin binds G9a and EZH2 in wildtype progenitors and that this interaction is enhanced in the HDAC3-binding mutant progenitors S54F and Q133H. We next showed H3K9me2 and H3K27me3 are enriched at the nuclear periphery in these same mutants. We then chose to

target catalytic activity of both G9a and EZH2 with small molecule inhibitors. We demonstrate that inhibition of either histone methyltransferase failed to rescue commitment or myotube formation to wildtype levels in emerlin-null cells expressing Q133H or S54F. Enrichment of H3K9me2 and H3K27me3 at the nuclear periphery upon increased emerlin-HMT binding in the emerlin HDAC3-binding mutants suggests emerlin is important for deposition of these marks or for

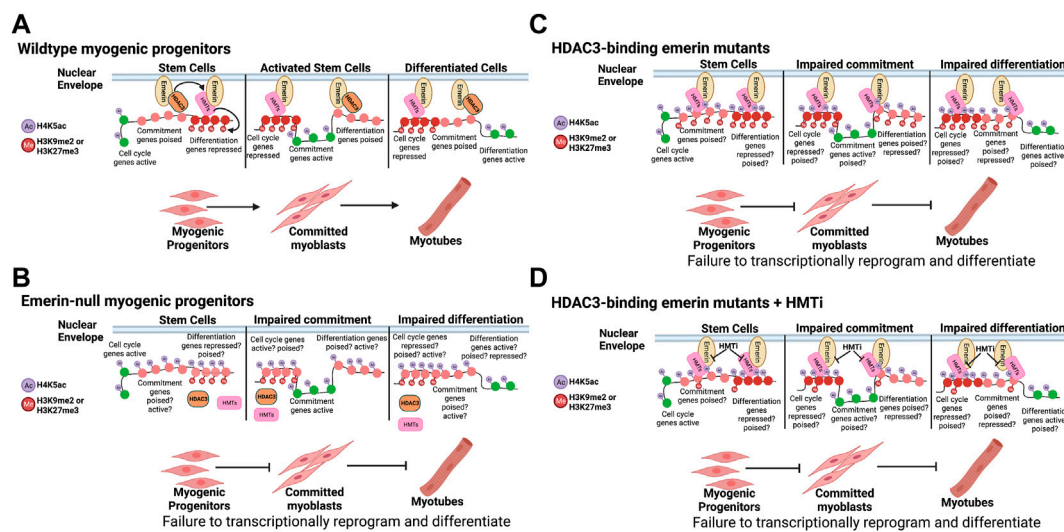


FIGURE 7

Model. (A) Wildtype myogenic progenitors dynamically reorganize their genome to coordinate the temporal expression of the differentiation program. (B) Cells lacking emerin fail to coordinate the temporal expression of key myogenic loci due to failure to dynamically reorganize the genome. (C) HDAC3-binding emerin mutants are predicted to exhibit dually acetylated and methylated chromatin states on key myogenic loci, leading to failure to coordinate their temporal expression. (D) Failure of HMT inhibition to rescue differentiation of HDAC3-binding emerin mutants is predicted to be due to the hyperacetylation of H4K5 on key myogenic loci independent of their methylation status. This is consistent with the role of HDAC3 in fLAD organization during myogenic and cardiomyogenic differentiation (Demmerle et al., 2012, 2013; Poleshko et al., 2017). This figure was created using BioRender software.

recruitment of chromatin containing these marks to the nuclear envelope.

The emerin-HDAC3 interaction is important for the coordinated temporal relocation of fLADs during myogenic differentiation (Demmerle et al., 2013). However, altering HMT activity fails to rescue differentiation, suggesting these changes are not important for myogenic differentiation. This supports a model whereby emerin helps maintain stably repressed H3K9me2/3 and H3K27me3 cLADs at the nuclear envelope through its interactions with HMTs. In this model (Figure 7) it is the interaction of emerin, as well as other unidentified nuclear envelope proteins, with HMTs that help establish cLADs, while the emerin-HDAC3 interaction modulates the dynamic localization of key myogenic loci (fLADs), including *MyoD*, *Myf5*, *Pax3/7*. Here, wildtype myogenic progenitors nuclear envelope-associated HMTs help organize cLADs (Figure 7A; H3K9me2/H3K27me3) at the nuclear lamina. In emerin mutants that disrupt HDAC3 binding, HDAC3 fails to localize to the periphery resulting in greater EZH2/G9a at the nuclear envelope, and by extension, increased H3K9me2 and H3K27me3 at the nuclear envelope (Figure 7C). In this model, increased H3K9me2 and H3K27me3 would be coincident with increases in H4K5ac at the nuclear envelope, since HDAC3 is not present at the periphery. When HMT activity is inhibited, this blocks methylation of H3K9 or H3K27, which we predict preferentially affects cLAD organization

(Figure 7D). The lack of HDAC3 at the nuclear envelope would still result in hyperacetylation of LADs, which we predict are specifically important for fLAD localization (Figure 7D). This is supported by the failure of myogenic fLADs (e.g., *Myf5*) to localize correctly in emerin-null or emerin S54F mutant progenitors and its failure to rescue differentiation (Demmerle et al., 2013; Iyer and Holaska, 2020). In this model the increased, aberrant H4K5 acetylation of the myogenic fLADs results in their misexpression regardless of HMT activity at the nuclear envelope (Figures 7C,D). However, we do not know whether these fLADs are methylated at H3K9 or H3K27 in these myogenic progenitors and thus are similar to 'poised genes' or if they lack H3K9 or H3K27 methylation and resemble transcriptionally active genes. Future studies will identify post-translational modifications at these myogenic fLADs to examine these possibilities.

It is possible that HMTs could be important for fLAD organization and HDAC3 could be important for its reorganization, as our studies and our proposed model fail to differentiate between these possibilities. For example, emerin-null and mutant progenitors have reduced global H3K27me3 and H3K9me2/3—a potential contributor to their impaired differentiation. Future studies will be necessary to investigate the effect of increasing global H3K9 and H3K27 methylation using specific demethylase inhibitors. More experiments are also necessary to examine how specific myogenic loci are dynamically

localized and how this correlates with their specific chromatin post-translational modification states in emerin mutant myogenic progenitors.

Although these and our previous studies (Demmerle et al., 2013; Bossone et al., 2020; Iyer and Holaska, 2020) support this model (Figure 7), there are other models that need to be considered. One such model would be that HDAC3 catalytic activity is dispensable for fLAD formation or localization, as shown in cardiomyocytes (Poleshko et al., 2017), suggestive that the role of HDAC3 is to tether repressed chromatin. Similarly, HMTs may function as a tether for repressed chromatin. In this regard, HDAC3-binding emerin mutants are able to bind more HMTs and therefore localize more H3K9me2/3 or H3K27me3 to the nuclear envelope. If HMT binding to emerin at the nuclear periphery renders them catalytically inactive, we would expect decreased total amounts of H3K9me2/3 and H3K27me3 in the absence of emerin or HDAC3 which is consistent with previous data (Knutson et al., 2008; Bhaskara et al., 2010; Demmerle et al., 2013; Bossone et al., 2020). A second model would be that methylation of H3K9 and H3K27 may require deacetylation of H4K5 to recruit HMTs independent of any HDAC3-HMT interaction. It is also possible that two distinct complexes form containing emerin-HDAC3-fLADs and emerin-HMT-cLADs. A third model would be that HDAC3 stimulates nuclear envelope recruitment of H3K9me2 by deacetylating H3K9ac. Although HDAC3 has not been shown to directly deacetylate H3K9, we and others have shown that loss of HDAC3 or emerin results in increased H3K9ac and decreased H3K9me2/3 (Knutson et al., 2008; Bhaskara et al., 2010; Demmerle et al., 2013). Future studies are needed to determine which model(s) is correct.

It is unclear from these studies as to whether emerin binds directly to EZH2 or G9a. Emerin may bind EZH2 and G9a through binding to their respective complex components. EZH2 and G9a may also interact with emerin through other known binding proteins. One candidate protein is Msx1. Emerin was shown to bind Msx1 and bridge an interaction between EZH2 and emerin (Ma et al., 2019). G9a was also shown to interact with Msx1 (Wang and Abate-Shen, 2012a), so it is possible Msx1 mediates the binding of emerin to HMTs.

The functional interaction of emerin with EZH2 and Msx1 is important for myogenic differentiation. Emerin knockdown in proliferating C2C12 myoblasts was shown to displace EZH2 and H3K27me3 from the nuclear periphery (Ma et al., 2019), suggesting emerin binding to EZH2 organizes repressive chromatin at the periphery (Wang and Abate-Shen, 2012b). Further, the catalytic activity of EZH2 was essential for myogenic differentiation (Carette et al., 2004). These results are consistent with previous experiments showing myoblasts treated with EZH2 shRNA exhibit impaired differentiation and delayed the expression of myogenic genes (Adhikari and

Davie, 2018). One pathway in which EZH2 is important for myogenic differentiation is the Wnt pathway (Markiewicz et al., 2006; Iyer et al., 2017; Iyer and Holaska, 2020). The Wnt pathway is activated after muscle injury to regulate myogenic differentiation (Brack et al., 2008) and is regulated by EZH2 and the PRC2 complex (Adhikari et al., 2019) by inhibition of Wnt antagonists. Interestingly, the Wnt pathway is dysfunctional in emerin-null and emerin mutant myogenic progenitors (Iyer et al., 2017; Iyer and Holaska, 2020).

Although the relative levels of H3K9me2 and H3K27me3 at the nuclear envelope are increased in HDAC3-binding emerin mutants, we do not observe more EZH2 or G9a at the nuclear envelope. This could be due to epitope masking of EZH2 or G9a upon binding to emerin at the nuclear envelope. Alternatively, it is possible that in live cells the interactions between EZH2 or G9a and emerin are more transient, as might be expected for an enzyme. This transient interaction would likely be sufficient to add the H3K9me2/3 or H3K27me3 modification. In this scenario, the conditions of the immunoprecipitation may increase the stability of the interactions between emerin and EZH2 that occurs in cells. Lastly, the interaction between emerin, Msx1, and G9a or EZH2 may mask the epitopes of G9a or EZH2 only when bound to Msx1 in cells. In this scenario more binding of G9a or EZH2 to emerin *via* Msx1 would be seen *in vitro*, but this increase would be masked in cells. Expression of exogenous G9a or EZH2 will be used in future experiments to test these possibilities.

In summary, it is clear the coordinated temporal reorganization of the genome occurs progressively, as some myogenic differentiation genes become active while cell cycle regulation and mitotic genes are silenced. Thus, this process occurs through multiple steps, all of which are crucial for proper differentiation into myotubes. It is possible that the failure to rescue myotube formation we observed in G9a and EZH2 inhibition experiments is a consequence of enriched H4K5ac from loss of HDAC3 interaction in S54F, Q133H, or emerin-null progenitors. One potential explanation would be that deacetylation of H4K5 is a critical step in the myogenic differentiation program. Further, the binding of HDAC3 to these regions would help limit the amount of more stable chromatin repression by limiting the amount of EZH2 or G9a at the nuclear envelope, thereby allowing precise control of the regions to be methylated with H3K9me2 or H3K27me3. In this way, emerin may also be important for maintaining homeostasis of H3K9me2 and H3K27me3 localization at the nuclear periphery, as well as its dynamic reorganization during differentiation. We posit that the interaction of S54F or Q133H emerin with EZH2 or G9a-containing complexes lack proper regulation due to their inability to bind HDAC3, resulting in defective chromatin organization at the nuclear periphery. Cells lacking emerin also exhibit a decrease in repressive marks, likely due to this inability to properly regulate repressive chromatin organization and are thus unable to appropriately

repress cell cycle genes. Previous data from our lab and the experiments in this study strongly suggest emerlin plays multiple roles in regulating dynamic genomic organization at the nuclear periphery.

Data availability statement

The raw data supporting the conclusion of this article will be made available by the authors, without undue reservation.

Author contributions

JMH and NM conceived and designed the experiments; NM performed the experiments; NM, and JMH analyzed the data; JMH contributed reagents/materials/analysis tools; NM, and JMH wrote the paper. All authors have read and agreed to the published version of the manuscript.

Funding

This work was supported by a grant from the National Institute of Arthritis, and Musculoskeletal and Skin Diseases (R15AR069935 to JH) and a grant from the New Jersey Commission on Cancer Research (JH). The content is solely the responsibility of the authors and does not necessarily represent the official views of the National Institutes of Health or the New Jersey Commission on Cancer Research. The WW Smith Charitable Trust, or the New Jersey Commission on Cancer Research. This work was also supported by Rowan University under the Camden Health Research Initiative.

References

- Adhikari, A., and Davie, J. (2018). JARID2 and the PRC2 complex regulate skeletal muscle differentiation through regulation of canonical Wnt signaling. *Epigenetics Chromatin* 11 (1), 46. doi:10.1186/s13072-018-0217-x
- Adhikari, A., Mainali, P., and Davie, J. K. (2019). JARID2 and the PRC2 complex regulate the cell cycle in skeletal muscle. *J. Biol. Chem.* 294 (51), 19451–19464. doi:10.1074/jbc.RA119.010060
- Battisti, V., Pontis, J., Boyarchuk, E., Fritsch, L., Robin, P., Ait-Si-Ali, S., et al. (2016). Unexpected distinct roles of the related histone H3 lysine 9 methyltransferases G9a and g9a-like protein in myoblasts. *J. Mol. Biol.* 428 (11), 2329–2343. doi:10.1016/j.jmb.2016.03.029
- Bharathy, N., Ling, B. M., and Taneja, R. (2013). Epigenetic regulation of skeletal muscle development and differentiation. *Subcell. Biochem.* 61, 139–150. doi:10.1007/978-94-007-4525-4_7
- Bhaskara, S., Knutson, S. K., Jiang, G., Chandrasekharan, M. B., Wilson, A. J., Zheng, S., et al. (2010). Hdac3 is essential for the maintenance of chromatin structure and genome stability. *Cancer Cell* 18 (5), 436–447. doi:10.1016/j.ccr.2010.10.022
- Bianchi, M., Renzini, A., Adamo, S., and Moresi, V. (2017). Coordinated actions of MicroRNAs with other epigenetic factors regulate skeletal muscle development and adaptation. *Int. J. Mol. Sci.* 18 (4), E840. doi:10.3390/ijms18040840
- Bione, S., Maestrini, E., Rivella, S., Mancini, M., Regis, S., Romeo, G., et al. (1994). Identification of a novel X-linked gene responsible for Emery-Dreifuss muscular dystrophy. *Nat. Genet.* 8 (4), 323–327. doi:10.1038/ng1294-323
- Bossone, K. A., Ellis, J. A., and Holaska, J. M. (2020). Histone acetyltransferase inhibition rescues differentiation of emerlin-deficient myogenic progenitors. *Muscle Nerve* 62 (1), 128–136. doi:10.1002/mus.26892
- Brack, A. S., Conboy, I. M., Conboy, M. J., Shen, J., and Rando, T. A. (2008). A temporal switch from notch to Wnt signaling in muscle stem cells is necessary for normal adult myogenesis. *Cell Stem Cell* 2 (1), 50–59. doi:10.1016/j.stem.2007.10.006
- Caretti, G., Di Padova, M., Micales, B., Lyons, G. E., and Sartorelli, V. (2004). The Polycomb Ezh2 methyltransferase regulates muscle gene expression and skeletal muscle differentiation. *Genes Dev.* 18 (21), 2627–2638. doi:10.1101/gad.1241904
- Collins, C. M., Ellis, J. A., and Holaska, J. M. (2017). MAPK signaling pathways and HDAC3 activity are disrupted during differentiation of emerlin-null myogenic progenitor cells. *Dis. Model. Mech.* 10 (4), 385–397. doi:10.1242/dmm.028787
- Demmerle, J., Koch, A. J., and Holaska, J. M. (2013). Emerlin and histone deacetylase 3 (HDAC3) cooperatively regulate expression and nuclear positions of MyoD, Myf5, and Pax7 genes during myogenesis. *Chromosome Res.* 21 (8), 765–779. doi:10.1007/s10577-013-9381-9
- Demmerle, J., Koch, A. J., and Holaska, J. M. (2012). The nuclear envelope protein emerlin binds directly to histone deacetylase 3 (HDAC3) and activates HDAC3 activity. *J. Biol. Chem.* 287 (26), 22080–22088. doi:10.1074/jbc.M111.325308
- Emmett, M. J., and Lazar, M. A. (2019). Integrative regulation of physiology by histone deacetylase 3. *Nat. Rev. Mol. Cell Biol.* 20 (2), 102–115. doi:10.1038/s41580-018-0076-0

Acknowledgments

We thank the Department of Biomedical Sciences at Cooper Medical School of Rowan University for providing funding for this work. We thank Ashvin Iyer for helping to create the cell lines used in this study. We thank the members of Holaska's lab for the numerous discussions pertaining to this manuscript.

Conflict of interest

The authors declare that the research was conducted in the absence of any commercial or financial relationships that could be construed as a potential conflict of interest.

Publisher's note

All claims expressed in this article are solely those of the authors and do not necessarily represent those of their affiliated organizations, or those of the publisher, the editors and the reviewers. Any product that may be evaluated in this article, or claim that may be made by its manufacturer, is not guaranteed or endorsed by the publisher.

Supplementary material

The Supplementary Material for this article can be found online at: <https://www.frontiersin.org/articles/10.3389/fcell.2022.1007120/full#supplementary-material>

- Harr, J. C., Luperchio, T. R., Wong, X., Cohen, E., Wheelan, S. J., and Reddy, K. L. (2015). Directed targeting of chromatin to the nuclear lamina is mediated by chromatin state and A-type lamins. *J. Cell Biol.* 208 (1), 33–52. doi:10.1083/jcb.201405110
- Heller, S. A., Shih, R., Kalra, R., and Kang, P. B. (2020). Emery-Dreifuss muscular dystrophy. *Muscle Nerve* 61 (4), 436–448. doi:10.1002/mus.26782
- Holaska, J. M., and Wilson, K. L. (2007). An emerin "proteome": Purification of distinct emerin-containing complexes from HeLa cells suggests molecular basis for diverse roles including gene regulation, mRNA splicing, signaling, mechanosensing, and nuclear architecture. *Biochemistry* 46 (30), 8897–8908. doi:10.1021/bi602636m
- Iyer, A., and Holaska, J. M. (2020). EDMD-causing emerin mutant myogenic progenitors exhibit impaired differentiation using similar mechanisms. *Cells* 9 (6), E1463. doi:10.3390/cells9061463
- Iyer, A., Koch, A. J., and Holaska, J. M. (2017). Expression profiling of differentiating emerin-null myogenic progenitor identifies molecular pathways implicated in their impaired differentiation. *Cells* 6 (4), E38. doi:10.3390/cells6040038
- Kind, J., Pagie, L., de Vries, S. S., Nahidiazar, L., Dey, S. S., Bienko, M., et al. (2015). Genome-wide maps of nuclear lamina interactions in single human cells. *Cell* 163 (1), 134–147. doi:10.1016/j.cell.2015.08.040
- Knutson, S. K., Chyla, B. J., Amann, J. M., Bhaskara, S., Huppert, S. S., and Hiebert, S. W. (2008). Liver-specific deletion of histone deacetylase 3 disrupts metabolic transcriptional networks. *EMBO J.* 27 (7), 1017–1028. doi:10.1038/emboj.2008.51
- Koch, A. J., and Holaska, J. M. (2014). Emerin in health and disease. *Semin. Cell Dev. Biol.* 29, 95–106. doi:10.1016/j.semcdb.2013.12.008
- Ling, B. M., Bharathy, N., Chung, T. K., Kok, W. K., Li, S., Tan, Y. H., et al. (2012). Lysine methyltransferase G9a methylates the transcription factor MyoD and regulates skeletal muscle differentiation. *Proc. Natl. Acad. Sci. U. S. A.* 109 (3), 841–846. doi:10.1073/pnas.111628109
- Luperchio, T. R., Wong, X., and Reddy, K. L. (2014). Genome regulation at the peripheral zone: Lamina associated domains in development and disease. *Curr. Opin. Genet. Dev.* 25, 50–61. doi:10.1016/j.gde.2013.11.021
- Ma, Z., Shi, H., Shen, Y., Li, H., Yang, Y., Yang, J., et al. (2019). Emerin anchors Mx1 and its protein partners at the nuclear periphery to inhibit myogenesis. *Cell Biosci.* 9, 34. doi:10.1186/s13578-019-0296-9
- Markiewicz, E., Tilgner, K., Barker, N., van de Wetering, M., Clevers, H., Dorobek, M., et al. (2006). The inner nuclear membrane protein emerin regulates beta-catenin activity by restricting its accumulation in the nucleus. *EMBO J.* 25 (14), 3275–3285. doi:10.1038/sj.emboj.7601230
- Meuleman, W., Peric-Hupkes, D., Kind, J., Beaudry, J. B., Pagie, L., Kellis, M., et al. (2013). Constitutive nuclear lamina-genome interactions are highly conserved and associated with A/T-rich sequence. *Genome Res.* 23 (2), 270–280. doi:10.1101/gr.141028.112
- Moser, M. A., Hagelkruys, A., and Seiser, C. (2014). Transcription and beyond: The role of mammalian class I lysine deacetylases. *Chromosoma* 123 (1–2), 67–78. doi:10.1007/s00412-013-0441-x
- Mozzetta, C., Pontis, J., Fritsch, L., Robin, P., Portoso, M., Proux, C., et al. (2014). The histone H3 lysine 9 methyltransferases G9a and GLP regulate polycomb repressive complex 2-mediated gene silencing. *Mol. Cell* 53 (2), 277–289. doi:10.1016/j.molcel.2013.12.005
- Peric-Hupkes, D., Meuleman, W., Pagie, L., Bruggeman, S. W., Solovei, I., Brugman, W., et al. (2010). Molecular maps of the reorganization of genome-nuclear lamina interactions during differentiation. *Mol. Cell* 38 (4), 603–613. doi:10.1016/j.molcel.2010.03.016
- Poleshko, A., Shah, P. P., Gupta, M., Babu, A., Morley, M. P., Manderfield, L. J., et al. (2017). Genome-nuclear lamina interactions regulate cardiac stem cell lineage restriction. *Cell* 171 (3), 573–587. e514. doi:10.1016/j.cell.2017.09.018
- Poulard, C., Noureddine, L. M., Pruvost, L., and Le Romancer, M. (2021). Structure, activity, and function of the protein lysine methyltransferase G9a. *Life (Basel)* 11 (10), 1082. doi:10.3390/life11101082
- Ranade, D., Pradhan, R., Jayakrishnan, M., Hegde, S., and Sengupta, K. (2019). Lamin A/C and Emrin depletion impacts chromatin organization and dynamics in the interphase nucleus. *BMC Mol. Cell Biol.* 20 (1), 11. doi:10.1186/s12860-019-0192-5
- Shinkai, Y., and Tachibana, M. (2011). H3K9 methyltransferase G9a and the related molecule GLP. *Genes Dev.* 25 (8), 781–788. doi:10.1101/gad.2027411
- Tachibana, M., Ueda, J., Fukuda, M., Takeda, N., Ohta, T., Iwanari, H., et al. (2005). Histone methyltransferases G9a and GLP form heteromeric complexes and are both crucial for methylation of euchromatin at H3-K9. *Genes Dev.* 19 (7), 815–826. doi:10.1101/gad.1284005
- Tan, J. Z., Yan, Y., Wang, X. X., Jiang, Y., and Xu, H. E. (2014). EZH2: Biology, disease, and structure-based drug discovery. *Acta Pharmacol. Sin.* 35 (2), 161–174. doi:10.1038/aps.2013.161
- Towbin, B. D., Gonzalez-Aguilera, C., Sack, R., Gaidatzis, D., Kalck, V., Meister, P., et al. (2012). Step-wise methylation of histone H3K9 positions heterochromatin at the nuclear periphery. *Cell* 150 (5), 934–947. doi:10.1016/j.cell.2012.06.051
- van Steensel, B., and Belmont, A. S. (2017). Lamina-associated domains: Links with chromosome architecture, heterochromatin, and gene repression. *Cell* 169 (5), 780–791. doi:10.1016/j.cell.2017.04.022
- Wang, J., and Abate-Shen, C. (2012a). The MSX1 homeoprotein recruits G9a methyltransferase to repressed target genes in myoblast cells. *PLoS One* 7 (5), e37647. doi:10.1371/journal.pone.0037647
- Wang, J., and Abate-Shen, C. (2012b). Transcriptional repression by the Msx1 homeoprotein is associated with global redistribution of the H3K27me3 repressive mark to the nuclear periphery. *Nucleus* 3 (2), 155–161. doi:10.4161/nucl.19477
- Wang, J., Kumar, R. M., Biggs, V. J., Lee, H., Chen, Y., Kagey, M. H., et al. (2011). The Msx1 homeoprotein recruits polycomb to the nuclear periphery during development. *Dev. Cell* 21 (3), 575–588. doi:10.1016/j.devcel.2011.07.003
- Wang, Z., Zang, C., Rosenfeld, J. A., Schones, D. E., Barski, A., Cuddapah, S., et al. (2008). Combinatorial patterns of histone acetylations and methylations in the human genome. *Nat. Genet.* 40 (7), 897–903. doi:10.1038/ng.154
- Wong, X., Luperchio, T. R., and Reddy, K. L. (2014). NET gains and losses: The role of changing nuclear envelope proteomes in genome regulation. *Curr. Opin. Cell Biol.* 28, 105–120. doi:10.1016/j.celb.2014.04.005
- Yang, Y., Fan, X., Yan, J., Chen, M., Zhu, M., Tang, Y., et al. (2021). A comprehensive epigenome atlas reveals DNA methylation regulating skeletal muscle development. *Nucleic Acids Res.* 49 (3), 1313–1329. doi:10.1093/nar/gkaa1203
- Zhang, X., Zhao, X., Fiskus, W., Lin, J., Lwin, T., Rao, R., et al. (2012). Coordinated silencing of MYC-mediated miR-29 by HDAC3 and EZH2 as a therapeutic target of histone modification in aggressive B-Cell lymphomas. *Cancer Cell* 22 (4), 506–523. doi:10.1016/j.ccr.2012.09.003
- Zheng, X., Kim, Y., and Zheng, Y. (2015). Identification of lamin B-regulated chromatin regions based on chromatin landscapes. *Mol. Biol. Cell* 26 (14), 2685–2697. doi:10.1091/mbc.E15-04-0210



OPEN ACCESS

EDITED BY

Eric C Schirmer,
University of Edinburgh,
United Kingdom

REVIEWED BY

James Holaska,
Cooper Medical School of Rowan
University, United States
Rajan Jain,
Penn Medicine, United States

*CORRESPONDENCE

Antoine Muchir,
a.muchir@institut-myologie.org

SPECIALTY SECTION

This article was submitted to Nuclear
Organization and Dynamics,
a section of the journal
Frontiers in Cell and Developmental
Biology

RECEIVED 29 August 2022

ACCEPTED 26 September 2022

PUBLISHED 07 October 2022

CITATION

Kervella M, Jahier M, Meli AC and
Muchir A (2022), Genome organization
in cardiomyocytes expressing mutated
A-type lamins.
Front. Cell Dev. Biol. 10:1030950.
doi: 10.3389/fcell.2022.1030950

COPYRIGHT

© 2022 Kervella, Jahier, Meli and
Muchir. This is an open-access article
distributed under the terms of the
[Creative Commons Attribution License](#)
(CC BY). The use, distribution or
reproduction in other forums is
permitted, provided the original
author(s) and the copyright owner(s) are
credited and that the original
publication in this journal is cited, in
accordance with accepted academic
practice. No use, distribution or
reproduction is permitted which does
not comply with these terms.

Genome organization in cardiomyocytes expressing mutated A-type lamins

Marie Kervella¹, Maureen Jahier², Albano C. Meli¹ and
Antoine Muchir^{2*}

¹PhyMedExp, University of Montpellier, INSERM, CNRS, Montpellier, France, ²Sorbonne Université, INSERM U974, Institute of Myology, Center of Research in Myology, Paris, France

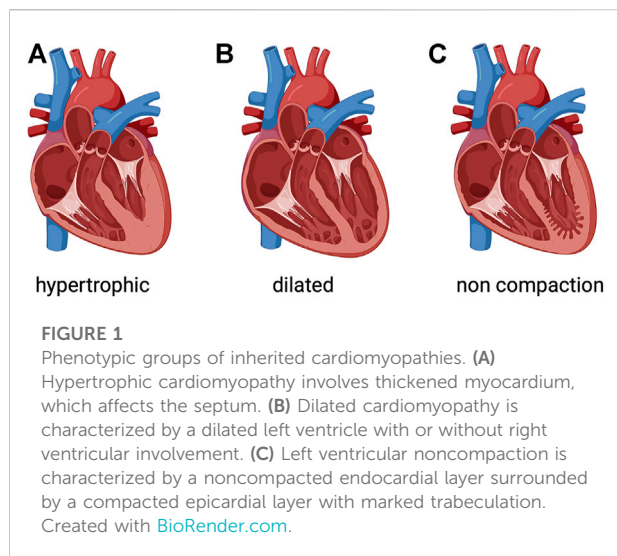
Cardiomyopathy is a myocardial disorder, in which the heart muscle is structurally and functionally abnormal, often leading to heart failure. Dilated cardiomyopathy is characterized by a compromised left ventricular function and contributes significantly to the heart failure epidemic, which represents a staggering clinical and public health problem worldwide. Gene mutations have been identified in 35% of patients with dilated cardiomyopathy. Pathogenic variants in *LMNA*, encoding nuclear A-type lamins, are one of the major causative causes of dilated cardiomyopathy (i.e. *CardioLaminopathy*). A-type lamins are type V intermediate filament proteins, which are the main components of the nuclear lamina. The nuclear lamina is connected to the cytoskeleton on one side, and to the chromatin on the other side. Among the models proposed to explain how *CardioLaminopathy* arises, the “chromatin model” posits an effect of mutated A-type lamins on the 3D genome organization and thus on the transcription activity of tissue-specific genes. Chromatin contacts with the nuclear lamina *via* specific genomic regions called lamina-associated domains lamina-associated domains. These LADs play a role in the chromatin organization and gene expression regulation. This review focuses on the identification of LADs and chromatin remodeling in cardiac muscle cells expressing mutated A-type lamins and discusses the methods and relevance of these findings in disease.

KEYWORDS

LMNA, nuclear lamins, cardiomyopathy, genome organization, LADs, lamina-associated domains

Introduction

The global prevalence of heart failure is approximately 26 million patients and the economic load related to this condition is approximately US\$120 billion (Groenewegen et al., 2020). The large burden of heart failure implies that developing compelling management strategies is paramount. Cardiomyopathy is a condition associated with contractile dysfunction of the heart, often leading to heart failure. Cardiomyopathies are a clinically heterogeneous group of cardiac muscle disorders, which can be either genetic (Figure 1) or systemic (Schultheiss et al., 2019; Hershberger et al., 2021). Dilated



cardiomyopathy, the most common form, has an estimated prevalence of >0.4% in the general population. Dilated cardiomyopathy is a condition where the heart muscle becomes enlarged and weakened, resulting in poor left ventricular function defined as a left ventricular ejection fraction <45% (Ziaieian and Fonarow, 2016). Despite current strategies to aggressively manage dilated cardiomyopathy, it remains a common cause of heart failure and a reference for cardiac transplantation. Notwithstanding progresses in reducing heart failure-related mortality, hospitalizations for heart failure remain very frequent and rates of readmissions continue to rise. Presumably, it is important and necessary to increase our knowledge on the pathophysiology of cardiomyopathies to unveil novel molecular/cellular mechanisms for future therapeutic approaches (Leviner et al., 2015).

Cardiolaminopathy

Among the most common genes implicated in dilated cardiomyopathy, it has been estimated that mutations in *LMNA* gene accounts for about a 10th of familial dilated cardiomyopathy, thus representing one of the major causative genes (Taylor et al., 2003). Affected patients often exhibit early conduction defects before left ventricle dysfunction and dilatation occur. *CardioLaminopathy* usually presents in early to mid-adulthood with symptomatic conduction system disease or arrhythmias, or with dilated cardiomyopathy. *CardioLaminopathy* has an intrusive clinical progression with higher rates of aggressive arrhythmias and faster course towards heart failure than most other cardiomyopathies (Taylor et al., 2003). Given the increased awareness among physicians, cardiologists now use defibrillators in order to avoid sudden death from aggressive ventricular arrhythmias, and pharmacological interventions to improve heart failure symptoms

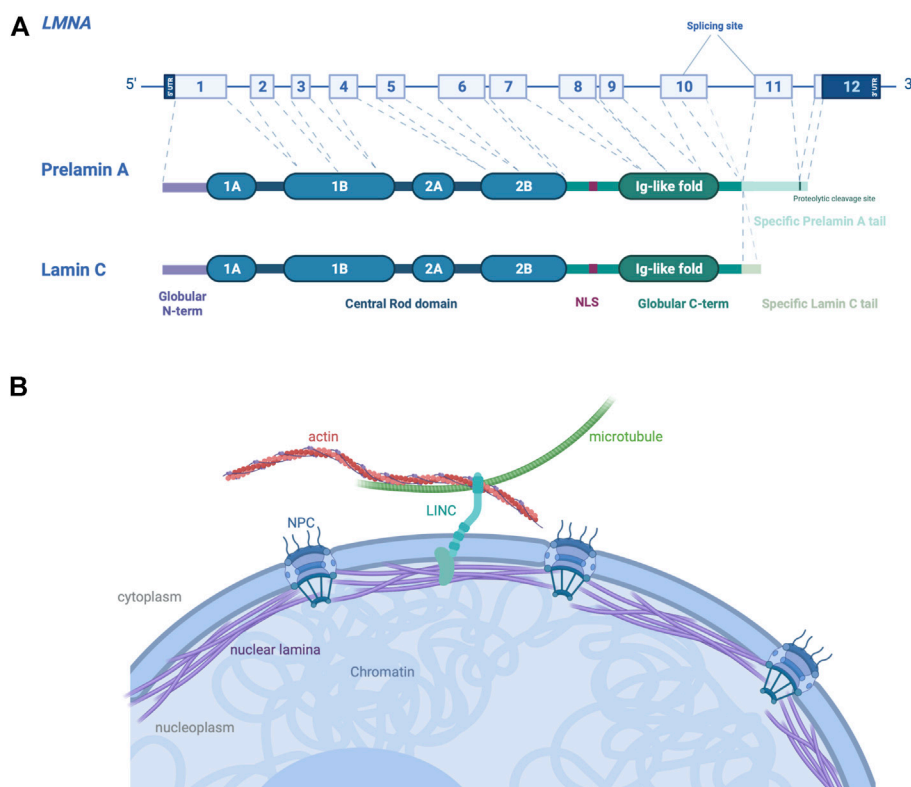
(Meune et al., 2006). Once dilated cardiomyopathy is clinically detected, the management for *CardioLaminopathy* follows the standard of care for heart failure. It is unclear whether early use of these therapeutic drugs prior detectable cardiac dysfunction can modify the aggressive nature of *CardioLaminopathy*. There is no definitive treatment for the progressive cardiac dilatation and loss of contractility in *CardioLaminopathy*, short of heart transplantation.

Nuclear A-type lamins

LMNA encodes nuclear A-type lamins. Lamins are class V intermediate filament proteins forming the main component of the nuclear lamins, a fibrous meshwork underlining the inner nuclear membrane of most eukaryotic cells (Wong et al., 2022). In mammalian somatic cells, four major lamin isoforms are found, encoded by two different genes. *LMNB1* and *LMNB2* genes encode lamins B1 and B2 respectively, which are ubiquitously expressed in cells during development. *LMNA* gene encodes A-type lamins, lamins A and C, obtained via an alternative pre-mRNA splicing (Figure 2A), which are mainly expressed in most differentiated cells (Dittmer and Misteli, 2011). A-type lamins interact both with the cytoskeleton in the cytoplasm through the LINC complex (Linker of nucleoskeleton and cytoskeleton), and with the chromatin in the nucleoplasm (Méjat, 2010) (Figure 2B). The LINC complex is a large protein complex composed of SUN and KASH domain proteins, present at the inner and outer nuclear membrane respectively (Haque et al., 2006; McGee et al., 2006). SUN proteins interact with several components of the nucleoskeleton, whereas KASH proteins interact with cytoskeleton through their large cytoplasmic protein domains (Jahed et al., 2021). The LINC complex has been shown to be involved in several biological processes including meiosis, DNA damage repair and gene expression (Wong et al., 2021b). By its location and protein interactions, the LINC complex provides a physical continuum between cytoskeleton and nuclear proteins, allows to withstand and transfer forces across the nucleus (Lombardi et al., 2011).

Given their interaction with LINC complex and chromatin, A-type lamins are involved in a plethora of biophysical and biochemical processes from the extracellular environment to the nuclear interior. A-type lamins participate to the signal mechanotransduction and regulation of the nucleus stiffness and shape (Broers et al., 2004; Lammerding et al., 2004), as well as in chromatin organization, gene regulation, DNA replication, RNA splicing and genome protection from mechanical cues (Dechat et al., 2008; Shimi et al., 2008; Bertero et al., 2019a; Cho et al., 2019).

Cardiomyocytes, by their intrinsic properties, are constantly subject to mechanical stress. Hence, the nuclei must resist these mechanical cues and correctly transmit the mechanical signal inside the nuclei to convert into a biochemical signal and modulate gene expression. In cardiomyocytes, the level of A-type lamins is finely regulated in response to a mechanical

**FIGURE 2**

Schematic representation of A-type A/C and their localization in cells. **(A)** *LMNA* gene encodes the A-type lamins, with prelamins A and lamin C generated by alternative RNA splicing being the major somatic cell isoforms. **(B)** Schematic view of A-type lamins, proteins of the nuclear lamina on the inner aspect of the inner nuclear membrane, cause autosomal dominant EDMD. The interactions between A-type lamins with SUN and KASH proteins form the LINC complex, connecting the nucleus to cytoskeleton in the cytoplasm of somatic cells. Created with [BioRender.com](https://www.biorender.com).

stimulus, to prevent nuclear rupture and protect the genome integrity (Cho et al., 2019). Mutations in A-type lamins could alter the signal mechanotransduction and thus contribute to the pathogenesis of *CardioLaminopathy* (Jaalouk and Lammerding, 2009). The mammalian nucleus is a highly specialized organelle, which maintains the genome integrity. The nuclear lamina plays an essential role of mechanotransducer, mechanosensor and participate to the chromatin organization. However, the specific mechanistic roles of A-type lamins in this last process in a cardiomyocyte remain obscure (Carmosino et al., 2014). In this review, we discuss recent findings supporting the role of A-type lamins in the organization and regulation of chromatin in *Cardiolaminopathy*.

Chromatin compartmentalization in mammalian cells

A-type lamins have been shown to be involved in genomic organization (Guelen et al., 2008; Paulsen et al., 2018; Guerreiro and Kind, 2019), recruitment of epigenetic regulators (Auguste et al.,

2020) and gene expression (van Steensel and Belmont, 2017). In mammalian nucleus, the genome is highly organized in a tissue-dependent manner. Each chromosome is located in a distinct region called “chromosome territories” (Figure 3) (Cremer and Cremer, 2010), containing two different chromosomal compartments, named A and B (Lieberman-Aiden et al., 2009). A-compartments are gene-rich chromatin regions, enriched in active chromatin marks (H3K36me3, H3K79me2, H3K27ac and H3K4me3) and are preferentially embedded in the center of the nucleus. B-compartments are poor-gene and repressive chromatin marks enriched at the nuclear periphery (H3K9me2/3, H3K27me3) (Bertero and Rosa-Garrido, 2021). The only genes present in B-compartments are silenced or weakly transcribed (Guelen et al., 2008). In B-compartments, large chromatin domains bound to nuclear lamins are referred as *lamina-associated domains* (LADs) (Figure 3) (Guelen et al., 2008; Kind et al., 2013; Amendola and Steensel, 2015; Leemans et al., 2019).

In mammals, A-type lamins interact with hundreds of LADs, which are regions ranging from 0.1–10 megabases in size detected on all chromosomes (Briand and Collas, 2020). LADs were first mapped by DNA adenine methyltransferase (DamID)

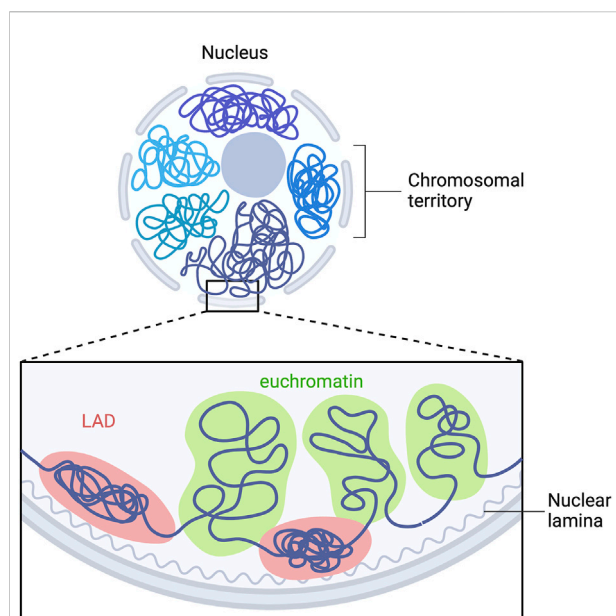


FIGURE 3

LADs organization in mammalian cells. Model depicting the interaction of multiple LADs with the nuclear lamina. Repressed LADs are located at the nuclear periphery and are composed of “gene-desert” regions, which are enriched in heterochromatin marks. Euchromatin is located within the nucleoplasm and is transcriptional active. Adapted from “Chromosome Organization in Nucleus: TADs”, by BioRender.com. Retrieved from <https://app.biorender.com/biorender-templates>.

identification in *Drosophila* (Steensel and Henikoff, 2000; Pickersgill et al., 2006) and later by chromatin immunoprecipitation sequencing (ChIP-seq) (Lund et al., 2014, 2015; Gesson et al., 2016; Cheedipudi et al., 2019; Shah et al., 2021). LADs are predominantly located at the nuclear periphery and are composed of “gene-desert” regions enriched in heterochromatin marks (Kind et al., 2013; Harr et al., 2015).

During mitosis (Wong et al., 2021a) or disease (Cheedipudi et al., 2019), LADs can be reorganized leading to a compartment change and aberrant gene expression (Zheng et al., 2018; Kim et al., 2019) (Figure 2). A-type lamins have been traditionally seen as associated with heterochromatin and transcriptional silencing. However, recent genome-wide approaches show that A-type lamins could be associated with promoters and enhancers outside the LADs, and regulate transcription and chromatin topology of key differentiation gene programs (Leemans et al., 2019).

Methods to identify and visualize LADs

A comprehensive knowledge of the structural features and dynamics of chromatin is essential to understand cellular

mechanisms involving DNA. Though, little is known about the dynamics of chromatin arrangement despite that the scientific community has gained important insights into the higher-order spatial organization of eukaryotic genomes. Several methods have enabled the discovery of higher-order chromatin structure, and notably to study and visualize the LADs organization within the nucleus.

A large variety of proteins bind to specific parts of the genome to regulate gene expression and chromatin structure. In ChIP experiment (Figure 4A), the interacting part of DNA with a protein of interest (lamin A/C for example) are chemically cross-linked together, and DNA is sheared into small fragments. Next, an antibody specific to the protein of interest is used to extract the DNA-protein complex by immunoprecipitation and the extracted DNA sequences are identified by sequencing (ChIP-seq) approaches (Park, 2009).

DamID is a powerful method used to map the genomic interaction sites of these proteins (Figure 4B) (Greil et al., 2006). It is based on fusing a protein of interest to *Escherichia coli* DNA adenine methyltransferase (Dam). Expression of this fusion protein *in vivo* leads to the addition of a methylation group to the adenine in GATC sequences (adenine-6-methylation (^{m6}A)). Because adenine methylation does not occur endogenously in eukaryotic cells, it provides a unique tag to mark protein interaction sites. The adenine-methylated DNA fragments are next isolated using a specific endonuclease, and are sequenced after PCR amplification. This method allows the identification of LADs in diseases caused by mutations in A-type lamins (Guelen et al., 2008; Peric-Hupkes et al., 2010; Zullo et al., 2012; Perovanovic et al., 2016; Harr et al., 2020). In combination with the DamID technology, ^{m6}A-Tracer method turns out to be a powerful tool to track LADs in living cells (Kind et al., 2013). ChIP-seq and DamID methods are both genomic DNA-binding profiling methods. However, DamID and ChIP-seq approaches each have their strengths and weaknesses. ChIP-seq method provides a snapshot of protein occupancy at a single location on DNA, whereas DamID method relies on DNA adenine methylation, which occurs over a period of several hours. Also, DamID method could give information of chromatin-binding events *in vivo*, whereas ChIP-seq method is only performed *in vitro* (Aughey et al., 2019). For a review of an elusive comparison between DamID and ChIP-seq approaches, please refer to (Aughey and Southall, 2016).

The arrangement of chromatin being intimately linked to the gene expression, it is of relevance to study the open state of the chromatin. This has been made possible by the assay for transposase-accessible chromatin with high-throughput sequencing (ATAC-seq) (Figure 4C). This approach allows to map the chromatin accessibility at the genome-wide scale with an *in vitro* transposition of sequencing adaptors into native chromatin (Buenrostro et al., 2013; Grandi et al., 2022). Prokaryotic Tn5 transposase is integrated into accessible chromatin regions. The combination of sequencing adaptors

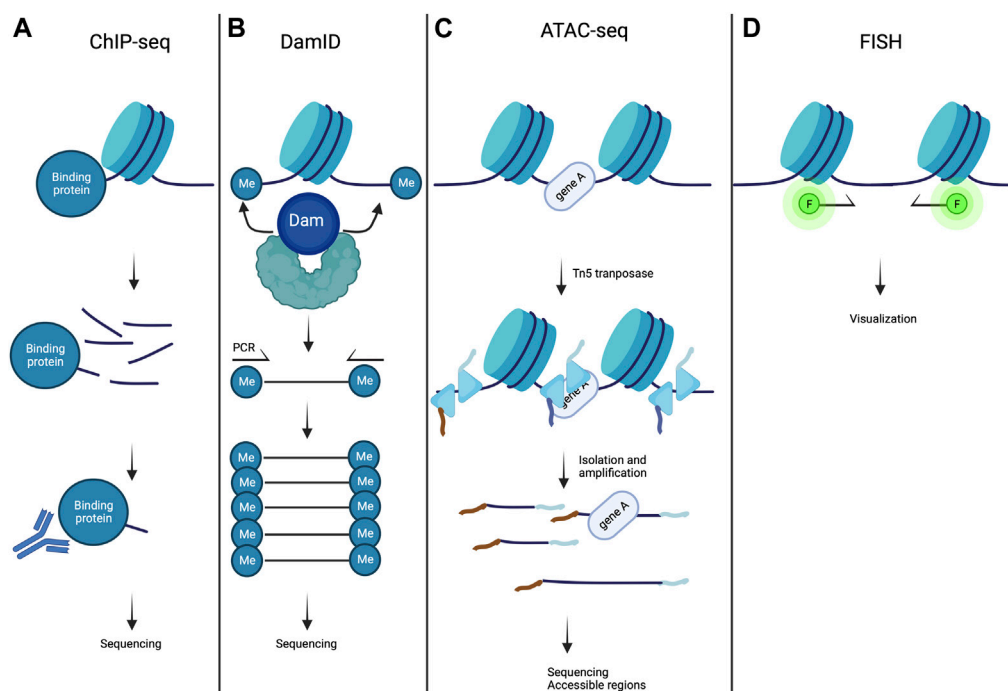


FIGURE 4

Methods to study chromatin organization. (A) In ChIP-seq experiments, chromatin is fragmented and magnetic beads conjugated to antibody specific to the target protein are used to precipitate chromatin fragments bound to the protein of interest. This is then followed by sequencing and mapped onto the genome assembly. (B) In DamID, a fusion protein is created consisting of dam methyltransferase and a protein of interest, resulting in local methylation of adenines in GATC sequences on the chromatin. The genomic methylation pattern can be mapped using sequencing. (C) ATAC-seq is a methodology used for identifying open chromatin regions. Chromatin is incubated with Tn5 transposase to simultaneously fragment and index the exposed DNA fragments. This is then followed by sequencing. (D) In FISH methods, DNA loci of interest are labeled with immunofluorescent DNA sequence specific or chromosome paint probes and are visualized by fluorescent microscopy. Created with BioRender.com.

and Tn5 transposase integration allows to simultaneously fragment and sequence the open chromatin regions (Buenrostro et al., 2015). ATAC-seq method can be used in combination with ChIP-seq and DamID to correlate LADs spatial organization and gene expression with a chromatin region opening (Lee et al., 2019). A recent methodology development, ATAC-seq, allowed to visualize open chromatin regions, by replacing the sequencing by fluorescent adaptors (Chen et al., 2016).

It is also essential to visualize regions of the genome, in order to reveal their individual relationships with nuclear structures in single cells. This is achieved by DNA fluorescence *in situ* hybridization (FISH) and more recently, by 3D-FISH (FISH on 3D-preserved nuclei with immunofluorescence) in cells (Clements et al., 2016). 3D-FISH allows to study individual locus or discrete number of loci within the nucleus (Szabo et al., 2021). In 3D-FISH methods, (Figure 4D) DNA loci of interest are labeled with immunofluorescent DNA sequence specific or chromosome paint probes and visualized by fluorescent microscopy (Jensen, 2014). This approach is efficient to study the nuclear organization at the single-cell

level. More recently, a quantitative high-resolution imaging approach, which combines FISH, array tomography imaging, and multiplexed immunostaining, has been implemented for investigating chromatin organization in complex tissues (Linhoff et al., 2015). 3D-FISH is thus a method of choice to study and visualize LADs and its location in *Cardiolaminopathy* (Kind et al., 2013; Paulsen et al., 2017; Bertero et al., 2019b; Salvarani et al., 2019).

Chromatin reorganization in cardiolaminopathy

Specific cellular and molecular mechanisms of pathogenesis and progression of *Cardiolaminopathy* remain unclear and are still under investigation. Several hypotheses have been proposed attempting to link the pathophysiology of this disease to known or emerging functions of A-type lamins, among which the “chromatin hypothesis”. This model is based on the interaction between A-type lamins and chromatin via LADs. This hypothesis suggests that a cell-type specific chromatin

reorganization caused by a disruption of A-type lamins protein expression in *Cardiolaminopathy*, leads to an abnormal gene expression and thus participates to the pathogenesis.

The “chromatin model” is supported by different studies. It emerges from recent works suggesting that *CardioLaminopathy* results from dysregulated gene expression as a consequence of LADs reorganization in cardiomyocytes. In fact, these LADs play a role for chromatin organization and gene expression regulation (Guelen et al., 2008; Shimi et al., 2008; Zullo et al., 2012; Solovei et al., 2013). It has been shown that the organization of the LADs is altered in *CardioLaminopathy* (Perovanovic et al., 2016; Shah et al., 2021). Due to the interaction between A-type lamins and chromatin, dysregulated gene expression has emerged as a plausible mechanism to partially explain the pathogenesis of *CardioLaminopathy*. One study focused on the organization of LADs in *CardioLaminopathy* using ChIP-Seq approach and RNA-sequencing in explanted hearts from patients (Cheedipudi et al., 2019). The authors highlighted the role of LADs in the regulation of gene expression, and identified several transcription factors involved in biological processes, such as cell death/survival, cell cycle and metabolism (Cheedipudi et al., 2019). These findings demonstrated that a reorganization of LADs associated with alteration of gene profile expression are occurring in *CardioLaminopathy*. This was recently strongly supported by a study from another group (Shah et al., 2021). This study was based on the differentiation of cardiomyocytes, adipocytes and hepatocytes derived from iPSCs from patients with *cardiolaminopathy*. The authors showed that mutations in A-type lamins result in abnormal gene regulation from peripheral chromatin regions only in cardiomyocytes cell types. With this study, Shah and collaborators provided evidence not only of the LADs reorganization in *Cardiolaminopathy* but also of the cell-type specific organization of several LADs and the link between LADs-chromatin interaction with cell identity. This study thus supports the tissue-specificity of the phenotypes observed in *Cardiolaminopathy*. Bertero and others studied chromosome conformation in cardiomyocytes derived from iPSCs from patient with *CardioLaminopathy* carrying the *LMNA* p. R225X mutation (Bertero et al., 2019b). The authors reported a switch from A- and B-compartments restricted at only ~1% of the genome, resulting in transcriptional activation of genes shifting from nuclear periphery to the nuclear interior. The limited chromatin compartment change thus challenges the “chromatin model”, as chromosomal compartmentation may not be the primary pathogenic mechanism in *CardioLaminopathy*. The distribution of open chromatin was biased towards the nuclear periphery in cardiomyocytes derived from iPSCs from patient with *CardioLaminopathy* carrying the *LMNA* p. K117fs mutation, compared with isogenic control cells (Lee et al., 2019). Using a combination of ChIP-seq and ATAC-seq approaches (see section ‘methods to identify and visualize LADs’), Lee and collaborators have shown that the abnormal

conformation of open chromatin is accompanied by an increase of open chromatin marks of the LADs gene promoters and a decrease of LADs association with A-type lamins. These results suggest that *LMNA* p. K117f mutation leads to local changes in LADs leading to transcriptional activation. Another study using cardiomyocytes derived from iPSCs from patient with *CardioLaminopathy* carrying the *LMNA* p. K219T mutation showed that conduction abnormalities are caused by repression of *SCN5A*, a gene encoding a sodium channel, due to epigenetics changes (Salvarani et al., 2019). *SCN5A* may be included in a LAD that shifts from the nuclear interior towards the nuclear periphery in *CardioLaminopathy* (Lund et al., 2013). Hence, epigenetic state of tissue-specific genes could lead to transcriptional silencing in LADs (Leemans et al., 2019). These data showed that even a slightly change in chromatin organization in mutant cells can still participate to phenotype observed in *Cardiolaminopathy*.

A-type lamins are mostly located at the nuclear periphery and bind LADs but a pool of these proteins can be associated with the open chromatin (euchromatin) (Gesson et al., 2014). Recently, two studies have shown an alteration of A-type lamins interaction with euchromatin in dilated cardiomyopathy (Zhang et al., 2021; Feng et al., 2022). Collectively, all these studies participate to understand the underlying mechanisms of the disease pathogenesis.

The mammalian genome is organized in different three-dimensional levels, which are finely regulated during normal and pathological development (Zheng and Xie, 2019). In this review, we focused on the LADs organization and reorganization in cardiac disease context but other levels of three-dimensional genome organization can be disrupted in cardiac diseases (Meaburn et al., 2007; Mewborn et al., 2010; Rosa-Garrido et al., 2017; Chapski et al., 2021). A better knowledge of the regulation at different three-dimensional scales of genome organization could then help to better understand the development of cardiac diseases.

This review targets the genome organization specifically in cardiomyocytes. However, studying other cardiac cell type present in the heart environment (e.g., cardiac fibroblasts and endothelial cells) could participate to further understand the pathogenesis of *Cardiolaminopathy* (Mewborn et al., 2010; Perovanovic et al., 2016; Ramirez-Martinez et al., 2021).

Open questions and future directions

Recent advances to study chromatin organization shed exciting new light on the pathogenesis of *CardioLaminopathy*. Here, we have outlined recent findings and methods that uncovered the role of chromatin compartment dysregulation in both mice and humans, giving novel insights into the nature of cardiomyocyte dysfunction during disease progression. Nevertheless, there is still a long list of open questions that needs to be answered. While recent studies have

elegantly identified the role of chromatin regulation during the pathogenesis of *CardioLaminopathy*, the distinct roles of chromosomal compartmentation remain elusive. Application of selective tools targeting only the context-dependent A-type lamins gene expression by Cre recombinase-mediated gene targeting or defined drugs might provide new insights into the nature of chromatin organization in the heart. To date, little is known about the temporal regulation of chromatin organization and the transcriptional level during development of *CardioLaminopathy*. Analyzing chromatin organization and gene regulation in heart along the progression of the disease will illuminate another aspect of genome regulation and help to identify specialized functions for the pathogenesis of age-related disease. In addition, whether such chromatin phenotypes are detrimental or beneficial for disease progression still remain unclear. Answering such critical questions, together with profiling heterogeneous subclusters of chromatin organization in healthy and diseased situations, can open new avenues for the development of therapeutic targeting of cardiomyocytes in *CardioLaminopathy*. These studies open up new perspectives in an attempt to explain the pathophysiology of *Cardiolaminopathies* and pinpoint possible new A-type lamins functions still unexplored.

Author contributions

AMu and MK performed data collection (literature reviewing) and prepared the original draft of the manuscript.

AMu, AMe and MK revised and wrote the final version of the manuscript. All authors revised and edited the manuscript for critically important intellectual content.

Funding

This work was supported by the Association Française contre les Myopathies, Institut National de la Santé et de la Recherche Médicale and Sorbonne Université. MK received a funding from Région Occitanie.

Conflict of interest

The authors declare that the research was conducted in the absence of any commercial or financial relationships that could be construed as a potential conflict of interest.

Publisher's note

All claims expressed in this article are solely those of the authors and do not necessarily represent those of their affiliated organizations, or those of the publisher, the editors and the reviewers. Any product that may be evaluated in this article, or claim that may be made by its manufacturer, is not guaranteed or endorsed by the publisher.

References

- Amendola, M., and Steensel, B. (2015). Nuclear lamins are not required for lamina-associated domain organization in mouse embryonic stem cells. *EMBO Rep.* 16, 610–617. doi:10.15252/embr.201439789
- Aughey, G. N., Cheetham, S. W., and Southall, T. D. (2019). DamID as a versatile tool for understanding gene regulation. *Development* 146, dev173666. doi:10.1242/dev.173666
- Aughey, G. N., and Southall, T. D. (2016). Dam it's good! DamID profiling of protein-DNA interactions. *Wiley Interdiscip. Rev. Dev. Biol.* 5, 25–37. doi:10.1002/wdev.205
- Auguste, G., Rouhi, L., Matkovich, S. J., Coarfa, C., Robertson, M. J., Czernuszewicz, G., et al. (2020). BET bromodomain inhibition attenuates cardiac phenotype in myocyte-specific lamin A/C-deficient mice. *J. Clin. Invest.* 130, 4740–4758. doi:10.1172/JCI135922
- Bertero, A., Fields, P. A., Ramani, V., Bonora, G., Yardimci, G. G., Reinecke, H., et al. (2019a). Dynamics of genome reorganization during human cardiogenesis reveal an RBM20-dependent splicing factory. *Nat. Commun.* 10, 1538. doi:10.1038/s41467-019-09483-5
- Bertero, A., Fields, P. A., Smith, A. S. T., Leonard, A., Beussman, K., Sniadecki, N. J., et al. (2019b). Chromatin compartment dynamics in a haploinsufficient model of cardiac laminopathy. *J. Cell Biol.* 218, 2919–2944. doi:10.1083/jcb.201902117
- Bertero, A., and Rosa-Garrido, M. (2021). Three-dimensional chromatin organization in cardiac development and disease. *J. Mol. Cell. Cardiol.* 151, 89–105. doi:10.1016/j.jmcc.2020.11.008
- Briand, N., and Collas, P. (2020). Lamina-associated domains: Peripheral matters and internal affairs. *Genome Biol.* 21, 85. doi:10.1186/s13059-020-02003-5
- Broers, J. L. V., Peeters, E. A. G., Kuijpers, H. J. H., Endert, J., Bouten, C. V. C., Oomens, C. W. J., et al. (2004). Decreased mechanical stiffness in LMNA-/- cells is caused by defective nucleo-cytoskeletal integrity: Implications for the development of laminopathies. *Hum. Mol. Genet.* 13, 2567–2580. doi:10.1093/hmg/ddh295
- Buenrostro, J. D., Giresi, P. G., Zaba, L. C., Chang, H. Y., and Greenleaf, W. J. (2013). Transposition of native chromatin for fast and sensitive epigenomic profiling of open chromatin, DNA-binding proteins and nucleosome position. *Nat. Methods* 10, 1213–1218. doi:10.1038/nmeth.2688
- Buenrostro, J. D., Wu, B., Chang, H. Y., and Greenleaf, W. J. (2015). ATAC-seq: A method for assaying chromatin accessibility genome-wide. *Curr. Protoc. Mol. Biol.* 109, 1–21. doi:10.1002/0471142727.mb2129s109
- Carmosino, M., Torretta, S., Procino, G., Gerbino, A., Forleo, C., Favale, S., et al. (2014). Role of nuclear Lamin A/C in cardiomyocyte functions: Lamin A/C in cardiomyocytes physiology. *Biol. Cell* 106, 346–358. doi:10.1111/boc.201400033
- Chapski, D. J., Cabaj, M., Morselli, M., Mason, R. J., Soehalim, E., Ren, S., et al. (2021). Early adaptive chromatin remodeling events precede pathologic phenotypes and are reinforced in the failing heart. *J. Mol. Cell. Cardiol.* 160, 73–86. doi:10.1016/j.jmcc.2021.07.002
- Cheedipudi, S. M., Matkovich, S. J., Coarfa, C., Hu, X., Robertson, M. J., Sweet, M., et al. (2019). Genomic reorganization of lamin-associated domains in cardiac myocytes is associated with differential gene expression and DNA methylation in human dilated cardiomyopathy. *Circ. Res.* 124, 1198–1213. doi:10.1161/CIRCRESAHA.118.314177
- Chen, X., Shen, Y., Draper, W., Buenrostro, J. D., Litzenburger, U., Cho, S. W., et al. (2016). ATAC-se reveals the accessible genome by transposase-mediated imaging and sequencing. *Nat. Methods* 13, 1013–1020. doi:10.1038/nmeth.4031
- Cho, S., Vashisth, M., Abbas, A., Majkut, S., Vogel, K., Xia, Y., et al. (2019). Mechanosensing by the lamina protects against nuclear rupture, DNA damage, and cell-cycle arrest. *Dev. Cell* 49, 920–935. e5. doi:10.1016/j.devcel.2019.04.020

- Clements, C. S., Bikkul, U., Ahmed, M. H., Foster, H. A., Godwin, L. S., and Bridger, J. M. (2016). "Visualizing the spatial relationship of the genome with the nuclear envelope using fluorescence *in situ* hybridization," in *The nuclear envelope methods in molecular biology*. Editors S. Shackleton, P. Collas, and E. C. Schirmer (New York, NY: Springer New York), 387–406. doi:10.1007/978-1-4939-3530-7_24
- Cremer, T., and Cremer, M. (2010). Chromosome territories. *Cold Spring Harb. Perspect. Biol.* 2, a003889. doi:10.1101/cshperspect.a003889
- Dechat, T., Pflieger, K., Sengupta, K., Shimi, T., Shumaker, D. K., Solimando, L., et al. (2008). Nuclear lamins: Major factors in the structural organization and function of the nucleus and chromatin. *Genes Dev.* 22, 832–853. doi:10.1101/gad.1652708
- Dittmer, T. A., and Misteli, T. (2011). The lamin protein family. *Genome Biol.* 12, 222. doi:10.1186/gb-2011-12-5-222
- Feng, Y., Cai, L., Hong, W., Zhang, C., Tan, N., Wang, M., et al. (2022). Rewiring of 3D chromatin topology orchestrates transcriptional reprogramming and the development of human dilated cardiomyopathy. *Circulation* 145, 1663–1683. doi:10.1161/CIRCULATIONAHA.121.055781
- Gesson, K., Rescheneder, P., Skoruppa, M. P., von Haeseler, A., Dechat, T., and Foisner, R. (2016). A-type lamins bind both hetero- and euchromatin, the latter being regulated by lamina-associated polypeptide 2 alpha. *Genome Res.* 26, 462–473. doi:10.1101/gr.196220.115
- Gesson, K., Vidak, S., and Foisner, R. (2014). Lamina-associated polypeptide (LAP)2α and nucleoplasmic lamins in adult stem cell regulation and disease. *Semin. Cell Dev. Biol.* 29, 116–124. doi:10.1016/j.semcdb.2013.12.009
- Grandi, F. C., Modi, H., Kampman, L., and Corces, M. R. (2022). Chromatin accessibility profiling by ATAC-seq. *Nat. Protoc.* 17, 1518–1552. doi:10.1038/s41596-022-00692-9
- Greil, F., Moorman, C., and van Steensel, B. (2006). "[16] DamID: Mapping of *in vivo* protein–genome interactions using tethered DNA adenine methyltransferase," in *Methods in enzymology* (Germany: Elsevier), 342–359. doi:10.1016/S0076-6879(06)10016-6
- Groenewegen, A., Rutten, F. H., Mosterd, A., and Hoes, A. W. (2020). Epidemiology of heart failure. *Eur. J. Heart Fail.* 22, 1342–1356. doi:10.1002/ehf.1858
- Guelen, L., Pagie, L., Brasset, E., Meuleman, W., Faza, M. B., Talhout, W., et al. (2008). Domain organization of human chromosomes revealed by mapping of nuclear lamina interactions. *Nature* 453, 948–951. doi:10.1038/nature06947
- Guerreiro, I., and Kind, J. (2019). Spatial chromatin organization and gene regulation at the nuclear lamina. *Curr. Opin. Genet. Dev.* 55, 19–25. doi:10.1016/j.gde.2019.04.008
- Haque, F., Lloyd, D. J., Smallwood, D. T., Dent, C. L., Shanahan, C. M., Fry, A. M., et al. (2006). SUN1 interacts with nuclear lamin A and cytoplasmic nesprins to provide a physical connection between the nuclear lamina and the cytoskeleton. *Mol. Cell. Biol.* 26, 3738–3751. doi:10.1128/MCB.26.10.3738-3751.2006
- Harr, J. C., Luperchio, T. R., Wong, X., Cohen, E., Wheelan, S. J., and Reddy, K. L. (2015). Directed targeting of chromatin to the nuclear lamina is mediated by chromatin state and A-type lamins. *J. Cell Biol.* 208, 33–52. doi:10.1083/jcb.201405110
- Harr, J. C., Schmid, C. D., Muñoz-Jiménez, C., Romero-Bueno, R., Kalck, V., Gonzalez-Sandoval, A., et al. (2020). Loss of an H3K9me anchor rescues laminopathy-linked changes in nuclear organization and muscle function in an Emery-Dreifuss muscular dystrophy model. *Genes Dev.* 34, 560–579. doi:10.1101/gad.332213.119
- Hershberger, R. E., Cowan, J., Jordan, E., and Kinnamon, D. D. (2021). The complex and diverse genetic architecture of dilated cardiomyopathy. *Circ. Res.* 128, 1514–1532. doi:10.1161/CIRCRESAHA.121.318157
- Jaalouk, D. E., and Lammerding, J. (2009). Mechanotransduction gone awry. *Nat. Rev. Mol. Cell Biol.* 10, 63–73. doi:10.1038/nrm2597
- Jahed, Z., Domkam, N., Ornowski, J., Yerima, G., and Mofrad, M. R. K. (2021). Molecular models of LINC complex assembly at the nuclear envelope. *J. Cell Sci.* 134, jcs258194. doi:10.1242/jcs.258194
- Jensen, E. (2014). Technical review: *In situ* hybridization: AR insights. *Anat. Rec.* 297, 1349–1353. doi:10.1002/ar.22944
- Kim, Y., Zheng, X., and Zheng, Y. (2019). Role of lamins in 3D genome organization and global gene expression. *Nucleus* 10, 33–41. doi:10.1080/19491034.2019.1578601
- Kind, J., Pagie, L., Ortabozkoyun, H., Boyle, S., de Vries, S. S., Janssen, H., et al. (2013). Single-cell dynamics of genome–nuclear lamina interactions. *Cell* 153, 178–192. doi:10.1016/j.cell.2013.02.028
- Lammerding, J., Schulze, P. C., Takahashi, T., Kozlov, S., Sullivan, T., Kamm, R. D., et al. (2004). Lamin A/C deficiency causes defective nuclear mechanics and mechanotransduction. *J. Clin. Invest.* 113, 370–378. doi:10.1172/JCI19670
- Lee, J., Termglinchan, V., Diecke, S., Itzhaki, I., Lam, C. K., Garg, P., et al. (2019). Activation of PDGF pathway links LMNA mutation to dilated cardiomyopathy. *Nature* 572, 335–340. doi:10.1038/s41586-019-1406-x
- Leemans, C., van der Zwalm, M. C. H., Brueckner, L., Comoglio, F., van Schaik, T., Pagie, L., et al. (2019). Promoter-intrinsic and local chromatin features determine gene repression in LADs. *Cell* 177, 852–864. e14. doi:10.1016/j.cell.2019.03.009
- Leviner, D. B., Hochhauser, E., and Arad, M. (2015). Inherited cardiomyopathies—novel therapies. *Pharmacol. Ther.* 155, 36–48. doi:10.1016/j.pharmthera.2015.08.003
- Lieberman-Aiden, E., van Berkum, N. L., Williams, L., Imakaev, M., Ragoczy, T., Telling, A., et al. (2009). Comprehensive mapping of long-range interactions reveals folding principles of the human genome. *Science* 326, 289–293. doi:10.1126/science.1181369
- Linhoff, M. W., Garg, S. K., and Mandel, G. (2015). A high-resolution imaging approach to investigate chromatin architecture in complex tissues. *Cell* 163, 246–255. doi:10.1016/j.cell.2015.09.002
- Lombardi, M. L., Jaalouk, D. E., Shanahan, C. M., Burke, B., Roux, K. J., and Lammerding, J. (2011). The interaction between nesprins and sun proteins at the nuclear envelope is critical for force transmission between the nucleus and cytoskeleton. *J. Biol. Chem.* 286, 26743–26753. doi:10.1074/jbc.M111.233700
- Lund, E. G., Duband-Goulet, I., Oldenburg, A., Buendia, B., and Collas, P. (2015). Distinct features of lamin A-interacting chromatin domains mapped by ChIP-seq—sequencing from sonicated or micrococcal nuclease-digested chromatin. *Nucleus* 6, 30–39. doi:10.4161/19491034.2014.990855
- Lund, E., Oldenburg, A. R., and Collas, P. (2014). Enriched domain detector: A program for detection of wide genomic enrichment domains robust against local variations. *Nucleic Acids Res.* 42, e92. doi:10.1093/nar/gku324
- Lund, E., Oldenburg, A. R., Delbarre, E., Freberg, C. T., Duband-Goulet, I., Eskeland, R., et al. (2013). Lamin A/C-promoter interactions specify chromatin state-dependent transcription outcomes. *Genome Res.* 23, 1580–1589. doi:10.1101/gr.159400.113
- McGee, M. D., Rillo, R., Anderson, A. S., and Starr, D. A. (2006). UNC-83 is a KASH protein required for nuclear migration and is recruited to the outer nuclear membrane by a physical interaction with the SUN protein UNC-84. *Mol. Biol. Cell* 17, 1790–1801. doi:10.1091/mbc.e05-09-0894
- Meaburn, K. J., Cabuy, E., Bonne, G., Levy, N., Morris, G. E., Novelli, G., et al. (2007). Primary laminopathy fibroblasts display altered genome organization and apoptosis. *Aging Cell* 6, 139–153. doi:10.1111/j.1474-9726.2007.00270.x
- Méjat, A., and Misteli, T. (2010). LINC complexes in health and disease. *Nucleus* 1, 40–52. doi:10.4161/nucl.1.1.10530
- Meune, C., Van Berlo, J. H., Anselme, F., Bonne, G., Pinto, Y. M., and Duboc, D. (2006). Primary prevention of sudden death in patients with lamin A/C gene mutations. *N. Engl. J. Med.* 354, 209–210. doi:10.1056/NEJMc052632
- Mewborn, S. K., Puckelwartz, M. J., Abusineh, F., Fahrenbach, J. P., Zhang, Y., MacLeod, H., et al. (2010). Altered chromosomal positioning, compaction, and gene expression with a lamin A/C gene mutation. *PLoS ONE* 5, e14342. doi:10.1371/journal.pone.0014342
- Park, P. J. (2009). ChIP-seq: Advantages and challenges of a maturing technology. *Nat. Rev. Genet.* 10, 669–680. doi:10.1038/nrg2641
- Paulsen, J., Liyakat Ali, T. M., and Collas, P. (2018). Computational 3D genome modeling using Chrom3D. *Nat. Protoc.* 13, 1137–1152. doi:10.1038/nprot.2018.009
- Paulsen, J., Sekelja, M., Oldenburg, A. R., Barateau, A., Briand, N., Delbarre, E., et al. (2017). Chrom3D: Three-dimensional genome modeling from hi-C and nuclear lamin-genome contacts. *Genome Biol.* 18, 21. doi:10.1186/s13059-016-1146-2
- Peric-Hupkes, D., Meuleman, W., Pagie, L., Bruggeman, S. W. M., Solovei, I., Brugman, W., et al. (2010). Molecular maps of the reorganization of genome–nuclear lamina interactions during differentiation. *Mol. Cell* 38, 603–613. doi:10.1016/j.molcel.2010.03.016
- Perovanovic, J., Dell'Orso, S., Gnouchi, V. F., Jaiswal, J. K., Sartorelli, V., Vigouroux, C., et al. (2016). Laminopathies disrupt epigenomic developmental programs and cell fate. *Sci. Transl. Med.* 8, 335ra58. doi:10.1126/scitranslmed.aad4991
- Pickersgill, H., Kalverda, B., de Wit, E., Talhout, W., Fornerod, M., and van Steensel, B. (2006). Characterization of the *Drosophila melanogaster* genome at the nuclear lamina. *Nat. Genet.* 38, 1005–1014. doi:10.1038/ng1852
- Ramirez-Martinez, A., Zhang, Y., Chen, K., Kim, J., Cenik, B. K., McAnally, J. R., et al. (2021). The nuclear envelope protein Net39 is essential for muscle nuclear

integrity and chromatin organization. *Nat. Commun.* 12, 690. doi:10.1038/s41467-021-20987-x

Rosa-Garrido, M., Chapski, D. J., Schmitt, A. D., Kimball, T. H., Karbassi, E., Monte, E., et al. (2017). High-resolution mapping of chromatin conformation in cardiac myocytes reveals structural remodeling of the epigenome in heart failure. *Circulation* 136, 1613–1625. doi:10.1161/CIRCULATIONAHA.117.029430

Salvarani, N., Crasto, S., Miragoli, M., Bertero, A., Paulis, M., Kunderfranco, P., et al. (2019). The K219T-Lamin mutation induces conduction defects through epigenetic inhibition of SCN5A in human cardiac laminopathy. *Nat. Commun.* 10, 2267. doi:10.1038/s41467-019-09929-w

Schultheiss, H. P., Fairweather, D., Caforio, A. L. P., Escher, F., Hershberger, R. E., Lipshultz, S. E., et al. (2019). Dilated cardiomyopathy. *Nat. Rev. Dis. Primer* 5, 32. doi:10.1038/s41572-019-0084-1

Shah, P. P., Lv, W., Rhoades, J. H., Poleshko, A., Abbey, D., Caporizzo, M. A., et al. (2021). Pathogenic LMNA variants disrupt cardiac lamina-chromatin interactions and de-repress alternative fate genes. *Cell Stem Cell* 28, 938–954.e9. doi:10.1016/j.stem.2020.12.016

Shimi, T., Pflieger, K., Kojima, S., Pack, C.-G., Solovei, I., Goldman, A. E., et al. (2008). The A- and B-type nuclear lamin networks: Microdomains involved in chromatin organization and transcription. *Genes Dev.* 22, 3409–3421. doi:10.1101/gad.1735208

Solovei, I., Wang, A. S., Thanisch, K., Schmidt, C. S., Krebs, S., Zwerger, M., et al. (2013). LBR and lamin A/C sequentially tether peripheral heterochromatin and inversely regulate differentiation. *Cell* 152, 584–598. doi:10.1016/j.cell.2013.01.009

Steensel, B., and Henikoff, S. (2000). Identification of *in vivo* DNA targets of chromatin proteins using tethered Dam methyltransferase. *Nat. Biotechnol.* 18, 424–428. doi:10.1038/74487

Szabo, Q., Cavalli, G., and Bantignies, F. (2021). “Higher-order chromatin organization using 3D DNA fluorescent *in situ* hybridization,” in *Capturing chromosome conformation methods in molecular Biology*. Editors B. Bodega and C. Lanzuolo (New York, NY: Springer US), 221–237. doi:10.1007/978-1-0716-0664-3_13

Taylor, M. R. G., Fain, P. R., Sinagra, G., Robinson, M. L., Robertson, A. D., Carniel, E., et al. (2003). Natural history of dilated cardiomyopathy due to lamin A/C gene mutations. *J. Am. Coll. Cardiol.* 41, 771–780. doi:10.1016/S0735-1097(02)02954-6

van Steensel, B., and Belmont, A. S. (2017). Lamina-associated domains: Links with chromosome architecture, heterochromatin, and gene repression. *Cell* 169, 780–791. doi:10.1016/j.cell.2017.04.022

Wong, X., Hoskins, V. E., Melendez-Perez, A. J., Harr, J. C., Gordon, M., and Reddy, K. L. (2021a). Lamin C is required to establish genome organization after mitosis. *Genome Biol.* 22, 305. doi:10.1186/s13059-021-02516-7

Wong, X., Loo, T.-H., and Stewart, C. L. (2021b). LINC complex regulation of genome organization and function. *Curr. Opin. Genet. Dev.* 67, 130–141. doi:10.1016/j.gde.2020.12.007

Wong, X., Melendez-Perez, A. J., and Reddy, K. L. (2022). The nuclear lamina. *Cold Spring Harb. Perspect. Biol.* 14, a040113. doi:10.1101/cshperspect.a040113

Zhang, X., Shao, X., Zhang, R., Zhu, R., and Feng, R. (2021). Integrated analysis reveals the alterations that LMNA interacts with euchromatin in LMNA mutation-associated dilated cardiomyopathy. *Clin. Epigenetics* 13, 3. doi:10.1186/s13148-020-00996-1

Zheng, H., and Xie, W. (2019). The role of 3D genome organization in development and cell differentiation. *Nat. Rev. Mol. Cell Biol.* 20, 535–550. doi:10.1038/s41580-019-0132-4

Zheng, X., Hu, J., Yue, S., Kristiani, L., Kim, M., Sauria, M., et al. (2018). Lamins organize the global three-dimensional genome from the nuclear periphery. *Mol. Cell* 71, 802–815. e7. doi:10.1016/j.molcel.2018.05.017

Ziaeeian, B., and Fonarow, G. C. (2016). Epidemiology and aetiology of heart failure. *Nat. Rev. Cardiol.* 13, 368–378. doi:10.1038/nrcardio.2016.25

Zullo, J. M., Demarco, I. A., Piqué-Regi, R., Gaffney, D. J., Epstein, C. B., Spooner, C. J., et al. (2012). DNA sequence-dependent compartmentalization and silencing of chromatin at the nuclear lamina. *Cell* 149, 1474–1487. doi:10.1016/j.cell.2012.04.035



OPEN ACCESS

EDITED BY

Joanna M. Bridger,
Brunel University London,
United Kingdom

REVIEWED BY

Ohad Medalia,
University of Zurich, Switzerland
Thomas Cremer,
Ludwig Maximilian University of Munich,
Germany

*CORRESPONDENCE

Giovanna Lattanzi,
giovanna.lattanzi@cnr.it

[†]These authors share first authorship

SPECIALTY SECTION

This article was submitted to Nuclear Organization and Dynamics, a section of the journal Frontiers in Cell and Developmental Biology

RECEIVED 12 August 2022

ACCEPTED 24 October 2022

PUBLISHED 16 November 2022

CITATION

Capanni C, Schena E, Di Giampietro ML, Montecucco A, Mattioli E and Lattanzi G (2022), The role of prelamin A post-translational maturation in stress response and 53BP1 recruitment. *Front. Cell Dev. Biol.* 10:1018102. doi: 10.3389/fcell.2022.1018102

COPYRIGHT

© 2022 Capanni, Schena, Di Giampietro, Montecucco, Mattioli and Lattanzi. This is an open-access article distributed under the terms of the [Creative Commons Attribution License \(CC BY\)](#). The use, distribution or reproduction in other forums is permitted, provided the original author(s) and the copyright owner(s) are credited and that the original publication in this journal is cited, in accordance with accepted academic practice. No use, distribution or reproduction is permitted which does not comply with these terms.

The role of prelamin A post-translational maturation in stress response and 53BP1 recruitment

Cristina Capanni^{1,2†}, Elisa Schena^{1,2†},
Maria Letizia Di Giampietro^{1†}, Alessandra Montecucco³,
Elisabetta Mattioli^{1,2} and Giovanna Lattanzi^{1,2*}

¹CNR Institute of Molecular Genetics “Luigi Luca Cavalli-Sforza”, Unit of Bologna, Bologna, Italy, ²IRCCS Rizzoli Orthopedic Institute, Bologna, Italy, ³CNR Institute of Molecular Genetics “Luigi Luca Cavalli-Sforza”, Pavia, Italy

Lamin A is a main constituent of the nuclear lamina and contributes to nuclear shaping, mechano-signaling transduction and gene regulation, thus affecting major cellular processes such as cell cycle progression and entry into senescence, cellular differentiation and stress response. The role of lamin A in stress response is particularly intriguing, yet not fully elucidated, and involves prelamin A post-translational processing. Here, we propose prelamin A as the tool that allows lamin A plasticity during oxidative stress response and permits timely 53BP1 recruitment to DNA damage foci. We show that while PCNA ubiquitination, p21 decrease and H2AX phosphorylation occur soon after stress induction in the absence of prelamin A, accumulation of non-farnesylated prelamin A follows and triggers recruitment of 53BP1 to lamin A/C complexes. Then, the following prelamin A processing steps causing transient accumulation of farnesylated prelamin A and maturation to lamin A reduce lamin A affinity for 53BP1 and favor its release and localization to DNA damage sites. Consistent with these observations, accumulation of prelamin A forms in cells under basal conditions impairs histone H2AX phosphorylation, PCNA ubiquitination and p21 degradation, thus affecting the early stages of stress response. As a whole, our results are consistent with a physiological function of prelamin A modulation during stress response aimed at timely recruitment/release of 53BP1 and other molecules required for DNA damage repair. In this context, it becomes more obvious how farnesylated prelamin A accumulation to toxic levels alters timing of DNA damage signaling and 53BP1 recruitment, thus contributing to cellular senescence and accelerated organismal aging as observed in progeroid laminopathies.

KEYWORDS

lamin A/C, prelamin A, DNA damage repair, laminopathies, premature ageing, Hutchinson-Gilford Progeria Syndrome (HGPS), 53BP1, oxidative stress response

Introduction

Lamin A is the main splicing product of *LMNA* gene and a key constituent of the nuclear lamina (Cenni et al., 2020a). The newly transcribed lamin A precursor, known as prelamin A, is 18 amino acids longer than mature lamin A and undergoes four post-translational modifications at its C-terminal CaaX box including farnesylation by the protein farnesyl transferase, double cleavage by the metalloprotease ZMPSTE24 and carboxymethylation by the methyltransferase Icm1 (Cenni et al., 2014; Cenni et al., 2020a). This series of events, starting from the full-length newly translated protein known as non-farnesylated prelamin A, leads to production of full-length farnesylated prelamin A, farnesylated prelamin A lacking the last three amino acids and carboxymethylated and farnesylated prelamin A (Cenni et al., 2020a). Since processing steps are very fast under basal conditions, prelamin A forms are barely detectable in most cells and tissues. However, prelamin A levels are transiently increased upon oxidative stress (Liu et al., 2013; Cenni et al., 2014) and farnesylated prelamin A is elevated during myogenic differentiation and in differentiated muscle cells (Mattioli et al., 2011). On the other hand, *LMNA* gene mutations may affect prelamin A processing leading to toxic accumulation of different lamin A precursors, a condition that causes lipodystrophic and progeroid laminopathies (Capanni et al., 2005; Filesi et al., 2005; Cenni et al., 2014; Cenni et al., 2020a; Benedicto et al., 2022; Chen et al., 2022; Wang et al., 2022). Moreover, toxic levels of prelamin A are accumulated in tissues subjected to stress due to pathological conditions as occurs in the cardiovascular system of patients affected by chronic kidney disease (Ragnauth et al., 2010; Liu et al., 2013).

We previously demonstrated that transient reduction of prelamin A processing rate occurs in response to oxidative stress and non-farnesylated prelamin A is accumulated at the early stage of oxidative stress response (Mattioli et al., 2019). At later stages, farnesylated prelamin A becomes detectable, while only mature lamin A is present in fibroblasts after return to basal conditions (Mattioli et al., 2019). Slow-down of prelamin A processing in cells subjected to oxidative stress is in part due to downregulation of the prelamin A endoprotease ZMPSTE24 (Cenni et al., 2014; Mattioli et al., 2019), but the initial event leading to accumulation of non-farnesylated prelamin A remains unknown. However, transient prelamin A accumulation during stress response contributes to modulation of lamin A/C-HDAC2 interaction and HDAC2-dependent transcriptional regulation of p21 (Mattioli et al., 2018). In fact, lamin A/C-HDAC2 complexes are decreased few hours after the onset of DNA damage response and reformed after completion of DNA repair (Mattioli et al., 2018). Lamin A/C binding to HDAC2 favors deacetylase activity, while release of lamin A/C reduces enzyme activity and favors acetylation of histone substrates including those at the p21 gene promoter (Mattioli

et al., 2018). This condition triggers upregulation of p21 during stress response. In this respect, it is worth considering that p21 decrease is necessary at the early stages of DNA damage response to allow ubiquitination of PCNA and H2A histone phosphorylation at damaged DNA, while transient p21 increase is required to avoid replication of damaged DNA sequences and in all steps to modulate DNA damage repair mechanisms (Ticli et al., 2022). However, fine tuning of p21 levels is important as unscheduled increase of p21 is a main determinant of geroconversion (Blagosklonny, 2014; Cenni et al., 2020a). Thus, the regulatory role of prelamin A in stress response appears relevant.

Another interaction involving lamin A/C during DNA damage response is the one with 53BP1, a protein recruited to DNA damage sites that in turn contributes to recruitment of other repair factors (Etourneau et al., 2021; Paiano et al., 2021). Altered nuclear recruitment of 53BP1 has been observed in HGPS cells and ascribed to the dominant negative effect of progerin (a truncated form of farnesylated prelamin A) (Gonzalez-Suarez et al., 2011; Kreienkamp et al., 2016). On the other hand, we showed that sub-toxic levels of prelamin A contribute to 53BP1 availability in nuclei under physiological conditions and positively influence DNA repair rate in cells from long-lived individuals (Cenni et al., 2014). Moreover, we showed that non-farnesylated prelamin A accumulation occurs a few hours after oxidative stress induction, while farnesylated prelamin A is increased after 24 h and only mature lamin A is present in nuclei upon stress recovery (Mattioli et al., 2018; Mattioli et al., 2019). Here, we hypothesized that, under non-pathological conditions, modulation of lamin A/C-53BP1 binding during oxidative stress response could be linked to transient accumulation of specific prelamin A forms, i.e., non-farnesylated prelamin A or farnesylated carboxymethylated prelamin A. To test this hypothesis, we induced accumulation of those prelamin A forms, triggered an oxidative stress condition and measured the effects on 53BP1- lamin A/C interaction and 53BP1 recruitment to DNA damage foci. We also tested the effect of aberrant prelamin A accumulation at the very early stages of stress response, when only mature lamin A is detectable in nuclei. Soon after oxidative stress induction, PCNA mono-ubiquitination occurs in response to DNA damage, an event that requires reduction of p21 levels and in turn triggers gamma-H2AX histone activation (Ticli et al., 2022). Our data show that aberrant accumulation of prelamin A forms at the very early stages of stress response alters timing of PCNA ubiquitination and reduces H2AX phosphorylation. On the other hand, a few hours after stress induction, non-farnesylated prelamin A favors recruitment of 53BP1 to lamin A/C complexes, while the following prelamin A processing steps, yielding farnesylated prelamin A and mature lamin A, progressively reduce lamin A affinity for 53BP1 and favor its timely release and localization to DNA damage sites.

Materials and methods

Cell cultures

Human skin fibroblasts and HeLa cells were cultured at 37°C with 5% CO₂ in Dulbecco's Modified Eagle's Medium (DMEM) containing 10% heat inactivated fetal calf serum (FCS), 2 mM L-glutamine, 50 µg/ml penicillin and 50 µg/ml streptomycin. Human skin fibroblasts were from the BioLaM biobank at IGM CNR and Rizzoli Orthopedic Institute (approval prot. Gen. 0018250 del 05/09/2016). Human fibroblasts were transiently transfected with full length FLAG-tagged prelamin A (LA-WT, pCI mammalian expression vector) and mutated constructs LA-C661M, LA-L647R FuGene reagent (Roche) (Cenni et al., 2020b). The HeLa *LMNA* (*LMNA*^{-/-}) and ZMPSTE24 (*ZMPSTE24*^{-/-}) knockout cell lines (Cenni et al., 2020b) were generated using CRISPR-Cas9 mediated genome editing technology. The guide RNA sequence which targets the first exon of the gene was: 5'- CCTTCGCATCACCGA GTCTGAAG-3' for *LMNA* and 5'- GGCCGAGAAGCGTATCTTCGGGG-3' for ZMPSTE24 as described before (Robijns et al., 2016). Constructs containing the Cas9 nuclease and selection markers were obtained from Addgene (#48138 and 48139) and published protocols were followed.

In human fibroblasts the accumulation of non-farnesylated prelamin A was obtained using 10 µM mevinolin (Sigma) in growth medium for 18 h while the accumulation of farnesylated and carboxymethylated-prelamin A was obtained using 50 µg/ml indinavir for 72 h. Oxidative stress was induced by the addition of H₂O₂ (100 µM) to the growth medium 4 h before harvesting cells (Mattioli et al., 2019). Treatment of HeLa cells with H₂O₂ was performed as follow. After 24 h of culture, cells were treated with H₂O₂ (200 µM) and cells were collected at different time-points (see Figure 6) in order to follow the oxidative stress response. Lonafarnib treatment (1 µM) was performed 18 h before H₂O₂ administration.

Immunofluorescence analysis

Human skin fibroblasts grown on coverslips were fixed in methanol at -20°C for 7 min. Samples were incubated with PBS containing 4% BSA to saturate non-specific binding and incubated with primary antibodies and secondary antibodies. The nuclei were then counterstained with 4,6-diamino-2-phenylindole (DAPI). The slides were mounted with an anti-fade reagent in glycerol and observed. Immunofluorescence microscopy was performed using a Nikon E600 epifluorescence microscope and a Nikon oil-immersion objective [×100 magnification, 1.3 NA (numerical aperture)]. Photographs were taken using a Nikon digital camera (DXm) and NIS-Element BR2.20 software. All images were taken at

similar exposures within an experiment for each antibody. Images were processed using Adobe Photoshop (Adobe Systems).

Proximity ligation assay

Proximity Ligation Assay (PLA) experiments were performed using kits from Sigma-Aldrich: Duolink® *in situ* Detection Reagents Orange (DUO92007). Briefly, methanol-fixed cells were saturated with saturated 4%-BSA and incubated with anti-lamin A/C (Santa Cruz sc-376248) and anti-P53BP1 (Cell Signaling 4937) primary antibodies overnight at 4°C. Thereafter, slides were incubated for 1 h at 37°C with secondary antibody-conjugated PLA probe. Ligation solution was added to each sample and slides were incubated in a humidity chamber for 30 min at 37°C. Ligation solution was removed with washing buffer and amplification solution was added. Slides were incubated in a humidity chamber for 100 min at 37°C and then washed with wash buffers. DNA was counterstained with DAPI and samples were observed by a Nikon Eclipse Ni fluorescence microscope equipped with a digital CCD camera and NIS Elements AR 4.3 software. Quantitative analysis was performed using Duolink Image Tool software (Sigma) by counting 300 nuclei per sample.

Western blotting

For western blotting analysis cells were processed in lysis buffer containing 20 mM Tris-HCl, pH 7.5, 1% SDS, 1 mM Na₃VO₄, 1 mM PMSF, 5% β-mercaptoethanol and protease inhibitors. 15 µg of solubilized protein were subjected to SDS gradient gel (5%–20%) electrophoresis and transferred to nitrocellulose membrane overnight at 4°C. Incubation with primary antibodies was performed for the indicated time. Bands were revealed using the Amersham ECL detection system and analyzed with ImageJ.

Antibodies

The antibodies employed in this study were: anti-lamin A (Abcam ab26300, diluted 1:1000 overnight at 4°C for immunofluorescence analysis) anti-prelamin A (Merck MABT858, diluted 1:500 for 1 h for Western blot analysis and 1:800 overnight at 4°C for immunofluorescence analysis) anti-lamin A/C mouse monoclonal (Santa Cruz sc-376248, diluted 1:1000 1 h for Western blot analysis); anti-PCNA mouse monoclonal (Santa Cruz sc-56, diluted 1:200 1 h for Western blot analysis); anti-P21 rabbit monoclonal (Invitrogen MA5-14949, diluted 1:2000 overnight at 4°C for Western blot analysis); anti-gamma-H2AX mouse monoclonal (Abcam

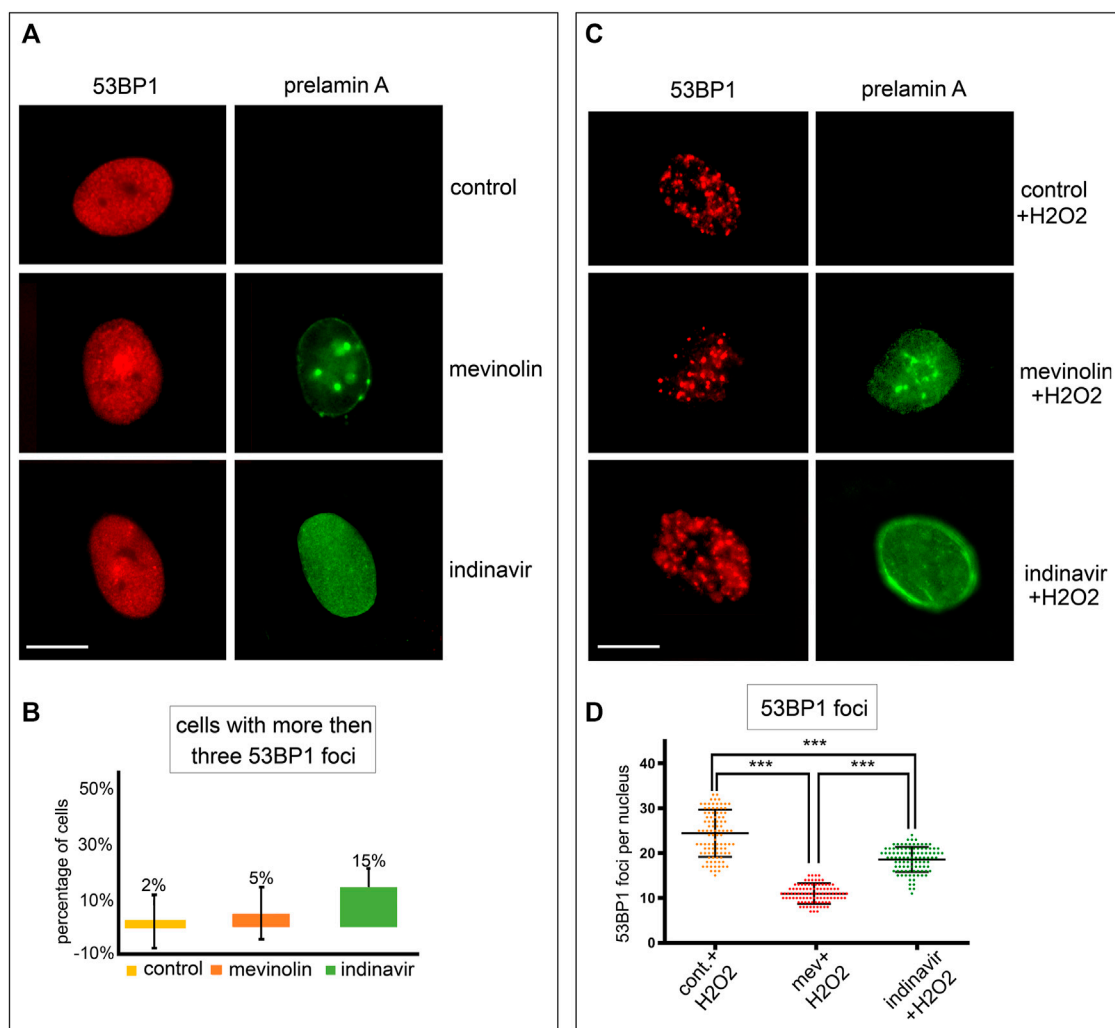


FIGURE 1

Stress-induced 53BP1 foci in human dermal fibroblasts accumulating prelamins A forms. **(A)** Immunofluorescence staining of 53BP1 and prelamins A in untreated, mevinolin- and indinavir-treated cells. 53BP1 (red), prelamins A (green). Bar, 10 μ m. **(B)** Quantitative analysis of the number of fibroblasts showing more than three 53BP1 foci per nucleus. Experiments were conducted in triplicate and 200 cells per sample were counted. Data reported in the graphs are mean values \pm standard deviation. **(C)** Immunofluorescence staining of 53BP1 and prelamins A in untreated or mevinolin treated fibroblasts upon oxidative stress induction. 53BP1 (red), prelamins A (green). Bar, 10 μ m. **(D)** Dot plot of the number of 53BP1 foci per nucleus in human dermal fibroblasts subjected to oxidative stress. Experiments were conducted in triplicate, data analyzed were based on an average of 100 cells. Error bars, mean \pm SD. Comparison between the groups was determined by using the one-way ANOVA test. Asterisks show statistical significance (***, $p < 0.001$).

26350, diluted 1:2000 for 1 h for Western blot analysis); anti-actin goat polyclonal (SCBT I-19, diluted 1:2000 for 1 h for Western blot analysis); anti-P53BP1 (Cell Signalling 4937, diluted 1:10 overnight at 4°C for immunofluorescence analysis); anti-non-farnesylated prelamins A rabbit polyclonal (Diatheva ANT0046 diluted 1:100 overnight at 4°C for immunofluorescence analysis); anti-farnesylated prelamins A rabbit polyclonal (Diatheva ANT0045 diluted 1:10 overnight at 4°C for immunofluorescence analysis); anti-FLAG mouse monoclonal (Sigma-Aldrich M2 1:100 1 h at room temperature for immunofluorescence analysis).

Results

Prelamins A affects formation of 53BP1 foci under oxidative stress in human dermal fibroblasts

Different prelamins A forms were accumulated in human dermal fibroblasts by using prelamins A processing inhibitors. They act on well-known mechanisms, either by inhibiting farnesyl production (mevinolin, which causes accumulation of non-farnesylated prelamins A) or blocking ZMPSTE24 activity

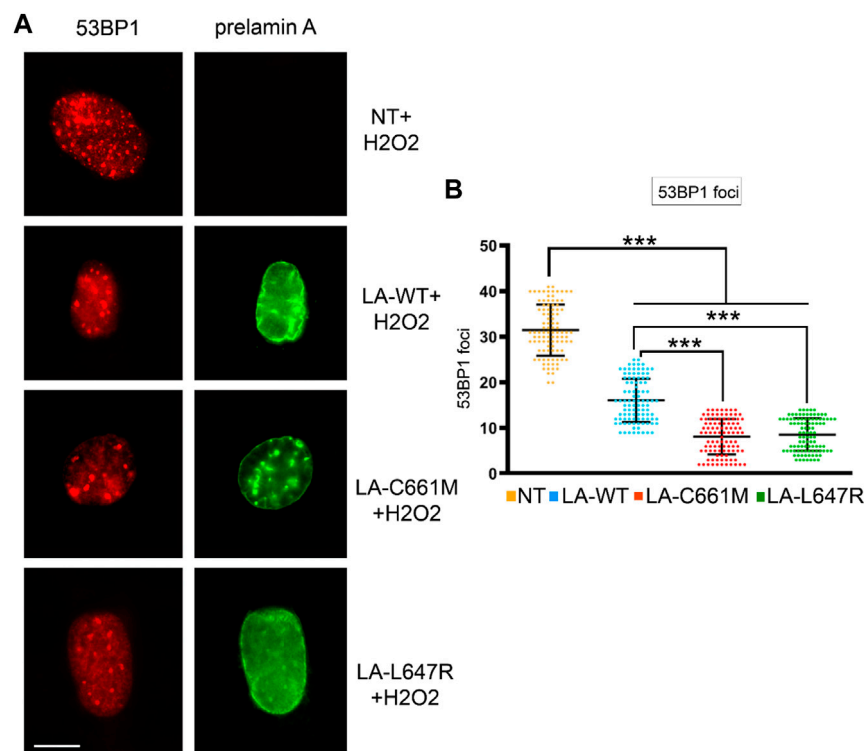


FIGURE 2

Stress-induced 53BP1 foci in human dermal fibroblasts overexpressing prelamins A mutants. **(A)** Immunofluorescence detection of 53BP1 (red) and FLAG-tagged prelamins A (green) in non-transfected fibroblasts (NT) or fibroblasts expressing wild-type prelamins A (LA-WT), non-farnesylated prelamins A (LA-C661M) or farnesylated and carboxymethylated prelamins A (LA-L647R) upon H₂O₂ administration. Bar, 10 μ m. **(B)** Dot plot showing the number of 53BP1 foci per nucleus as detected in (A). Experiments were conducted in triplicate, data analyzed were based on an average of 100 cells. Error bars, mean \pm SD. Comparison between the groups was determined by using the one-way ANOVA test. Asterisks show statistical significance (***, $p < 0.001$).

(indinavir, which causes accumulation of farnesylated and carboxymethylated prelamins A) (Coffinier et al., 2007; Dominici et al., 2009; Mattioli et al., 2019). Non-farnesylated prelamins A was undetectable in untreated fibroblasts (Figure 1A). In mevinolin-treated cells, non-farnesylated prelamins A was observed at the nuclear rim and in intranuclear foci (Figure 1A). In fibroblasts treated with indinavir, farnesylated prelamins A was observed at the nuclear rim and in the nucleoplasm (Figure 1A).

53BP1 localization was analyzed in cells that accumulated different prelamins A forms or mature lamin A under basal conditions or upon oxidative stress induction.

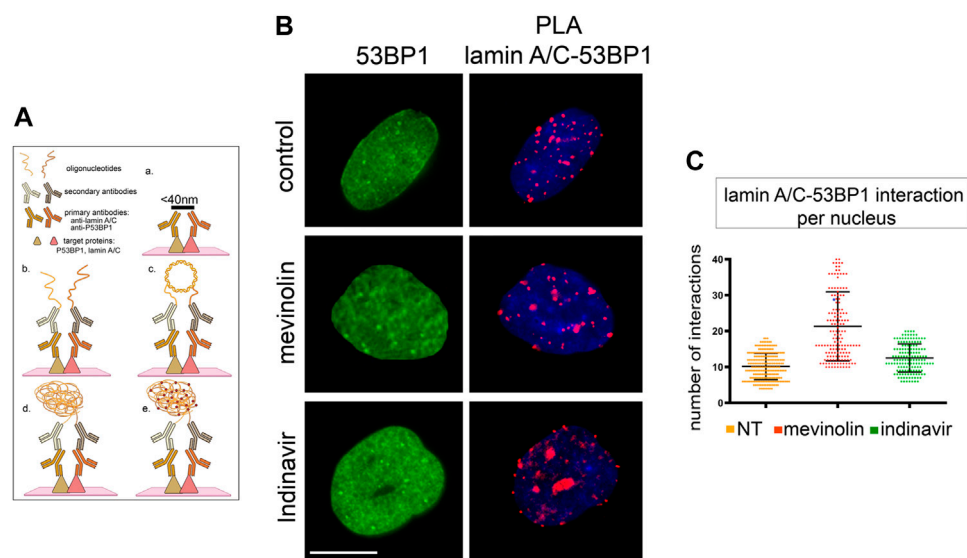
In unperturbed human dermal fibroblasts, 53BP1 was localized in the nucleoplasm (Figure 1A) or it was detected as one or two intensely labeled foci, while more than three 53BP1-labeled nuclear foci were observed in 2% of cells (Figures 1A,B). In this study, we assumed that cells showing three or more intranuclear 53BP1 foci were involved in the DNA damage response process.

Under basal conditions, the number of cells showing more than three 53BP1 foci in the nucleus was not significantly different between untreated and mevinolin-or indinavir-treated cells as

calculated by statistical analysis, although a slight increase was observed in cells that accumulated farnesylated prelamins A upon indinavir treatment (Figures 1A,B).

In cells subjected to oxidative stress, a different scenario was observed. Four hours after H₂O₂ treatment, 53BP1 was recruited to DNA damage sites and multiple 53BP1-labeled foci were detected in all fibroblast nuclei (Figure 1C). However, relative to cells that did not accumulate prelamins A, reduced 53BP1 recruitment in foci was observed in cells accumulating farnesylated prelamins A, while the lowest number of 53BP1 foci was detected in cells that accumulated non-farnesylated prelamins A (Figures 1C,D).

To support these observations, we overexpressed different prelamins A forms in human dermal fibroblasts and induced oxidative stress. In cells expressing LA-C661M (non-farnesylated prelamins A) a lower number of 53BP1 foci was observed with respect to cells expressing LA-WT (fully processable prelamins A) or LA-L647R (farnesylated prelamins A) (Figure 2). However, relative to mock-transfected cells, fibroblasts overexpressing any LMNA plasmid showed a significantly reduced number of 53BP1 foci, possibly due to accumulation of non-farnesylated prelamins A under

**FIGURE 3**

53BP1-lamin A/C binding in human dermal fibroblasts accumulating prelamins A, (A) Schematic representation of PLA protocol showing primary antibodies and interactors analysed in this study (created with BioRender.com). The maximum distance between interactors that allows direct binding and detection by PLA is indicated on the black bar in panel a. Binding of primary antibodies and secondary antibody-bound probes is shown in panel b. Ligase-catalysed oligonucleotide annealing is shown in c. Amplification of oligonucleotides is represented in d, incorporation of fluorescent probes is represented in e. (B) 53BP1 localization and PLA of lamin A/C-53BP1 interactions in untreated, mevinolin- or indinavir-treated cells. 53BP1 was detected by immunofluorescence labeling with a specific antibody (green). Interactions between lamin A/C and 53BP1 are revealed as red signals. Chromatin was counterstained with DAPI (blue). Bar, 10 μm . (C) Dot plot showing the number of PLA signals per nucleus as detected in (B). Experiments were conducted in triplicate, data analyzed were based on an average of 100 cells. Error bars, mean \pm SD. Comparison between the groups was determined by using the one-way ANOVA test.

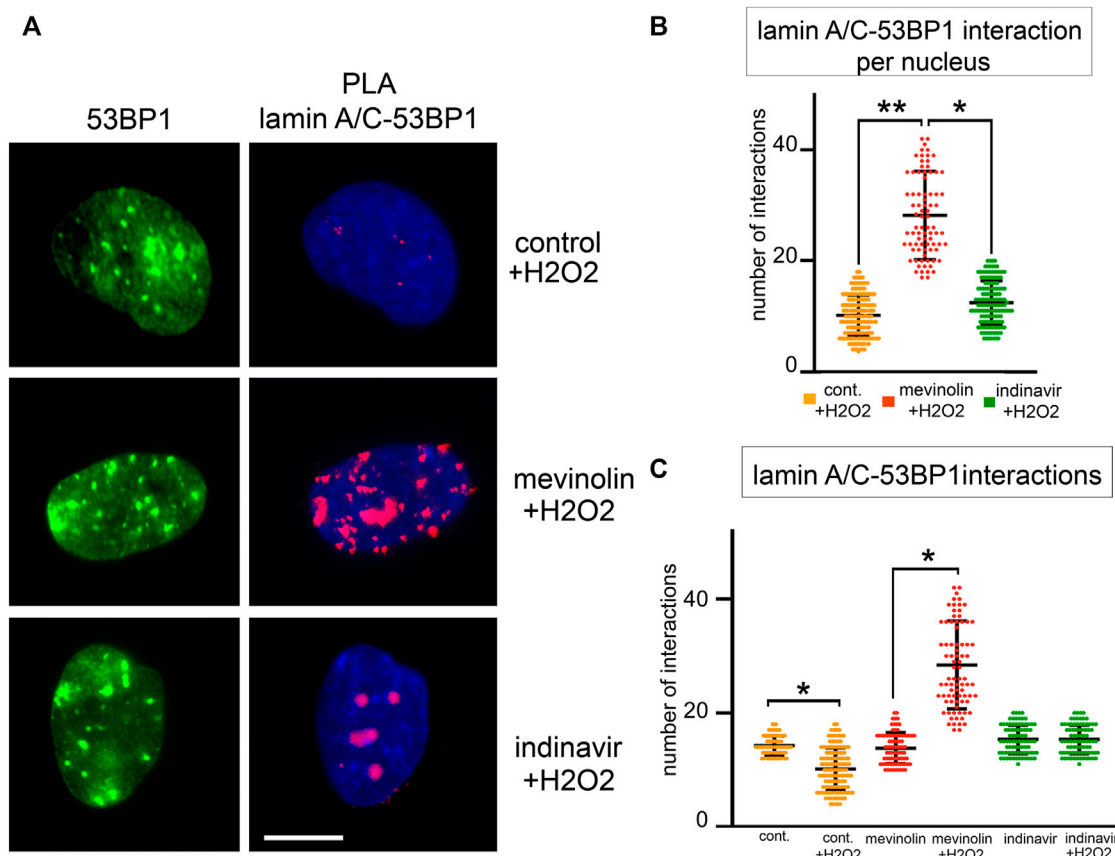
overexpression conditions. We have observed similar behavior in other experimental settings (Capanni et al., 2012) and this observation may explain the reduced recruitment of 53BP1 to DNA damage foci even in LA-L647R (farnesylated prelamins A) with respect to LA-WT (fully processable prelamins A) (Figure 2). To avoid any bias due to overexpression conditions, the following experiments were only performed in cells that accumulated prelamins A due to mevinolin or indinavir administration.

Accumulation of non-farnesylated prelamins A increases 53BP1 recruitment to lamin A/C complexes upon oxidative stress in human dermal fibroblasts

It has been demonstrated that 53BP1, through its Tudor domain, is able to bind lamin A/C and that this interaction is abrogated by DNA-damage (Gibbs-Seymour et al., 2015). Our hypothesis was that the accumulation of prelamins A forms could affect 53BP1 interaction with lamin A/C. Thus, we analyzed the interaction between lamin A/C and 53BP1 through Proximity Ligation Assay (PLA) (Figure 3A) (Mattioli et al., 2018).

Under basal conditions, a direct interaction was detected between lamin A/C and 53BP1 (Figure 3B). In mevinolin- or indinavir-treated cells, the number of interactions between lamin A/C and 53BP1 was not significantly different from that measured in untreated cells (Figure 3C).

Then, we analyzed 53BP1-lamin A/C complexes and formation of 53BP1 foci upon oxidative stress induction (Figure 4A–C). Four hours after H₂O₂ treatment, the highest number of 53BP1-lamin A/C complexes was measured in cells that accumulated non-farnesylated prelamins A, while binding signals were reduced in cells that accumulated farnesylated prelamins A and the lowest number of PLA signals was measured in cells that did not accumulate prelamins A ($p < 0.001$, Figure 4B). When comparing unperturbed and H₂O₂-treated cells (Figure 4C), the number of protein complexes was significantly reduced under stress conditions in the absence of prelamins A inhibitors ($p < 0.001$), significantly increased in mevinolin-treated fibroblasts accumulating non-farnesylated prelamins A ($p < 0.001$) and unaffected in indinavir-treated fibroblasts that accumulated farnesylated prelamins A (Figure 4C). As a whole, these results were consistent with previous studies showing release of lamin A/C-

**FIGURE 4**

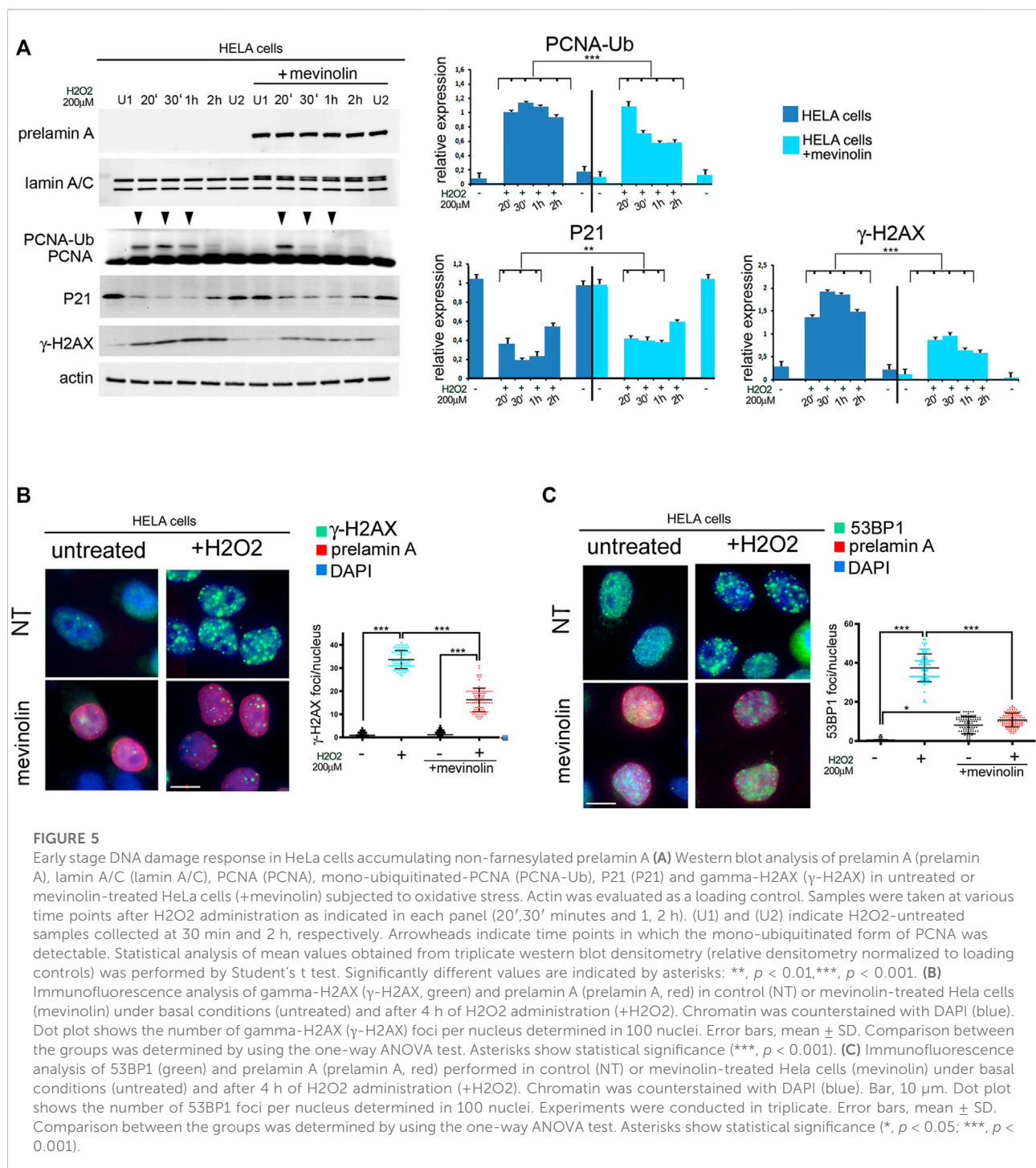
53BP1-lamin A/C binding in human dermal fibroblasts accumulating prelamins A subjected to oxidative stress. **(A)** Proximity ligation assay (PLA) showing lamin A/C-53BP1 interactions in untreated, mevinolin- and indinavir-treated fibroblasts upon oxidative stress induction. 53BP1 was detected by immunofluorescence labeling with a specific antibody (green). Interactions between lamin A/C and 53BP1 are revealed as red PLA signals. Chromatin was counterstained with DAPI (blue). Bar, 10 μ m. **(B)** Dot plot showing the number of PLA signals per nucleus in fibroblasts subjected to oxidative stress. Experiments were conducted in triplicate and 100 nuclei per sample were analyzed. Comparison between the groups was determined by using the one-way ANOVA test. Error bars, mean \pm SD. Asterisks show statistical significance (*, $p < 0.05$; **, $p < 0.01$). **(C)** Dot plot comparing PLA signals corresponding to lamin A/C-53BP1 interactions in fibroblasts left untreated (control) or subjected to H₂O₂ for 4 h (+H₂O₂). Untreated cells (cont.), mevinolin treated cells (mevinolin), indinavir treated cells (indinavir). Experiments were conducted in triplicate and 100 nuclei per sample were analyzed. Comparison between the groups was determined by using the one-way ANOVA test. Error bars, mean \pm SD. Asterisks show statistical significance (*, $p < 0.05$; **, $p < 0.01$).

53BP1 complexes upon DNA damage as a determinant of proper DNA damage response dynamics (Gonzalez-Suarez et al., 2011; Gibbs-Seymour et al., 2015) and provided evidence that prelamins A interferes with this process.

Farnesylated prelamins A affects the early stages of stress response and 53BP1 distribution in ZMPSTE24 $-/-$ HeLa cells

While the above reported data suggested a role for prelamins A in recruitment of 53BP1 during stress response, we did not observe prelamins A increase within 2 h upon stress induction (Figure 5A).

Thus, we suspected that prelamins A accumulation could have a toxic effect at the very early stages of oxidative stress response. To test this hypothesis, we first assessed the effect of non-farnesylated prelamins A accumulation by measuring H2AX phosphorylation in mevinolin-treated HeLa cells soon after oxidative stress induction. In untreated and mevinolin-treated cells, phosphorylation of H2AX increased at all examined stages of oxidative stress response, including the very early time points (Figure 5A). However, lower levels of phosphorylated H2AX were detected in cells that accumulated non-farnesylated prelamins A (Figure 5A). Moreover, ubiquitination of PCNA, which is required at this stage to permit trans-lesion DNA synthesis (Cazzalini et al., 2003; Paiano et al., 2021; Tidi et al., 2022), occurred in untreated cells, while it was significantly less efficient in the presence of



non-farnesylated prelamin A (Figure 5A). As p21-PCNA interaction is modulated at this stage through PCNA ubiquitination, which influences p21 degradation (Zlatanou et al., 2011), we also investigated p21 levels. In cells that did not accumulate any prelamin A form, p21 levels linearly decreased in the first stages of the stress response (20, 30 min, and 1 h) and started to increase 2 h after stress induction (Figure 5A). In the

presence of non-farnesylated prelamin A, p21 decrease was observed 20 min after stress induction, while further decrease at the following time points was not observed and increased levels were detected 2 h after H2O2 administration (Figure 5A). The whole evaluation of these results supported the view that accumulation of non-farnesylated prelamin A attenuates the early DNA damage response.

Immunofluorescence analysis showed that phosphorylated H2AX at DNA damage foci was not affected by non-farnesylated prelamin A accumulation under basal conditions (Figure 5B). However, upon oxidative stress induction, while phosphorylated H2AX was detected in foci in cells that did not accumulate prelamin A, a reduced number of phosphorylated H2AX foci was formed in cells that had accumulated non-farnesylated prelamin A (Figure 5B).

53BP1 distribution was slightly affected by non-farnesylated prelamin A accumulation (mevinolin) under basal conditions (Figure 5C). However, in HeLa cells subjected to H₂O₂, 53BP1 foci were efficiently formed in the absence of prelamin A, while a significantly lower number of foci was detected in mevinolin-treated cells 4 h after stress induction (Figure 5C). Thus, similar effects of non-farnesylated prelamin A were determined in fibroblasts (Figure 1B) and HeLa cells (Figure 5C).

Then, to check the effect of farnesylated prelamin A on early cellular response to oxidative stress, we took advantage of ZMPSTE24 silenced HeLa cells (ZMPSTE24^{-/-} cells) obtained by CRISPR/Cas9 gene editing. These cells accumulate farnesylated prelamin A in the absence of mature lamin A (Mattoli et al., 2019; Cenni et al., 2020b). Compared to ZMPSTE24^{+/+} cells, PCNA ubiquitination was impaired in ZMPSTE24^{-/-} cells (Figure 6A), while p21 levels were elevated under basal conditions and barely decreased upon stress induction (Figure 6A). In particular, p21 reduction was observed soon after oxidative stress induction, but fluctuation of protein levels was observed during 2 h observation (Figure 6A). Moreover, lower levels of phosphorylated H2AX were detected in ZMPSTE24^{-/-} cells upon stress induction as compared to cells that did not accumulate prelamin A (Figure 6A). The latter results showed that farnesylated prelamin A accumulation to toxic levels alters p21 modulation, ubiquitination of PCNA and H2AX phosphorylation. The whole evaluation of our data indicated that accumulation of any prelamin A form affects the very early stages of stress response and the most negative effect is observed with farnesylated prelamin A. These results were relevant to the understanding of laminopathic diseases featuring prelamin A accumulation, as the developmental disorder Restrictive Dermopathy and the progeroid syndromes Mandibuloacral Dysplasia and HGPS. As current clinical trials for progeroid laminopathies are based on inhibition of prelamin A farnesylation, we decided to investigate to which extent impairing prelamin A farnesylation in ZMPSTE24^{-/-} cells could improve early stress response. To this end, ZMPSTE24^{-/-} cells were treated with the farnesyl-transferase inhibitor Lonafarnib, which is currently used in HGPS clinical trials (Gordon et al., 2018). In Lonafarnib-treated ZMPSTE24^{-/-} cells, rescue of PCNA mono-ubiquitination was observed during the early stages of stress response (Figure 6B). Lonafarnib also increased H2AX phosphorylation levels suggesting improved recruitment of DNA damage response factors (Figure 6B).

Regarding phosphorylated H2AX distribution, we did not observe any significant difference between wild-type and ZMPSTE24^{-/-} HeLa cells under basal conditions (Figure 6C, graph). Further, lonafarnib did not affect phosphorylated H2AX under basal conditions (Figure 6C). Interestingly, oxidative stress caused a slightly (not significantly) increased number of phosphorylated H2AX foci in untreated ZMPSTE24^{-/-} HeLa cells, while foci were significantly enhanced in lonafarnib-treated cells subjected to H₂O₂ (Figure 6C).

As demonstrated in human dermal fibroblasts (Figures 1B, 2), formation of 53BP1 foci upon oxidative stress induction was reduced in HeLa cells that accumulated farnesylated prelamin A (Figure 6D). In fact, in ZMPSTE24^{-/-} HeLa cells subject to H₂O₂, a lower number of 53BP1 foci was detected relative to wild-type HeLa cells (Figure 6D, graph). However, lonafarnib treatment elicited an unexpected effect both under basal conditions and upon oxidative stress induction. In fact, the number of 53BP1 foci increased in lonafarnib-treated ZMPSTE24^{-/-} HeLa cells in the absence of any stress stimulus (Figure 6D), while H₂O₂ treatment did not determine any further increase of 53BP1-labeled foci (Figure 6D). Taken together, phosphorylated H2AX and 53BP1 dynamics observed in ZMPSTE24^{-/-} HeLa cells indicate that accumulation of farnesylated prelamin A uncouples DNA damage signaling (H2AX phosphorylation) from 53BP1 recruitment to damaged DNA. However, while lonafarnib restores phosphorylated H2AX recruitment, it appears ineffective towards 53BP1.

Discussion

Our results bring us to the hypothesis schematically represented in Figure 7. Briefly, in cells subjected to oxidative stress, only mature lamin A is present at the very early stage of response, a condition permitting p21 decrease and PCNA ubiquitination, along with increase of H2AX phosphorylation. A few hours after stress induction, prelamin A processing is slowed-down leading to accumulation of non-farnesylated prelamin A, which elicits recruitment of 53BP1 to lamin A/C complexes and a low number of 53BP1-containing DNA damage foci. Accumulation of farnesylated prelamin A, which follows due to progression of protein maturation, causes partial release of 53BP1 from lamin A/C binding and increase of 53BP1-labeled foci. At the last stage, mature lamin A is produced, a condition associated with almost complete release of 53BP1 from lamin A/C complexes and 53BP1 targeting to DNA damage foci. Consistent with this dynamics, prelamin A accumulation affects the very early stage of stress response by impairing p21 decrease, PCNA ubiquitination and H2AX phosphorylation (Figure 7).

Prelamin A undergoes a complex post-translational processing yielding mature lamin A. This process causes formation of four different intermediates, among which, we

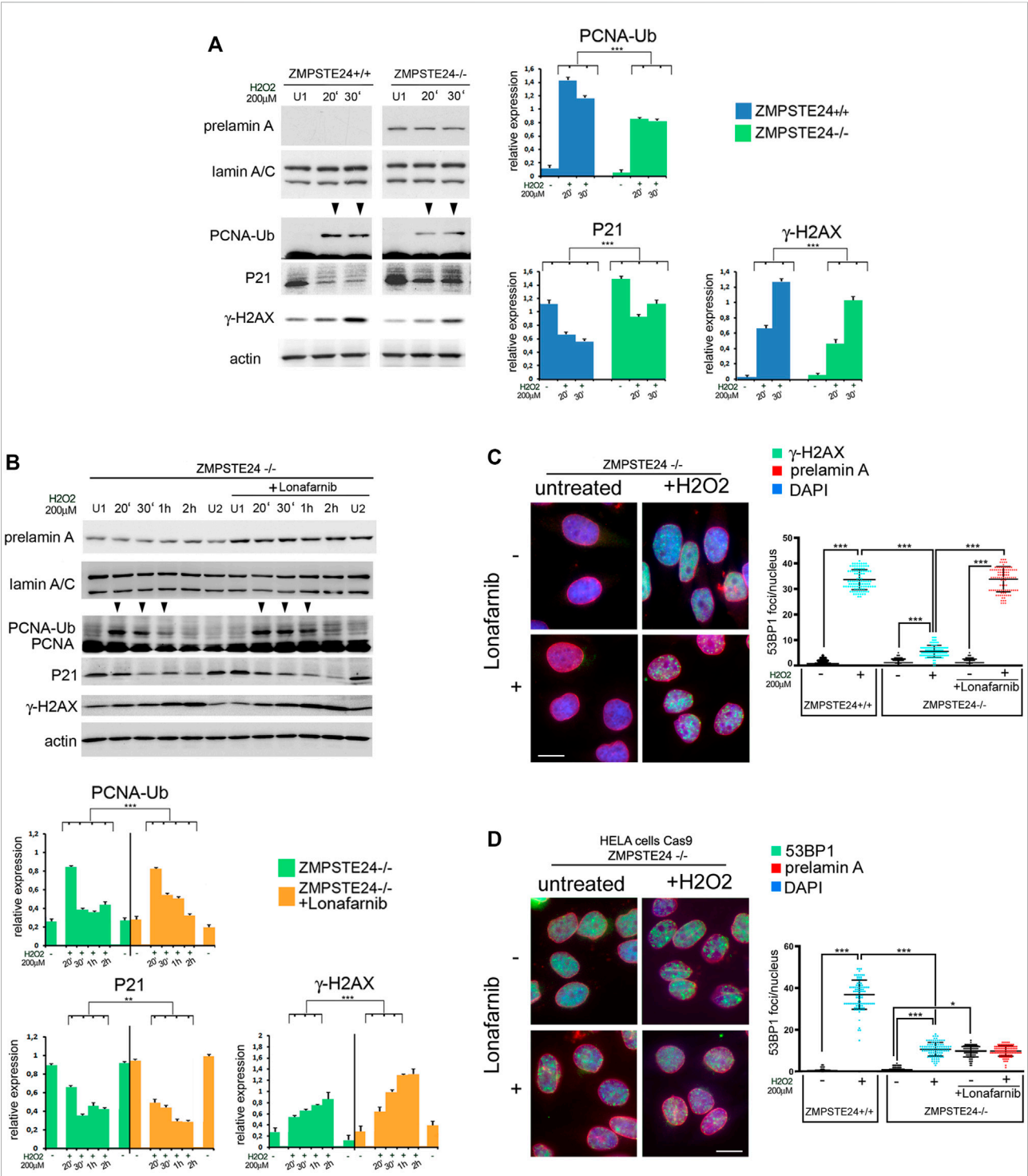
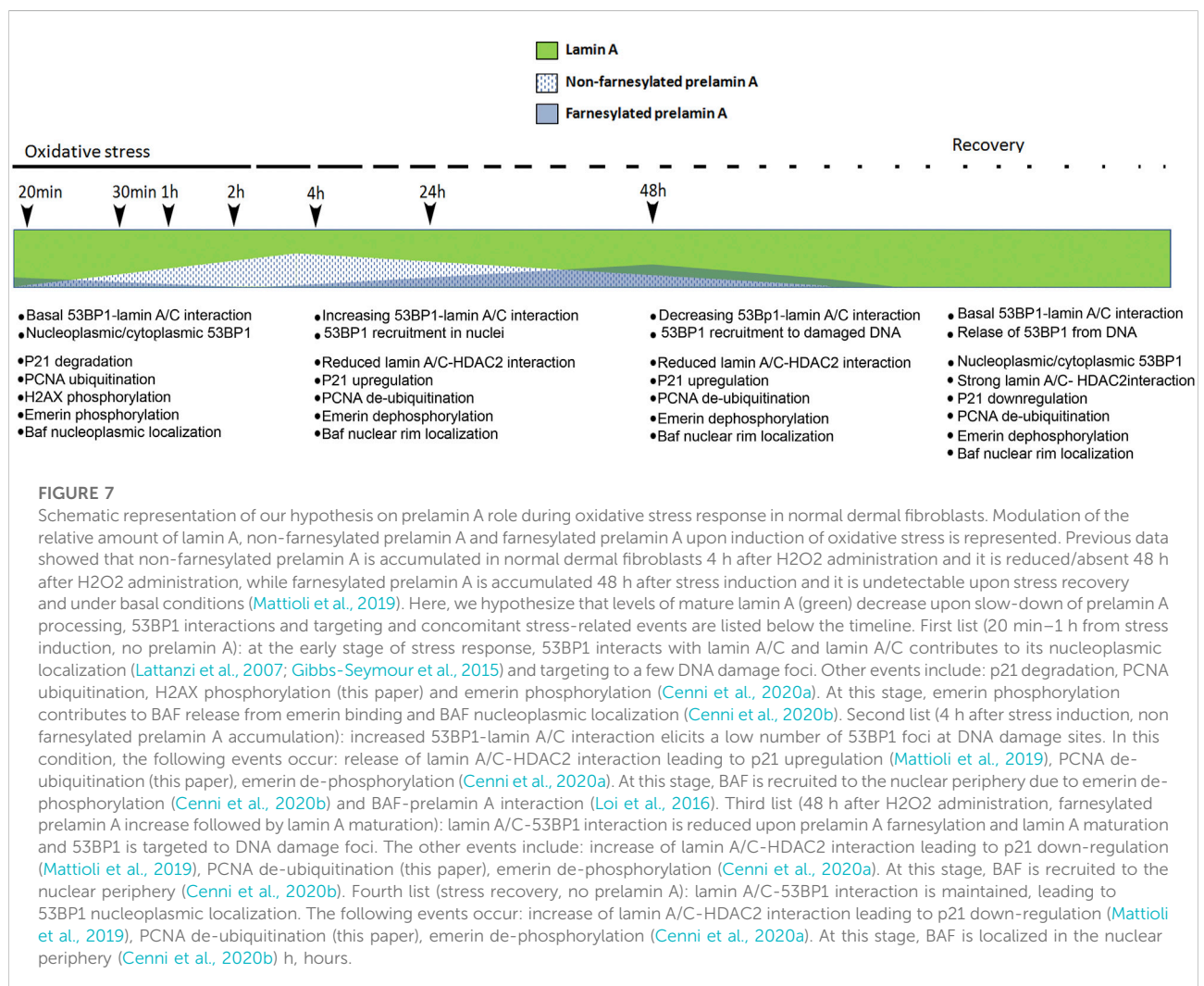


FIGURE 6 Early stage DNA damage response in ZMPSTE24^{-/-} HeLa cells accumulating farnesylated prelamin A (A) Western blot analysis performed in ZMPSTE24^{+/+} (ZMPSTE24^{+/+}) and ZMPSTE24^{-/-} HeLa cells (ZMPSTE^{-/-}) subjected to oxidative stress (H2O2). Prelamin A (prelamin A), lamin A/C (lamin A/C), mono-ubiquitinated-PCNA (PCNA-Ub), P21 (P21) and gamma-H2AX (γ-H2AX) bands are shown. Actin was evaluated as a protein loading control. (U1) indicates H2O2-untreated samples collected at 30 min, while 20' and 30' indicates samples collected after 20 and 30 minutes after H2O2 administration respectively. Arrowheads indicate time points in which the mono-ubiquitinated form of PCNA was detectable. Statistical analysis of mean values obtained from triplicate western blot densitometry (relative densitometry normalized to loading controls) was performed by Student's t test. Significantly different values are indicated by asterisks: *** = $p < 0.001$. (B) Western blot analysis performed in ZMPSTE24^{-/-} HeLa cells (ZMPSTE24^{-/-}) subjected to oxidative stress (H2O2) in the presence or absence of Lonafarnib (+Lonafarnib). Prelamin A (prelamin A), lamin A/C (lamin A/C), mono-ubiquitinated-PCNA (PCNA-Ub), P21 (P21) and gamma-H2AX (γ-H2AX) bands are shown. Actin was evaluated as a protein loading control. (U1) indicates H2O2-untreated samples collected at 30 min, while 20' and 30' indicates samples collected after 20 and 30 minutes after H2O2 administration respectively. Arrowheads indicate time points in which the mono-ubiquitinated form of PCNA was detectable. Statistical analysis of mean values obtained from triplicate western blot densitometry (relative densitometry normalized to loading controls) was performed by Student's t test. Significantly different values are indicated by asterisks: *** = $p < 0.001$. (C) Immunofluorescence analysis performed in ZMPSTE24^{-/-} HeLa cells (ZMPSTE24^{-/-}) subjected to oxidative stress (H2O2) in the presence or absence of Lonafarnib (+Lonafarnib). 53BP1 foci (53BP1 foci/nucleus), prelamin A (prelamin A) and DAPI (DAPI) are shown. Statistical analysis of mean values obtained from triplicate immunofluorescence analysis (relative densitometry normalized to loading controls) was performed by Student's t test. Significantly different values are indicated by asterisks: *** = $p < 0.001$. (D) Immunofluorescence analysis performed in HELa cells Cas9 ZMPSTE24^{-/-} (HELa cells Cas9 ZMPSTE24^{-/-}) subjected to oxidative stress (H2O2) in the presence or absence of Lonafarnib (+Lonafarnib). 53BP1 foci (53BP1 foci/nucleus), prelamin A (prelamin A) and DAPI (DAPI) are shown. Statistical analysis of mean values obtained from triplicate immunofluorescence analysis (relative densitometry normalized to loading controls) was performed by Student's t test. Significantly different values are indicated by asterisks: *** = $p < 0.001$. (Continued)

FIGURE 6 (Continued)

A/C), PCNA (PCNA), mono-ubiquitinated-PCNA (PCNA-Ub), P21 (P21) and gamma- H2AX (γ -H2AX) bands are shown. Actin was evaluated as a protein loading control. Samples were taken at various time points after H₂O₂ administration as indicated in each panel. (U1) and (U2) indicate H₂O₂-untreated samples collected at 30 min and 2 h, respectively. Arrowheads indicate time points in which the mono-ubiquitinated form of PCNA was detectable. Statistical analysis of mean values obtained from triplicate western blot densitometry (relative densitometry normalized to loading controls) was performed by Student's *t* test. Significantly different values are indicated by asterisks: **, *p* < 0.01, ***, *p* < 0.001. (C) Immunofluorescence analysis of gamma-H2AX (γ -H2AX, green) and prelamin A (prelamin A, red) performed in control or Lonafarnib-treated ZMPSTE24^{-/-} HeLa cells under basal condition (untreated) and after 4 h of H₂O₂ administration (+H₂O₂). Chromatin was counterstained with DAPI (blue). Dot plot shows the number of gamma-H2AX foci in ZMPSTE24^{+/+} and ZMPSTE24^{-/-} HeLa cells. Experiments were conducted in triplicate and 100 nuclei per sample were analyzed. Error bars, mean \pm SD. Comparison between the groups was determined by using the one-way ANOVA test. Asterisks show statistical significance (***, *p* < 0.001). Bar, 10 μ m. (D) Immunofluorescence analysis of 53BP1 (green) and prelamin A (prelamin A, red) performed in control or Lonafarnib-treated ZMPSTE24^{-/-} HeLa cells under basal condition (untreated) and after 4 h of H₂O₂ administration (+H₂O₂). Chromatin was counterstained with DAPI (blue). Dot plot shows the number of gamma-H2AX foci in ZMPSTE24^{+/+} and ZMPSTE24^{-/-} HeLa cells. Experiments were conducted in triplicate and 100 nuclei per sample were analyzed. Comparison between the groups was determined by using the one-way ANOVA test. Asterisks show statistical significance (*, *p* < 0.05; ***, *p* < 0.001). Bar, 10 μ m.



analysed non-farnesylated prelamin A and carboxymethylated-farnesylated prelamin A (Mattioli et al., 2019; Cenni et al., 2020a). To accumulate prelamin A and test

its physiological role, we decided to block its processing by using specific inhibitors and detect the endogenous proteins. In fact, any mutation in the *LMNA* sequence aimed at

impairing prelamin A processing may either lead to expression of a pathogenetic prelamin A mutant (as in the case of *LMNA* L647R, which is associated with a progeroid laminopathy (Wang et al., 2016; Wang et al., 2022)) or cause toxic levels of prelamin A (Capanni et al., 2012). We can consider mevinolin and indinavir-treated cells as representative of a condition of prelamin A accumulation below the threshold level of toxicity leading to disease. On the other hand, as prelamin A is not accumulated at the very early stage of stress response, increasing its levels at that stage elicits a non-physiological condition that helps elucidating its pathogenetic pathway(s). It is worth considering that *ZMPSTE24*^{-/-} cells feature fully blocked prelamin A processing, thus representing a true pathological condition, while all other experimental settings used in this study recapitulate transient accumulation of different prelamin A forms in cells that also express mature lamin A, as occurs a few hours after H₂O₂ administration (Ragnauth et al., 2010; Cenni et al., 2014; Mattioli et al., 2019). It has been shown that prelamin A accumulation during DDR reduces lamin A/C binding to HDAC2 thus allowing chromatin relaxation due to histone H3K9 and H4K20 acetylation (Mattioli et al., 2018). Moreover, reduced lamin A/C-HDAC2 interaction during DDR affects HDAC2 activity and increases the expression of p21, an HDAC2-regulated gene (Mattioli et al., 2018). As a whole, transient impairment of HDAC2-lamin A/C interaction during DDR is necessary to set chromatin and p21 in a condition allowing DNA repair (Mattioli et al., 2018).

In that context, we investigated how prelamin A accumulation interferes with lamin A/C-53BP1 binding and formation of 53BP1 foci at DNA damage sites. PLA experiments confirmed the interaction between lamin A/C and 53BP1, supporting direct binding between the two proteins (Etourneau et al., 2021). Our results show that, under basal conditions, the presence of non-farnesylated prelamin A does not affect lamin A/C-53BP1 interaction. Consistent with this observation, formation of 53BP1 foci in nuclei is not increased in cells accumulating non-farnesylated prelamin A. This observation is relevant as it rules out major toxic effects of therapeutic treatments based on prelamin A farnesylation inhibitors as statins or FTIs, at least in dermal fibroblasts. Considering that 53BP1 foci are minimally increased under basal conditions even in cells accumulating farnesylated prelamin A, we suggest that prelamin A does not cause DNA damage *per se*, while it interferes with DNA damage repair (Cenni et al., 2014; Cenni et al., 2020a). In fact, upon induction of oxidative stress, prelamin A strongly affects 53BP1 dynamics. Non-farnesylated prelamin A is accumulated a few hours after stress induction and favours 53BP1 recruitment to lamin A/C complexes in the nucleoplasm (Lattanzi et al., 2007), possibly to collect all available protein, while the following prelamin A processing steps, ultimately eliciting mature lamin A, reduce the amount of nuclear lamina-associated 53BP1 and allow its

targeting to newly damaged DNA sequences during stress response (Figure 7).

Another aspect of prelamin A-related 53BP1 dynamics is highlighted by the comparison of the number of interactions in untreated *versus* H₂O₂-treated cells that accumulated a specific form of prelamin A. Upon oxidative stress induction, the number of protein complexes was significantly increased in cells that accumulated non-farnesylated prelamin A, while it was reduced in cells that only expressed mature lamin A. Importantly, any oxidative stress-dependent modification (increase or decrease) in the amount of lamin A/C-53BP1 interactions relative to non-stressed cells was abolished in the presence of farnesylated prelamin A and a sort of unresponsive or locked condition was apparently established. This observation is particularly relevant to the understanding of pathological accumulation of farnesylated prelamin A. Previous studies have shown impaired 53BP1 recruitment to DNA damage foci in the presence of L647R-prelamin A (uncleavable farnesylated prelamin A (Cobb et al., 2016) and other progeria-linked prelamin A forms (Starke et al., 2013) including progerin, the truncated form of farnesylated prelamin A accumulated in HGPS (Starke et al., 2013; Kreienkamp et al., 2016). Here, we propose that persistent accumulation of farnesylated prelamin A negatively impacts two main stages of DNA damage repair. First, by affecting PCNA, P21 and H2AX modifications required at the very early stages of DDR and secondly by freezing a physiological step of farnesylated prelamin A accumulation occurring during DDR under physiological conditions. Other mechanisms and players affect 53BP1 during DDR under pathological or even physiological conditions (Mayca Pozo et al., 2017). For instance, the presence of progerin has been shown to mediate cathepsin L-mediated 53BP1 degradation (Kreienkamp et al., 2016; Mayca Pozo et al., 2017). On the other hand, it has been recently demonstrated that lamin B1 forms complexes with 53BP1 and plays a key role in the regulation 53BP1 recruitment during ionizing radiation-induced DNA damage repair (Etourneau et al., 2021). Interestingly, the authors showed that upregulation of lamin B1 alters 53BP1 recruitment to DNA damage foci by strengthening lamin B1-53BP1 complexes, while that mechanism does not involve lamin A, at least in tumour cells (Etourneau et al., 2021). It should be interesting to investigate whether prelamin B is also accumulated in cells under stress conditions as well as the interplay between lamin B1 or prelamin A platforms recruiting 53BP1. In this study, we further show that toxic levels of farnesylated prelamin A impair PCNA mono-ubiquitination at the early stage of stress response. Mono-ubiquitination of PCNA is a key step in the activation of TLS, a DNA damage response mechanism necessary to bypass DNA lesions encountered during replication. The recruitment of polymerases specialized in DNA synthesis through damaged bases at the stalled replication fork is governed by the PCNA mono-ubiquitination, which increases the PCNA affinity for pol η (Ma et al., 2020). In this context,

p21 plays a fundamental role as a negative regulator of DNA synthesis across a lesion (Soria and Gottifredi, 2010). In fact, p21 binding to PCNA impedes PCNA ubiquitination and PCNA-polymerase η interaction (Ticli et al., 2022). Here we show that the high amount of p21 elicited by unscheduled accumulation of prelamin A forms at the very early stage of DNA damage response (Mattioli et al., 2018 and, 2019) affects PCNA dynamics. This defect might add to impaired down regulation of *CDKN1A* gene upon recovery from DNA damage that occurs in cells that accumulate toxic levels of prelamin A forms as previously described in HGPS fibroblasts (Mattioli et al., 2018) and contribute to the setting of conditions that favour cellular senescence. Preventing prelamin A farnesylation improved PCNA mono-ubiquitination in ZMPSTE24 silenced cells. As progerin is a form of farnesylated prelamin A, we suggest that lonafarnib efficacy in HGPS clinical trials could in part involve improvement of PCNA processing in cells facing DNA damage. As BRCA1 supports the mono-ubiquitination of PCNA by regulating the recruitment of ubiquitinating enzymes (Tian et al., 2013), and a strong reduction in the amount of BRCA1 protein has been described in HGPS fibroblasts (Kreienkamp et al., 2016), we cannot rule out the possibility that progerin or even prelamin A accumulation could contribute to impaired PCNA ubiquitination by altering both BRCA1 and p21 levels. It is worth noting that lonafarnib treatment of ZMPSTE24^{-/-} HeLa cells was also effective in restoring phosphorylated H2AX recruitment upon oxidative stress, but did not increase the number of 53BP1-labeled foci under the same conditions. This observation was not unexpected as we had observed in fibroblasts that accumulation of non-farnesylated prelamin A (that occurs in mevinolin- or lonafarnib-treated cells) slowed-down formation of 53BP1 foci due to recruitment of 53BP1 to lamin A/C complexes. However, the apparent uncoupling between H2AX phosphorylation and 53BP1 foci formation in lonafarnib-treated ZMPSTE24^{-/-} cells could in part explain partial rescue of the HGPS cellular phenotype upon lonafarnib administration.

Our study here reported has been performed in dermal fibroblasts and epithelial cells. This represents a limitation of the study, as different prelamin A-related dynamics might occur in different cell types, also depending on different nuclear envelope interactors of lamin A/C (Tingey et al., 2019; Czapiewski et al., 2022). A possibility exists that prelamin A in either form, governs timing of DNA damage repair thus fitting repair dynamics to pre-existing cellular conditions. This could be the case of myotubes and muscle cells, where farnesylated prelamin A is detectable even in the absence of stress conditions (Mattioli et al., 2011). Moreover, provided that an analogous mechanism of 53BP1 modulation is mediated by lamin B1 in bone or epithelial tumour cells (Etourneau et al., 2021), it should be interesting to investigate whether different lamin platforms anchor 53BP1 in transformed cells.

Conclusion

The whole evaluation of different players involved in DDR will allow us to discriminate whether prelamin A accumulation is a trigger of DNA damage or an activator of DNA repair factors under different stress conditions. In our opinion, both hypotheses can be true, as we see that modulation of prelamin A post-translational processing rate contributes to proper timing of DNA damage repair. As a consequence, altered prelamin A modulation may impair DNA damage repair and increase the amount of unrepaired DNA.

As a whole, our data show that prelamin A does not induce *per se* DNA-damage when transiently accumulated at low levels in the absence of stress stimuli. However, soon after stress induction, prelamin A accumulation appears to impair proper DNA damage response due to inhibition of PCNA ubiquitination. On the other hand, transient increase of prelamin A levels at the following stages is crucial to modulate 53BP1 targeting to DNA-damage sites. We can assess that non-farnesylated prelamin A favours recruitment of 53BP1 to lamin A/C-containing complexes, while prelamin A processing allows timely 53BP1 release. Based on previous and present observations, we suggest that the increased lamin A/C-53BP1 interaction occurring in the presence of non-farnesylated prelamin A helps collecting all available 53BP1 from inside and outside the nuclei. Alternatively, recruitment of 53BP1 by non-farnesylated prelamin A could establish a priority in damaged DNA to be repaired. It will be interesting to establish to which damaged sequences is 53BP1 targeted in the presence of non-farnesylated prelamin A, if those sequences are within lamina-associated chromatin domains (LADs) (Robson et al., 2017; Bellanger et al., 2022; Madsen-Osterbye et al., 2022), correspond to the most recently damaged DNA or are they selected by any lamin A/nuclear envelope-related tissue-specific mechanism (Mattioli et al., 2011; Czapiewski et al., 2022).

In this context, we propose that senescent cells are accumulated in patients affected by progeroid laminopathies due to unscheduled or impaired activation of prelamin A-regulated DNA damage repair mechanisms under oxidative stress conditions. Thus, clearly the genome defect is a cause of the pathology. However, we suggest that other prelamin A-dependent events not related to DNA damage response, as for instance remodeling of specific chromatin domains (Bellanger et al., 2022) or recruitment of chromatin binding proteins as BAF, LAP2alpha or HDAC2 (Lattanzi et al., 2007; Mattioli et al., 2008; Mattioli et al., 2011; Camozzi et al., 2014; Loi et al., 2016; Mattioli et al., 2018) contribute to the onset of organismal ageing when one or more prelamin A forms are stabilized. As a whole, we believe that un-processable prelamin A forms cannot accomplish their main role of sensors of “environmental changes” and timely activators of specific stress responses (Cenni et al., 2020a) as any of these

functions relies on modulation of prelamin A maturation rate or establishment of transient interactions at the prelamin A-specific C-terminal domain. This has been shown for p21, HDAC2, LAP2alpha, Oct-1, BAF in cells subjected to oxidative stress and all these proteins impact on genome functional organization (Mattioli et al., 2008; Cenni et al., 2014; Mattioli et al., 2018; Mattioli et al., 2019; Cenni et al., 2020b). On the other hand, it is too complex of an issue to be able to completely rule out that other functions of the prelamin A are indirectly responsible for the increases in DNA damage. For instance, a direct consequence of the accumulation of progerin or toxic levels of wild-type prelamin A is a dramatic remodeling of the whole nuclear envelope (Columbaro et al., 2005; Columbaro et al., 2010; Pellegrini et al., 2015; Squarzone et al., 2021) with deleterious effects on cytoskeleton interactions (Balmus et al., 2018) and chromatin spatial organization leading to formation of damaged cytoplasmic DNA (Graziano et al., 2018; Kreienkamp et al., 2018). This in turn may activate inflammatory responses driven by the NF- κ B and Jak/STAT pathway (Liu et al., 2019; Squarzone et al., 2021) and cause chromatin reorganization as a response to inflammation. From this point of view, the pathology is a cause of genome defects. As all these considerations can be considered acceptable, it is not surprising that a vicious circle set up in progeroid laminopathies leads to worsening of cellular and organism phenotype in a very short time-frame. Our results and the above reported considerations may contribute to unravelling fine tuning of DNA damage repair mechanisms and chromatin dynamics, which occur under physiological conditions and avoid genome instability and cancer on one side and cellular and organismal aging on the other side.

Data availability statement

The raw data supporting the conclusion of this article will be made available by the authors, without undue reservation.

References

- Balmus, G., Larrieu, D., Barros, A. C., Collins, C., Abrudan, M., Demir, M., et al. (2018). Targeting of Nat10 enhances healthspan in A mouse model of human accelerated aging syndrome. *Nat. Commun.* 9, 1700. doi:10.1038/s41467-018-03770-3
- Bellanger, A., Madsen-Osterbye, J., Galigniana, N. M., and Collas, P. (2022). Restructuring of lamina-associated domains in senescence and cancer. *Cells* 11, 1846. doi:10.3390/cells11111846
- Benedicto, I., Chen, X., Bergo, M. O., and Andres, V. (2022). Progeria: A perspective on potential drug targets and treatment strategies. *Expert Opin. Ther. Targets* 26, 393–399. doi:10.1080/14728222.2022.2078699
- Blagosklonny, M. V. (2014). Geroconversion: Irreversible step to cellular senescence. *Cell Cycle* 13, 3628–3635. doi:10.4161/15384101.2014.985507
- Camozzi, D., Capanni, C., Cenni, V., Mattioli, E., Columbaro, M., Squarzone, S., et al. (2014). Diverse lamin-dependent mechanisms interact to control chromatin dynamics. Focus on laminopathies. *Nucleus* 5, 427–440. doi:10.4161/nucl.36289
- Capanni, C., Mattioli, E., Columbaro, M., Lucarelli, E., Parnik, V. K., Novelli, G., et al. (2005). Altered pre-lamin A processing is a common mechanism leading to lipodystrophy. *Hum. Mol. Genet.* 14, 1489–1502. doi:10.1093/hmg/ddi158
- Capanni, C., Squarzone, S., Cenni, V., D'apice, M. R., Gambineri, A., Novelli, G., et al. (2012). Familial partial lipodystrophy, mandibuloacral Dysplasia and restrictive dermopathy feature barrier-to-autointegration factor (baf) nuclear redistribution. *Cell Cycle* 11, 3568–3577. doi:10.4161/cc.21869
- Cazzalini, O., Perucca, P., Riva, F., Stivala, L. A., Bianchi, L., Vannini, V., et al. (2003). P21cdkn1a does not interfere with loading of pcna at dna replication sites, but inhibits subsequent binding of dna polymerase delta at the G1/S phase transition. *Cell Cycle* 2, 596–603.
- Cenni, V., Capanni, C., Mattioli, E., Columbaro, M., Wehnert, M., Ortolani, M., et al. (2014). Rapamycin treatment of mandibuloacral Dysplasia cells rescues localization of chromatin-associated proteins and cell cycle dynamics. *Aging (Albany Ny)* 6, 755–770. doi:10.18632/aging.100680

Author contributions

CC: Study design, western blotting, cell cultures, experimental plan, manuscript drafting. ES: Cell cultures, statistical analyses; MLDG: Cell cultures, immunofluorescence analysis, PLA; AM: Experimental plan, manuscript reviewing; EM: PLA experiments; GL study design, experimental plan, manuscript drafting, fund raising.

Funding

This study was supported by AIPROSAB Grant 3/2020 and 3/2021, by PRF Grant 2019/76 and by the CNR project NutrAge 2022.

Acknowledgments

The authors thank Despina Kiriakidu for the technical support.

Conflict of interest

The authors declare that the research was conducted in the absence of any commercial or financial relationships that could be construed as a potential conflict of interest.

Publisher's note

All claims expressed in this article are solely those of the authors and do not necessarily represent those of their affiliated organizations, or those of the publisher, the editors and the reviewers. Any product that may be evaluated in this article, or claim that may be made by its manufacturer, is not guaranteed or endorsed by the publisher.

- Cenni, V., Capanni, C., Mattioli, E., Schena, E., Squarzone, S., Bacalini, M. G., et al. (2020a). Lamin A involvement in ageing processes. *Ageing Res. Rev.* 62, 101073. doi:10.1016/j.arr.2020.101073
- Cenni, V., Squarzone, S., Loi, M., Mattioli, E., Lattanzi, G., and Capanni, C. (2020b). Emerin phosphorylation during the early phase of the oxidative stress response influences emerin-baf interaction and baf nuclear localization. *Cells* 9, E1415. doi:10.3390/cells9061415
- Chen, X., Yao, H., Andres, V., Berge, M. O., and Kashif, M. (2022). Status of treatment strategies for hutchinson-gilford progeria syndrome with a focus on prelamin A: A posttranslational modification. *Basic Clin. Pharmacol. Toxicol.* 131, 217–223. doi:10.1111/bcpt.13770
- Cobb, A. M., Larrieu, D., Warren, D. T., Liu, Y., Srivastava, S., Smith, A. J. O., et al. (2016). Prelamin A impairs 53bp1 nuclear entry by mislocalizing Nup153 and disrupting the ran gradient. *Ageing Cell* 15, 1039–1050. doi:10.1111/accel.12506
- Coffinier, C., Hudon, S. E., Farber, E. A., Chang, S. Y., Hrycyna, C. A., Young, S. G., et al. (2007). Hiv protease inhibitors block the zinc metalloproteinase Zmpste24 and lead to an accumulation of prelamin A in cells. *Proc. Natl. Acad. Sci. U. S. A.* 104, 13432–13437. doi:10.1073/pnas.0704212104
- Columbaro, M., Capanni, C., Mattioli, E., Novelli, G., Parnai, V. K., Squarzone, S., et al. (2005). Rescue of heterochromatin organization in hutchinson-gilford progeria by drug treatment. *Cell. Mol. Life Sci.* 62, 2669–2678. doi:10.1007/s00018-005-5318-6
- Columbaro, M., Mattioli, E., Schena, E., Capanni, C., Cenni, V., Levy, N., et al. (2010). Prelamin A processing and functional effects in restrictive dermatopathy. *Cell Cycle* 9, 4766–4768. doi:10.4161/cc.9.23.14210
- Czapiewski, R., Batrakou, D. G., De Las Heras, J. I., Carter, R. N., Sivakumar, A., Slivinska, M., et al. (2022). Genomic loci mispositioning in Tmem120a knockout mice yields latent lipodystrophy. *Nat. Commun.* 13, 321. doi:10.1038/s41467-021-27869-2
- Dominici, S., Fiori, V., Magnani, M., Schena, E., Capanni, C., Camozzi, D., et al. (2009). Different prelamin A forms accumulate in human fibroblasts: A study in experimental models and progeria. *Eur. J. Histochem.* 53, 43–52. doi:10.4081/ejh.2009.43
- Etourneau, L., Moussa, A., Rass, E., Genet, D., Willaume, S., Chabance-Okumura, C., et al. (2021). Lamin B1 sequesters 53bp1 to control its recruitment to dna damage. *Sci. Adv.* 7, eabb3799. doi:10.1126/sciadv.abb3799
- Filesi, I., Gullotta, F., Lattanzi, G., D'apice, M. R., Capanni, C., Nardone, A. M., et al. (2005). Alterations of nuclear envelope and chromatin organization in mandibuloacral Dysplasia, A rare form of laminopathy. *Physiol. Genomics* 23, 150–158. doi:10.1152/physiolgenomics.00060.2005
- Gibbs-Seymour, I., Markiewicz, E., Bekker-Jensen, S., Maitland, N., and Hutchison, C. J. (2015). Lamin A/C-dependent interaction with 53bp1 promotes cellular responses to dna damage. *Ageing Cell* 14, 162–169. doi:10.1111/accel.12258
- Gonzalez-Suarez, I., Redwood, A. B., Grotzky, D. A., Neumann, M. A., Cheng, E. H., Stewart, C. L., et al. (2011). A new pathway that regulates 53bp1 stability implicates cathepsin L and vitamin D in dna repair. *Embo J.* 30, 3383–3396. doi:10.1038/emboj.2011.225
- Gordon, L. B., Shappell, H., Massaro, J., D'agostino, R. B., Sr., Brazier, J., et al. (2018). Association of lonafarnib treatment vs No treatment with mortality rate in patients with hutchinson-gilford progeria syndrome. *Jama* 319, 1687–1695. doi:10.1001/jama.2018.3264
- Graziano, S., Kreienkamp, R., Coll-Bonfill, N., and Gonzalo, S. (2018). Causes and consequences of genomic instability in laminopathies: Replication stress and interferon response. *Nucleus* 9, 258–275. doi:10.1080/19491034.2018.1454168
- Kreienkamp, R., Croke, M., Neumann, M. A., Bedia-Diaz, G., Graziano, S., Dusso, A., et al. (2016). Vitamin D receptor signaling improves hutchinson-gilford progeria syndrome cellular phenotypes. *Oncotarget* 7, 30018–30031. doi:10.18632/oncotarget.9065
- Kreienkamp, R., Graziano, S., Coll-Bonfill, N., Bedia-Diaz, G., Cybulla, E., Vindigni, A., et al. (2018). A cell-intrinsic interferon-like response links replication stress to cellular aging caused by progerin. *Cell Rep.* 22, 2006–2015. doi:10.1016/j.celrep.2018.01.090
- Lattanzi, G., Columbaro, M., Mattioli, E., Cenni, V., Camozzi, D., Wehnert, M., et al. (2007). Pre-lamin A processing is linked to heterochromatin organization. *J. Cell. Biochem.* 102, 1149–1159. doi:10.1002/jcb.21467
- Liu, C., Arnold, R., Henriques, G., and Djabali, K. (2019). Inhibition of jak-stat signaling with baricitinib reduces inflammation and improves cellular homeostasis in progeria cells. *Cells* 8, E1276. doi:10.3390/cells8101276
- Liu, Y., Drozdov, I., Shroff, R., Beltran, L. E., and Shanahan, C. M. (2013). Prelamin A accelerates vascular calcification via activation of the dna damage response and senescence-associated secretory phenotype in vascular smooth muscle cells. *Circ. Res.* 112, E99–E109. doi:10.1161/CIRCRESAHA.111.300543
- Loi, M., Cenni, V., Duchi, S., Squarzone, S., Lopez-Otin, C., Foisner, R., et al. (2016). Barrier-to-autointegration factor (baf) involvement in prelamin A-related chromatin organization changes. *Oncotarget* 7, 15662–15677. doi:10.18632/oncotarget.6697
- Ma, X., Tang, T. S., and Guo, C. (2020). Regulation of translesion dna synthesis in mammalian cells. *Environ. Mol. Mutagen.* 61, 680–692. doi:10.1002/em.22359
- Madsen-Osterbye, J., Bellanger, A., Galigniana, N. M., and Collas, P. (2022). Biology and model predictions of the dynamics and heterogeneity of chromatin-nuclear lamina interactions. *Front. Cell Dev. Biol.* 10, 913458. doi:10.3389/fcell.2022.913458
- Mattioli, E., Andrenacci, D., Garofalo, C., Principe, S., Scotlandi, K., Remondini, D., et al. (2018). Altered modulation of lamin A/C-Hdac2 interaction and P21 expression during oxidative stress response in hgps. *Ageing Cell* 17, E12824. doi:10.1111/accel.12824
- Mattioli, E., Andrenacci, D., Mai, A., Valente, S., Robijns, J., De Vos, W. H., et al. (2019). Statins and histone deacetylase inhibitors affect lamin A/C - histone deacetylase 2 interaction in human cells. *Front. Cell Dev. Biol.* 7, 6. doi:10.3389/fcell.2019.00006
- Mattioli, E., Columbaro, M., Capanni, C., Maraldi, N. M., Cenni, V., Scotlandi, K., et al. (2011). Prelamin A-mediated recruitment of Sun1 to the nuclear envelope directs nuclear positioning in human muscle. *Cell Death Differ.* 18, 1305–1315. doi:10.1038/cdd.2010.183
- Mattioli, E., Columbaro, M., Capanni, C., Santi, S., Maraldi, N. M., D'apice, M. R., et al. (2008). Drugs affecting prelamin A processing: Effects on heterochromatin organization. *Exp. Cell Res.* 314, 453–462. doi:10.1016/j.yexcr.2007.11.012
- Mayca Pozo, F., Tang, J., Bonk, K. W., Keri, R. A., Yao, X., and Zhang, Y. (2017). Regulatory cross-talk determines the cellular levels of 53bp1 protein, A critical factor in dna repair. *J. Biol. Chem.* 292, 5992–6003. doi:10.1074/jbc.M116.760645
- Paiano, J., Zolnerowich, N., Wu, W., Pavani, R., Wang, C., Li, H., et al. (2021). Role of 53bp1 in end protection and dna synthesis at dna breaks. *Genes Dev.* 35, 1356–1367. doi:10.1101/gad.348667.121
- Pellegrini, C., Columbaro, M., Capanni, C., D'apice, M. R., Cavallo, C., Murdocca, M., et al. (2015). All-trans retinoic acid and rapamycin normalize Hutchinson progeria fibroblast phenotype. *Oncotarget* 6, 29914–29928. doi:10.18632/oncotarget.4939
- Ragnauth, C. D., Warren, D. T., Liu, Y., McNair, R., Tajsic, T., Figg, N., et al. (2010). Prelamin A acts to accelerate smooth muscle cell senescence and is a novel biomarker of human vascular aging. *Circulation* 121, 2200–2210. doi:10.1161/CIRCULATIONAHA.109.902056
- Robijns, J., Molenberghs, F., Sieprath, T., Corne, T. D., Verschuuren, M., and De Vos, W. H. (2016). *In silico* synchronization reveals regulators of nuclear ruptures in lamin A/C deficient model cells. *Sci. Rep.* 6, 30325. doi:10.1038/srep30325
- Robson, M. I., De Las Heras, J. I., Czapiewski, R., Sivakumar, A., Kerr, A. R. W., and Schirmer, E. C. (2017). Constrained release of lamina-associated enhancers and genes from the nuclear envelope during T-cell activation facilitates their association in chromosome compartments. *Genome Res.* 27, 1126–1138. doi:10.1101/gr.212308.116
- Soria, G., and Gottfredi, V. (2010). PcnA-coupled P21 degradation after dna damage: The exception that confirms the rule? *Dna Repair (Amst)* 9, 358–364. doi:10.1016/j.dnarep.2009.12.003
- Squarzone, S., Schena, E., Sabatelli, P., Mattioli, E., Capanni, C., Cenni, V., et al. (2021). Interleukin-6 neutralization ameliorates symptoms in prematurely aged mice. *Ageing Cell* 20, E13285. doi:10.1111/accel.13285
- Starke, S., Meinke, P., Camozzi, D., Mattioli, E., Pfaffle, R., Siekmeyer, M., et al. (2013). Progeroid laminopathy with restrictive dermatopathy-like features caused by an isodisomic lmna mutation P.R435c. *Ageing (Albany NY)* 5, 445–459. doi:10.18632/aging.100566
- Tian, F., Sharma, S., Zou, J., Lin, S. Y., Wang, B., Rezvani, K., et al. (2013). Brcal promotes the ubiquitination of pcna and recruitment of translesion polymerases in response to replication blockade. *Proc. Natl. Acad. Sci. U. S. A.* 110, 13558–13563. doi:10.1073/pnas.1306534110
- Ticli, G., Cazzalini, O., Stivala, L. A., and Prosperi, E. (2022). Revisiting the function of P21(cdkn1a) in dna repair: The influence of protein interactions and stability. *Int. J. Mol. Sci.* 23, 7058. doi:10.3390/ijms23137058
- Tingey, M., Mudumbi, K. C., Schirmer, E. C., and Yang, W. (2019). Casting A wider net: Differentiating between inner nuclear envelope and outer nuclear envelope transmembrane proteins. *Int. J. Mol. Sci.* 20, E5248. doi:10.3390/ijms20215248
- Wang, Y., Lichter-Konecki, U., Anyane-Yebo, K., Shaw, J. E., Lu, J. T., Ostlund, C., et al. (2016). A mutation abolishing the Zmpste24 cleavage site in prelamin A causes A progeroid disorder. *J. Cell Sci.* 129, 1975–1980. doi:10.1242/jcs.187302
- Wang, Y., Shilagardi, K., Hsu, T., Odinamadu, K. O., Maruyama, T., Wu, W., et al. (2022). Abolishing the prelamin A Zmpste24 cleavage site leads to progeroid phenotypes with near-normal longevity in mice. *Proc. Natl. Acad. Sci. U. S. A.* 119, e2118695119. doi:10.1073/pnas.2118695119
- Zlatanou, A., Despras, E., Braz-Petta, T., Boubakour-Azzouz, I., Pouvelle, C., Stewart, G. S., et al. (2011). The hms2-hmsh6 complex acts in concert with monoubiquitinated pcna and pol eta in response to oxidative dna damage in human cells. *Mol. Cell* 43, 649–662. doi:10.1016/j.molcel.2011.06.023



OPEN ACCESS

EDITED BY

Eric C. Schirmer,
University of Edinburgh,
United Kingdom

REVIEWED BY

Susana Gonzalo-Hervas,
Saint Louis University, United States
Fred Dick,
Western University, Canada
Jop Kind,
Hubrecht Institute (KNAW), Netherlands

*CORRESPONDENCE

Kundan Sengupta,
✉ kunsen@iiserpune.ac.in

†These authors have contributed equally
to this work

SPECIALTY SECTION

This article was submitted to Nuclear
Organization and Dynamics,
a section of the journal
Frontiers in Cell and Developmental
Biology

RECEIVED 12 October 2022

ACCEPTED 05 December 2022

PUBLISHED 16 December 2022

CITATION

Balaji AK, Saha S, Deshpande S, Poola D
and Sengupta K (2022), Nuclear
envelope, chromatin organizers,
histones, and DNA: The many achilles
heels exploited across cancers.
Front. Cell Dev. Biol. 10:1068347.
doi: 10.3389/fcell.2022.1068347

COPYRIGHT

© 2022 Balaji, Saha, Deshpande, Poola
and Sengupta. This is an open-access
article distributed under the terms of the
[Creative Commons Attribution License
\(CC BY\)](https://creativecommons.org/licenses/by/4.0/). The use, distribution or
reproduction in other forums is
permitted, provided the original
author(s) and the copyright owner(s) are
credited and that the original
publication in this journal is cited, in
accordance with accepted academic
practice. No use, distribution or
reproduction is permitted which does
not comply with these terms.

Nuclear envelope, chromatin organizers, histones, and DNA: The many achilles heels exploited across cancers

A. K. Balaji[†], Santam Saha[†], Shruti Deshpande[†], Darshini Poola
and Kundan Sengupta^{*}

Chromosome Biology Lab (CBL), Indian Institute of Science Education and Research, Pune,
Maharashtra, India

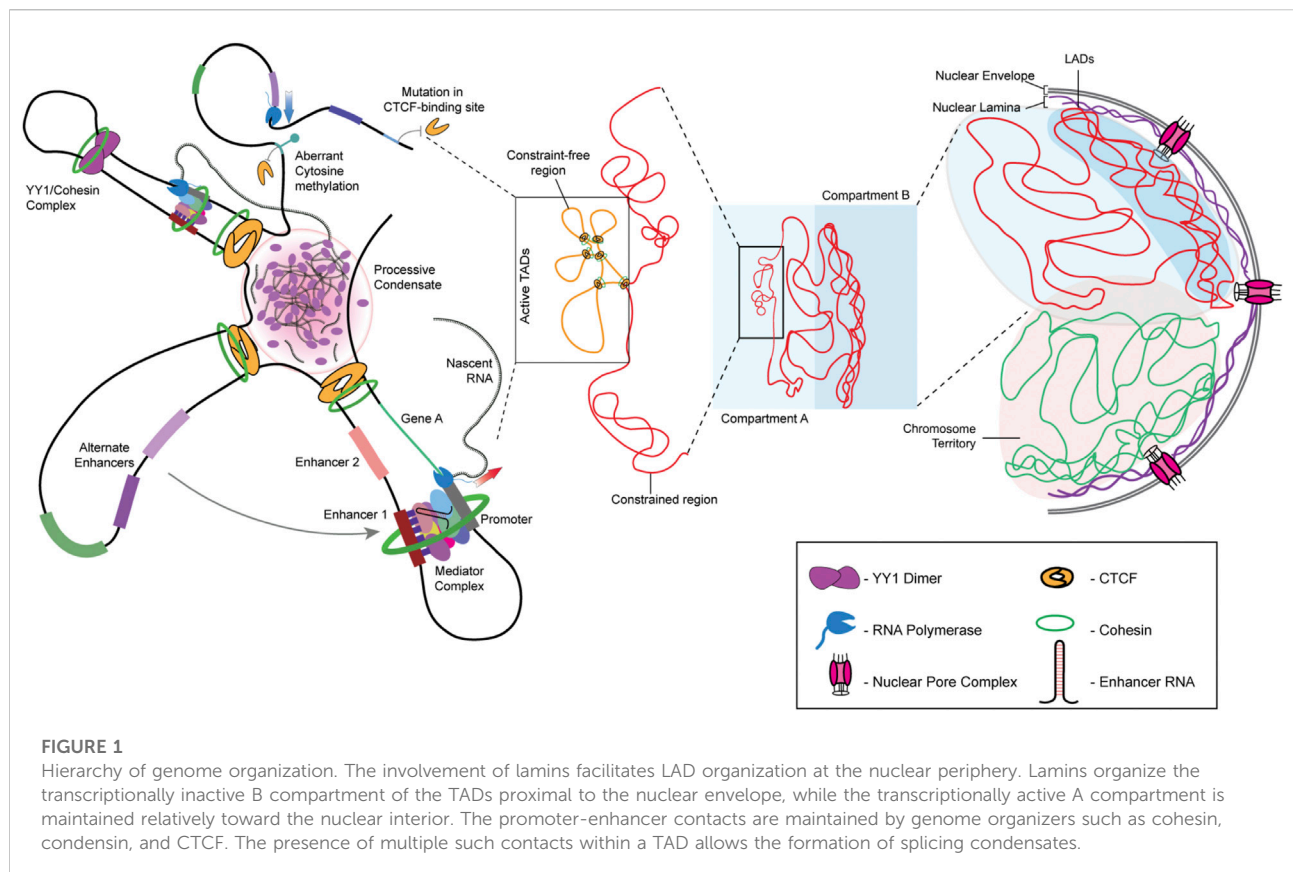
In eukaryotic cells, the genome is organized in the form of chromatin composed of DNA and histones that organize and regulate gene expression. The dysregulation of chromatin remodeling, including the aberrant incorporation of histone variants and their consequent post-translational modifications, is prevalent across cancers. Additionally, nuclear envelope proteins are often deregulated in cancers, which impacts the 3D organization of the genome. Altered nuclear morphology, genome organization, and gene expression are defining features of cancers. With advances in single-cell sequencing, imaging technologies, and high-end data mining approaches, we are now at the forefront of designing appropriate small molecules to selectively inhibit the growth and proliferation of cancer cells in a genome- and epigenome-specific manner. Here, we review recent advances and the emerging significance of aberrations in nuclear envelope proteins, histone variants, and oncohistones in deregulating chromatin organization and gene expression in oncogenesis.

KEYWORDS

lamins, heterochromatin, genome organization, nuclear envelope, oncohistones, histone variants

1 Introduction

Each chromosome occupies a unique sub-volume in the interphase nucleus, referred to as a chromosome territory (Cremer and Cremer, 2001). A chromosome territory encompasses intra- and inter-chromatin interactions, further fine-tuned by histone modifications. Analyses of chromatin interactions have revealed the organization of chromatin into two distinct compartments—A and B. Compartment A is composed of gene-rich, open chromatin localized toward the nuclear interior. In contrast, compartment B is gene-poor, has a compact conformation, and is localized toward the nuclear periphery. Closer inspection using variants of chromosome conformation capture assays, such as 3C, 4C, and Hi-C, reveals that the 3D genome architecture of a nucleus is intricately organized into Topologically Associating Domains (TADs), where



stretches of chromatin physically interact in a regulated manner to modulate gene expression within the TAD (Figure 1) (Szabo et al., 2019). The loop extrusion model of chromatin organization forms the basis of TAD-mediated genome organization, where chromatin loops are extruded by chromatin organizers and cohesin complexes and are delimited by CTCF-binding factor (CTCF), another chromatin organizer (Fudenberg et al., 2016; Nuebler et al., 2018). TADs organize looping-in of sequences ~1 Mb (in mammals) apart within close proximity, enabling enhancer-promoter contacts for the spatiotemporal regulation of gene expression (Chetverina et al., 2017). Interestingly, chromatin stretches with the same type of histone modifications show a propensity to interact and compartmentalize in the 3D space of the nucleus, thus revealing CTCF-cohesin-independent chromatin folding mechanisms. For instance, H3K27me3 histone modifications function as a signal for long-range chromatin interactions during hematopoietic stem cell differentiation (Zhang X et al., 2020). Notably, in addition to CTCF, genome organizers such as cohesin and condensin are required for the recruitment of transcription cofactors. Cohesin and CTCF function as boundary elements that collectively maintain genome architecture, which is prudently rigid and guardedly dynamic (Phillips-Cremins et al., 2013). Furthermore, chromatin

remodelers alter local chromatin dynamics in response to cell signaling events. The maintenance of TADs is critical since disruption of TAD organization is associated with developmental diseases and cancers (Lupianez et al., 2015; Akdemir et al., 2020). In cancers, the aberrant activation of cell signaling pathways relays erratic signals to the nucleus, which alters chromatin organization and transcriptional outputs of the cell. It remains to be examined how chromatin and its organizers respond to aberrant oncogenic signaling in cancer cells.

The double-membraned nucleus functions as the primary protector of the genome. In metazoans, the nucleus not only harbors the genome but also works in tandem with the differentially-compacted chromatin to regulate its tissue-specific spatial and functional organization. The nuclear envelope comprises the nuclear lamina that maintains nuclear integrity and regulates gene expression and is interspersed with Nuclear Pore Complexes (NPCs), whose primary function is to regulate nuclear transport (Lin et al., 2018). Though the chromatin in contact with the nuclear lamina is frequently repressed, NPCs additionally contribute to the regulation of gene expression. Furthermore, owing to the role of NPCs in chromatin organization and function, Nucleoporins (Nups), the class of proteins that comprise the NPC, are also involved in

regulating stemness and cell fate determination (D'Angelo et al., 2012). Interestingly, nucleoporins crosstalk with the chromatin organizer CTCF, which functions as a boundary element between TADs, while facilitating intra-TAD interaction. For instance, the nucleoporins Nup153 and Nup93, along with CTCF, regulate the transcriptional activity of the HOX gene cluster during early development and differentiation (Kadota et al., 2020; Labade et al., 2021).

In metazoans, type V intermediate filament proteins, the lamins, maintain the structural and functional integrity of the nucleus (Aebi et al., 1986; Gruenbaum and Foisner, 2015). The nuclear lamina is predominantly composed of two lamin sub-types—the A-type lamins that include lamins A and C (a spliced variant of lamin A), and the B-type lamins that comprise separately-encoded lamins B1 and B2 (in vertebrates). Each lamin sub-type harbors post-translational modifications (PTMs), exponentially increasing the functional diversity of lamins. Nuclear lamins regulate replication-dependent cell cycle progression, DNA damage repair, genome stability, and 3D organization of the genome (Moir et al., 2000; Bronshtein et al., 2015; Earle et al., 2020). Nuclear lamina interacts with stretches of chromatin that are in proximity to the nuclear periphery, referred to as Lamina-Associated Domains (LADs). LADs are typically repressed, barring exceptions where a subset of euchromatin interacts with lamin B1 and are categorized as euchromatic LADs (eLADs) (Guelen et al., 2008; Pascual-Reguant et al., 2018).

Chromatin in eukaryotes is organized as DNA wrapped around histone octamers, forming nucleosomes. Further, the linker histone H1 is incorporated with the nucleosomes constituting the fundamental units of the chromatin fiber—the chromatosomes (Zhang and Li, 2017). Histones are among the most widely modified proteins, and each modification has the unique ability to regulate gene expression (Turner, 1993; Millán-Zambrano et al., 2022). Actively transcribing genomic regions localized away from the nuclear periphery are often associated with active histone marks such as H3K4me3, H3K9ac, and H3K27ac, deposited by histone remodelers such as KMT2, CBP, and p300, respectively (Ogryzko et al., 1996; Rao and Dou, 2015). On the other hand, histone modifications such as H3K9me2/3, H3K27me3, and H4K20me1 are associated with transcriptional repression. The combination of active and inactive marks fine-tunes transcriptional output (Kimura, 2013; Talbert and Henikoff, 2021). Of note, repressive histone marks such as H3K9me2/3 and H3K27me3, deposited by INM-interacting histone-remodeling complexes such as SUV39H1/2 and the Polycomb Repressor Complex 2 (PRC2) complex, are often enriched on LADs (Shumaker et al., 2006; Cesarini et al., 2015; Harr et al., 2015). These histone-remodeling complexes interact with lamins and maintain the associated chromatin in a state of repression (Marullo et al., 2016; Salvarani et al., 2019; Bianchi et al., 2020; Siegenfeld et al., 2022).

Cancer cells exhibit a remarkable interplay between aberrant genome organization and deregulated transcription. The cancer genome harbors mutations in both coding and non-coding regions, selectively providing tumorigenic cells with a proliferative advantage to outcompete normal cells (Moreno and Basler, 2004; Pon and Marra, 2015; Bailey et al., 2021). For instance, incorporating non-canonical histone variants alters nucleosome stability, often resulting in altered replication and transcription (Bönisch et al., 2012; Henikoff and Smith, 2015; Buschbeck and Hake, 2017). In solid tumors, mutant chromatin remodelers differentially recruit histone modifiers that confer chemoresistance (Drosos et al., 2022). These cancer-associated mutant histones are referred to as oncohistones, which are now emerging as a class of prominent biomarkers of cancers (Bočkaj et al., 2021). In this review, we address the molecular and mechanistic underpinnings of nuclear envelope factors, their crosstalk with chromatin, and their pivotal role in cancer initiation and progression.

2 Nuclear envelope and lamins

The nuclear envelope is a crucial barrier between the cytoplasm and the nucleus and functions as a protector of the genome. The nuclear envelope consists of an outer and inner nuclear membrane (ONM and INM, respectively) and NPCs. The INM is lined on the inner side by a protein meshwork referred to as the nuclear lamina, which is composed of type V intermediate filament proteins—the A- and B-type lamins. The A-type lamins, lamin A/C, are produced as two somatic isoforms of prelamin A by alternative mRNA splicing at exon 10 of the LMNA gene (Machiels et al., 1996). Lamin A bears a CaaX motif at its C-terminal end, which is farnesylated, in contrast to lamin C, which does not contain the CaaX motif or undergo farnesylation (Vorburger et al., 1989). Notably, mature lamin A is formed by the loss of farnesylation inside the nucleus. On the other hand, the predominant B-type lamins—lamins B1 and B2 are permanently-farnesylated products of two separate genes—LMNB1 and LMNB2. Lamins interact with chromatin, either directly or through transmembrane proteins of the INM—lamin B receptor (LBR), MAN1, and Emerin (Ye and Worman, 1996; Holaska and Wilson, 2007; Demmerle et al., 2012). Apart from biochemical cues, the nucleus directly perceives mechanical signals through the LINC complex, involving Nesprin and SUN proteins (Figure 2). Nesprins, which extend from the ONM to the perinuclear space, directly interact with cytoskeletal proteins such as vimentin, actin, and microtubules (Ketema et al., 2013; Gimpel et al., 2017; Li et al., 2021). Mechanical cues are subsequently propagated *via* the interaction with the SUN and KASH domain proteins (Starr and Fischer, 2005; Tzur et al., 2006). These lines of evidence suggest that the coordinated functioning of nuclear lamins, nucleoporins, and LINC complex factors is central to the functional organization of the nucleus and the genome.

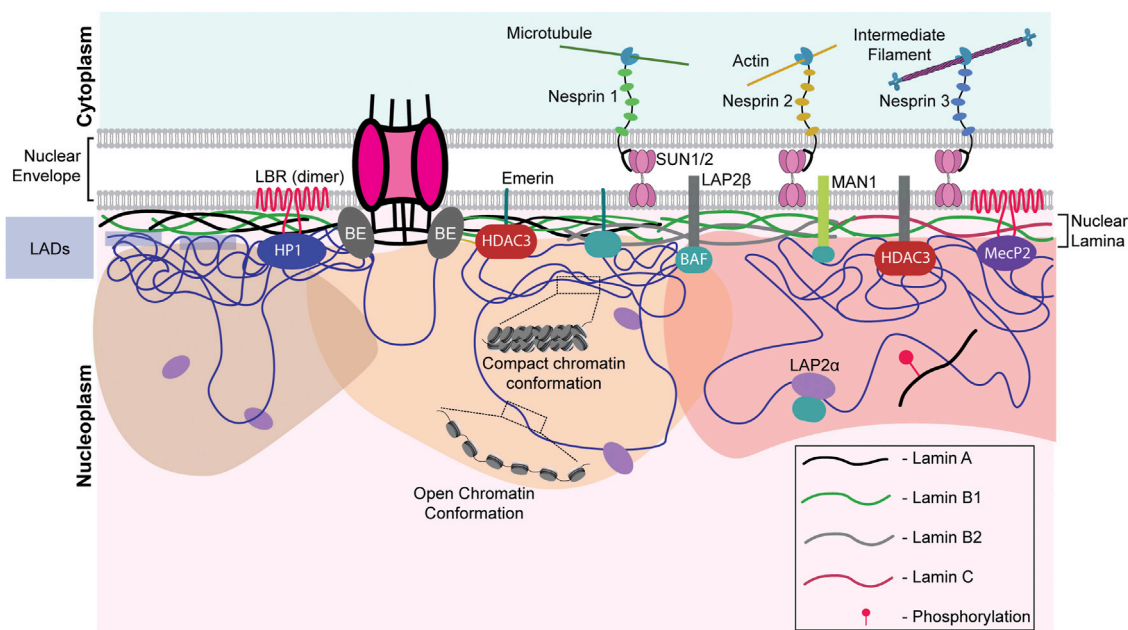


FIGURE 2

Nuclear envelope architecture and its role in genome organization. A schematic model showing the INM proteome involved in maintaining genome organization. Nesprins communicate external mechanical cues to the nucleus *via* the SUN1/2 complex. The regions of the genome contacting the nuclear lamina, the LADs, are maintained in a heterochromatic state. Phosphorylated lamin A binds to active enhancers in the nuclear interior. LAP2 α interacts with intra-nuclear lamin A/C and could be regulating its functioning. Chromatin remodelers such as HDACs and sirtuins are often associated with the INM proteins such as emerin, MAN1, LAP2 β , lamins, and LBR. NPCs are also associated with chromatin. LAP2 α - lamina Associated Peptide 2 α , LBR - lamin B receptor, BE - Barrier Element, HP1—Heterochromatin Protein 1, HDAC—histone deacetylase, SUN1/2—Sad1/unc-84 protein-like 1/2 and MeCP2—methyl CpG-binding protein 2.

Aberrations in nuclear morphology, such as invaginations, blebs, and micronuclei, serve as histological markers for grading tumor progression and often correlate with carcinogenesis. For instance, Haematoxylin-Eosin (HE) staining of papillary thyroid carcinoma cells and colon adenocarcinoma revealed enlarged nuclei with irregular morphology compared to normal cells with smaller and spherical nuclei (Fischer, 2020). Furthermore, nearly 90% of solid tumors are characterized by aneuploidy, which predominantly involves deletions and amplifications at the whole chromosomal and sub-chromosomal levels (Holland and Cleveland, 2012). CIN leads to transcriptional imbalances in a cell- and tissue-specific manner (Bakhoun et al., 2018; Benhra et al., 2018). Here, we focus on the mechanisms by which defects in the nuclear envelope manifest themselves, resulting in genomic instability and thereby contributing to cancer progression.

2.1 Role of aberrant nuclear envelope factors in cancers

The stability and integrity of LINC complex proteins and nuclear lamins are crucial for maintaining chromatin organization and genome stability, aberrations of which are

associated with various cancers (Sur et al., 2014). For instance, immunohistochemistry showed decreased expression of LMNA and LMNB1 in 7/8 primary gastric cancers and 6/8 gastric cancers, respectively (Moss et al., 1999). In addition, nuclear envelope proteins regulate chromosomal stability as they participate in cell cycle progression, chromosome segregation, and nuclear envelope assembly post-mitosis (Dechat et al., 2007; Kuga et al., 2014; Dubińska-Magiera et al., 2019).

Remarkably, nuclear morphology plays a vital role in modulating cell fate in the continuum of cancer progression (Capo-Chichi et al., 2016; Smith et al., 2018; Fischer, 2020). In particular, the loss of emerin and lamin A show aberrations in nuclear morphology, accompanied by an increased aggressiveness of cancer cells (Reis-Sobreiro et al., 2018; Bell et al., 2022). Consistent with this finding, ovarian cancers show decreased emerin and lamin A/C levels, accompanied by a progressive destabilization of the nuclear envelope (Capo-chichi et al., 2011). Lamin A/C-emerin co-depletion alters chromatin mobility, suggestive of their role in the maintenance of genome organization and function (Ranade et al., 2019). Intriguingly, depletion of lamin A/C mislocalized emerin, resulting in altered nuclear morphology and increased invasiveness of DU145 prostate cancer cells (Kong et al., 2012; Reis-Sobreiro et al., 2018).

The nuclear lamina is composed of three lamin sub-types and interacts with the LINC complex genes, and this confers a molecular redundancy on lamin function, which counters abrupt alterations in the lamina—predominantly in response to external cues. For instance, keratinocytes and fibroblasts of the skin derived from lamin A/C-knockout mice showed prolonged expression of LBR as compared to wild-type cells (Solovei et al., 2013). Similar buffering mechanisms were uncovered in EMD- and LMNA-null mice during development. While LAP2α was upregulated in myogenic cells derived from LMNA^{-/-} mice, cells derived from EMD-null mice showed a compensatory increase in lamin A expression (Melcon et al., 2006). However, the mechanistic basis of the transcriptional feedback circuits between lamin A/C and the nuclear envelope factors remains to be examined in greater detail.

The nuclear lamina functions as a docking site for anchoring LADs enriched in heterochromatin. For example, LBR tethers heterochromatin to the nuclear envelope in actively proliferating cancer cells during the early stages of mammalian development, while lamin A/C is a chromatin anchor in differentiated cells (Solovei et al., 2013; Lukášová et al., 2017). It is interesting to note that the loss of both LBR and lamin A/C results in the inversion of chromatin with heterochromatin toward the nuclear interior (Solovei et al., 2013), reiterating the significance of the nuclear lamina in chromatin organization and function. Furthermore, lamin B1 loss significantly increases nuclear bleb formation, while the depletion of lamin A/C shows morphological aberrations such as nuclear atypia, in addition to aneuploidy and CIN (Lammerding et al., 2006; Capo-chichi et al., 2011). Furthermore, destabilization of the nuclear envelope shows enhanced nuclear blebbing and micronuclei formation, which contribute to chromosomal losses and aneuploidy (Capo-Chichi et al., 2016). In addition to A and B-type lamins, peripheral heterochromatin provides additional stiffness, and its deregulation foreseeably weakens the nuclear envelope, contributing to the formation of nuclear blebs (Stephens et al., 2018). In summary, a stable nuclear envelope composition is required for genome organization facilitated by the maintenance of nuclear integrity by reinforcing nuclear stiffness.

Interestingly, the loss of lamin B1 shows CIN and DNA damage by destabilizing key Homologous Recombination (HR) pathway proteins such as Rad51 in U2OS cells (Liu et al., 2015). Correspondingly, A-type lamins regulate HR through transcriptional co-regulation of RAD51 and BRCA1 while modulating Non-Homologous End Joining (NHEJ) through 53BP1 in breast cancer cells (Redwood et al., 2011). Lamin A also regulates DNA damage repair (DDR) *via* its direct interaction with Hsp90—a molecular chaperone involved in protein folding and stability in ovarian cancer cells (Wang et al., 2021). Furthermore, whether the differential stoichiometry of the A and B-type lamins modulates NHEJ or HR pathways to repair damaged DNA in a cell-type- and cancer-specific manner remains an open question.

2.2 Role of nucleoporins in genome organization and cancers

Nuclear pore complexes (NPCs) are ~120 nm-wide structures in the nuclear envelope, which mediate selective transport in and out of the nucleus. In vertebrates, NPCs comprise nucleoporins (Nups), a group of ~30 proteins, to form a ~125MDa protein complex (Cronshaw et al., 2002; Cohen et al., 2012). In addition to nuclear transport, the NPCs regulate chromatin interaction and function (Zhou and Panté, 2010; Kadota et al., 2020). Further, Nups are classified into 1) on-pore Nups that are associated with the NPC and 2) off-pore Nups that exist both in the NPC and nucleoplasm. Nups that interact with and regulate essential genes in the genome include Nup93 (on-pore) and Nup153 (off-pore), which interact with super-enhancers, and function as major chromatin regulators (Baumann, 2016; Ibarra et al., 2016). Nup153 and Nup98, present near the nuclear basket of the NPC, communicate with a wide range of poised genes through interactions with CTCF (Pascual-Garcia et al., 2017). Certain on-pore Nups, such as Nup93, interact with and repress HOXA genes which are essential for early development (Labade et al., 2016). In the context of cancer progression, Nup93 facilitates metastasis by enhancing β-catenin import and upregulating EMT target genes, thus inducing epithelial-to-mesenchymal transition (EMT) in breast and hepatocellular cancers (Lin et al., 2022; Nataraj et al., 2022). The on-pore Nup210 interacts with SUN2 to regulate the expression of prometastatic mechanosensitive genes by impeding the spread of heterochromatin (Amin et al., 2021). Intriguingly, a non-canonical extranuclear function of the Nup107-160 complex is to stabilize bipolar spindle arrangement and prevent aneuploidy during each cell division, thus maintaining genome integrity (Orjalo et al., 2006).

Nups contribute to cancer progression by forming fusion proteins. For instance, the off-pore Nup98 is involved in multiple fusion proteins with transcriptional coactivators, histone methyltransferases, helicases, and in some instances, even orphan proteins (Wang et al., 2007; Yassin et al., 2010; Gough et al., 2011). During hematopoietic stem cell differentiation, HoxA7, HoxA9, and HoxA10 levels are upregulated, which progressively decrease as the hematopoietic cells differentiate further into various lineages. The Nup98 fusion protein alters gene expression resulting in Acute Myeloid Leukemia (AML). Intriguingly, in Nup98-NSD1 fusion protein-mediated AML, the fusion protein is recruited to the HoxA7, HoxA9, and HoxA10 gene loci. The FG-repeat (originating from Nup98) of the fusion protein interacts with HAT CBP/p300, leading to overexpression of the aforementioned Hox genes, contributing to AML. Nup98-PHD fusion proteins also promote AML progression *via* a similar mechanism (Wang et al., 2007, 2009). Thus, the aberrant localization and expression of Nups impact genome organization, contributing to oncogenesis. Taken together, the cellular machinery effectively copes with aberrant

2.3.1 Amplifications

It is well established that CIN and aneuploidy involving whole chromosomal and focal amplifications and deletions in the genome are defining features of cancer initiation and progression (Watanabe et al., 2001; Zhou et al., 2002; Kops et al., 2004). Interestingly, genes that encode for lamins are strikingly amplified as compared to the other nuclear envelope genes, implying that the very mechanisms that protect genomic integrity aberrate in cancers. TCGA analyses of nuclear envelope genes across patient samples revealed CNAs of the LMNA-coding sequence in ~13% of cancers. Breast cancer patient samples show the maximum extent of CNAs in LMNA in ~40% of the 211 patient samples (Figure 3A). However, the extent to which gene amplifications in LMNA correlate with changes in its transcript level remains unclear. An intriguing possibility is that transcriptional deregulation of lamin A/C potentially impacts expression levels of B-type lamins or LINC genes as a consequence of copy number amplifications of lamins and the stability of their interacting partners in a cell-type-specific manner.

2.3.2 Deletions

Interestingly, the LMNB1 gene shows a significant number of deletions across cancers. It is unique that LMNB1 and LMNB2 genes showed only deep deletions in ovarian cancers (Figures 3B,C). In ovarian cancer cells (HO-8910PM), decreased expression levels of lamin A/C correlate with increased cell migration and poor prognosis (Wang et al., 2019). Moreover, the lamin A:B stoichiometric ratio shows a dominance of A-type lamins in stiffer cartilaginous tissues, while B-type lamins are more prominent in softer tissues such as the brain (Swift et al., 2013). Nevertheless, if lamin A:B stoichiometry does modulate the malignant potential of cancer cells, the extent of complementation and the mechanisms that regulate the altered sub-interactome of the A- and B-type lamins remain to be uncovered.

2.3.3 Mutations in nuclear envelope genes—Nesprin (SYNE1)

We examined the status of mutations in genes that encode the nuclear envelope proteins across cancers using cBioPortal. This analysis revealed recurrent mutations in the Nesprin-1 gene—SYNE1 (Figure 3D). Markedly, the SYNE1 gene accumulates the highest number of missense mutations (271), followed by truncating (41) and splice mutations (12). A mutation in exon 33 of the SYNE1 gene modifies a conserved residue in spectrin repeat 11, showing aberrant mitotic phenotypes such as altered distance between the centrosome and the nucleus, potentially contributing to CIN in human hepatoma-derived Huh7 cells (Sur-Erdem et al., 2020). Furthermore, mutation analysis of SYNE1 revealed frequent missense mutations of T8362M across three different cancers—medulloblastoma, pancreatic adenocarcinoma, and

ovarian epithelial tumor. However, the physiological significance of these mutations remains to be elucidated. Do mutations in SYNE1 destabilize or hyperactivate mechanochemical signals into the nucleus and chromatin as a consequence of its altered interaction with LINC complex factors and actin? This could further contribute to increased communication with the microenvironment and the consequent proliferation of cancer cells.

3 Chromatin organizers in carcinogenesis

The genome is a highly dynamic collection of genes, their regulators, and massive stretches of DNA whose function is yet to be discovered. Maintenance of genome organization involves the concerted function of numerous proteins required for the regulation of chromatin organization and gene expression. The aberrant function of chromatin organizers is associated with cancers (Table 1). Here, we examine the contribution of major chromatin organizers, namely CTCF, cohesins, and condensins, to cancer progression.

3.1 CTCF

CCCTC-binding factor (CTCF) is a conserved zinc-finger protein that functions as a chromatin organizer and transcription factor. In association with cohesin, CTCF regulates the organization of gene loci and alternative splicing primed by its sequence-specific binding to CTCF sites. In addition, CTCF functions as an insulator to restrict the expansion of repressive marks (Dixon et al., 2012; Holwerda and de Laat, 2013). The human genome has ~55,000–65,000 CTCF binding sites, amongst which around ~5,000 are highly conserved across species (Yusufzai et al., 2004; Chen et al., 2012; Holwerda and de Laat, 2013), though CTCF occupancy remains tissue- and cancer-specific (Hanssen et al., 2017; Debaugny and Skok, 2020). As per the loop extrusion model for TAD formation, the cohesin complex moves along the chromatin, establishing a loop until it encounters an oriented CTCF dimer. Consequently, further advancement of the cohesin complex is aborted, thus demarcating TAD boundaries enriched in CTCF binding sites (Sanborn et al., 2015; Fudenberg et al., 2016). CTCF also prevents non-specific promoter-enhancer interaction by delimiting the loop size, thus augmenting enhancer-blocking mechanisms (Amankwaa et al., 2022). The Yin Yang 1 (YY1) protein interacts with cohesin and is enriched near enhancer-promoter contact sites, thus assisting CTCF in augmenting enhancer-promoter interaction (Figure 1) (Weintraub et al., 2017).

Aberrant expression or occupancy of CTCF is associated with breast, lung, endometrial, gastrointestinal, prostate, and skin

TABLE 1 Role of chromatin organizers in cancers.

Chromatin organizer	Gene	Cancer	Effect of dysregulation of gene	Reference
Cohesin	STAG2	Glioblastoma	Mutation in STAG2 leads to aneuploidy while its rescue enhances the chromosomal stability	Solomon et al. (2011)
	RAD21	Breast	Overexpression of RAD21 in MDA-MB-231 cells leads to poor prognosis and chemoresistance, while its knockdown reduces chemoresistance	Xu et al. (2011)
Condensin	NCAPH	Colorectal	In HCT116, NCAPH depletion decreases cell migration, arrests the cells in G2/M, and enhances apoptosis	Yin et al. (2017)
	NCAPG	Liver	NCAPG has a pro-proliferative effect in adenocarcinoma patients	Zhang et al. (2022)
	NCAPH	Prostate	Upregulation of NCAPH in prostate cancers promotes cell proliferation and helps in bypassing replication checkpoints, which might hinder cancer progression	Kim et al. (2019)
CTCF		Breast	CTCF and EGR1 reduce cell migration in TNBC cell line MDA-MB-231 by inducing the expression of Nm23-H1	Wong et al. (2021)

Mutations in genes that encode for chromatin organizers are implicated in carcinogenesis and impact chromosome organization, stability and transcriptional regulation.

cancers (Eldholm et al., 2014; Kemp et al., 2014; Poulos et al., 2016; Guo et al., 2018; Höflmayer et al., 2020). Of note, multiple mutations map to the DNA-binding zinc finger domain of CTCF across cancers (Bailey et al., 2021). CTCF binding to its target sites is sensitive to their methylation states. For instance, hypermethylation of CTCF binding sites shows a loss of insulation in isocitrate dehydrogenase (IDH) mutant gliomas (Flavahan et al., 2016). This further leads to the ectopic interaction of the IDH enhancer with PDGFRA (platelet-derived growth factor receptor alpha), leading to its constitutive expression and the development of gliomas (Figure 1). However, not all cancer-specific mutations in CTCF affect its binding. For instance, stop codon mutations in its N- and C-terminals, as well as in the zinc finger domain, may exhibit a dominant-negative effect by hindering interactions with functionally important cofactors, thus impeding CTCF function (Debaugny and Skok, 2020).

Analyzing patient data sets from TCGA reveals frequent loss of the CTCF gene in breast and prostate cancer patients, correlating with hypermethylation of CpG islands and hypomethylation of other parts of the genome. CTCF depletion in a prostate cancer cell line, HPECE6/E7, shows hypermethylation of CTCF binding sites, further downregulating respective gene expression (Damaschke et al., 2020). This indicates that CTCF binding to its target sites prevents CpG hypermethylation and safeguards chromatin architecture, not just by organizing the chromatin but also by maintaining it. This study further reveals that drug-induced hypomethylation using 5-aza-2 deoxycytidine (5dAza) rescued chromatin organization, reaffirming the importance of CTCF and its binding sites in cancers. However, 5dAza interacts with a wide range of targets and fails to act precisely on distinct TADs, thus raising the question of specificity in cancer therapies.

CTCF functions as a double-edged sword, acting both as an oncogene as well as a tumor suppressor in a cancer subtype-specific

manner. Ovarian cancers exemplify the oncogenic potential of CTCF, where metastatic lesions display elevated CTCF expression. Further, the depletion of CTCF in ovarian cancer cell lines (SKOV3 and A2780) decreased cell migration by consistently downregulating three metastasis-associated genes, including CTBP1, SRC, and SERPINE (Zhao et al., 2017). In contrast, CTCF positively regulates the expression of the metastatic suppressor, Nm23-H1, in breast cancers. Studies in the highly invasive MDA-MB-231 and the less invasive MCF-7 cells show that CTCF-dependent Nm23-H1 levels inversely correlate with cancer aggressiveness (Wong et al., 2021). The mechanism by which CTCF functions in a cancer-specific manner remains poorly understood.

Overall, changes in genome organization due to altered levels or aberrant recruitment of chromatin organizers contribute to cancer progression. However, experiments performed in cell culture models need to be complemented with insights from animal models and patient-derived tumor samples. Since adherent cell culture studies are usually performed on a monolayer of cells, these approaches do not mimic the tumor microenvironment, discounting factors such as nutrient accessibility, barrier tissue formation, and variation in drug response, among others. What effects chemotherapeutic agents have on TAD organization and gene expression *in vivo* remains an area of active study. Moreover, it is intriguing that environmental factors, such as diet and social interaction, also impinge on CTCF function and, therefore, chromatin organization and function (Davis et al., 2022; Wang R et al., 2022)—an interesting finding, given that extraneous environmental factors considerably contribute to an increase in the incidence of cancers.

3.2 Cohesin

Cohesins are multi-protein complexes essential for mitosis and meiosis, conserved from yeast to humans. The canonical

function of cohesins is to clasp sister chromatids together during the metaphase-to-anaphase transition. Apart from the aforementioned function, cohesin plays a vital role in maintaining inter-TAD and intra-TAD boundaries by looping chromatin in the interphase nucleus, allowing for regulated inter- and intra-TAD interactions (Matthews and Waxman, 2018; Barrington et al., 2019). This promotes enhancer-promoter contacts in a cell type-specific manner.

Through genome-wide sequencing, it is now apparent that cohesin accumulates a number of mutations in the coding region that alter the way it binds the chromatin and promotes aberrant genomic contacts leading to anomalous expression of various genes. Depletion of RAD21, a component of the cohesin complex, promotes enhanced expression of mesenchymal genes such as ITGA5 and TGF-B1 by altering the intrachromosomal chromatin contacts and creating active transcriptional units (Yun et al., 2016). Recent exome sequencing revealed that the STAG2 protein of cohesin is frequently mutated in cancers (Lawrence et al., 2014). It is interesting to note that STAG2 is involved in promoting regulated chromosomal contacts, the depletion of which enhances the loop extrusion and promotes aberrant genomic contacts (Adane et al., 2021; Richart et al., 2021). It remains unclear how the mutated STAG2 functions in cancer, elucidation of which might uncover a new therapeutic candidate. Moreover, the loss of cohesin function in cancers leads to increased replication stress and genomic instability (Leylek et al., 2020; Minchell et al., 2020). We surmise that cohesin mutations enhance genomic instability, facilitate clonal expansion, or enhance tumorigenic potential, eventually leading to cohesin loss of function in the clonal population. However, various lines of evidence suggest that mutations in the cohesin genes contribute to cancer initiation and progression by disrupting chromosome organization and transcriptional regulation (Table 1) (Leeke et al., 2014; Kojic et al., 2018; Antony et al., 2021).

3.3 Condensin

Like cohesins, condensins are multi-protein complexes required for chromosome assembly, condensation, and segregation during mitosis and meiosis. While cohesin clasps the sister chromatids together, condensin facilitates mitotic chromosome compaction by uniting the two distant portions of a single chromatid. Condensin isoforms have conserved structural maintenance of chromosome (SMC) proteins, SMC2 and SMC4, but differ in their non-SMC components. Interestingly, decreased condensin expression triggers CIN, consequently driving colorectal cancer progression (Baergen et al., 2019). In addition, mutations in the C-terminal residues R551 and S556 of CAPH2, a condensin II subunit, lead to genomic instability in the human retinal pigment epithelial

(RPE1) cell line (Weyburne and Bosco, 2021). Another line of evidence shows the involvement of the condensin complex in maintaining chromosomal stability *via* its recruitment to the pericentromeric regions. The binding of cell cycle regulators pRB and E2F1 to the pericentromeric regions cause replication stress. Studies reveal that these factors recruit condensin II to form a complex in the pericentromeric chromatin, thus regulating replication fidelity and cell ploidy (Coschi et al., 2014). This agrees with an increase in the γ H2A.X marker at the pericentromeric region, accompanied by enhanced repeat instability, on depletion of condensin (Samoshkin et al., 2012). However, the precise function of condensin II and the mechanistic basis of its safeguarding function against replicative stress remains to be deciphered.

Apart from chromatin compaction, condensins also play moonlighting roles that include facilitating enhancer RNA transcription and enhancer-promoter looping in condensin-bound ER α (Estrogen Receptor α)-sensitive enhancers in breast cancers by recruiting p300 and RIP140 (Li et al., 2015). Immunoprecipitation of condensins followed by mass spectroscopy or Rapid immunoprecipitation mass spectrometry of endogenous proteins (RIME) during dynamic processes such as cell transformation may reveal other non-canonical functions (Mohammed et al., 2016). Considering the limited number of therapeutic approaches available to combat triple-negative breast cancers (TNBC), it is encouraging that the knockdown of condensin I complex protein NCAPD2 curtailed cell proliferation and invasion. These lines of evidence implicate NCAPD2 expression as a prognostic marker of TNBC patients suggesting a potential therapeutic candidate (Zhang Y et al., 2020). An in-depth biochemical and molecular characterization assumes significance as condensins emerge as potential therapeutic targets for human cancers (Wang et al., 2018).

4 Impact of non-canonical histones and oncohistones on chromatin organization in cancers

Non-canonical histone variants occasionally replace canonical histones in the genome, often serving two main purposes. First, histone variants are dynamically incorporated throughout the interphase with the regular nucleosomal turnover of canonical histones to sustain nucleosomal stability. Secondly, additional regulatory domains, interactors, and PTMs in non-canonical histones offer supplementary mechanisms for the control of epigenetic regulation. Since cancers are characterized by large-scale remodeling of their epigenetic landscape, canonical histones in cancers are occasionally interchanged with histone variants (Vardabasso et al., 2015). Structurally, histones are composed of amino- and carboxy-terminal tails and a globular histone fold domain (HFD). Specific mutations in histone genes tend to confer oncogenic

properties to cells, and these mutant histones are referred to as oncohistones (Mohammad and Helin, 2017). Mutations occur both in the tail and globular domains, with different consequences. While tail domain mutants cause a global loss of both active and inactive histone marks, the globular domain destabilizes the nucleosome. Here, we review the functional diversity and regulatory mechanisms involved in genome organization by some non-canonical and oncohistones while discussing the scope for further research in the field.

4.1 H3 variants

The histone variant H3.3 functions as a space-filling histone when canonical H3 is evicted from the nucleosome, thus maintaining nucleosomal stability (Ray-Gallet et al., 2011). The incorporation of histone H3.3 facilitates the enrichment of active marks on chromatin associated with dynamic histone turnovers, such as transcriptionally active promoters and enhancers of active genes (Lin et al., 2013; Ha et al., 2014). Contrastingly, histone H3.3 is also incorporated in repeat-rich and repressed telomeres, where H3.3 is incorporated into the nucleosomes and further methylated to H3.3K9me3. The H3.3K9me3 mark is vital for maintaining the integrity of constitutively heterochromatinized telomeres (Udugama et al., 2015). Specific chaperone complexes facilitate the incorporation of the histone H3.3 into different regions in the genome. In the euchromatin, H3.3 is incorporated by the HIRA complex (Shi et al., 2017; Yu et al., 2021; Yang et al., 2022), while DAXX/ATRX complexes incorporate H3.3 in the telomeric and pericentric heterochromatin (Goldberg et al., 2010; Lewis et al., 2010; Heaphy et al., 2011). Of note, DAXX/ATRX is mutated in classes of gliomas, sarcomas, and pancreatic neuroendocrine tumors and is involved in differential H3.3 deposition, thereby deregulating gene expression profiles (Heaphy et al., 2011; Yuen and Knoepfler, 2013; Ren et al., 2018). Deposition of the H3.3 variant in the telomeric regions might potentially contribute to the maintenance of cancer stem cells within tumors by activating embryonic stem cell dynamics and promoting alternative lengthening of telomeres (ALT) (Wong et al., 2009; Gulve et al., 2022). Moreover, the H3.3 recruiter ATRX is also localized to the nuclear periphery with the lamins, suggesting a possible interaction between H3.3, the telomere complex, and lamins, which collectively regulate telomere organization (Pennarun et al., 2021; Teng et al., 2021).

Histone composition in the nucleosome, especially the incorporation of oncohistones, affects the expression of a wide range of genes. For instance, H3/H3.3K27M tail domain mutations accelerate neural stem cell self-renewal by dysregulating neural development genes in diffuse intrinsic pontine gliomas (DIPGs) (Mohammad and Helin, 2017; Larson et al., 2019; Nacev et al., 2019). H3G34V/R and H3.3G34W/L histone tail domain mutations are found in

pediatric high-grade gliomas and giant cell tumors of the bone, respectively. Several *in vitro* and *in vivo* studies reveal that both the oncohistones, H3.3K27M and H3.3G34W/L/V/R, reduce H3K27me3 levels, resulting in the aberrant expression of Polycomb-group (PcG)-mediated heterochromatinized genes, though the results are more promising in *in vitro* systems (Mohammad and Helin, 2017). H3.3K27M tumors have enhanced expression of genes associated with neural development, where H3K27me3 loss released bivalent promoters from their poised state (Larson et al., 2019). Likewise, the H3.3K36M mutation, found in 90% of chondroblastomas, shows a parallel trend of decreasing H3K36 di- and tri-methylation, PTMs involved in RNA polymerase elongation (Jha and Strahl, 2014; Fang et al., 2016; Sahu and Lu, 2022). A possible mechanism is reducing methylation levels by the selective sequestration of histone methyltransferases, NSD2, SETD2, and PRC2, creating a dominant negative effect (Figure 4D). Intriguingly, these oncohistones affect multiple histone marks. For instance, the H3.3K36M mutation, despite decreasing H3K36 methylation, increases the deposition of H3K27me3 marks. This leads to the mobilization of the polycomb repressor complex 1 (PRC1) away from its target sites, resulting in aberrations of PcG-regulated heterochromatin and an altered epigenetic profile (Bjerke et al., 2013; Chan et al., 2013; Lu et al., 2016). It remains an open question as to why the tail domain mutants of H3.3 are spatially confined in a hindbrain tissue-specific manner. Surprisingly, the H3.3K27M mutant promotes CIN and induces NHEJ-mediated DNA damage response through the DNA end-processing enzyme Polynucleotide Kinase 3'-Phosphatase (PNKP) (Rondinelli et al., 2022). The rationale underlying the deposition of H3.3 mutants on stalled forks despite the presence of other canonical histones remains unclear. Although oncohistones function as discrete entities, the mechanistic basis underlying their potential regulatory crosstalk would be a tantalizing finding to unravel.

4.2 H2A and H2B variants

All histones exist as multiple variants that modulate gene expression, barring histone H4, which has only one variant. Histone H2A and H2B cumulatively have 15 non-canonical histone variants, out of which 11 are H2A variants—H2A.X, H2A.Z.1, H2A.Z.2.1, H2A.Z.2.2, H2A.Bbd, H2A.J, H2A.B, TH2A, H2A.P, macroH2A.1.1, macroH2A.2, and macroH2A1.2, and four are H2B variants—H2BE, H2B.S.M, TH2B, and H2B.W (Oberdoerffer and Miller, 2022), which are often dysregulated in cancers (Figure 4A). γ H2A.X, a histone H2A subclass phosphorylated at S139, functions as a molecular beacon that detects DNA damage in the genome (Mah et al., 2010). Of note, the lack of H2A.X causes lethality in mice exposed to γ -irradiation, establishing its importance in

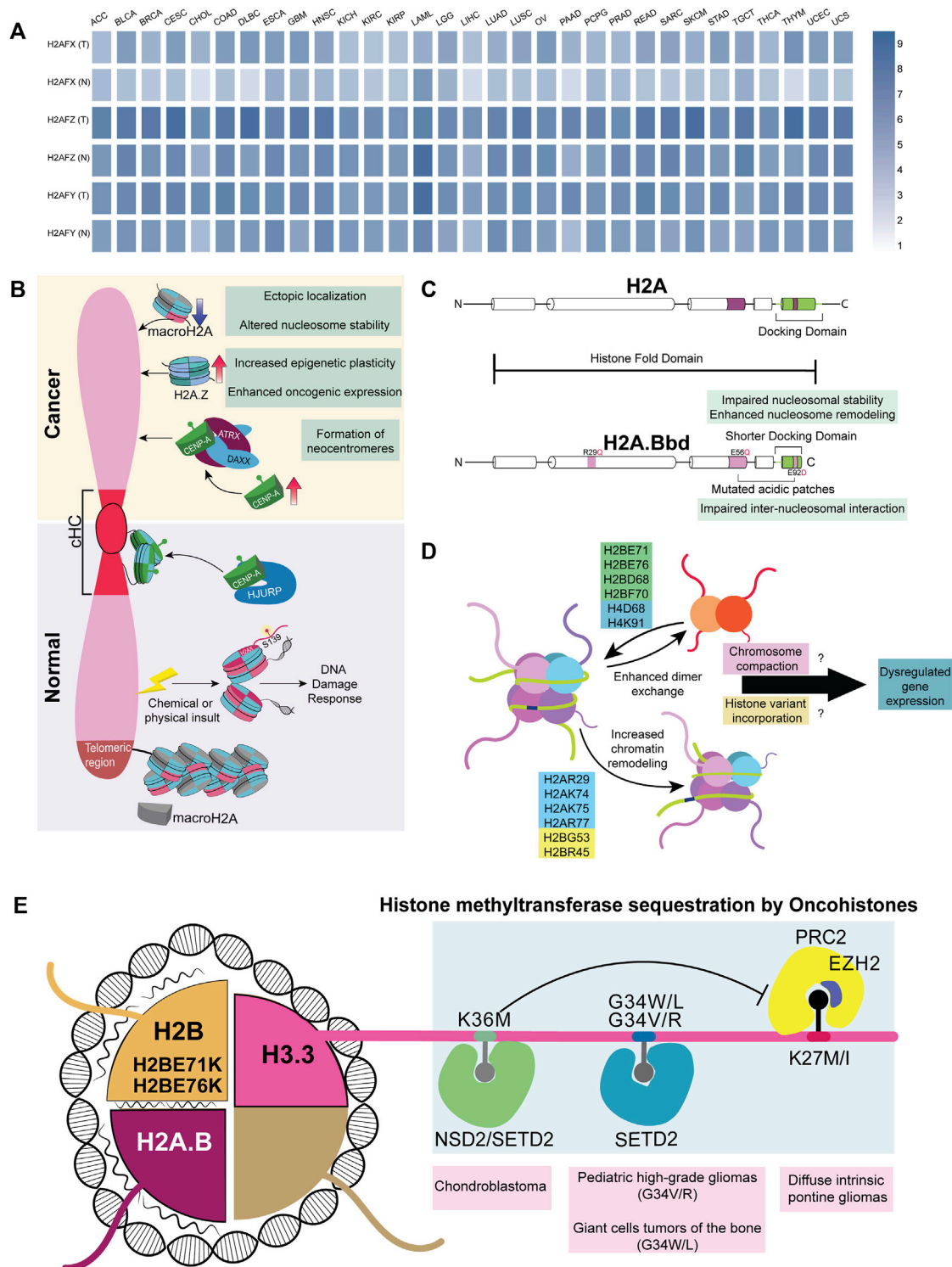


FIGURE 4

Histone variants and mutants in cancer (A) A heatmap representing various non-canonical histones across 31 different cancers; data curated from GEPIA2. Genes H2AFX, H2AFZ, and H2AFY code for H2A.X, H2A.Z.1, and macroH2A, respectively (B) Difference in the recruitment of non-canonical histones in normal versus cancer cells. cHC—Constitutive heterochromatin (C) Comparison between canonical H2A and non-canonical histone H2A.B (D) Mutations in the globular domain of core histones (H2B, H2A, and H4) to enhance dimer exchange and chromatin remodeling. This further dysregulates the expression of genes involved in differentiation (E) Oncohistones, mutations in the tail and globular domains are found in different cancers. Tail domain mutations sequester histone methyltransferases, while globular domain mutants destabilize the nucleosome, altering the expression of various genes.

maintaining genome stability (Celeste et al., 2002). Surprisingly, H2A.X is also involved in sustaining the self-renewal capacity of pluripotent stem cells (Turinetto et al., 2012). We speculate an H2A.X-dependent mechanism involved in the sustenance and regulation of cancer stem cells (Kim et al., 2012). As the guardian of the genome, the significance of H2A.X in facilitating metastasis was demonstrated when the knockdown of H2A.X induced EMT through the upregulation of transcription factors Twist1, ZEB, and SLUG (mesenchymal markers) in HCT116 colorectal cancer and MCF10A non-tumorigenic breast epithelial cell lines (Weyemi et al., 2016). This strongly suggests alternate functions of H2A.X in various aspects of gene regulation in addition to its role in the DNA damage response machinery.

Both H2A.Z and H3.3 maintain an open conformation of chromatin in nucleosome-depleted regions of the promoter for transcription factors to interact with gene promoters resulting in their transcriptional upregulation (Jin et al., 2009). Consistent with the requirement to transcribe genes, H2A.Z facilitates access to transcribing genomic regions by destabilizing the nucleosome, which is important in regulating stem-cell renewal and differentiation (Buschbeck and Hake, 2017). In cancers, canonical H2A is often replaced by its non-canonical variants H2A.Z.1.1 and H2A.Z.2. Remarkably, these isoforms are upregulated and positively correlate with resistance to chemotherapy in malignant stages of melanoma and pancreatic ductal adenocarcinoma (Vardabasso et al., 2015; Ávila-López et al., 2021). Furthermore, overexpression of H2A.Z correlates with poor prognosis in estrogen receptor-positive breast cancer (Hua et al., 2008). The non-canonical histone variant, macroH2A (mH2A), has a macro-domain and is involved in the inactivation of the X chromosome in mammals (Chadwick et al., 2001). In contrast to other histones, mH2A has a stabilizing effect on the nucleosome and can mediate both gene activation and repression. Notably, the depletion of mH2A dysregulates gene expression in at least nine cancers (Zink and Hake, 2016). However, the recruitment mechanism of mH2A is yet to be completely elucidated.

H2A.Bbd, a member of the short H2A family, is a testis and brain-specific histone variant overexpressed predominantly in Diffuse Large B-cell Lymphomas (DLBCLs) (Chew et al., 2021). Interestingly, H2A.B harbors multiple H2A mutations in its sequence. These include R29Q (DNA binding site mutant) and E92L (acidic-patch mutant) (Figure 4C). Furthermore, H2A.B's truncated C-terminal tail compromises its nucleosomal compaction and, if expressed ectopically, might cause dysregulated gene regulation (González-Romero et al., 2008; Bagert et al., 2021; Chew et al., 2021; Kohestani and Wereszczynski, 2021). From a vantage point, wild-type H2A.B has already evolved into an oncohistone with the ability to promote nucleosomal instability (Bagert et al., 2021). H2B, another histone H2 variant, has the highest number of

nucleosome-destabilizing mutations in the globular domain at E71 and E76 (Nacev et al., 2019; Bagert et al., 2021).

Essentially, tail-domain mutants are well-characterized, but not limited to, H3.3. The same is true for globular domain mutations, which are better documented for histone H2 (Nacev et al., 2019). Mutation data shows that 80% of the most frequent mutations in histones occur in their globular domain (Nacev et al., 2019). Many of these mutations in the globular domain enhance chromatin remodeling and histone dimer exchange, which correlates with the altered expression of genes involved in differentiation across patients with different cancers (Bagert et al., 2021). However, the mechanism and contribution of these mutations to cancers remain largely uncharacterized. We surmise that mutations in the globular domain of histones induce nucleosomal instability, which affects chromatin compaction both during mitosis and interphase. Moreover, histones bearing mutations in their globular domains mutant histones can increase the chances of incorporating histone variants, potentially altering gene expression. The temporal preference for the incorporation of histones, both dependent on and independent of replication, adds an additional layer of complexity (Figure 4E). Interestingly, 47% of the missense mutations in histones H2A, H2B, H3, and H4 show a conversion of glutamic acid residues to lysine or glutamine (Nacev et al., 2019), suggestive of 1) altered DNA-histone interactions 2) aberrations in PTM patterns of histones owing to an increase in the number of lysine and glutamine residues. Such a contribution of novel histone PTMs to carcinogenesis remains to be elucidated.

4.3 CENP-A

Apart from the role of histones in regulating transcription, histones are essential for modulating DNA damage response, genome organization, and chromosome maintenance. CENP-A, a centromere-specific H3 variant, is necessary and sufficient to ensure the structural and functional organization of the centromere. Heterochromatinization at the centromere is achieved by recruiting RNAi-based DICER machinery and SUV methyltransferases (Peters et al., 2003; Folco et al., 2008). Moreover, heterochromatic regions are associated with the nuclear envelope components, contributing to an additional layer of regulation (Towbin et al., 2012; Solovei et al., 2013; Ebrahimi et al., 2018; Iglesias et al., 2020). For instance, LBR and B-type lamins are involved in the organization of the pericentric heterochromatin in the interphase nucleus (Shimi et al., 2008; Dechat et al., 2010; Lukášová et al., 2018). Centromeres and telomeres are enriched in constitutive heterochromatin marks that frequently localize to the LADs in the genome (Haaf and Schmid, 1991; Weierich et al., 2003; Raz et al., 2008; Bloom, 2014), with a subset of heterochromatic domains clustering

around nucleoli as perinucleolar heterochromatin (Alcobia et al., 2000; Gdula et al., 2013).

The two fundamental functions of CENP-A include 1) centromere formation and maintenance and 2) nucleation of checkpoint assembly proteins involved in chromosomal segregation. The organization of the centromere is dynamic during the various cell cycle stages, contributing to chromatin reorganization. During the early G1 phase, CENP-A molecules form a rosette-like structure nucleated by HJURP, facilitating a 3D ring-like organization during the G1 phase (Figure 4B). During mitosis, this structure is reoriented to form a rod-like pattern (Andronov et al., 2019). Elevated levels of CENP-A form neo-centromeres due to its mislocalization along the chromosomal arms, resulting in the misorientation of microtubule fibers on the kinetochore. This leads to the abnormal segregation of chromosomes, resulting in chromosomal translocations and breakage (Barnhart et al., 2011; Sun et al., 2016). It is now established that CENP-A is recruited to DNA double-strand breaks, and its depletion leads to an impaired DDR (Zeitlin et al., 2009; Lawrence et al., 2015; Stirpe and Heun, 2022). This highlights that CENP-A is recruited to sites other than the centromeric regions, although the exact role of CENP-A in DDR remains to be characterized. The ectopic overexpression of CENP-A increases the tolerance limit to DNA insults and enhances chemoresistance (Lacoste et al., 2014). The mechanism of CENP-A recruitment to DNA breakage sites and the consequent molecular signals required for its residence and dislodgement remains to be elucidated.

5 Chromatin organization during senescence

Cellular senescence is a state of dormancy where the cell ceases to divide. Senescence involves shortened telomeres, increased DNA damage, stalled replication, nuclear deformities, mitochondrial dysfunction, and aberrant genome organization (Di Micco et al., 2021). After a somatic cell crosses the Hayflick limit, it reaches replicative senescence because of the end replication problem, i.e., progressive shortening of telomeres with each division cycle due to the inherent inability of DNA polymerases to correctly replicate the cytosine-rich telomere lagging-strand (Hayflick and Moorhead, 1961; Harley et al., 1990). Interestingly, this limit is often bypassed by neoplastic cells, making them immortal (Autexier and Greider, 1996). As aging progresses, the DDR machinery is compromised, predominantly increasing the predisposition to breast, prostate, lung, and colon cancers (Rossi et al., 2007; de Magalhães, 2013). Normally, these functions are tightly regulated, and the activation of oncogenes leads to aberrant replication fork progression, resulting in Oncogene-Induced Senescence (OIS) (Serrano et al., 1997; Di Micco et al., 2006; Rocha et al., 2022). It is noteworthy that cancer cells often evade

OIS by altering cellular levels of p16^{INK4A}, a cell cycle blocker (McLaughlin-Drubin et al., 2013).

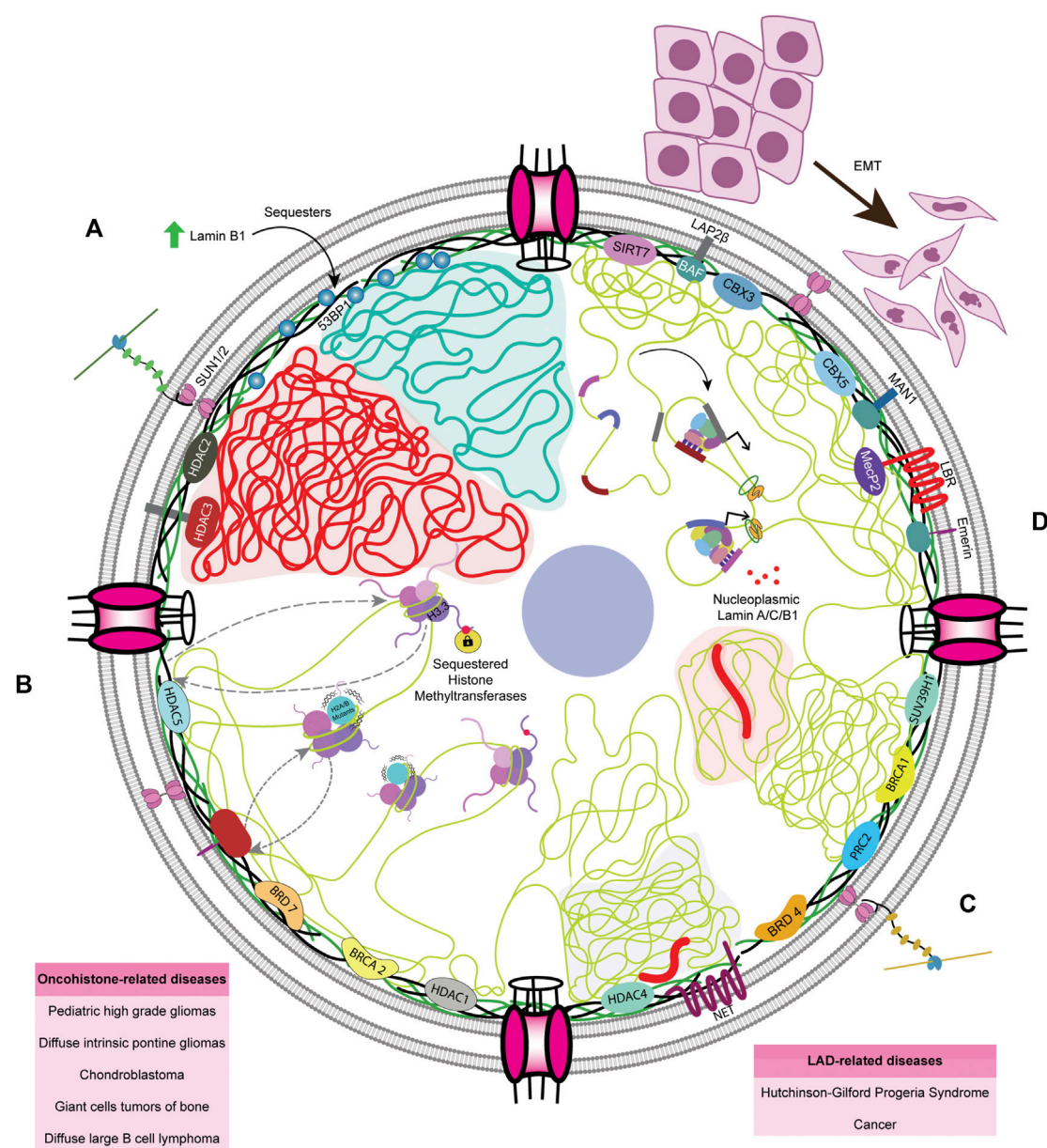
Remarkably, extensive topological changes in chromatin compartmentalization accompany senescence, obfuscating the spatial separation between the A and B compartments. Microscopy and polymer modeling of chromatin reveals that the spatial organization of chromatin compartments is drastically altered in tumor cells. Following this finding, an additional intermediate Compartment I has been proposed that interacts with both A and B compartments in normal tissue and inclines toward the B compartment in cancerous tissue (Johnstone et al., 2020). Cells undergoing OIS show dramatic changes in chromatin architecture, with the formation of Senescence Associated Heterochromatin Foci (SAHF), characteristically enriched with facultative heterochromatic marks such as H3K9me1/2, H3K20me3, along with high-mobility group proteins and non-canonical histones such as mH2A (Narita et al., 2003; Zhang et al., 2007; Nelson et al., 2016). Chromatin polymer modeling suggests that SAHF can mobilize specific loci adjacent to heterochromatic domains in close proximity to each other in the 3D space of the nucleus, enhancing their activity in cell adhesion and cancer-related signaling (Sati et al., 2020). Alongside activating specific genes, the SAHF also affects cell proliferation by epigenetically repressing E2F target genes through the recruitment of pRB and heterochromatin factors (Narita et al., 2003). Moreover, SAHFs are not found in cells going through quiescence (Aird and Zhang, 2013). In agreement with this, the silencing of E2F-responsive elements and the formation of SAHF are characteristic of only irreversibly arrested cells, thus hinting towards an Rb-mediated mechanism for stabilizing the senescent phenotype.

The induction of senescence in cancer cells serves as a traditional therapeutic approach by targeting p53, mTOR, PI3K, and BCL-2 family proteins using senolytic agents (Lee et al., 2010; Muñoz-Espín et al., 2013; Laberge et al., 2015). However, challenges in targeting cancer cells are contributed to by tumor heterogeneity since aged patients have higher numbers of senescent cells, which can lead to fatal off-target effects by senolytic agents (Wang L et al., 2022).

6 Perspectives

6.1 Effect of lamin mutations on genome organization during cancer progression and senescence

The LADs are parts of chromatin domains that are largely in a state of repression. Surprisingly, the simultaneous loss of all lamin forms in mouse embryonic stem cells did not change the overall TAD structure but reorganized the inter- and intra-TAD interactions, further altering transcriptional

**FIGURE 5**

Lacunae in the field of genome organization and nuclear envelope (A) Lamin B1 is upregulated in most cancers, as per TCGA data, and overexpression of Lamin B1 expression sequesters 53BP1, a major orchestrator of NHEJ pathway. The precise mechanisms as to how cancer cells overcome 53BP1 sequestration is unknown (B) Incorporation of both tail and globular domain mutants leads to dysregulated gene expression through various mechanisms, though it remains unclear whether nuclear lamina has any role in either mitigating or worsening it. Globular domain mutations, when associated with the LADs, could be altering the spatial localization of gene loci. (C) The nuclear envelope maintains heterochromatin. LADs form a significant portion of the human genome and are regulated by the lamina and its associated complexes, the deregulation of which often leads to HGPS and cancer (D) Furthermore, in EMT and cancer progression, phosphorylated lamin A/C and B1 are associated with enhancer sequences, but the role of this association remains to be elucidated.

output (Zheng et al., 2018). It is interesting to note that although lamins are known to organize heterochromatin proximal to the nuclear border, they also modulate the organization of transcriptionally-active euchromatin within

the nuclear interior (Pascual-Reguant et al., 2018; Ikegami et al., 2020).

Ovarian cancers harbor homozygous deletion in the LMNB1 gene, while the loss of lamin A/C leads to poor

prognosis and enhanced metastatic potential of cells (Capo-chichi et al., 2011). In the context of senescence, lamin A/C directly interacts with the telomeric protein TRF2, which facilitates the insertion of 3' overhangs into telomeric DNA, resulting in T-loop formation that protects the telomere ends and slows cellular senescence in a cell-type specific manner. Mutations in LMNA, like those found in Hutchinson-Gilford progeria syndrome (HGPS), destabilize lamin A/C-TRF2 interaction, further leading to telomere loss and accelerated cellular aging (Wood et al., 2014).

Additionally, TCGA data retrieved from GEPIA2 shows that most of the cancers show upregulated levels of lamin B1. It is known that lamin B1 overexpression sequesters 53BP1, a crucial mediator of the NHEJ pathway (Etourneau et al., 2021). It remains to be elucidated how a majority of the cancers overexpressing lamin B1 manage to steer the DDR to specific NHEJ pathways (Bouwman et al., 2010) (Figure 5A). Furthermore, lamins repress the activation of mobile transposable elements that trigger chromosomal instability (Andrenacci et al., 2020). During the later stages of cellular aging, the association of lamin with transposable elements declines, coupled with the loss of heterochromatin, leading to aberrant gene expression and type-I interferon response (De Cecco et al., 2019; Cenni et al., 2020). The mechanisms by which chromatin organizers function in cancer cells will facilitate the design of specific small molecule inhibitors.

6.2 Interactors of LMNA during cancer progression

Lamin A regulates gene expression by interacting with various chromatin modifiers, the deregulation of which promotes cancers. For instance, lamin A directly interacts with and prevents the proteasomal degradation of SUV39H1, the writer of the H3K9me3 inactive mark (Liu et al., 2013), the dysregulation of which results in HGPS (Figure 5C). Correspondingly, the PcG proteins that deposit the H3K27me3 inactive mark interact with lamins (Cesarini et al., 2015; Marullo et al., 2016). Notably, lamin loss leads to an anomalous distribution of PcG proteins, eventually resulting in dysregulated gene expression and accelerated cancer progression. HDAC2 also plays an active role in heterochromatinization by interacting with LMNA at the nuclear periphery (Mattioli et al., 2018; Santi et al., 2020; Murray-Nerger and Cristea, 2021). However, the molecular mechanisms involving lamin-mediated regulation of inactive H3K9me3 and H3K27me3 and active H3K4me3 marks are yet to be uncovered.

In cancers, chromatin organizers harbor mutations in various domains, resulting in their deregulated activity and altered binding to chromatin or lamins. For instance, sarcomas harbor high-frequency H3.3G34R and H3.3K36M mutations

that directly prevent the binding of H3K36me2/3 writer NSD1/2, thus reducing PRC2-H3K36me2 interaction and increasing H3K27me3 levels (Lu et al., 2016). The interaction between SMARCB1 and NSD1 is essential for the deposition of H3K36me2 in the genome, which is a marker for better prognosis in sarcoma. Mutated SMARCB1 is unable to bind to NSD1 but binds to PRC2, leading to an increase in H3K27me3 with poor prognosis in cancer patients (Drosos et al., 2022). Such atypical deposition of inactive histone marks dilutes their occupancy in normally-repressed genes, reorienting the genomic regions localized to the nuclear periphery. As a result, genes typically localized to the nuclear periphery, such as the mesenchymal progenitor genes in the facultative LADs, become de-repressed (Lu et al., 2016). Hence, we surmise a potential crosstalk between the nuclear lamins, chromatin regulators, and oncohistones in the initiation and sustenance of cancer progression.

6.3 Crosstalk between the nuclear envelope and oncohistones

The nuclear lamina is primarily associated with inactive histone marks at the nuclear periphery. However, lamins also modulate active euchromatin (Zheng et al., 2018). How the peripheral and nucleoplasmic pools of lamins engage in chromatin dynamics and impinge on the transcriptional regulation mediated by oncohistones such as H3.3K27M/I, H3.3G34W/V/L/R, H3.3K36M, or H2A is unclear (Figure 5B). In addition, components of the nuclear envelope, namely Nups and LINC complex factors, also participate in chromatin organization. Moreover, lamins are required for chromatin organization, although their potential role in the incorporation of oncohistones by chaperones remains unclear (Figure 5B). The extent of lamin A/C phosphorylation correlates with lamin A/C levels in the DU145 prostate cancer cell line, though this remains to be verified experimentally across cancers (Kong et al., 2012). Phosphorylated lamin A/C and unphosphorylated, probably nucleoplasmic lamin B1, associate with active enhancers and transcribing genes, respectively, which contradicts the conventional function of LADs in gene repression (Guelen et al., 2008; Ikegami et al., 2020). However, the exact role of phosphorylated Lamin A/C in modulating enhancer regions remains an enigma. In addition, the association of lamin B1 with eLADs and higher expression of fibronectin, vimentin, and twist highlight the role of lamin B1 in metastasis (Pascual-Reguant et al., 2018), although its exact purpose of lamin B1 in compartment A remains to be elucidated (Figure 5D). Interestingly, lamin B1 has been shown to localize to the TAD borders of eLADs, opening the possibility of its interaction with border elements such as CTCF and cohesin.

7 Conclusion

In summary, it is beyond any doubt that genetic mutations, aberrations in chromatin organization, incorporation of oncohistones, deregulated transcription, and defects in nuclear envelope organization and function collectively deregulate the cellular and molecular processes of cancers. Novel therapeutic targets will be identified by leveraging high-resolution single-cell approaches, such as sc-ChIP-seq, sc-ATAC-seq, and sc-Hi-C, with high-content imaging, including high-resolution FISH. Furthermore, molecular and biochemical assays remain the mainstay for the elucidation of molecular mechanisms. Collectively, these lines of evidence reveal that aberrant genome architecture serves as a precursor and promoter of cancer initiation and progression.

Author contributions

AKB, SS, SD, DP, and KS wrote the manuscript. SS, SD, and DP prepared the illustrations.

References

- Adane, B., Alexe, G., Seong, B. K. A., Lu, D., Hwang, E. E., Hnisz, D., et al. (2021). STAG2 loss rewires oncogenic and developmental programs to promote metastasis in Ewing sarcoma. *Cancer Cell* 39, 827–844. e10. doi:10.1016/j.ccell.2021.05.007
- Aebi, U., Cohn, J., Buhle, L., and Gerace, L. (1986). The nuclear lamina is a meshwork of intermediate-type filaments. *Nature* 323, 560–564. doi:10.1038/323560a0
- Aird, K. M., and Zhang, R. (2013). Detection of senescence-associated heterochromatin foci (SAHF). *Methods Mol. Biol.* 965, 185–196. doi:10.1007/978-1-62703-239-1_12
- Akdemir, K. C., Le, V. T., Chandran, S., Li, Y., Verhaak, R. G., Beroukhim, R., et al. (2020). PCAWG Structural Variation Working Group, PCAWG Consortium Disruption of chromatin folding domains by somatic genomic rearrangements in human cancer. *Nat. Genet.* 52, 294–305. doi:10.1038/s41588-019-0564-y
- Alcobia, I., Dilão, R., and Parreira, L. (2000). Spatial associations of centromeres in the nuclei of hematopoietic cells: Evidence for cell-type-specific organizational patterns. *Blood* 95, 1608–1615. doi:10.1182/blood.V95.5.1608.005k32_1608_1615
- Amankwaa, B., Schoborg, T., and Labrador, M. (2022). α -tubulin and β -tubulin: Insulator proteins exhibit *in vivo* liquid-liquid phase separation properties. *Life Sci. Alliance* 5, e202201536. doi:10.26508/lsa.202201536
- Amin, R., Shukla, A., Zhu, J. J., Kim, S., Wang, P., Tian, S. Z., et al. (2021). Nuclear pore protein NUP210 depletion suppresses metastasis through heterochromatin-mediated disruption of tumor cell mechanical response. *Nat. Commun.* 12, 7216. doi:10.1038/s41467-021-27451-w
- Andrenacci, D., Cavaliere, V., and Lattanzi, G. (2020). The role of transposable elements activity in aging and their possible involvement in laminopathies diseases. *Ageing Res. Rev.* 57, 100995. doi:10.1016/j.arr.2019.100995
- Andronov, L., Ouararhni, K., Stoll, L., Klaholz, B. P., and Hamiche, A. (2019). CENP-A nucleosome clusters form rosette-like structures around HJURP during G1. *Nat. Commun.* 10, 4436. doi:10.1038/s41467-019-12383-3
- Antony, J., Chin, C. V., and Horsfield, J. A. (2021). Cohesin mutations in cancer: Emerging therapeutic targets. *Int. J. Mol. Sci.* 22, 6788. doi:10.3390/ijms22136788
- Autexier, C., and Greider, C. W. (1996). Telomerase and cancer: Revisiting the telomere hypothesis. *Trends Biochem. Sci.* 21, 387–391. doi:10.1016/S0968-0004(96)10042-6
- Ávila-López, P. A., Guerrero, G., Nuñez-Martínez, H. N., Peralta-Alvarez, C. A., Hernández-Montes, G., Álvarez-Hilario, L. G., et al. (2021). H2A.Z overexpression suppresses senescence and chemosensitivity in pancreatic ductal adenocarcinoma. *Oncogene* 40, 2065–2080. doi:10.1038/s41388-021-01664-1
- Baergen, A. K., Jeusset, L. M., Lichtensztejn, Z., and McManus, K. J. (2019). Diminished condensin gene expression drives chromosome instability that may contribute to colorectal cancer pathogenesis. *Cancers (Basel)* 11, 1066. doi:10.3390/cancers11081066
- Bagert, J. D., Mitchener, M. M., Patriotis, A. L., Dul, B. E., Wojcik, F., Nacev, B. A., et al. (2021). Oncohistone mutations enhance chromatin remodeling and alter cell fates. *Nat. Chem. Biol.* 17, 403–411. doi:10.1038/s41589-021-00738-1
- Bailey, C. G., Gupta, S., Mettler, C., Amarasekera, P. M. S., O'Young, P., Kyaw, W., et al. (2021). Structure-function relationships explain CTCF zinc finger mutation phenotypes in cancer. *Cell. Mol. Life Sci.* 78, 7519–7536. doi:10.1007/s00018-021-03946-z
- Bakhoum, S. F., Ngo, B., Laughney, A. M., Cavallo, J.-A., Murphy, C. J., Ly, P., et al. (2018). Chromosomal instability drives metastasis through a cytosolic DNA response. *Nature* 553, 467–472. doi:10.1038/nature25432
- Barnhart, M. C., Kuich, P. H. J. L., Stellfox, M. E., Ward, J. A., Bassett, E. A., Black, B. E., et al. (2011). HJURP is a CENP-A chromatin assembly factor sufficient to form a functional de novo kinetochore. *J. Cell Biol.* 194, 229–243. doi:10.1083/jcb.201012017
- Barrington, C., Georgopoulou, D., Pezic, D., Varsally, W., Herrero, J., and Hadjir, S. (2019). Enhancer accessibility and CTCF occupancy underlie asymmetric TAD architecture and cell type specific genome topology. *Nat. Commun.* 10, 2908. doi:10.1038/s41467-019-10725-9
- Baumann, K. (2016). Nuclear organization: NUP-Tial binding to super-enhancers. *Nat. Rev. Mol. Cell Biol.* 17, 738–739. doi:10.1038/nrm.2016.158
- Bell, E. S., Shah, P., Zuela-Sopilniak, N., Kim, D., Varlet, A.-A., Morival, J. L. P., et al. (2022). Low lamin A levels enhance confined cell migration and metastatic capacity in breast cancer. *Oncogene* 41, 4211–4230. doi:10.1038/s41388-022-02420-9
- Benhra, N., Barrio, L., Muzzopappa, M., and Milán, M. (2018). Chromosomal instability induces cellular invasion in epithelial tissues. *Dev. Cell* 47, 161–174. doi:10.1016/j.devcel.2018.08.021
- Bianchi, A., Mozzetta, C., Pegoli, G., Lucini, F., Valsoni, S., Rosti, V., et al. (2020). Dysfunctional polycomb transcriptional repression contributes to lamin A/C-dependent muscular dystrophy. *J. Clin. Invest.* 130, 2408–2421. doi:10.1172/JCI128161
- Bjerke, L., Mackay, A., Nandhabalan, M., Burford, A., Jury, A., Popov, S., et al. (2013). Histone H3.3. mutations drive pediatric glioblastoma through upregulation of MYCN. *Cancer Discov.* 3, 512–519. doi:10.1158/2159-8290.CD-12-0426

Funding

We gratefully acknowledge support from Science & Engineering Board (SERB), Grant#CRG/2020/002563 and intramural funding support from IISER-Pune.

Conflict of interest

The authors declare that the research was conducted in the absence of any commercial or financial relationships that could be construed as a potential conflict of interest.

Publisher's note

All claims expressed in this article are solely those of the authors and do not necessarily represent those of their affiliated organizations, or those of the publisher, the editors and the reviewers. Any product that may be evaluated in this article, or claim that may be made by its manufacturer, is not guaranteed or endorsed by the publisher.

- Bloom, K. S. (2014). Centromeric heterochromatin: The primordial segregation machine. *Annu. Rev. Genet.* 48, 457–484. doi:10.1146/annurev-genet-120213-092033
- Bockaj, I., Martini, T. E. I., de Camargo Magalhães, E. S., Bakker, P. L., Meeuwse-de Boer, T. G. J., Armandari, I., et al. (2021). The H3.3K27M oncohistone affects replication stress outcome and provokes genomic instability in pediatric glioma. *PLoS Genet.* 17, e1009868. doi:10.1371/journal.pgen.1009868
- Bönisch, C., Schneider, K., Pünzeler, S., Wiedemann, S. M., Bielmeier, C., Bocola, M., et al. (2012). H2A.Z.2.2 is an alternatively spliced histone H2A.Z variant that causes severe nucleosome destabilization. *Nucleic Acids Res.* 40, 5951–5964. doi:10.1093/nar/gks267
- Bouwman, P., Aly, A., Escandell, J. M., Pieterse, M., Bartkova, J., van der Gulden, H., et al. (2010). 53BP1 loss rescues BRCA1 deficiency and is associated with triple-negative and BRCA-mutated breast cancers. *Nat. Struct. Mol. Biol.* 17, 688–695. doi:10.1038/nsmb.1831
- Bronstein, I., Kepten, E., Kanter, I., Berezin, S., Lindner, M., Redwood, A. B., et al. (2015). Loss of lamin A function increases chromatin dynamics in the nuclear interior. *Nat. Commun.* 6, 8044. doi:10.1038/ncomms9044
- Buschbeck, M., and Hake, S. B. (2017). Variants of core histones and their roles in cell fate decisions, development and cancer. *Nat. Rev. Mol. Cell Biol.* 18, 299–314. doi:10.1038/nrm.2016.166
- Capo-chichi, C. D., Cai, K. Q., Simpkins, F., Ganjei-Azar, P., Godwin, A. K., and Xu, X.-X. (2011). Nuclear envelope structural defects cause chromosomal numerical instability and aneuploidy in ovarian cancer. *BMC Med.* 9, 28. doi:10.1186/1741-7015-9-28
- Capo-Chichi, C. D., Yeasky, T. M., Smith, E. R., and Xu, X.-X. (2016). Nuclear envelope structural defect underlies the main cause of aneuploidy in ovarian carcinogenesis. *BMC Cell Biol.* 17, 37. doi:10.1186/s12860-016-0114-8
- Celeste, A., Petersen, S., Romanienko, P. J., Fernandez-Capetillo, O., Chen, H. T., Sedelnikova, O. A., et al. (2002). Genomic instability in mice lacking histone H2AX. *Science* 296, 922–927. doi:10.1126/science.1069398
- Cenni, V., Capanni, C., Mattioli, E., Schena, E., Squarzone, S., Bacalini, M. G., et al. (2020). Lamin A involvement in ageing processes. *Ageing Res. Rev.* 62, 101073. doi:10.1016/j.arr.2020.101073
- Cerami, E., Gao, J., Dogrusoz, U., Gross, B. E., Sumer, S. O., Aksoy, B. A., et al. (2012). The cBio cancer genomics portal: An open platform for exploring multidimensional cancer genomics data. *Cancer Discov.* 2, 401–404. doi:10.1158/2159-8290.CD-12-0095
- Cesarini, E., Mozzetta, C., Marullo, F., Gregoret, F., Gargiulo, A., Columbaro, M., et al. (2015). Lamin A/C sustains PcG protein architecture, maintaining transcriptional repression at target genes. *J. Cell Biol.* 211, 533–551. doi:10.1083/jcb.201504035
- Chadwick, B. P., Valley, C. M., and Willard, H. F. (2001). Histone variant macroH2A contains two distinct macrochromatin domains capable of directing macroH2A to the inactive X chromosome. *Nucleic Acids Res.* 29, 2699–2705. doi:10.1093/nar/29.13.2699
- Chan, K.-M., Fang, D., Gan, H., Hashizume, R., Yu, C., Schroeder, M., et al. (2013). The histone H3.3K27M mutation in pediatric glioma reprograms H3K27 methylation and gene expression. *Genes Dev.* 27, 985–990. doi:10.1101/gad.217778.113
- Chen, G. K., Chang, X., Curtis, C., and Wang, K. (2013). Precise inference of copy number alterations in tumor samples from SNP arrays. *Bioinformatics* 29, 2964–2970. doi:10.1093/bioinformatics/btt521
- Chen, H., Tian, Y., Shu, W., Bo, X., and Wang, S. (2012). Comprehensive identification and annotation of cell type-specific and ubiquitous CTCF-binding sites in the human genome. *PLoS ONE* 7, e41374. doi:10.1371/journal.pone.0041374
- Chetverina, D., Fujioka, M., Erokhin, M., Georgiev, P., Jaynes, J. B., and Schedl, P. (2017). Boundaries of loop domains (insulators): Determinants of chromosome form and function in multicellular eukaryotes. *BioEssays* 39 (3), 1600233. doi:10.1002/bies.201600233
- Chew, G.-L., Bleakley, M., Bradley, R. K., Malik, H. S., Henikoff, S., Molaro, A., et al. (2021). Short H2A histone variants are expressed in cancer. *Nat. Commun.* 12, 490. doi:10.1038/s41467-020-20707-x
- Cohen, S., Etingov, I., and Panté, N. (2012). Effect of viral infection on the nuclear envelope and nuclear pore complex. *Int. Rev. Cell Mol. Biol.* 299, 117–159. doi:10.1016/B978-0-12-394310-1.00003-5
- Coschi, C. H., Ishak, C. A., Gallo, D., Marshall, A., Talluri, S., Wang, J., et al. (2014). Haploinsufficiency of an RB-E2F1-Condensin II complex leads to aberrant replication and aneuploidy. *Cancer Discov.* 4, 840–853. doi:10.1158/2159-8290.CD-14-0215
- Cremer, T., and Cremer, C. (2001). Chromosome territories, nuclear architecture and gene regulation in mammalian cells. *Nat. Rev. Genet.* 2, 292–301. doi:10.1038/35066075
- Cronshaw, J. M., Krutchinsky, A. N., Zhang, W., Chait, B. T., and Matunis, M. J. (2002). Proteomic analysis of the mammalian nuclear pore complex. *J. Cell Biol.* 158, 915–927. doi:10.1083/jcb.200206106
- Damaschke, N. A., Gawdzik, J., Avilla, M., Yang, B., Svaren, J., Roopra, A., et al. (2020). CTCF loss mediates unique DNA hypermethylation landscapes in human cancers. *Clin. Epigenetics* 12, 80. doi:10.1186/s13148-020-00869-7
- D'Angelo, M. A., Gomez-Cavazos, J. S., Mei, A., Lackner, D. H., and Hetzer, M. W. (2012). A change in nuclear pore complex composition regulates cell differentiation. *Dev. Cell* 22, 446–458. doi:10.1016/j.devcel.2011.11.021
- Davis, L., Rayi, P. R., Getselter, D., Kaphzan, H., and Elliott, E. (2022). CTCF in parvalbumin-expressing neurons regulates motor, anxiety and social behavior and neuronal identity. *Mol. Brain* 15, 30. doi:10.1186/s13041-022-00916-9
- De Cecco, M., Ito, T., Petrashen, A. P., Elias, A. E., Skvir, N. J., Criscione, S. W., et al. (2019). L1 drives IFN in senescent cells and promotes age-associated inflammation. *Nature* 566, 73–78. doi:10.1038/s41586-018-0784-9
- de Magalhães, J. P. (2013). How ageing processes influence cancer. *Nat. Rev. Cancer* 13, 357–365. doi:10.1038/nrc3497
- Debaugny, R. E., and Skok, J. A. (2020). CTCF and CTCFL in cancer. *Curr. Opin. Genet. Dev.* 61, 44–52. doi:10.1016/j.gde.2020.02.021
- Dechat, T., Adam, S. A., Taimen, P., Shimi, T., and Goldman, R. D. (2010). Nuclear lamins. *Cold Spring Harb. Perspect. Biol.* 2, a000547. doi:10.1101/cshperspect.a000547
- Dechat, T., Shimi, T., Adam, S. A., Rusinol, A. E., Andres, D. A., Spielmann, H. P., et al. (2007). Alterations in mitosis and cell cycle progression caused by a mutant lamin A known to accelerate human aging. *Proc. Natl. Acad. Sci. U. S. A.* 104, 4955–4960. doi:10.1073/pnas.0700854104
- Demmerle, J., Koch, A. J., and Holaska, J. M. (2012). The nuclear envelope protein emerlin binds directly to histone deacetylase 3 (HDAC3) and activates HDAC3 activity. *J. Biol. Chem.* 287, 22080–22088. doi:10.1074/jbc.M111.325308
- Di Micco, R., Fumagalli, M., Cicalese, A., Piccinin, S., Gasparini, P., Luise, C., et al. (2006). Oncogene-induced senescence is a DNA damage response triggered by DNA hyper-replication. *Nature* 444, 638–642. doi:10.1038/nature05327
- Di Micco, R., Krizhanovsky, V., Baker, D., and d'Adda di Fagagna, F. (2021). Cellular senescence in ageing: From mechanisms to therapeutic opportunities. *Nat. Rev. Mol. Cell Biol.* 22, 75–95. doi:10.1038/s41580-020-00314-w
- Dixon, J. R., Selvaraj, S., Yue, F., Kim, A., Li, Y., Shen, Y., et al. (2012). Topological domains in mammalian genomes identified by analysis of chromatin interactions. *Nature* 485, 376–380. doi:10.1038/nature11082
- Drosos, Y., Myers, J. A., Xu, B., Mathias, K. M., Beane, E. C., Radko-Juettner, S., et al. (2022). NSD1 mediates antagonism between SWI/SNF and polycomb complexes and is required for transcriptional activation upon EZH2 inhibition. *Mol. Cell* 82, 2472–2489. e8. doi:10.1016/j.molcel.2022.04.015
- Dubińska-Magiera, M., Kozioł, K., Machowska, M., Piekarczyk, K., Filipczak, D., and Rzepecki, R. (2019). Emerin is required for proper nucleus reassembly after mitosis: Implications for new pathogenetic mechanisms for laminopathies detected in EDMD1 patients. *Cells* 8, 1. doi:10.3390/cells8030240
- Earle, A. J., Kirby, T. J., Fedorchak, G. R., Isermann, P., Patel, J., Iruvanti, S., et al. (2020). Mutant lamins cause nuclear envelope rupture and DNA damage in skeletal muscle cells. *Nat. Mat.* 19, 464–473. doi:10.1038/s41563-019-0563-5
- Ebrahimi, H., Masuda, H., Jain, D., and Cooper, J. P. (2018). Distinct “safe zones” at the nuclear envelope ensure robust replication of heterochromatic chromosome regions. *eLife* 7, e32911. doi:10.7554/eLife.32911
- Eldholm, V., Haugen, A., and Zienoldin, S. (2014). CTCF mediates the TERT enhancer-promoter interactions in lung cancer cells: Identification of a novel enhancer region involved in the regulation of TERT gene. *Int. J. Cancer* 134, 2305–2313. doi:10.1002/ijc.28570
- Etourneau, L., Moussa, A., Rass, E., Genet, D., Willaume, S., Chabance-Oumura, C., et al. (2021). Lamin B1 sequesters 53BP1 to control its recruitment to DNA damage. *Sci. Adv.* 7, eabb3799. doi:10.1126/sciadv.abb3799
- Fang, D., Gan, H., Lee, J.-H., Han, J., Wang, Z., Riest, S. M., et al. (2016). The histone H3.3K36M mutation reprograms the epigenome of chondroblastomas. *Science* 352, 1344–1348. doi:10.1126/science.aae0065
- Fischer, E. G. (2020). Nuclear morphology and the biology of cancer cells. *Acta Cytol.* 64, 511–519. doi:10.1159/000508780
- Flavahan, W. A., Drier, Y., Liao, B. B., Gillespie, S. M., Venteicher, A. S., Stemmer-Rachamimov, A. O., et al. (2016). Insulator dysfunction and oncogene activation in IDH mutant gliomas. *Nature* 529, 110–114. doi:10.1038/nature16490
- Folco, H. D., Pidoux, A. L., Urano, T., and Allshire, R. C. (2008). Heterochromatin and RNAi are required to establish CENP-A chromatin at centromeres. *Science* 319, 94–97. doi:10.1126/science.1150944

- Fudenberg, G., Imakaev, M., Lu, C., Goloborodko, A., Abdennur, N., and Mirny, L. A. (2016). Formation of chromosomal domains by loop extrusion. *Cell Rep.* 15, 2038–2049. doi:10.1016/j.celrep.2016.04.085
- Gao, J., Aksoy, B. A., Dogrusoz, U., Dresdner, G., Gross, B., Sumer, S. O., et al. (2013). Integrative analysis of complex cancer genomics and clinical profiles using the cBioPortal. *Sci. Signal.* 6, pii. doi:10.1126/scisignal.2004088
- Gdula, M. R., Poterlowicz, K., Mardaryev, A. N., Sharov, A. A., Peng, Y., Fessing, M. Y., et al. (2013). Remodeling of three-dimensional organization of the nucleus during terminal keratinocyte differentiation in the epidermis. *J. Invest. Dermatol.* 133, 2191–2201. doi:10.1038/jid.2013.66
- Gimpel, P., Lee, Y. L., Sobota, R. M., Calvi, A., Koullourou, V., Patel, R., et al. (2017). Nesprin-1 α -Dependent microtubule nucleation from the nuclear envelope via Akap450 is necessary for nuclear positioning in muscle cells. *Curr. Biol.* 27, 2999–3009. doi:10.1016/j.cub.2017.08.031
- Goldberg, A. D., Banaszynski, L. A., Noh, K.-M., Lewis, P. W., Elsaesser, S. J., Stadler, S., et al. (2010). Distinct factors control histone variant H3.3 localization at specific genomic regions. *Cell* 140, 678–691. doi:10.1016/j.cell.2010.01.003
- González-Romero, R., Méndez, J., Ausió, J., and Eirín-López, J. M. (2008). Quickly evolving histones, nucleosome stability and chromatin folding: All about histone H2A.Bbd. *Gene* 413, 1–7. doi:10.1016/j.gene.2008.02.003
- Gough, S. M., Slape, C. I., and Aplan, P. D. (2011). NUP98 gene fusions and hematopoietic malignancies: Common themes and new biologic insights. *Blood* 118, 6247–6257. doi:10.1182/blood-2011-07-328880
- Gruenbaum, Y., and Foisner, R. (2015). Lamins: Nuclear intermediate filament proteins with fundamental functions in nuclear mechanics and genome regulation. *Annu. Rev. Biochem.* 84, 131–164. doi:10.1146/annurev-biochem-060614-034115
- Guelen, L., Pagie, L., Brasset, E., Meuleman, W., Faza, M. B., Talhout, W., et al. (2008). Domain organization of human chromosomes revealed by mapping of nuclear lamina interactions. *Nature* 453, 948–951. doi:10.1038/nature06947
- Gulve, N., Su, C., Deng, Z., Soldan, S. S., Vladimirova, O., Wickramasinghe, J., et al. (2022). DAXX-ATRAX regulation of p53 chromatin binding and DNA damage response. *Nat. Commun.* 13, 5033. doi:10.1038/s41467-022-32680-8
- Guo, Y. A., Chang, M. M., Huang, W., Ooi, W. F., Xing, M., Tan, P., et al. (2018). Mutation hotspots at CTCF binding sites coupled to chromosomal instability in gastrointestinal cancers. *Nat. Commun.* 9, 1520. doi:10.1038/s41467-018-03828-2
- Ha, M., Kraushaar, D. C., and Zhao, K. (2014). Genome-wide analysis of H3.3 dissociation reveals high nucleosome turnover at distal regulatory regions of embryonic stem cells. *Epigenetics Chromatin* 7, 38. doi:10.1186/1756-8935-7-38
- Haaf, T., and Schmid, M. (1991). Chromosome topology in mammalian interphase nuclei. *Exp. Cell Res.* 192, 325–332. doi:10.1016/0014-4827(91)90048-y
- Hanssen, L. L. P., Kassouf, M. T., Oudelaar, A. M., Biggs, D., Preece, C., Downes, D. J., et al. (2017). Tissue-specific CTCF-cohesin-mediated chromatin architecture delimits enhancer interactions and function *in vivo*. *Nat. Cell Biol.* 19, 952–961. doi:10.1038/ncb3573
- Harley, C. B., Futcher, A. B., and Greider, C. W. (1990). Telomeres shorten during ageing of human fibroblasts. *Nature* 345, 458–460. doi:10.1038/345458a0
- Harr, J. C., Luperchio, T. R., Wong, X., Cohen, E., Wheelan, S. J., and Reddy, K. L. (2015). Directed targeting of chromatin to the nuclear lamina is mediated by chromatin state and A-type lamins. *J. Cell Biol.* 208, 33–52. doi:10.1083/jcb.201405110
- Hayflick, L., and Moorhead, P. S. (1961). The serial cultivation of human diploid cell strains. *Exp. Cell Res.* 25, 585–621. doi:10.1016/0014-4827(61)90192-6
- Heaphy, C. M., de Wilde, R. F., Jiao, Y., Klein, A. P., Edil, B. H., Shi, C., et al. (2011). Altered telomeres in tumors with ATRX and DAXX mutations. *Science* 333, 425. doi:10.1126/science.1207313
- Henikoff, S., and Smith, M. M. (2015). Histone variants and epigenetics. *Cold Spring Harb. Perspect. Biol.* 7, a019364. doi:10.1101/cshperspect.a019364
- Höflmayer, D., Steinhoff, A., Hube-Magg, C., Kluth, M., Simon, R., Burandt, E., et al. (2020). Expression of CCCTC-binding factor (CTCF) is linked to poor prognosis in prostate cancer. *Mol. Oncol.* 14, 129–138. doi:10.1002/1878-0261.12597
- Holaska, J. M., and Wilson, K. L. (2007). An emerin “proteome”: Purification of distinct emerin-containing complexes from HeLa cells suggests molecular basis for diverse roles including gene regulation, mRNA splicing, signaling, mechanosensing, and nuclear architecture. *Biochemistry* 46, 8897–8908. doi:10.1021/bi602636m
- Holland, A. J., and Cleveland, D. W. (2012). Losing balance: The origin and impact of aneuploidy in cancer. *EMBO Rep.* 13, 501–514. doi:10.1038/embor.2012.55
- Holwerda, S. J. B., and de Laat, W. (2013). Ctf: The protein, the binding partners, the binding sites and their chromatin loops. *Philos. Trans. R. Soc. Lond. B Biol. Sci.* 368, 20120369. doi:10.1098/rstb.2012.0369
- Hua, S., Kallen, C. B., Dhar, R., Baquero, M. T., Mason, C. E., Russell, B. A., et al. (2008). Genomic analysis of estrogen cascade reveals histone variant H2A.Z associated with breast cancer progression. *Mol. Syst. Biol.* 4, 188. doi:10.1038/msb.2008.25
- Ibarra, A., Benner, C., Tyagi, S., Cool, J., and Hetzer, M. W. (2016). Nucleoporin-mediated regulation of cell identity genes. *Genes Dev.* 30, 2253–2258. doi:10.1101/gad.287417.116
- Iglesias, N., Paulo, J. A., Tatarakis, A., Wang, X., Edwards, A. L., Bhanu, N. V., et al. (2020). Native chromatin proteomics reveals a role for specific nucleoporins in heterochromatin organization and maintenance. *Mol. Cell* 77, 51–66. e8. doi:10.1016/j.molcel.2019.10.018
- Ikegami, K., Secchia, S., Almakki, O., Lieb, J. D., and Moskowitz, I. P. (2020). Phosphorylated lamin A/C in the nuclear interior binds active enhancers associated with abnormal transcription in progeria. *Dev. Cell* 52, 699–713. doi:10.1016/j.devcel.2020.02.011
- Jha, D. K., and Strahl, B. D. (2014). An RNA polymerase II-coupled function for histone H3K36 methylation in checkpoint activation and DSB repair. *Nat. Commun.* 5, 3965. doi:10.1038/ncomms4965
- Jin, C., Zang, C., Wei, G., Cui, K., Peng, W., Zhao, K., et al. (2009). H3.3/H2A.Z double variant-containing nucleosomes mark “nucleosome-free regions” of active promoters and other regulatory regions. *Nat. Genet.* 41, 941–945. doi:10.1038/ng.409
- Johnstone, S. E., Reyes, A., Qi, Y., Adriaens, C., Hegazi, E., Pelka, K., et al. (2020). Large-scale topological changes restrain malignant progression in colorectal cancer. *Cell* 182, 1474–1489. doi:10.1016/j.cell.2020.07.030
- Kadota, S., Ou, J., Shi, Y., Lee, J. T., Sun, J., and Yildirim, E. (2020). Nucleoporin 153 links nuclear pore complex to chromatin architecture by mediating CTCF and cohesin binding. *Nat. Commun.* 11, 2606. doi:10.1038/s41467-020-16394-3
- Kemp, C. J., Moore, J. M., Moser, R., Bernard, B., Teater, M., Smith, L. E., et al. (2014). CTCF haploinsufficiency destabilizes DNA methylation and predisposes to cancer. *Cell Rep.* 7, 1020–1029. doi:10.1016/j.celrep.2014.04.004
- Ketema, M., Kreft, M., Secades, P., Janssen, H., and Sonnenberg, A. (2013). Nesprin-3 connects plectin and vimentin to the nuclear envelope of Sertoli cells but is not required for Sertoli cell function in spermatogenesis. *Mol. Biol. Cell* 24, 2454–2466. doi:10.1091/mbc.E13-02-0100
- Kim, J. H., Youn, Y., Kim, K.-T., Jang, G., and Hwang, J.-H. (2019). Non-SMC condensin I complex subunit H mediates mature chromosome condensation and DNA damage in pancreatic cancer cells. *Sci. Rep.* 9, 17889. doi:10.1038/s41598-019-54478-3
- Kim, S.-Y., Rhee, J. G., Song, X., Prochowick, E. V., Spitz, D. R., and Lee, Y. J. (2012). Breast cancer stem cell-like cells are more sensitive to ionizing radiation than non-stem cells: Role of ATM. *PLoS ONE* 7, e50423. doi:10.1371/journal.pone.0050423
- Kimura, H. (2013). Histone modifications for human epigenome analysis. *J. Hum. Genet.* 58, 439–445. doi:10.1038/jhg.2013.66
- Kohestani, H., and Wereszczynski, J. (2021). Effects of H2A.B incorporation on nucleosome structures and dynamics. *Biophys. J.* 120, 1498–1509. doi:10.1016/j.bpj.2021.01.036
- Kojic, A., Cuadrado, A., De Koninck, M., Giménez-Llorente, D., Rodríguez-Corsino, M., Gómez-López, G., et al. (2018). Distinct roles of cohesin-SA1 and cohesin-SA2 in 3D chromosome organization. *Nat. Struct. Mol. Biol.* 25, 496–504. doi:10.1038/s41594-018-0070-4
- Kong, L., Schäfer, G., Bu, H., Zhang, Y., Zhang, Y., and Klocker, H. (2012). Lamin A/C protein is overexpressed in tissue-invading prostate cancer and promotes prostate cancer cell growth, migration and invasion through the PI3K/AKT/PTEN pathway. *Carcinogenesis* 33, 751–759. doi:10.1093/carcin/bgs022
- Kops, G. J. P. L., Foltz, D. R., and Cleveland, D. W. (2004). Lethality to human cancer cells through massive chromosome loss by inhibition of the mitotic checkpoint. *Proc. Natl. Acad. Sci. U. S. A.* 101, 8699–8704. doi:10.1073/pnas.0401142101
- Kuga, T., Nie, H., Kazami, T., Satoh, M., Matsushita, K., Nomura, F., et al. (2014). Lamin B2 prevents chromosome instability by ensuring proper mitotic chromosome segregation. *Oncogenesis* 3, e94. doi:10.1038/oncsis.2014.6
- Labade, A. S., Karmodiya, K., and Sengupta, K. (2016). HOXA repression is mediated by nucleoporin Nup93 assisted by its interactors Nup188 and Nup205. *Epigenetics Chromatin* 9, 54. doi:10.1186/s13072-016-0106-0
- Labade, A. S., Salvi, A., Kar, S., Karmodiya, K., and Sengupta, K. (2021). Nup93 and CTCF modulate spatiotemporal dynamics and function of the HOXA gene locus during differentiation. *J. Cell Sci.* 134, jcs259307. doi:10.1242/jcs.259307
- Laberge, R.-M., Sun, Y., Orjalo, A. V., Patil, C. K., Freund, A., Zhou, L., et al. (2015). MTOR regulates the pro-tumorigenic senescence-associated secretory

- phenotype by promoting IL1A translation. *Nat. Cell Biol.* 17, 1049–1061. doi:10.1038/ncb3195
- Lacoste, N., Woolfe, A., Tachiwana, H., Gareu, A. V., Barth, T., Cantaloube, S., et al. (2014). Mislocalization of the centromeric histone variant CenH3/CENP-A in human cells depends on the chaperone DAXX. *Mol. Cell* 53, 631–644. doi:10.1016/j.molcel.2014.01.018
- Lammerding, J., Fong, L. G., Ji, J. Y., Reue, K., Stewart, C. L., Young, S. G., et al. (2006). Lamins A and C but not lamin B1 regulate nuclear mechanics. *J. Biol. Chem.* 281, 25768–25780. doi:10.1074/jbc.M513511200
- Larson, J. D., Kasper, L. H., Paugh, B. S., Jin, H., Wu, G., Kwon, C.-H., et al. (2019). Histone H3.3 K27M accelerates spontaneous brainstem glioma and drives restricted changes in bivalent gene expression. *Cancer Cell* 35, 140–155. doi:10.1016/j.ccell.2018.11.015
- Lawrence, K. S., Chau, T., and Engebrecht, J. (2015). DNA damage response and spindle assembly checkpoint function throughout the cell cycle to ensure genomic integrity. *PLoS Genet.* 11, e1005150. doi:10.1371/journal.pgen.1005150
- Lawrence, M. S., Stojanov, P., Mermel, C. H., Robinson, J. T., Garraway, L. A., Golub, T. R., et al. (2014). Discovery and saturation analysis of cancer genes across 21 tumour types. *Nature* 505, 495–501. doi:10.1038/nature12912
- Lee, J. J., Lee, J. H., Ko, Y. G., Hong, S. I., and Lee, J. S. (2010). Prevention of premature senescence requires JNK regulation of Bcl-2 and reactive oxygen species. *Oncogene* 29, 561–575. doi:10.1038/onc.2009.355
- Leeke, B., Marsman, J., O'Sullivan, J. M., and Horsfield, J. A. (2014). Cohesin mutations in myeloid malignancies: Underlying mechanisms. *Exp. Hematol. Oncol.* 3, 13. doi:10.1186/2162-3619-3-13
- Lewis, P. W., Elsaesser, S. J., Noh, K.-M., Stadler, S. C., and Allis, C. D. (2010). Daxx is an H3.3-specific histone chaperone and cooperates with ATRX in replication-independent chromatin assembly at telomeres. *Proc. Natl. Acad. Sci. U. S. A.* 107, 14075–14080. doi:10.1073/pnas.1008850107
- Leyk, T. R., Jussiet, L. M., Lichtensztein, Z., and McManus, K. J. (2020). Reduced expression of genes regulating cohesion induces chromosome instability that may promote cancer and impact patient outcomes. *Sci. Rep.* 10, 592. doi:10.1038/s41598-020-57530-9
- Li, W., Hu, Y., Oh, S., Ma, Q., Merkurjev, D., Song, X., et al. (2015). Condensin I and II complexes license full estrogen receptor α -dependent enhancer activation. *Mol. Cell* 59, 188–202. doi:10.1016/j.molcel.2015.06.002
- Li, Y.-L., Cheng, X.-N., Lu, T., Shao, M., and Shi, D.-L. (2021). Syne2b/Nesprin-2 is required for actin organization and epithelial integrity during epiboly movement in zebrafish. *Front. Cell Dev. Biol.* 9, 671887. doi:10.3389/fcell.2021.671887
- Lin, C.-J., Conti, M., and Ramalho-Santos, M. (2013). Histone variant H3.3 maintains a decondensed chromatin state essential for mouse preimplantation development. *Development* 140, 3624–3634. doi:10.1242/dev.095513
- Lin, C.-S., Liang, Y., Su, S.-G., Zheng, Y.-L., Yang, X., Jiang, N., et al. (2022). Nucleoporin 93 mediates β -catenin nuclear import to promote hepatocellular carcinoma progression and metastasis. *Cancer Lett.* 526, 236–247. doi:10.1016/j.canlet.2021.11.001
- Lin, D. H., Correia, A. R., Cai, S. W., Huber, F. M., Jette, C. A., and Hoelz, A. (2018). Structural and functional analysis of mRNA export regulation by the nuclear pore complex. *Nat. Commun.* 9, 2319. doi:10.1038/s41467-018-04459-3
- Liu, B., Wang, Z., Zhang, L., Ghosh, S., Zheng, H., and Zhou, Z. (2013). Depleting the methyltransferase Suv39h1 improves DNA repair and extends lifespan in a progeria mouse model. *Nat. Commun.* 4, 1868. doi:10.1038/ncomms2885
- Liu, N.-A., Sun, J., Kono, K., Horikoshi, Y., Ikura, T., Tong, X., et al. (2015). Regulation of homologous recombinational repair by lamin B1 in radiation-induced DNA damage. *FASEB J.* 29, 2514–2525. doi:10.1096/fj.14-265546
- Lu, C., Jain, S. U., Hoelper, D., Bechet, D., Molden, R. C., Ran, L., et al. (2016). Histone H3K36 mutations promote sarcomagenesis through altered histone methylation landscape. *Science* 352, 844–849. doi:10.1126/science.aac7272
- Lukášová, E., Kovářik, A., and Kozubek, S. (2018). Consequences of lamin B1 and lamin B receptor downregulation in senescence. *Cells* 7, 1. doi:10.3390/cells7020011
- Lukášová, E., Kovářik, A., Bacóřiková, A., Falk, M., and Kozubek, S. (2017). Loss of lamin B receptor is necessary to induce cellular senescence. *Biochem. J.* 474, 281–300. doi:10.1042/BCJ20160459
- Lupiáñez, D. G., Kraft, K., Heinrich, V., Krawitz, P., Brancati, F., Klopocki, E., et al. (2015). Disruptions of topological chromatin domains cause pathogenic rewiring of gene-enhancer interactions. *Cell* 161, 1012–1025. doi:10.1016/j.cell.2015.04.004
- Machiels, B. M., Zorenc, A. H., Endert, J. M., Kuipers, H. J., van Eys, G. J., Ramaekers, F. C., et al. (1996). An alternative splicing product of the lamin A/C gene lacks exon 10. *J. Biol. Chem.* 271, 9249–9253. doi:10.1074/jbc.271.16.9249
- Mah, L. J., El-Osta, A., and Karagiannis, T. C. (2010). gammaH2AX: a sensitive molecular marker of DNA damage and repair. *Leukemia* 24, 679–686. doi:10.1038/leu.2010.6
- Marullo, F., Cesarini, E., Antonelli, L., Gregoret, F., Oliva, G., and Lanzuolo, C. (2016). Nucleoplasmic Lamin A/C and Polycomb group of proteins: An evolutionarily conserved interplay. *Nucleus* 7, 103–111. doi:10.1080/19491034.2016.1157675
- Matthews, B. J., and Waxman, D. J. (2018). Computational prediction of CTCF/cohesin-based intra-TAD loops that insulate chromatin contacts and gene expression in mouse liver. *eLife* 7, e34077. doi:10.7554/eLife.34077
- Mattioli, E., Andrenacci, D., Garofalo, C., Prencipe, S., Scotlandi, K., Remondini, D., et al. (2018). Altered modulation of lamin A/C-HDAC2 interaction and p21 expression during oxidative stress response in HGPS. *Aging Cell* 17, e12824. doi:10.1111/acel.12824
- McLaughlin-Drubin, M. E., Park, D., and Munger, K. (2013). Tumor suppressor p16INK4A is necessary for survival of cervical carcinoma cell lines. *Proc. Natl. Acad. Sci. U. S. A.* 110, 16175–16180. doi:10.1073/pnas.1310432110
- Melcon, G., Kozlov, S., Cutler, D. A., Sullivan, T., Hernandez, L., Zhao, P., et al. (2006). Loss of emerin at the nuclear envelope disrupts the Rb1/E2F and MyoD pathways during muscle regeneration. *Hum. Mol. Genet.* 15, 637–651. doi:10.1093/hmg/ddi479
- Millán-Zambrano, G., Burton, A., Bannister, A. J., and Schneider, R. (2022). Histone post-translational modifications - cause and consequence of genome function. *Nat. Rev. Genet.* 23, 563–580. doi:10.1038/s41576-022-00468-7
- Minchell, N. E., Keszthelyi, A., and Baxter, J. (2020). Cohesin causes replicative DNA damage by trapping DNA topological stress. *Mol. Cell* 78, 739–751. e8. doi:10.1016/j.molcel.2020.03.013
- Mohammad, F., and Helin, K. (2017). Oncohistones: Drivers of pediatric cancers. *Genes Dev.* 31, 2313–2324. doi:10.1101/gad.309013.117
- Mohammed, H., Taylor, C., Brown, G. D., Papachristou, E. K., Carroll, J. S., and D'Santos, C. S. (2016). Rapid immunoprecipitation mass spectrometry of endogenous proteins (RIME) for analysis of chromatin complexes. *Nat. Protoc.* 11, 316–326. doi:10.1038/nprot.2016.020
- Moir, R. D., Spann, T. P., Herrmann, H., and Goldman, R. D. (2000). Disruption of nuclear lamin organization blocks the elongation phase of DNA replication. *J. Cell Biol.* 149, 1179–1192. doi:10.1083/jcb.149.6.1179
- Moreno, E., and Basler, K. (2004). dMyc transforms cells into super-competitors. *Cell* 117, 117–129. doi:10.1016/s0092-8674(04)00262-4
- Moss, S. F., Krivosheyev, V., de Souza, A., Chin, K., Gaetz, H. P., Chaudhary, N., et al. (1999). Decreased and aberrant nuclear lamin expression in gastrointestinal tract neoplasms. *Gut* 45, 723–729. doi:10.1136/gut.45.5.723
- Muñoz-Espín, D., Cañamero, M., Maraver, A., Gómez-López, G., Contreras, J., Murillo-Cuesta, S., et al. (2013). Programmed cell senescence during mammalian embryonic development. *Cell* 155, 1104–1118. doi:10.1016/j.cell.2013.10.019
- Murray-Nerger, L. A., and Cristea, I. M. (2021). Lamin post-translational modifications: Emerging toggles of nuclear organization and function. *Trends biochem. Sci.* 46, 832–847. doi:10.1016/j.tibs.2021.05.007
- Nacev, B. A., Feng, L., Bagert, J. D., Lemiesz, A. E., Gao, J., Soshnev, A. A., et al. (2019). The expanding landscape of "oncohistone" mutations in human cancers. *Nature* 567, 473–478. doi:10.1038/s41586-019-1038-1
- Narita, M., Nunez, S., Heard, E., Narita, M., Lin, A. W., Hearn, S. A., et al. (2003). Rb-mediated heterochromatin formation and silencing of E2F target genes during cellular senescence. *Cell* 113, 703–716. doi:10.1016/s0092-8674(03)00401-x
- Nataraj, N. B., Noronha, A., Lee, J. S., Ghosh, S., Mohan Raju, H. R., Sekar, A., et al. (2022). Nucleoporin-93 reveals a common feature of aggressive breast cancers: Robust nucleocytoplasmic transport of transcription factors. *Cell Rep.* 38, 110418. doi:10.1016/j.celrep.2022.110418
- Nelson, D. M., Jaber-Hijazi, F., Cole, J. J., Robertson, N. A., Pawlikowski, J. S., Norris, K. T., et al. (2016). Mapping H4K20me3 onto the chromatin landscape of senescent cells indicates a function in control of cell senescence and tumor suppression through preservation of genetic and epigenetic stability. *Genome Biol.* 17, 158. doi:10.1186/s13059-016-1017-x
- Nuebler, J., Fudenberg, G., Imakaev, M., Abdennur, N., and Mirny, L. A. (2018). Chromatin organization by an interplay of loop extrusion and compartmental segregation. *Proc. Natl. Acad. Sci. U. S. A.* 115, E6697–E6706. doi:10.1073/pnas.1717730115
- Oberdoerffer, P., and Miller, K. M. (2022). Histone H2A variants: Diversifying chromatin to ensure genome integrity. *Semin. Cell Dev. Biol.* 135, 59–72. doi:10.1016/j.semcdb.2022.03.011
- Ogryzko, V. V., Schiltz, R. L., Russanova, V., Howard, B. H., and Nakatani, Y. (1996). The transcriptional coactivators p300 and CBP are histone acetyltransferases. *Cell* 87, 953–959. doi:10.1016/s0092-8674(00)82001-2

- Orjalo, A. V., Arnaoutov, A., Shen, Z., Boyarchuk, Y., Zeitlin, S. G., Fontoura, B., et al. (2006). The Nup107-160 nucleoporin complex is required for correct bipolar spindle assembly. *Mol. Biol. Cell* 17, 3806–3818. doi:10.1091/mbc.E05-11-1061
- Pascual-García, P., Debo, B., Aleman, J. R., Talamas, J. A., Lan, Y., Nguyen, N. H., et al. (2017). Metazoan nuclear pores provide a scaffold for poised genes and mediate induced enhancer-promoter contacts. *Mol. Cell* 66, 63–76. doi:10.1016/j.molcel.2017.02.020
- Pascual-Reguant, L., Blanco, E., Galan, S., Le Dily, F., Cuartero, Y., Serra-Bardens, G., et al. (2018). Lamin B1 mapping reveals the existence of dynamic and functional euchromatin lamin B1 domains. *Nat. Commun.* 9, 3420. doi:10.1038/s41467-018-05912-z
- Pennarun, G., Picotto, J., Etourneau, L., Redavid, A.-R., Certain, A., Gauthier, L. R., et al. (2021). Increase in lamin B1 promotes telomere instability by disrupting the shelterin complex in human cells. *Nucleic Acids Res.* 49, 9886–9905. doi:10.1093/nar/gkab761
- Peters, A. H. F. M., Kubicek, S., Mechtler, K., O'Sullivan, R. J., Derijck, A. A. H. A., Perez-Burgos, L., et al. (2003). Partitioning and plasticity of repressive histone methylation states in mammalian chromatin. *Mol. Cell* 12, 1577–1589. doi:10.1016/s1097-2765(03)00477-5
- Phillips-Cremins, J. E., Sauria, M. E. G., Sanyal, A., Gerasimova, T. I., Lajoie, B. R., Bell, J. S. K., et al. (2013). Architectural protein subclasses shape 3D organization of genomes during lineage commitment. *Cell* 153, 1281–1295. doi:10.1016/j.cell.2013.04.053
- Pon, J. R., and Marra, M. A. (2015). Driver and passenger mutations in cancer. *Annu. Rev. Pathol.* 10, 25–50. doi:10.1146/annurev-pathol-012414-040312
- Poulos, R. C., Thoms, J. A. I., Guan, Y. F., Unnikrishnan, A., Pimanda, J. E., and Wong, J. W. H. (2016). Functional mutations form at CTCF-cohesin binding sites in melanoma due to uneven nucleotide excision repair across the motif. *Cell Rep.* 17, 2865–2872. doi:10.1016/j.celrep.2016.11.055
- Ranade, D., Pradhan, R., Jayakrishnan, M., Hegde, S., and Sengupta, K. (2019). Lamin A/C and Emerin depletion impacts chromatin organization and dynamics in the interphase nucleus. *BMC Mol. Cell Biol.* 20, 11. doi:10.1186/s12860-019-0192-5
- Rao, R. C., and Dou, Y. (2015). Hijacked in cancer: The KMT2 (MLL) family of methyltransferases. *Nat. Rev. Cancer* 15, 334–346. doi:10.1038/nrc3929
- Ray-Gallet, D., Woolfe, A., Vassias, I., Pellentz, C., Lacoste, N., Puri, A., et al. (2011). Dynamics of histone H3 deposition *in vivo* reveal a nucleosome gap-filling mechanism for H3.3 to maintain chromatin integrity. *Mol. Cell* 44, 928–941. doi:10.1016/j.molcel.2011.12.006
- Raz, V., Vermolen, B. J., Garini, Y., Onderwater, J. J. M., Mommaas-Kienhuis, M. A., Koster, A. J., et al. (2008). The nuclear lamina promotes telomere aggregation and centromere peripheral localization during senescence of human mesenchymal stem cells. *J. Cell Sci.* 121, 4018–4028. doi:10.1242/jcs.034876
- Redwood, A. B., Perkins, S. M., Vanderwaal, R. P., Feng, Z., Biehl, K. J., Gonzalez-Suarez, I., et al. (2011). A dual role for A-type lamins in DNA double-strand break repair. *Cell Cycle* 10, 2549–2560. doi:10.4161/cc.10.15.16531
- Reis-Sobreira, M., Chen, J.-F., Novitskaya, T., You, S., Morley, S., Steadman, K., et al. (2018). Emerin deregulation links nuclear shape instability to metastatic potential. *Cancer Res.* 78, 6086–6097. doi:10.1158/0008-5472.CAN-18-0608
- Ren, X., Tu, C., Tang, Z., Ma, R., and Li, Z. (2018). Alternative lengthening of telomeres phenotype and loss of ATRX expression in sarcomas. *Oncol. Lett.* 15, 7489–7496. doi:10.3892/ol.2018.8318
- Richart, L., Lapi, E., Pancaldi, V., Cuenca-Ardura, M., Pau, E. C.-S., Madrid-Mencia, M., et al. (2021). STAG2 loss-of-function affects short-range genomic contacts and modulates the basal-luminal transcriptional program of bladder cancer cells. *Nucleic Acids Res.* 49, 11005–11021. doi:10.1093/nar/gkab864
- Rocha, A., Dalgarno, A., and Neretti, N. (2022). The functional impact of nuclear reorganization in cellular senescence. *Brief. Funct. Genomics* 21, 24–34. doi:10.1093/bfgp/elab012
- Rondinelli, B., Giacomini, G., Piquet, S., Chevallier, O., Dabin, J., Bai, S.-K., et al. (2022). Aberrant DNA repair is a vulnerability in histone H3.3-mutant brain tumors. *BioRxiv* 1, 1. doi:10.1101/2022.09.29.510093
- Rossi, D. J., Bryder, D., Seita, J., Nussenzweig, A., Hoeijmakers, J., and Weissman, I. L. (2007). Deficiencies in DNA damage repair limit the function of haematopoietic stem cells with age. *Nature* 447, 725–729. doi:10.1038/nature05862
- Sahu, V., and Lu, C. (2022). Oncohistones: Hijacking the histone code. *Annu. Rev. Cancer Biol.* 6, 293–312. doi:10.1146/annurev-cancerbio-070120-102521
- Salvarani, N., Crasto, S., Miragoli, M., Bertero, A., Paulis, M., Kunderfranco, P., et al. (2019). The K219T-Lamin mutation induces conduction defects through epigenetic inhibition of SCN5A in human cardiac laminopathy. *Nat. Commun.* 10, 2267. doi:10.1038/s41467-019-09929-w
- Samoshkin, A., Dulev, S., Loukinov, D., Rosenfeld, J. A., and Strunnikov, A. V. (2012). Condensin dysfunction in human cells induces nonrandom chromosomal breaks in anaphase, with distinct patterns for both unique and repeated genomic regions. *Chromosoma* 121, 191–199. doi:10.1007/s00412-011-0353-6
- Sanborn, A. L., Rao, S. S. P., Huang, S.-C., Durand, N. C., Huntley, M. H., Jewett, A. I., et al. (2015). Chromatin extrusion explains key features of loop and domain formation in wild-type and engineered genomes. *Proc. Natl. Acad. Sci. U. S. A.* 112, E6456–E6465. doi:10.1073/pnas.1518552112
- Santi, S., Cenni, V., Capanni, C., Lattanzi, G., and Mattioli, E. (2020). PCAF involvement in lamin A/C-HDAC2 interplay during the early phase of muscle differentiation. *Cells* 9, 1. doi:10.3390/cells9071735
- Sati, S., Bonev, B., Szabo, Q., Jost, D., Bensadoun, P., Serra, F., et al. (2020). 4D genome rewiring during oncogene-induced and replicative senescence. *Mol. Cell* 78, 522–538. doi:10.1016/j.molcel.2020.03.007
- Serrano, M., Lin, A. W., McCurrach, M. E., Beach, D., and Lowe, S. W. (1997). Oncogenic ras provokes premature cell senescence associated with accumulation of p53 and p16INK4a. *Cell* 88, 593–602. doi:10.1016/s0092-8674(00)81902-9
- Shi, L., Wen, H., and Shi, X. (2017). The histone variant H3.3 in transcriptional regulation and human disease. *J. Mol. Biol.* 429, 1934–1945. doi:10.1016/j.jmb.2016.11.019
- Shimi, T., Pflieger, K., Kojima, S., Pack, C.-G., Solovei, I., Goldman, A. E., et al. (2008). The A- and B-type nuclear lamin networks: Microdomains involved in chromatin organization and transcription. *Genes Dev.* 22, 3409–3421. doi:10.1101/gad.1735208
- Shumaker, D. K., Dechat, T., Kohlmaier, A., Adam, S. A., Bozovsky, M. R., Erdos, M. R., et al. (2006). Mutant nuclear lamin A leads to progressive alterations of epigenetic control in premature aging. *Proc. Natl. Acad. Sci. U. S. A.* 103, 8703–8708. doi:10.1073/pnas.0602569103
- Siegenfeld, A. P., Roseman, S. A., Roh, H., Lue, N. Z., Wagen, C. C., Zhou, E., et al. (2022). Polycarb-lamina antagonism partitions heterochromatin at the nuclear periphery. *Nat. Commun.* 13, 4199. doi:10.1038/s41467-022-31857-5
- Smith, E. R., Capo-Chichi, C. D., and Xu, X.-X. (2018). Defective nuclear lamina in aneuploidy and carcinogenesis. *Front. Oncol.* 8, 529. doi:10.3389/fonc.2018.00529
- Solomon, D. A., Kim, T., Diaz-Martinez, L. A., Fair, J., Elkahloun, A. G., Harris, B. T., et al. (2011). Mutational inactivation of STAG2 causes aneuploidy in human cancer. *Science* 333, 1039–1043. doi:10.1126/science.1203619
- Solovei, I., Wang, A. S., Thanisch, K., Schmidt, C. S., Krebs, S., Zwerger, M., et al. (2013). LBR and lamin A/C sequentially tether peripheral heterochromatin and inversely regulate differentiation. *Cell* 152, 584–598. doi:10.1016/j.cell.2013.01.009
- Starr, D. A., and Fischer, J. A. (2005). KASH 'n' karry: The KASH domain family of cargo-specific cytoskeletal adaptor proteins. *Bioessays* 27, 1136–1146. doi:10.1002/bies.20312
- Stephens, A. D., Liu, P. Z., Banigan, E. J., Almassalha, L. M., Backman, V., Adam, S. A., et al. (2018). Chromatin histone modifications and rigidity affect nuclear morphology independent of lamins. *Mol. Biol. Cell* 29, 220–233. doi:10.1091/mbc.E17-06-0410
- Stirpe, A., and Heun, P. (2022). The ins and outs of CENP-A: Chromatin dynamics of the centromere-specific histone. *Semin. Cell Dev. Biol.* 135, 24–34. doi:10.1016/j.semcdb.2022.04.003
- Sun, X., Clermont, P.-L., Jiao, W., Helgason, C. D., Gout, P. W., Wang, Y., et al. (2016). Elevated expression of the centromere protein-A (CENP-A)-encoding gene as a prognostic and predictive biomarker in human cancers. *Int. J. Cancer* 139, 899–907. doi:10.1002/ijc.30133
- Sur, I., Neumann, S., and Noegel, A. A. (2014). Nesprin-1 role in DNA damage response. *Nucleus* 5, 173–191. doi:10.4161/nucl.29023
- Sur-Erdem, I., Hussain, M. S., Asif, M., Pinarbasi, N., Aksu, A. C., and Noegel, A. A. (2020). Nesprin-1 impact on tumorigenic cell phenotypes. *Mol. Biol. Rep.* 47, 921–934. doi:10.1007/s11033-019-05184-w
- Swift, J., Ivanovska, I. L., Buxboim, A., Harada, T., Dingal, P. C. D. P., Pinter, J., et al. (2013). Nuclear lamin-A scales with tissue stiffness and enhances matrix-directed differentiation. *Science* 341, 1240104. doi:10.1126/science.1240104
- Szabo, Q., Bantignies, F., and Cavalli, G. (2019). Principles of genome folding into topologically associating domains. *Sci. Adv.* 5, eaaw1668. doi:10.1126/sciadv.aaw1668
- Talbert, P. B., and Henikoff, S. (2021). Histone variants at a glance. *J. Cell Sci.* 134, jcs244749. doi:10.1242/jcs.244749
- Teng, Y.-C., Sundaresan, A., O'Hara, R., Gant, V. U., Li, M., Martire, S., et al. (2021). ATRX promotes heterochromatin formation to protect cells from G-quadruplex DNA-mediated stress. *Nat. Commun.* 12, 3887. doi:10.1038/s41467-021-24206-5
- Towbin, B. D., González-Aguilera, C., Sack, R., Gaidatzis, D., Kalck, V., Meister, P., et al. (2012). Step-wise methylation of histone H3K9 positions heterochromatin at the nuclear periphery. *Cell* 150, 934–947. doi:10.1016/j.cell.2012.06.051

- Turinetto, V., Orlando, L., Sanchez-Ripoll, Y., Kumpfmüller, B., Storm, M. P., Porcedda, P., et al. (2012). High basal γH2AX levels sustain self-renewal of mouse embryonic and induced pluripotent stem cells. *Stem Cells* 30, 1414–1423. doi:10.1002/stem.1133
- Turner, B. M. (1993). *Decoding the nucleosome minireview*: Cell Press. 75 (1), 5–8. doi:10.1016/S0092-8674(05)80078-9
- Tzur, Y. B., Wilson, K. L., and Gruenbaum, Y. (2006). SUN-Domain proteins: “Velcro” that links the nucleoskeleton to the cytoskeleton. *Nat. Rev. Mol. Cell Biol.* 7, 782–788. doi:10.1038/nrm2003
- Udugama, M., M Chang, F. T., Chan, F. L., Tang, M. C., Pickett, H. A., R McGhie, J. D., et al. (2015). Histone variant H3.3 provides the heterochromatic H3 lysine 9 tri-methylation mark at telomeres. *Nucleic Acids Res.* 43, 10227–10237. doi:10.1093/nar/gkv847
- Vardabasso, C., Gaspar-Maia, A., Hasson, D., Pünzler, S., Valle-Garcia, D., Straub, T., et al. (2015). Histone variant H2A.Z.2 mediates proliferation and drug sensitivity of malignant melanoma. *Mol. Cell* 59, 75–88. doi:10.1016/j.molcel.2015.05.009
- Vorburger, K., Kitten, G. T., and Nigg, E. A. (1989). Modification of nuclear lamin proteins by a mevalonic acid derivative occurs in reticulocyte lysates and requires the cysteine residue of the C-terminal CXXM motif. *EMBO J.* 8, 4007–4013. doi:10.1002/j.1460-2075.1989.tb05833.x
- Wang, G. G., Cai, L., Pasillas, M. P., and Kamps, M. P. (2007). NUP98-NSD1 links H3K36 methylation to Hox-A gene activation and leukaemogenesis. *Nat. Cell Biol.* 9, 804–812. doi:10.1038/ncb1608
- Wang, G. G., Song, J., Wang, Z., Dormann, H. L., Casadio, F., Li, H., et al. (2009). Haematopoietic malignancies caused by dysregulation of a chromatin-binding PHD finger. *Nature* 459, 847–851. doi:10.1038/nature08036
- Wang, L., Lankhorst, L., and Bernards, R. (2022). Exploiting senescence for the treatment of cancer. *Nat. Rev. Cancer* 22, 340–355. doi:10.1038/s41568-022-00450-9
- Wang, R.-R., Qiu, X., Pan, R., Fu, H., Zhang, Z., Wang, Q., et al. (2022). Dietary intervention preserves β cell function in mice through CTCF-mediated transcriptional reprogramming. *J. Exp. Med.* 219, e20211779. doi:10.1084/jem.20211779
- Wang, X., Hughes, A. C., Brandão, H. B., Walker, B., Lierz, C., Cochran, J. C., et al. (2018). *In vivo* evidence for ATPase-dependent DNA translocation by the *Bacillus subtilis* SMC condensin complex. *Mol. Cell* 71, 841–847. e5. doi:10.1016/j.molcel.2018.07.006
- Wang, Y., Chen, Q., Wu, D., Chen, Q., Gong, G., He, L., et al. (2021). Lamin-A interacting protein Hsp90 is required for DNA damage repair and chemoresistance of ovarian cancer cells. *Cell Death Dis.* 12, 786. doi:10.1038/s41419-021-04074-z
- Wang, Y., Jiang, J., He, L., Gong, G., and Wu, X. (2019). Effect of lamin-A expression on migration and nuclear stability of ovarian cancer cells. *Gynecol. Oncol.* 152, 166–176. doi:10.1016/j.ygyno.2018.10.030
- Watanabe, T., Wu, T. T., Catalano, P. J., Ueki, T., Satriano, R., Haller, D. G., et al. (2001). Molecular predictors of survival after adjuvant chemotherapy for colon cancer. *N. Engl. J. Med.* 344, 1196–1206. doi:10.1056/NEJM200104193441603
- Weierich, C., Brero, A., Stein, S., von Hase, J., Cremer, C., Cremer, T., et al. (2003). Three-dimensional arrangements of centromeres and telomeres in nuclei of human and murine lymphocytes. *Chromosome Res.* 11, 485–502. doi:10.1023/a:1025016828544
- Weintraub, A. S., Li, C. H., Zamudio, A. V., Sigova, A. A., Hannett, N. M., Day, D. S., et al. (2017). YY1 is a structural regulator of enhancer-promoter loops. *Cell* 171, 1573–1588. doi:10.1016/j.cell.2017.11.008
- Weyburne, E., and Bosco, G. (2021). Cancer-associated mutations in the condensin II subunit CAPH2 cause genomic instability through telomere dysfunction and anaphase chromosome bridges. *J. Cell. Physiol.* 236, 3579–3598. doi:10.1002/jcp.30113
- Weyemi, U., Redon, C. E., Sethi, T. K., Burrell, A. S., Jailwala, P., Kasoji, M., et al. (2016). Twist1 and Slug mediate H2AX-regulated epithelial-mesenchymal transition in breast cells. *Cell Cycle* 15, 2398–2404. doi:10.1080/15384101.2016.1198864
- Wong, K. M., Song, J., and Wong, Y. H. (2021). CTCF and EGR1 suppress breast cancer cell migration through transcriptional control of Nm23-H1. *Sci. Rep.* 11, 491. doi:10.1038/s41598-020-79869-9
- Wong, L. H., Ren, H., Williams, E., McGhie, J., Ahn, S., Sim, M., et al. (2009). Histone H3.3 incorporation provides a unique and functionally essential telomeric chromatin in embryonic stem cells. *Genome Res.* 19, 404–414. doi:10.1101/gr.084947.108
- Wood, A. M., Rendtlew Danielsen, J. M., Lucas, C. A., Rice, E. L., Scalzo, D., Shimi, T., et al. (2014). TRF2 and lamin A/C interact to facilitate the functional organization of chromosome ends. *Nat. Commun.* 5, 5467. doi:10.1038/ncomms6467
- Xu, H., Yan, M., Patra, J., Natrajan, R., Yan, Y., Swagemakers, S., et al. (2011). Enhanced RAD21 cohesin expression confers poor prognosis and resistance to chemotherapy in high grade luminal, basal and HER2 breast cancers. *Breast Cancer Res.* 13, R9. doi:10.1186/bcr2814
- Yang, Y., Zhang, L., Xiong, C., Chen, J., Wang, L., Wen, Z., et al. (2022). HIRA complex presets transcriptional potential through coordinating depositions of the histone variants H3.3 and H2A.Z on the poised genes in mESCs. *Nucleic Acids Res.* 50, 191–206. doi:10.1093/nar/gkab1221
- Yassin, E. R., Abdul-Nabi, A. M., Takeda, A., and Yaseen, N. R. (2010). Effects of the NUP98-DDX10 oncogene on primary human CD34+ cells: Role of a conserved helicase motif. *Leukemia* 24, 1001–1011. doi:10.1038/leu.2010.42
- Ye, Q., and Worman, H. J. (1996). Interaction between an integral protein of the nuclear envelope inner membrane and human chromodomain proteins homologous to Drosophila HP1. *J. Biol. Chem.* 271, 14653–14656. doi:10.1074/jbc.271.25.14653
- Yin, L., Jiang, L.-P., Shen, Q.-S., Xiong, Q.-X., Zhuo, X., Zhang, L.-L., et al. (2017). NCAPH plays important roles in human colon cancer. *Cell Death Dis.* 8, e2680. doi:10.1038/cddis.2017.88
- Yu, G., Zhang, Y., Gupta, V., Zhang, J., MacCarthy, T., Duan, Z., et al. (2021). The role of HIRA-dependent H3.3 deposition and its modifications in the somatic hypermutation of immunoglobulin variable regions. *Proc. Natl. Acad. Sci. U. S. A.* 118, e2114743118. doi:10.1073/pnas.2114743118
- Yuen, B. T. K., and Knöpfel, P. S. (2013). Histone H3.3 mutations: A variant path to cancer. *Cancer Cell* 24, 567–574. doi:10.1016/j.ccr.2013.09.015
- Yun, J., Song, S.-H., Kim, H.-P., Han, S.-W., Yi, E. C., and Kim, T.-Y. (2016). Dynamic cohesin-mediated chromatin architecture controls epithelial-mesenchymal plasticity in cancer. *EMBO Rep.* 17, 1343–1359. doi:10.15252/embr.201541852
- Yusufzai, T. M., Tagami, H., Nakatani, Y., and Felsenfeld, G. (2004). CTCF tethers an insulator to subnuclear sites, suggesting shared insulator mechanisms across species. *Mol. Cell* 13, 291–298. doi:10.1016/s1097-2765(04)00029-2
- Zeitlin, S. G., Baker, N. M., Chapados, B. R., Soutoglou, E., Wang, J. Y. J., Berns, M. W., et al. (2009). Double-strand DNA breaks recruit the centromeric histone CENP-A. *Proc. Natl. Acad. Sci. U. S. A.* 106, 15762–15767. doi:10.1073/pnas.0908233106
- Zhang, H., and Li, T. (2017). Effects of spermidine and ATP on stabilities of chromatosomes and histone H1-depleted chromatosomes. *Bioorg. Med. Chem. Lett.* 27, 1149–1153. doi:10.1016/j.bmcl.2017.01.072
- Zhang, R., Ai, J., Wang, J., Sun, C., Lu, H., He, A., et al. (2022). NCAPG promotes the proliferation of hepatocellular carcinoma through the CKII-dependent regulation of PTEN. *J. Transl. Med.* 20, 325. doi:10.1186/s12967-022-03519-z
- Zhang, R., Chen, W., and Adams, P. D. (2007). Molecular dissection of formation of senescence-associated heterochromatin foci. *Mol. Cell. Biol.* 27, 2343–2358. doi:10.1128/MCB.02019-06
- Zhang, X., Jeong, M., Huang, X., Wang, X. Q., Wang, X., Zhou, W., et al. (2020). Large DNA methylation nadirs anchor chromatin loops maintaining hematopoietic stem cell identity. *Mol. Cell* 78, 506–521. doi:10.1016/j.molcel.2020.04.018
- Zhang, Y., Liu, F., Zhang, C., Ren, M., Kuang, M., Xiao, T., et al. (2020). Non-SMC condensin I complex subunit D2 is a prognostic factor in triple-negative breast cancer for the ability to promote cell cycle and enhance invasion. *Am. J. Pathol.* 190, 37–47. doi:10.1016/j.ajpath.2019.09.014
- Zhao, L., Yang, Y., Yin, S., Yang, T., Luo, J., Xie, R., et al. (2017). CTCF promotes epithelial ovarian cancer metastasis by broadly controlling the expression of metastasis-associated genes. *Oncotarget* 8, 62217–62230. doi:10.18632/oncotarget.19216
- Zheng, X., Hu, J., Yue, S., Kristiani, L., Kim, M., Sauria, M., et al. (2018). Lamins organize the global three-dimensional genome from the nuclear periphery. *Mol. Cell* 71, 802–815. doi:10.1016/j.molcel.2018.05.017
- Zhou, L., and Panté, N. (2010). The nucleoporin Nup153 maintains nuclear envelope architecture and is required for cell migration in tumor cells. *FEBS Lett.* 584, 3013–3020. doi:10.1016/j.febslet.2010.05.038
- Zhou, W., Goodman, S. N., Galizia, G., Lieto, E., Ferraraccio, F., Pignatelli, C., et al. (2002). Counting alleles to predict recurrence of early-stage colorectal cancers. *Lancet* 359, 219–225. doi:10.1016/S0140-6736(02)07448-2
- Zink, L.-M., and Hake, S. B. (2016). Histone variants: Nuclear function and disease. *Curr. Opin. Genet. Dev.* 37, 82–89. doi:10.1016/j.gde.2015.12.002



OPEN ACCESS

EDITED BY

Joanna M. Bridger,
Brunel University London, United Kingdom

REVIEWED BY

Ping Hu,
Shanghai Institute of Biochemistry and Cell
Biology (CAS), China
Ian Holt,
Robert Jones and Agnes Hunt
Orthopaedic Hospital NHS Trust,
United Kingdom

*CORRESPONDENCE

Peter Meinke,
✉ Peter.Meinke@med.uni-muenchen.de

SPECIALTY SECTION

This article was submitted to Nuclear
Organization and Dynamics,
a section of the journal
Frontiers in Cell and Developmental
Biology

RECEIVED 30 July 2022

ACCEPTED 27 December 2022

PUBLISHED 09 January 2023

CITATION

Todorow V, Hintze S, Schoser B and
Meinke P (2023), Nuclear envelope
transmembrane proteins involved in
genome organization are misregulated in
myotonic dystrophy type 1 muscle.
Front. Cell Dev. Biol. 10:1007331.
doi: 10.3389/fcell.2022.1007331

COPYRIGHT

© 2023 Todorow, Hintze, Schoser and
Meinke. This is an open-access article
distributed under the terms of the [Creative
Commons Attribution License \(CC BY\)](#).
The use, distribution or reproduction in
other forums is permitted, provided the
original author(s) and the copyright
owner(s) are credited and that the original
publication in this journal is cited, in
accordance with accepted academic
practice. No use, distribution or
reproduction is permitted which does not
comply with these terms.

Nuclear envelope transmembrane proteins involved in genome organization are misregulated in myotonic dystrophy type 1 muscle

Vanessa Todorow, Stefan Hintze, Benedikt Schoser and
Peter Meinke*

Friedrich-Baur-Institute at the Department of Neurology, University Hospital, LMU, Munich, Germany

Myotonic dystrophy type 1 is a multisystemic disorder with predominant muscle and neurological involvement. Despite a well described pathomechanism, which is primarily a global missplicing due to sequestration of RNA-binding proteins, there are still many unsolved questions. One such question is the disease etiology in the different affected tissues. We observed alterations at the nuclear envelope in primary muscle cell cultures before. This led us to reanalyze a published RNA-sequencing dataset of DM1 and control muscle biopsies regarding the misregulation of NE proteins. We could identify several muscle NE protein encoding genes to be misregulated depending on the severity of the muscle phenotype. Among these misregulated genes were NE transmembrane proteins (NETs) involved in nuclear-cytoskeletal coupling as well as genome organization. For selected genes, we could confirm that observed gene-misregulation led to protein expression changes. Furthermore, we investigated if genes known to be under expression-regulation by genome organization NETs were also misregulated in DM1 biopsies, which revealed that misregulation of two NETs alone is likely responsible for differential expression of about 10% of all genes being differentially expressed in DM1. Notably, the majority of NETs identified here to be misregulated in DM1 muscle are mutated in Emery-Dreifuss muscular dystrophy or clinical similar muscular dystrophies, suggesting a broader similarity on the molecular level for muscular dystrophies than anticipated. This shows not only the importance of muscle NETs in muscle health and disease, but also highlights the importance of the NE in DM1 disease progression.

KEYWORDS

nuclear envelope, myotonic dystrophy type 1, genome organization, muscle biopsy, nuclear envelope transmembrane proteins

Introduction

Myotonic dystrophy type 1 (DM1) is clinically characterized by multisystemic involvement with skeletal muscle and brain being the primarily affected organs. Clinical symptoms include myotonia, skeletal muscle weakness and wasting, cardiac arrhythmia, cataracts and insulin resistance, endocrine dysfunction, frontal balding and a shortened lifespan (Udd and Krahe, 2012; Thornton, 2014; Wenninger et al., 2018). An estimated prevalence of about one in 8,000 and the predominant muscle involvement make DM1 one of the most frequent muscular dystrophies in adulthood (Faustino and Cooper, 2003; Wheeler, 2008).

Genetically, DM1 is caused by a pathological CTG-repeat expansion in the 3'UTR of the DMPK (dystrophin myotonia protein kinase) gene (Fu et al., 1992). The extended repeat is

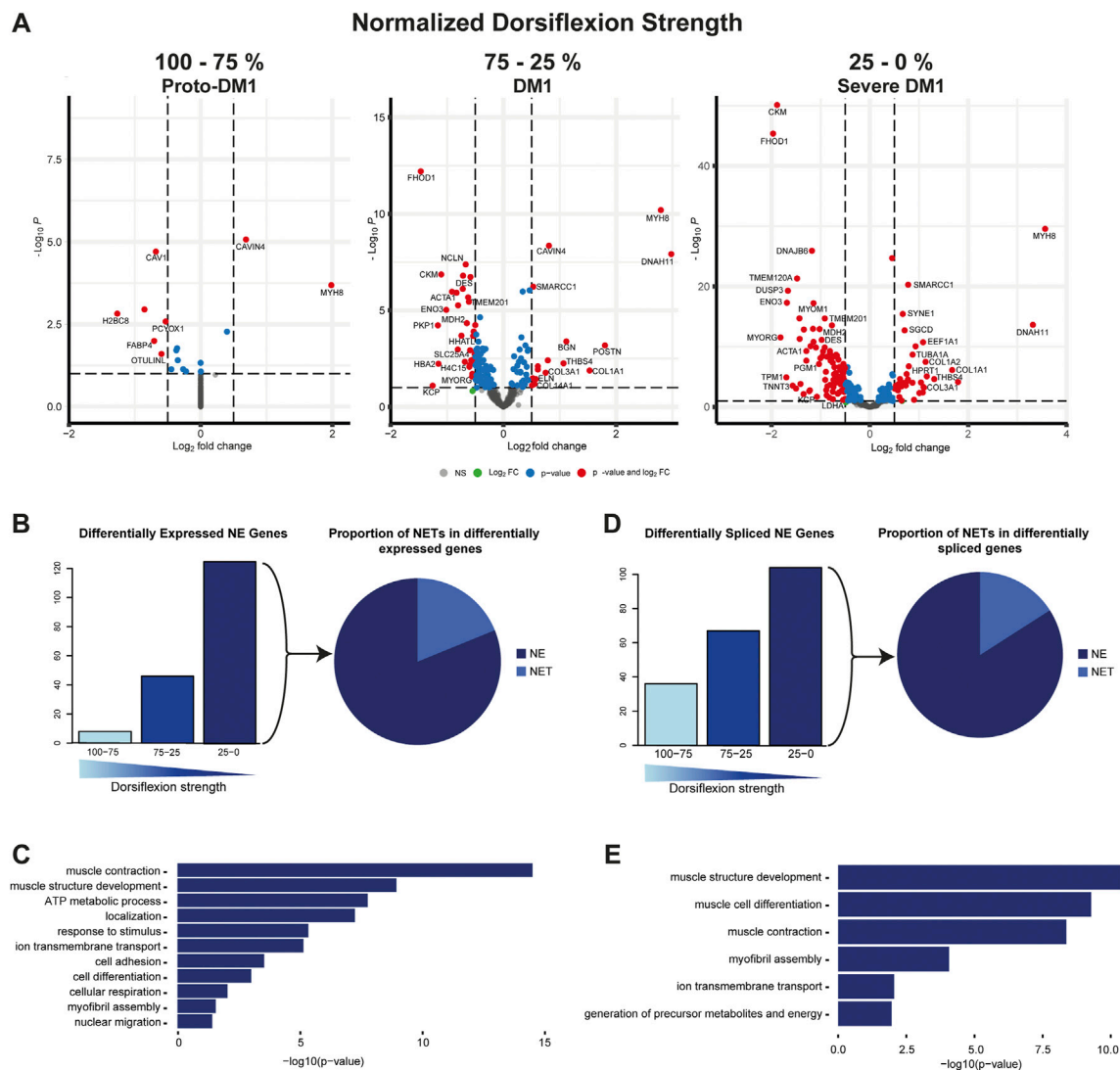


FIGURE 1

Muscle nuclear envelope (NE) proteins are differential expressed and spliced in DM1. (A) Gene expression of 386 muscle NE proteins for proto-DM1, DM1, and severe DM1 based on dorsiflexion strength. (B) Number of genes being differential expressed and the proportion of NE transmembrane proteins (NETs). (C) GO-term enrichment for the differential expressed muscle NE proteins. (D) Number of genes being differential spliced and the proportion of NETs. (E) GO-term enrichment for the differential spliced muscle NE proteins.

unstable, up to 35 CTG-repeats are found in healthy individuals, and between 35 and 49 repeats are considered to be a premutation (Udd and Krahe, 2012). The longer the repeat, the more severe the clinical presentation: between 50 and ~150 repeats usually result in a mild phenotype, a range from ~100 to ~1,000 repeats has been identified in patients with classical DM1, and more than 1000 CTG-triplets usually result in congenital DM, the most severe form of the disease. This rough correlation between repeat length and severity of the disease is non-linear (De Antonio et al., 2016), and there are other factors contributing to the clinical presentation. Maternal inheritance results in more severe symptoms than paternal inheritance, which may be due to an increased greater instability of mutant alleles in female meiosis or maternal-biased CpG methylation of the *DMPK* locus (Rakocevic-Stojanovic et al., 2005; Martorell et al., 2007; Barbé et al., 2017). The extended repeats are somatically unstable, usually resulting in increase of repeat length during the lifetime of an affected individual and

somatic mosaicism (Monckton et al., 1995; Wong et al., 1995). Especially for skeletal muscle it has been shown that repeats can be three- and 25-fold longer than in leukocytes (Thornton et al., 1994; Nakamori et al., 2013).

The mechanisms proposed to contribute to the DM1 phenotype include alternative splicing of several mRNAs (Ho et al., 2005; López-Martínez et al., 2020), altered transcriptional regulation (Ebralidze et al., 2004; Osborne et al., 2009), miRNA misregulation (Rau et al., 2011; Kalsotra et al., 2014; Shen et al., 2020) and inhibited translation (Huichalaf et al., 2010; Meola et al., 2013). The most intensively investigated mechanism is probably alternative splicing, caused by the formation of hairpin structures in the extended CUG-repeat containing *DMPK* RNA transcripts (Napierała and Krzyzosiak, 1997). These secondary structures sequester several RNA-binding proteins, with muscle-blind proteins (MBNL1-3) being the most prominent ones (Fardaei et al., 2001; Fardaei et al., 2002). This

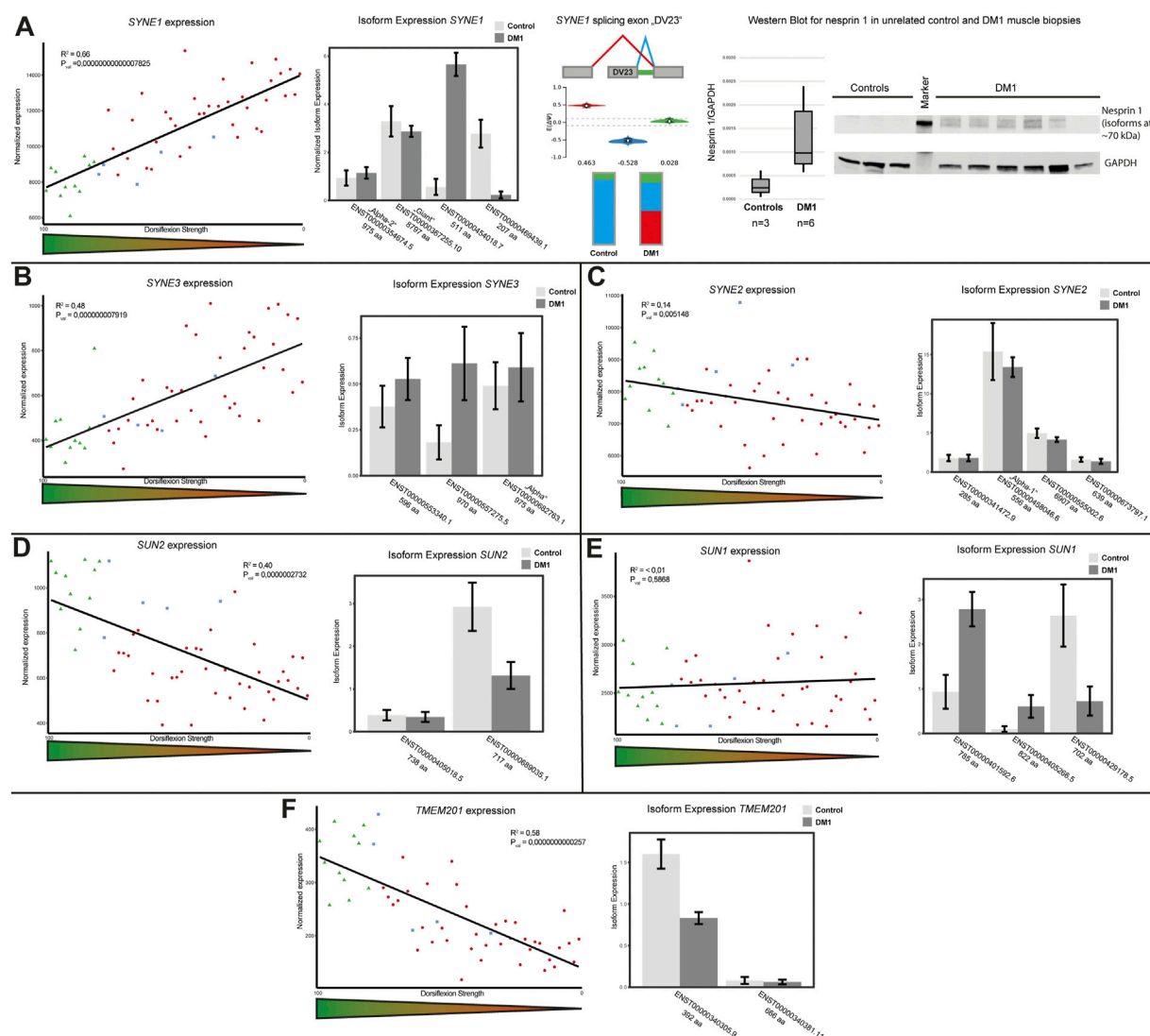


FIGURE 2

LINC (linker of nucleo- and cytoskeleton) complex protein expression and splicing is altered in DM1. (A) *SYNE1* gene expression is inversely correlated with dorsiflexion strength (left panel), there is a switch in isoform expression (second panel) and the muscle-specific DV23 exon is preferentially spliced out in DM1 (third panel). Western blot analysis confirms the expression changes for short nesprin isoforms (fourth panel). (B) *SYNE3* gene expression is inversely correlated with dorsiflexion strength (left panel), there is a switch in isoform expression (right panel). (C) *SYNE2* gene expression slightly correlates with dorsiflexion strength (left panel), there appears to be a general slight downregulation of several isoforms (right panel). (D) *SUN2* gene expression correlates with dorsiflexion strength (left panel), the main muscle isoform is downregulated (right panel). (E) *SUN1* gene expression is unaffected (left panel), but there is a switch in isoform expression (right panel). (F) *TMEM201* gene expression correlates with dorsiflexion strength (left panel), the main muscle isoform is downregulated (right panel).

results in a nucleoplasmic depletion of MBNL and therefore loss of function. Another splicing factor, CUGBP elav-like family member 1 (CELF1), gets stabilized in parallel by hyperphosphorylation causing a gain of function (Philips et al., 1998; Kuyumcu-Martinez et al., 2007). In total, this leads to a misbalance of splicing and a shift towards an embryonic splicing pattern. Missplicing of a set of muscle-specific genes including *TTN* (titin), *DMD* (dystrophin) (Yamashita et al., 2012), *CLCN1* (chloride voltage-gated channel 1) (Charlet et al., 2002; Mankodi et al., 2002), and *RYR1* (ryanodine receptor 1) (Kimura et al., 2005), among others, can be directly linked to specific DM1 symptoms.

Despite all this information, it is still unclear which mechanism is contributing to which extent, and if yet unknown factors add to the

development of this complex disease—especially in the different tissues affected. Intriguingly, alterations to the nuclear envelope (NE) structure and expression changes of NE transmembrane proteins (NETs) have been observed in primary DM1 myoblast and myotube cultures (Hintze et al., 2018; Meinke et al., 2018) as well as in patient fibroblasts (Rodríguez et al., 2015; Viegas et al., 2022). NE proteins are linked to a wide range of disorders, including myopathies and neuropathies. Cellular functions of the NE include the organization, regulation, and repair of the genome, signaling, and cellular mechanics (Meinke and Schirmer, 2016). The composition of the NE is at least partially tissue specific (Korfali et al., 2012), and the identification of NE proteins in skeletal muscle (Wilkie et al., 2011) allows to investigate the NE role in DM1.

Here we reanalyzed RNA-sequencing data from deep sequencing of DM1 and control muscle biopsies (Wang et al., 2019) regarding muscle NE proteins to gain some insight in the role of the NE in DM1 and its contribution to the phenotype.

Methods

Sequencing data

The transcriptomes of 44 DM1 and 11 control tibialis biopsies are publicly available in FASTQ format at GEO (GSE86356). Sample processing has been described in (Wang et al., 2019). One DM1 sample was excluded from further analysis due to insufficient quality as assessed with fastqc. Anonymized patient information can be found in the supplementary data of the original publication and includes the evaluation of the normalized dorsiflexion strength in percent with healthy individuals corresponding to 100% of strength. For the subsequent analysis, either all samples or subgroups according to dorsiflexion strength were used. The subgroups are as following: healthy/proto DM1 (dorsiflexion strength 100%–75%), DM1 (dorsiflexion strength 75%–25%), and severe DM1 (dorsiflexion strength 25%–0%).

Bioinformatical analyses

Alignment

Reads were either mapped with STAR v2.7 (Dobin et al., 2013) or Kallisto v0.46.0 (Bray et al., 2016) to the GRCh38 human reference genome. STAR generated BAM files were used for DESeq2 (Love et al., 2014), DEXSeq (Anders et al., 2012) and MAJIQ v2.3 (Vaquero-Garcia et al., 2016), Kallisto counts were used for isoformSwitchAnalyzer (Vitting-Seerup and Sandelin, 2019).

DESeq2

Aligned reads were counted using featureCounts and analyzed with a standard DESeq2 workflow in R v4.2 using the built-in normalization method (median of ratios). Principal component analysis (PCA) was used to plot the samples according to the two main parameters of variability PC1 and PC2, which showed that samples from healthy individuals clustered together, while DM1 patients are scattered along PC1, consistent with disease severity (Supplementary Figure S1). Genes with log2 foldchanges of $> |0.5|$ and p -values < 0.05 have been set to be significantly changed. Gprofiler2 was used for GO analysis. Volcanoplots were generated with EnhancedVolcano, other plots have been generated with ggplot2. For the expression scatter plots of selected nuclear envelope transmembrane proteins in Figure 2 and Figure 3, samples were ordered after the normalized dorsiflexion strength. Additionally, the analysis has been run separately for the above determined three subgroups to find NE associated proteins. All results are in Supplementary Table S1.

DEXSeq

Mapped reads were counted using the in-built python script of DEXSeq with python v3.9. Standard DEXSeq workflow in R v4.2 was followed and exons with less than 40 counts for all

samples filtered out. Exons with a log2FC of $> |0.5|$ and p -value < 0.05 have been set to be significantly changed. Here as well, analysis has been run separately for the above determined three subgroups to find NE associated proteins. All results are in Supplementary Table S2.

Isoformswitchanalyzer

Isoform counts generated by Kallisto were imported in R and abundance values were normalized *via* edgeR. Normalized isoform expressions were used to generate bar charts *via* the in-built isoformSwitchAnalyzer function switchPlotIsoExp (). For this, we focused on the severe DM1 group and compared it to healthy controls. All results are in Supplementary Table S3.

MAJIQ

Alternative splicing events were analyzed using MAJIQ in python v2.7, providing STAR generated BAM files and a GRCh38 gff3 file. The in-built deltapsi script was used to determine significantly altered splice events between DM1 and control with a confidence interval of .9 and percent-spliced-in (psi) values of $> |0.1|$. MAJIQ Voila was used to visualize the splice graphs. Exon cassette results in Supplementary Table S4.

Western blot

Whole protein extracts were generated from 10 μ m muscle sections using RIPA buffer and an ultrasonic sonicator with a MS73 tip (Bandelin Sonopuls) to lyse the sections. The proteins were separated by SDS gel electrophoresis using 4%–15% TGX gels (BioRad #456–8,087) and 10% TGX gels (BioRad #456–8,034). Western blotting was performed using the Trans-Blot® Turbo™ system (BioRad). Proteins were transferred to nitrocellulose membranes (Trans-Blot® Turbo™ RTA Transfer Kit #170–4,270). Membranes were blocked with 5% skim milk in 1xTBS/0.1% Tween® 20. Following primary antibodies were used: nesprin1 (provided by Didier Hodzic (Razafsky et al., 2013)), Tmem38a (Merck Millipore #06–1,005), Plpp7 (Proteintech #20635-1-AP). For quantification mouse antiGAPDH (Milipore #MAB374) was used. As secondary antibodies we used donkey anti-mouse IRDye 680RD and donkey anti-rabbit IRDye 800 CW. All western blot images were obtained using a Licor FC. Quantification was done using the Licor ImageStudio Software. Western blots were repeated at least three times to confirm the results. Full blots are shown in Supplementary Figure S2.

Muscle biopsies

Muscle biopsies were obtained from the Muscle Tissue Culture Collection (MTCC) at the Friedrich-Baur-Institute (Department of Neurology, LMU Klinikum, Ludwig-Maximilians-University, Munich, Germany). All materials were obtained with written informed consent of the donor. Ethical approval for this study was obtained from the ethical review committee at the Ludwig-Maximilians-University, Munich, Germany (reference 45–14).

Results

To analyze muscle NE protein expression and splicing in DM1 biopsies we used a list of 386 proteins identified by mass

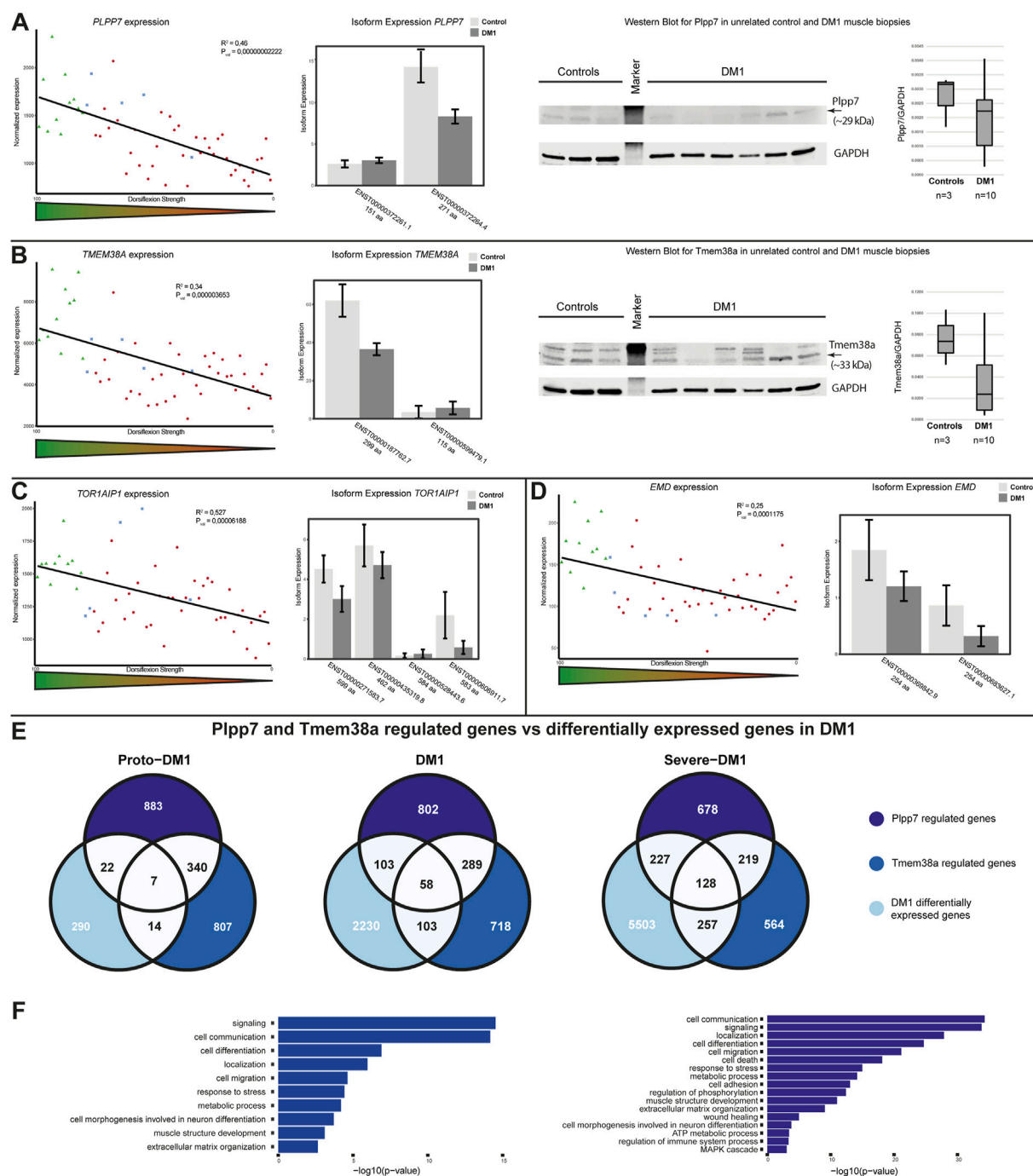


FIGURE 3

Genome organizing muscle nuclear envelope transmembrane protein (NET) expression is altered in DM1 and affects gene expression. (A) *PLPP7* gene expression is correlated with dorsiflexion strength (left panel), the main muscle isoform is downregulated (middle panel). Western blot analysis confirms the expression changes (right panel). (B) *TMEM38A* gene expression is correlated with dorsiflexion strength (left panel), the main muscle isoform is downregulated (middle panel). Western blot analysis confirms the expression changes (right panel). (C) *TOR1AIP1* gene expression is correlated with dorsiflexion strength (left panel), several isoforms are downregulated (right panel). (D) *EMD* gene expression is correlated with dorsiflexion strength (left panel), several isoforms only different in the UTR-region are downregulated (right panel). (E) Overlap between Ppp7 and Tmem38a regulated genes and DM1 differential expressed genes for proto-DM1, DM1, and severe DM1 based on dorsiflexion strength. (F) GO-term enrichment for the Ppp7 and Tmem38a regulated and DM1 differential expressed genes.

spectrometry of isolated muscle NEs (Wilkie et al., 2011; Korfali et al., 2012) (Supplemental Table S5). The genes encoding these 386 proteins were analyzed for alterations in expression or splicing in a published transcriptome dataset of 54 tibialis anterior muscle

biopsies (Wang et al., 2019). We decided to use the datasets of tibialis anterior muscles for our analyses as this muscle is predominantly affected in DM1 (Harper, 2001). These 54 tibialis anterior muscle biopsies originated from 11 unaffected individuals and

43 DM1 patients, all characterized for ankle dorsiflexion strength to quantify how much the muscle was affected. Based on these measurements the DM1 patients were characterized as proto-DM1, DM1 or severe DM1 (Wang et al., 2019).

Differential expression of muscle nuclear envelope proteins

First, read counts were analyzed using DESeq2. We identified two genes up and six genes being downregulated in proto-DM1, while in DM1 14 genes were up and 32 genes downregulated. In severe DM1, there was a further increase of NE-protein encoding genes being differentially expressed, 34 genes were up and 91 genes down (Figure 1A). The total number of genes encoding muscle NE proteins was accordingly increasing with loss of dorsiflexion strength (8, 46, 125; Figure 1B, left panel). Among these differentially expressed genes, the percentage of genes encoding proteins with a transmembrane domain was 11.2% (Figure 1B, right panel). Next, we were interested in which biological functions the protein products of these genes were involved. Pathway analysis revealed functions in muscle relevant processes like muscle contraction, muscle structure development, response to stimulus, and metabolic processes (Figure 1C; Supplementary Table S6).

Splicing alterations of muscle nuclear envelope proteins

Apart from differential expression, splicing alteration can impact the function of translated proteins—especially when considering that the main pathomechanism described in DM1 is an increase in alternative splicing. Similar to differential gene expression the number of genes affected by splice alterations did increase with reduced dorsiflexion strength. In proto-DM1, 36 genes were affected while in DM1 this number increased to 67 and in severe DM1 to 104 genes (Figure 1D, left panel). Among these differentially spliced genes, the percentage of genes encoding proteins with a transmembrane domain was 8.7% (Figure 1D, right panel). Pathway analysis of these alternatively spliced genes also revealed functions in muscle contraction, muscle structure development, and metabolic processes (Figure 1E; Supplementary Table S7).

Cytoskeletal associated NETs

We did describe alterations of the NE in primary DM1 myoblasts and myotubes before (Hintze et al., 2018; Meinke et al., 2018). There, we observed NE invaginations which indicated altered nuclear-cytoskeletal coupling and accordingly identified altered expression of several nesprin isoforms. Based on these data we screened differentially expressed and spliced genes for genes encoding LINC complex (linker of nucleoskeleton and cytoskeleton) and LINC-associated proteins. We identified the expression of *SYNE1*, encoding nesprin 1, to be inverse correlated with dorsiflexion strength (Figure 2A, left panel). As the *SYNE1* gene is giving rise to multiple nesprin isoforms by alternative splicing, we performed an isoform expression analysis. This showed that the expression changes were not caused by

alterations of the giant or muscle specific alpha-2 isoforms. Instead, there was a misregulation of other short isoforms, as illustrated for two isoforms containing neither the KASH nor the actin-binding domain. While a 207 amino acid (aa) isoform was downregulated a 511 aa isoform was strongly upregulated (Figure 2A, second panel). The *SYNE1* gene also came up in the MAJIQ analysis, with a preferential exclusion of a specific exon. This 69 nucleotide exon was identified in an early study (Apel et al., 2000) and later named Δ SR (Simpson and Roberts, 2008) and DV23 (Duong et al., 2014). It is evolutionary conserved and highly muscle-specific (Simpson and Roberts, 2008; Duong et al., 2014). We found this exon to be spliced out in about 50% of the transcripts in DM1 biopsies while it was almost exclusively spliced in in controls (Figure 2A, third panel). To verify the RNAseq data on protein level we performed Western blot on a set of unrelated control and DM1 muscle biopsies. An increased signal of several bands between 70 and 260 kDa in DM1 patients muscle indicates an upregulation of short nesprin 1 isoforms on protein level (Figure 2A, fourth panel; Supplementary Figure S2).

Similar to *SYNE1* the expression of *SYNE3*, encoding nesprin 3, was also inverse correlated with dorsiflexion strength (Figure 2B, left panel). Here the increased expression appears to originate from an upregulation of a 970 aa isoform, which differs from the “alpha isoform” (975 aa) by the loss of the amino acids 793 to 797 due to the usage of an alternative splice site (Figure 2B, right panel). Considering the differential expression of the nesprins 1 and 3 we decided to look also at *SYNE2*, but here we found only a very mild trend for a correlation of gene expression and dorsiflexion strength which may be caused by changes to the expression of the muscle isoform “alpha-1” (Figure 2C).

The nuclear side of the LINC complex consists of SUN proteins. The expression of *SUN2* was strongly correlated with dorsiflexion strength (Figure 2D, left panel). In terms of isoform expression, this seems to originate from a downregulation of the 717 aa isoform (Figure 2D, right panel). We also looked at expression of *SUN1*, but could not find clear correlation with dorsiflexion strength (Figure 2E, left panel). However, looking at the isoform expression we could see several alterations which seem to level out the total gene expression. While a 785 aa and a 822 aa isoform were upregulated, a 702 aa isoform was strongly downregulated (Figure 2E, right panel).

Samp1, which is encoded by the *TMEM201* gene, is functional associated to the LINC complex (Gudise et al., 2011). We found expression of Samp1 to strongly correlate with dorsiflexion strength (Figure 2F, left panel). The reduced expression is due to downregulation of the shorter isoform (392 aa), with the longer isoform (666 aa) being affected very little (Figure 2F, right panel).

Genome organizing mNETs

Samp1 has not only been described to be involved in the nucleoskeleton-cytoskeletal coupling *via* the LINC complex, but has also been shown to be involved in genome organization (Zuleger et al., 2013). This in addition to observed general gene expression changes here as well as in DM1 tissue culture systems (Todorow et al., 2021) prompted us to investigate muscle specific NETs involved in genome organization in more detail. We found in addition to *TMEM201* the expression of *PLPP7*, *TMEM38A*, *TOR1AIP1* and *EMD* to be altered.

For *PLPP7* we found a positive correlation of gene expression and dorsiflexion strength (Figure 3A, left panel). This was caused by

downregulation of the main isoform of the protein (271 aa) (Figure 3A, middle panel). We proceeded to confirm these expression changes on protein level by Western blot, which showed downregulation of Plpp7 in unrelated DM1 muscle biopsies (Figure 3A, right panel). Tmem38a expression was correlating in a similar manner as *PLPP7* with dorsiflexion strength (Figure 3B, left panel). Here the expression changes also seemingly originated from the main isoform (299 aa) (Figure 3B, middle panel). We could also confirm these results on protein level in unrelated samples (Figure 3B, right panel). We looked at two additional NETs known to be involved in genome organization, LAP1 (encoded by *TOR1AIP1*), and emerin (encoded by *EMD*). For both we found a clear correlation with dorsiflexion strength originating from a downregulation of all isoforms (Figures 3C, D).

Apart from the effect on expression and splicing of muscle NE proteins we were also interested in possible functional consequences. Plpp7 and Tmem38a are muscle specific NETs involved in genome organization, and the genes they contribute to regulate in C2C12 myotubes (which partially overlap) have been identified (Robson et al., 2016). To investigate whether the observed expression changes in DM1 muscle biopsies do have any functional relevance we proceeded to test the expression of these Plpp7 and Tmem38a co-regulated genes in the three subgroups. We could indeed find an overlap between genes regulated by both proteins in mouse myotubes and DM1 patient biopsies: in proto-DM1, there was an overlap of 43 genes, in DM1 264 genes, and in severe DM1 612 genes (Figure 3E). This made up 13, 11, and 10% of the overall differentially expressed genes in the DM1 samples, respectively. Next, we were interested in the biological functions of the genes under Plpp7 or Tmem38a control. Considering the number of genes, this analysis was possible for the DM1 and severe DM1 groups. The main enriched pathways were signaling, cell communication, cell migration, localization, response to stress and metabolic process (Figure 3F, Supplementary Table S8).

Discussion

The missplicing in DM1 is well investigated and there are many target genes of this missplicing described, which are contributing or likely contributing to the disease pathology. Yet, it still remains elusive which additional pathomechanisms are contributing to the development in DM1, and to which extent, especially in the different tissues affected. The NE has been shown to be much more than just a barrier separating the genome from the rest of the cell (de Las Heras et al., 2013), it hosts a tissue specific proteome and tissue specific as well as ubiquitously expressed NETs have been shown to be involved in controlling the intranuclear positioning and thus expression of genes, often in a tissue specific manner (Zuleger et al., 2011). We could previously identify NE alterations in muscle tissue culture systems of DM1, with likely effects on cell cycle control and differentiation (Hintze et al., 2018; Meinke et al., 2018). Investigating the involvement of the NE in DM1 mature muscle was therefore the logical follow up to unravel its role in the DM1 pathology.

The set of NE genes we investigated contained genes with and without transmembrane domains, as we did not want to exclude a possible contribution of NE-associated proteins. We could indeed find for both NE and NET encoding genes a high percentage of

differential expression and differential splicing. This highlighted the likelihood of an important role of NE proteins in DM1 as the GO-term analysis revealed that the most enriched processes of these differentially regulated genes are all relevant for muscle function.

We wanted to follow up on specific aspects of NE function. Considering the misregulation of nesprin proteins in DM1 muscle cell cultures (Hintze et al., 2018), which is a possible explanation for observed NE invaginations (Meinke et al., 2018), and the identification of mutations in *SYNE* and *SUN* in a clinically similar disease, EDMD (Zhang et al., 2007; Meinke et al., 2014), we looked at all components of the LINC complex. We could identify isoform-specific alterations in the expression of the *SYNE1*, *SYNE3*, *SUN1*, and *SUN2* genes—all core components of LINC complexes. Although there was no apparent change in the expression of the muscle-specific nesprin 1 isoform “alpha-2”, in about half of these transcripts a 23 aa exon (DV23) was spliced out in DM1 patients. As this exon has been shown to be included in 94% muscle *SYNE1* transcripts (Duong et al., 2014) this could indicate a loss of a muscle-specific nesprin 1 function. Furthermore, for Samp1, which has been identified as a LINC complex associated protein, there was also a downregulation of the major muscle isoform. This clearly indicates a likely weakening of the nuclear-cytoskeletal connection in DM1 muscle, which is going to impact on mechanotransduction as well as nuclei positioning. This is in line with observed missplicing of the myc box-dependent-interacting protein 1 (Bin1), which is involved in the formation of tubular invaginations of the plasma membrane that function in depolarization-contraction coupling (Fugier et al., 2011).

Another important aspect of the NE is the tissue specific regulation of gene expression by the recruitment of specific genes to the NE by tissue specific NETs. Examples for this are Plpp7 and Tmem38a, which have been shown to have important muscle functions (Robson et al., 2016). It is important to note that these proteins appear to have an additive effect, a knockdown of more than one resulted in stronger effects than single knockdowns (Robson et al., 2016). Thus, it is likely that a reduced expression of several NETs is also adding up to result in phenotypical consequences. We found both proteins to be downregulated on RNA and protein level, and by comparing DM1 differentially expressed genes to the genes identified under their expression control in mouse myoblasts, we could prove that we have similar effects in DM1. Intriguingly, mutations in *PLPP7*, *TMEM38A*, and *TMEM201* have been identified in muscular dystrophy patients with an EDMD-like phenotype (Meinke et al., 2020), which highlights the importance of these proteins in muscle disease. Misregulation of the two muscle NETs Plpp7 and Tmem38a alone does indeed account for about 10% of all differentially expressed genes in DM1 muscle. Since there are additional NETs misregulated in DM1 the actual effect is probably even more profound. It has been shown that Samp1 can also reposition chromosomes (Zuleger et al., 2013) and emerin directly binds histone deacetylase 3 (Demmerle et al., 2012), while LAP1 binds indirectly to chromatin (Foisner and Gerace, 1993). Notably, mutations in the genes encoding emerin and LAP1 also cause EDMD (Bione et al., 1994) respectively a very similar muscular dystrophy (Kayman-Kurekci et al., 2014). All in all, our data suggests that DM1 and EDMD share a broader common ground also on the cellular level rather than only in the symptomatology.

Data availability statement

The datasets presented in this study can be found in online repositories. The names of the repository/repositories and accession number(s) can be found in the article/[Supplementary Material](#).

Ethics statement

The studies involving human participants were reviewed and approved by Ethical review committee at the Ludwig-Maximilians-University, Munich, Germany. The patients/participants provided their written informed consent to participate in this study.

Author contributions

VT, SH, BS, and PM contributed to the conception and design of the experiments. PM and BS wrote the manuscript, SH performed the experiments, VT performed the bioinformatical analyses.

Funding

This work was funded by the Deutsche Forschungsgemeinschaft (DFG, German Research Foundation)—Projektnummer 470092532.

References

- Anders, S., Reyes, A., and Huber, W. (2012). Detecting differential usage of exons from RNA-seq data. *Genome Res.* 22 (10), 2008–2017. doi:10.1101/gr.133744.111
- Apel, E. D., Lewis, R. M., Grady, R. M., and Sanes, J. R. (2000). Syne-1, a dystrophin- and Klarsicht-related protein associated with synaptic nuclei at the neuromuscular junction. *J. Biol. Chem.* 275 (41), 31986–31995. doi:10.1074/jbc.M004775200
- Barbé, L., Lanni, S., López-Castel, A., Franck, S., Spits, C., Keymolen, K., et al. (2017). CpG methylation, a parent-of-origin effect for maternal-biased transmission of congenital myotonic dystrophy. *Am. J. Hum. Genet.* 100 (3), 488–505. doi:10.1016/j.ajhg.2017.01.033
- Bione, S., Maestrini, E., Rivella, S., Mancini, M., Regis, S., Romeo, G., et al. (1994). Identification of a novel X-linked gene responsible for Emery-Dreifuss muscular dystrophy. *Nat. Genet.* 8 (4), 323–327. doi:10.1038/ng1294-323
- Bray, N. L., Pimentel, H., Melsted, P., and Pachter, L. (2016). Erratum: Near-optimal probabilistic RNA-seq quantification. *Nat. Biotechnol.* 34 (8), 888. doi:10.1038/nbt0816-888d
- Charlet, B. N., Savkur, R. S., Singh, G., Philips, A. V., Grice, E. A., and Cooper, T. A. (2002). Loss of the muscle-specific chloride channel in type 1 myotonic dystrophy due to misregulated alternative splicing. *Mol. Cell* 10 (1), 45–53. doi:10.1016/s1097-2765(02)00572-5
- De Antonio, M., Dogan, C., Hamroun, D., Mati, M., Zerrouki, S., Eymard, B., et al. (2016). Unravelling the myotonic dystrophy type 1 clinical spectrum: A systematic registry-based study with implications for disease classification. *Rev. Neurol. Paris.* 172 (10), 572–580. doi:10.1016/j.neurol.2016.08.003
- de Las Heras, J. I., Meinke, P., Batrakou, D. G., Srsen, V., Zuleger, N., Kerr, A. R., et al. (2013). Tissue specificity in the nuclear envelope supports its functional complexity. *Nucleus* 4 (6), 460–477. doi:10.4161/nucl.26872
- Demmerle, J., Koch, A. J., and Holaska, J. M. (2012). The nuclear envelope protein emerin binds directly to histone deacetylase 3 (HDAC3) and activates HDAC3 activity. *J. Biol. Chem.* 287 (26), 22080–22088. doi:10.1074/jbc.M111.325308
- Dobin, A., Davis, C. A., Schlesinger, F., Drenkow, J., Zaleski, C., Jha, S., et al. (2013). Star: Ultrafast universal RNA-seq aligner. *Bioinformatics* 29 (1), 15–21. doi:10.1093/bioinformatics/bts635
- Duong, N. T., Morris, G. E., Lam, L. T., Zhang, Q., Sewry, C. A., Shanahan, C. M., et al. (2014). Nesprins: Tissue-specific expression of epsilon and other short isoforms. *PLoS One* 9 (4), e94380. doi:10.1371/journal.pone.0094380
- Ebrlidge, A., Wang, Y., Petkova, V., Ebrlidge, K., and Junghans, R. P. (2004). RNA leaching of transcription factors disrupts transcription in myotonic dystrophy. *Science* 303 (5656), 383–387. doi:10.1126/science.1088679
- Fardaei, M., Larkin, K., Brook, J. D., and Hamshire, M. G. (2001). *In vivo* co-localisation of MBNL protein with DMPK expanded-repeat transcripts. *Nucleic Acids Res.* 29 (13), 2766–2771. doi:10.1093/nar/29.13.2766
- Fardaei, M., Rogers, M. T., Thorpe, H. M., Larkin, K., Hamshire, M. G., Harper, P. S., et al. (2002). Three proteins, MBNL, MBLL and MBXL, co-localize *in vivo* with nuclear foci of expanded-repeat transcripts in DM1 and DM2 cells. *Hum. Mol. Genet.* 11 (7), 805–814. doi:10.1093/hmg/11.7.805
- Faustino, N. A., and Cooper, T. A. (2003). Pre-mRNA splicing and human disease. *Genes Dev.* 17 (4), 419–437. doi:10.1101/gad.1048803
- Foisner, R., and Gerace, L. (1993). Integral membrane proteins of the nuclear envelope interact with lamins and chromosomes, and binding is modulated by mitotic phosphorylation. *Cell* 73 (7), 1267–1279. doi:10.1016/0092-8674(93)90355-t
- Fu, Y. H., Pizzuti, A., Fenwick, R. G., Jr., King, J., Rajnarayan, S., Dunne, P. W., et al. (1992). An unstable triplet repeat in a gene related to myotonic muscular dystrophy. *Science* 255 (5049), 1256–1258. doi:10.1126/science.1546326
- Fugier, C., Klein, A. F., Hammer, C., Vassilopoulos, S., Ivarsson, Y., Toussaint, A., et al. (2011). Misregulated alternative splicing of BIN1 is associated with T tubule alterations and muscle weakness in myotonic dystrophy. *Nat. Med.* 17 (6), 720–725. doi:10.1038/nm.2374
- Gudise, S., Figueroa, R. A., Lindberg, R., Larsson, V., and Hallberg, E. (2011). Samp1 is functionally associated with the LINC complex and A-type lamina networks. *J. Cell Sci.* 124, 2077–2085. doi:10.1242/jcs.078923
- Harper, P. S. (2001). in *Myotonic dystrophy-the clinical picture Myotonic dystrophy*. Editor W. B. Saunders. third edition ed London, 17–46.
- Hintze, S., Knaier, L., Limmer, S., Schoser, B., and Meinke, P. (2018). Nuclear envelope transmembrane proteins in myotonic dystrophy type 1. *Front. Physiol.* 9, 1532. doi:10.3389/fphys.2018.01532
- Ho, T. H., Bundman, D., Armstrong, D. L., and Cooper, T. A. (2005). Transgenic mice expressing CUG-BP1 reproduce splicing mis-regulation observed in myotonic dystrophy. *Hum. Mol. Genet.* 14 (11), 1539–1547. doi:10.1093/hmg/ddi162
- Huichalaf, C., Sakai, K., Jin, B., Jones, K., Wang, G. L., Schoser, B., et al. (2010). Expansion of CUG RNA repeats causes stress and inhibition of translation in myotonic dystrophy 1 (DM1) cells. *FASEB J.* 24 (10), 3706–3719. doi:10.1096/fj.09-151159
- Kalsotra, A., Singh, R. K., Gurha, P., Ward, A. J., Creighton, C. J., and Cooper, T. A. (2014). The Mef2 transcription network is disrupted in myotonic dystrophy heart tissue, dramatically altering miRNA and mRNA expression. *Cell Rep.* 6 (2), 336–345. doi:10.1016/j.celrep.2013.12.025

Acknowledgments

We thank Prof. Eric C. Schirmer and Didier Hodzic for the antibodies provided to us.

Conflict of interest

The authors declare that the research was conducted in the absence of any commercial or financial relationships that could be construed as a potential conflict of interest.

Publisher's note

All claims expressed in this article are solely those of the authors and do not necessarily represent those of their affiliated organizations, or those of the publisher, the editors and the reviewers. Any product that may be evaluated in this article, or claim that may be made by its manufacturer, is not guaranteed or endorsed by the publisher.

Supplementary material

The Supplementary Material for this article can be found online at: <https://www.frontiersin.org/articles/10.3389/fcell.2022.1007331/full#supplementary-material>

- Kayman-Kurekci, G., Talim, B., Korkusuz, P., Sayar, N., Sarioglu, T., Oncel, I., et al. (2014). Mutation in TOR1AIP1 encoding LAP1B in a form of muscular dystrophy: A novel gene related to nuclear envelopopathies. *Neuromuscul. Disord.* 24 (7), 624–633. doi:10.1016/j.nmd.2014.04.007
- Kimura, T., Nakamori, M., Lueck, J. D., Pouliquin, P., Aoi, F., Fujimura, H., et al. (2005). Altered mRNA splicing of the skeletal muscle ryanodine receptor and sarcoplasmic/endoplasmic reticulum Ca²⁺-ATPase in myotonic dystrophy type 1. *Hum. Mol. Genet.* 14 (15), 2189–2200. doi:10.1093/hmg/ddi223
- Korfali, N., Wilkie, G. S., Swanson, S. K., Srsen, V., de Las Heras, J., Batrakou, D. G., et al. (2012). The nuclear envelope proteome differs notably between tissues. *Nucleus* 3 (6), 552–564. doi:10.4161/nucl.22257
- Kuyumcu-Martinez, N. M., Wang, G. S., and Cooper, T. A. (2007). Increased steady-state levels of CUGBP1 in myotonic dystrophy 1 are due to PKC-mediated hyperphosphorylation. *Mol. Cell* 28 (1), 68–78. doi:10.1016/j.molcel.2007.07.027
- López-Martínez, A., Soblechero-Martín, P., de-la-Puente-Ovejero, L., Nogales-Gadea, G., and Archavala-Gomez, V. (2020). An overview of alternative splicing defects implicated in myotonic dystrophy type I. *Genes* 11 (9), 1109. doi:10.3390/genes11091109
- Love, M. I., Huber, W., and Anders, S. (2014). Moderated estimation of fold change and dispersion for RNA-seq data with DESeq2. *Genome Biol.* 15 (12), 550. doi:10.1186/s13059-014-0550-8
- Mankodi, A., Takahashi, M. P., Jiang, H., Beck, C. L., Bowers, W. J., Moxley, R. T., et al. (2002). Expanded CUG repeats trigger aberrant splicing of ClC-1 chloride channel pre-mRNA and hyperexcitability of skeletal muscle in myotonic dystrophy. *Mol. Cell* 10 (1), 35–44. doi:10.1016/s1097-2765(02)00563-4
- Martorell, L., Cobo, A. M., Baiget, M., Naudo, M., Poza, J. J., and Parra, J. (2007). Prenatal diagnosis in myotonic dystrophy type 1. Thirteen years of experience: Implications for reproductive counselling in DM1 families. *Prenat. Diagn.* 27 (1), 68–72. doi:10.1002/pd.1627
- Meinke, P., Hintze, S., Limmer, S., and Schoser, B. (2018). Myotonic dystrophy-A progeroid disease? *Front. Neurol.* 9, 601. doi:10.3389/fneur.2018.00601
- Meinke, P., Kerr, A. R. W., Czapiewski, R., de Las Heras, J. I., Dixon, C. R., Harris, E., et al. (2020). A multistage sequencing strategy pinpoints novel candidate alleles for Emery-Dreifuss muscular dystrophy and supports gene misregulation as its pathomechanism. *EBioMedicine* 51, 102587. doi:10.1016/j.ebiom.2019.11.048
- Meinke, P., Mattioli, E., Haque, F., Antoku, S., Columbaro, M., Straatman, K. R., et al. (2014). Muscular dystrophy-associated SUN1 and SUN2 variants disrupt nuclear-cytoskeletal connections and myonuclear organization. *PLoS Genet.* 10 (9), e1004605. doi:10.1371/journal.pgen.1004605
- Meinke, P., and Schirmer, E. C. (2016). The increasing relevance of nuclear envelope myopathies. *Curr. Opin. Neurol.* 29 (5), 651–661. doi:10.1097/wco.0000000000000359
- Meola, G., Jones, K., Wei, C., and Timchenko, L. T. (2013). Dysfunction of protein homeostasis in myotonic dystrophies. *Histol. Histopathol.* 28 (9), 1089–1098. doi:10.14670/HH-28.1089
- Monckton, D. G., Wong, L. J., Ashizawa, T., and Caskey, C. T. (1995). Somatic mosaicism, germline expansions, germline reversions and intergenerational reductions in myotonic dystrophy males: Small pool PCR analyses. *Hum. Mol. Genet.* 4 (1), 1–8. doi:10.1093/hmg/4.1.1
- Nakamori, M., Sobczak, K., Puwanant, A., Welle, S., Eichinger, K., Pandya, S., et al. (2013). Splicing biomarkers of disease severity in myotonic dystrophy. *Ann. Neurol.* 74 (6), 862–872. doi:10.1002/ana.23992
- Napierala, M., and Krzyzosiak, W. J. (1997). CUG repeats present in myotonin kinase RNA form metastable "slippery" hairpins. *J. Biol. Chem.* 272 (49), 31079–31085. doi:10.1074/jbc.272.49.31079
- Osborne, R. J., Lin, X., Welle, S., Sobczak, K., O'Rourke, J. R., Swanson, M. S., et al. (2009). Transcriptional and post-transcriptional impact of toxic RNA in myotonic dystrophy. *Hum. Mol. Genet.* 18 (8), 1471–1481. doi:10.1093/hmg/ddp058
- Philips, A. V., Timchenko, L. T., and Cooper, T. A. (1998). Disruption of splicing regulated by a CUG-binding protein in myotonic dystrophy. *Science* 280 (5364), 737–741. doi:10.1126/science.280.5364.737
- Rakocevic-Stojanovic, V., Savic, D., Pavlovic, S., Lavernic, D., Stevic, Z., Basta, I., et al. (2005). Intergenerational changes of CTG repeat depending on the sex of the transmitting parent in myotonic dystrophy type I. *Eur. J. Neurol.* 12 (3), 236–237. doi:10.1111/j.1468-1331.2004.01075.x
- Rau, F., Freyermuth, F., Fugier, C., Villemin, J. P., Fischer, M. C., Jost, B., et al. (2011). Misregulation of miR-1 processing is associated with heart defects in myotonic dystrophy. *Nat. Struct. Mol. Biol.* 18 (7), 840–845. doi:10.1038/nsmb.2067
- Razafsky, D. S., Ward, C. L., Kolb, T., and Hodzic, D. (2013). Developmental regulation of linkers of the nucleoskeleton to the cytoskeleton during mouse postnatal retinogenesis. *Nucleus* 4 (5), 399–409. doi:10.4161/nucl.26244
- Robson, M. I., de Las Heras, J. I., Czapiewski, R., P. L. T., Booth, D. G., Kelly, D. A., et al. (2016). Tissue-specific gene repositioning by muscle nuclear membrane proteins enhances repression of critical developmental genes during myogenesis. *Mol. Cell* 62 (6), 834–847. doi:10.1016/j.molcel.2016.04.035
- Rodríguez, R., Hernández-Hernández, O., Magaña, J. J., González-Ramírez, R., García-López, E. S., and Cisneros, B. (2015). Altered nuclear structure in myotonic dystrophy type 1-derived fibroblasts. *Mol. Biol. Rep.* 42 (2), 479–488. doi:10.1007/s11033-014-3791-4
- Shen, X., Xu, F., Li, M., Wu, S., Zhang, J., Wang, A., et al. (2020). miR-322/-503 rescues myoblast defects in myotonic dystrophy type 1 cell model by targeting CUG repeats. *Cell Death Dis.* 11 (10), 891. doi:10.1038/s41419-020-03112-6
- Simpson, J. G., and Roberts, R. G. (2008). Patterns of evolutionary conservation in the nesprin genes highlight probable functionally important protein domains and isoforms. *Biochem. Soc. Trans.* 36, 1359–1367. doi:10.1042/bst0361359
- Thornton, C. A., Johnson, K., and Moxley, R. T., 3rd (1994). Myotonic dystrophy patients have larger CTG expansions in skeletal muscle than in leukocytes. *Ann. Neurol.* 35 (1), 104–107. doi:10.1002/ana.410350116
- Thornton, C. A. (2014). Myotonic dystrophy. *Neurol. Clin.* 32 (3), 705–719. viii. doi:10.1016/j.ncl.2014.04.011
- Todorow, V., Hintze, S., Kerr, A. R. W., Hehr, A., Schoser, B., and Meinke, P. (2021). Transcriptome analysis in a primary human muscle cell differentiation model for myotonic dystrophy type 1. *Int. J. Mol. Sci.* 22 (16), 8607. doi:10.3390/ijms22168607
- Udd, B., and Krahe, R. (2012). The myotonic dystrophies: Molecular, clinical, and therapeutic challenges. *Lancet Neurol.* 11 (10), 891–905. doi:10.1016/S1474-4422(12)70204-1
- Vaquero-Garcia, J., Barrera, A., Gazzara, M. R., González-Vallinas, J., Lahens, N. F., Hogenesch, J. B., et al. (2016). A new view of transcriptome complexity and regulation through the lens of local splicing variations. *Elife* 5, e11752. doi:10.7554/eLife.11752
- Viegas, D., Pereira, C. D., Martins, F., Mateus, T., da Cruz, E. S. O. A. B., Herdeiro, M. T., et al. (2022). Nuclear envelope alterations in myotonic dystrophy type 1 patient-derived fibroblasts. *Int. J. Mol. Sci.* 23 (1), 522. doi:10.3390/ijms23010522
- Vitting-Seerup, K., and Sandelin, A. (2019). IsoformSwitchAnalyzeR: Analysis of changes in genome-wide patterns of alternative splicing and its functional consequences. *Bioinformatics* 35 (21), 4469–4471. doi:10.1093/bioinformatics/btz247
- Wang, E. T., Treacy, D., Eichinger, K., Struck, A., Estabrook, J., Olafson, H., et al. (2019). Transcriptome alterations in myotonic dystrophy skeletal muscle and heart. *Hum. Mol. Genet.* 28 (8), 1312–1321. doi:10.1093/hmg/ddy432
- Wenninger, S., Montagnese, F., and Schoser, B. (2018). Core clinical phenotypes in myotonic dystrophies. *Front. Neurol.* 9, 303. doi:10.3389/fneur.2018.00303
- Wheeler, T. M. (2008). Myotonic dystrophy: Therapeutic strategies for the future. *Neurotherapeutics* 5 (4), 592–600. doi:10.1016/j.nurt.2008.08.001
- Wilkie, G. S., Korfali, N., Swanson, S. K., Malik, P., Srsen, V., Batrakou, D. G., et al. (2011). Several novel nuclear envelope transmembrane proteins identified in skeletal muscle have cytoskeletal associations. *Mol. Cell Proteomics* 10 (1), M110.003129. doi:10.1074/mcp.M110.003129
- Wong, L. J., Ashizawa, T., Monckton, D. G., Caskey, C. T., and Richards, C. S. (1995). Somatic heterogeneity of the CTG repeat in myotonic dystrophy is age and size dependent. *Am. J. Hum. Genet.* 56 (1), 114–122.
- Yamashita, Y., Matsuura, T., Shinmi, J., Amakusa, Y., Masuda, A., Ito, M., et al. (2012). Four parameters increase the sensitivity and specificity of the exon array analysis and disclose 25 novel aberrantly spliced exons in myotonic dystrophy. *J. Hum. Genet.* 57 (6), 368–374. doi:10.1038/jhg.2012.37
- Zhang, Q., Bethmann, C., Worth, N. F., Davies, J. D., Wasner, C., Feuer, A., et al. (2007). Nesprin-1 and -2 are involved in the pathogenesis of Emery Dreifuss muscular dystrophy and are critical for nuclear envelope integrity. *Hum. Mol. Genet.* 16 (23), 2816–2833. doi:10.1093/hmg/ddm238
- Zuleger, N., Boyle, S., Kelly, D. A., de las Heras, J. I., Lazou, V., Korfali, N., et al. (2013). Specific nuclear envelope transmembrane proteins can promote the location of chromosomes to and from the nuclear periphery. *Genome Biol.* 14 (2), R14. doi:10.1186/gb-2013-14-2-r14
- Zuleger, N., Robson, M. I., and Schirmer, E. C. (2011). The nuclear envelope as a chromatin organizer. *Nucleus* 2 (5), 339–349. doi:10.4161/nucl.2.5.17846

Frontiers in Cell and Developmental Biology

Explores the fundamental biological processes of life, covering intracellular and extracellular dynamics.

The world's most cited developmental biology journal, advancing our understanding of the fundamental processes of life. It explores a wide spectrum of cell and developmental biology, covering intracellular and extracellular dynamics.

Discover the latest Research Topics

[See more →](#)

Frontiers

Avenue du Tribunal-Fédéral 34
1005 Lausanne, Switzerland
frontiersin.org

Contact us

+41 (0)21 510 17 00
frontiersin.org/about/contact

